*Phil. Trans. R. Soc. Lond.* B **304**, 199–253 (1984) 
*Printed in Great Britain*

# CYTOCHROME OXIDASE PATCHES: A NEW CYTOARCHITECTONIC FEATURE OF MONKEY VISUAL CORTEX

BY J. C. HORTON

*Department of Neurobiology, Harvard Medical School, 25 Shattuck Street, Boston, Massachusetts, 02115, U.S.A.*

(*Communicated by T. N. Wiesel, For.Mem.R.S. – Received 28 February* 1983)

[Plates 1–27]

## CONTENTS

PAGE

1. INTRODUCTION 202

2. MATERIALS AND METHODS 204

3. RESULTS 207
   (*a*) Patches: a new cytoarchitectonic feature of monkey visual cortex 207
      (i) The cytochrome oxidase patches in coronal and tangential section 207
      (ii) Microscopic appearance of the cytochrome oxidase stain 208
      (iii) Correlation with other histochemical and structural stains 210
      (iv) A pattern in V2 212
   (*b*) Survey of cytochrome oxidase staining in visual cortex of non-macaque species 213
   (*c*) A direct projection from the lateral geniculate nucleus to the patches 214
      (i) HRP injection in the owl monkey 215
      (ii) HRP injection in the macaque monkey 216
      (iii) Interpretation of the HRP experiments 217
   (*d*) Alignment of patches and ocular dominance columns in macaque 218
   (*e*) Effect of eye removal on cytochrome oxidase staining 219
      (i) Effect on the lateral geniculate nucleus 219
      (ii) Effect on layer IVc of striate cortex 219
      (iii) Effect on the patches 222
      (iv) Summary of eye removal experiments 223
   (*f*) Effect of eyelid suture on cytochrome oxidase staining 224
      (i) Effect on the lateral geniculate nucleus 225
      (ii) Effect on the visual cortex 225
      (iii) Comparison of the effects of eye removal and eyelid suture 228
   (*g*) Pattern of patches in optic disk and monocular crescent regions of macaque striate cortex 229
      (i) Optic disc 229
      (ii) Monocular crescent 231

 [Published 17 January 1984

PAGE

(*h*) Correlation between cytochrome oxidase staining and 2-deoxyglucose uptake 232
(i) Stimulation with all orientations 233
(ii) Stimulation with a single orientation 234
(*i*) Cytochrome oxidase staining in fetal macaques 235

4. Discussion 237
(*a*) The geniculate projection to the patches 237
(*b*) Eye removal and eyelid suture experiments 238
(*c*) Findings in optic disc and monocular crescent regions 241
(*d*) Development of patches in the foetal monkey 242
(*e*) Lessons from comparative anatomical studies 244
(*f*) Interpretation of 2-deoxyglucose results 245
(*g*) Patches as the fundamental cytoarchitectonic unit of primate striate cortex 246

5. References 250

In normal macaque monkeys a histochemical stain for cytochrome oxidase activity revealed a striking pattern of regularly spaced patches in primary visual (striate, area 17, V1) cortex. The patches were most obvious in layers II and III, but also in layers I, IVb, V and VI; only in layers IVc and IVa were they absent. The patches were oval shaped, about 250 by 150 μm and aligned into rows spaced about 350 μm apart. Along each row a patch was located about every 550 μm; often patches in neighbouring rows were aligned, creating a square array. Their density was about one patch per 0.2 $mm^2$ (550 by 350 μm) in opercular cortex. The patches were also labelled preferentially by stains for lactate dehydrogenase, succinate dehydrogenase, acetylcholinesterase (AChE), and myelin.

In V2, a coarser pattern of broad parallel stripes labelled by cytochrome oxidase, lactate dehydrogenase, and AChE was present.

The cytochrome oxidase patches were absent in non-primate species like the cat, mink, tree shrew, mouse, rat, rabbit, and ground squirrel. However, they were present in all primate species examined, including the rhesus, cynomolgus, owl, and squirrel monkey, baboon, bushbaby, and human. While more species should be tested, it appears that the patches are a cytoarchitectonic feature unique to primate visual cortex.

In the owl monkey patches of anterogradely transported horseradish peroxidase (HRP) were found in layers IV$c_\alpha$, III, and II after injection of the tracer into the lateral geniculate nucleus (l.g.n.). They coincided exactly with the position of patches in adjacent sections processed for cytochrome oxidase. A similar result was obtained in the macaque, except that patches were not present in layer IV$c_\alpha$. These experiments established that the cytochrome oxidase patches receive a direct, patchy projection from the lateral geniculate body. However, retrogradely filled layer VI cells in the owl monkey bore no regular relation to the patches. In the macaque, the 'honeycomb' of geniculate terminals in layer IVa matched a similar honeycomb pattern of cytochrome oxidase staining. In the Nissl stain three sublayers in layer IVa were identified: the honeycomb was located in layer IV$a_\beta$. In V2, in the owl monkey the parallel stripes of enhanced cytochrome oxidase activity received a direct projection from l.g.n. or pulvinar.

In the macaque, after intraocular injection of [$^3$H]proline, the rows of patches in layers II and III lay in register with ocular dominance columns seen by transneuronal radioautography in layer IVc.

In another macaque, one eye was removed and the cortex stained for cytochrome oxidase, AChE and Nissl substance after six months survival. In layer IVc light and

dark bands corresponding to the ocular dominance columns were visible; surprisingly the dark cytochrome oxidase bands matched the light AChE and Nissl bands. The set of bands belonging to the missing eye was determined by examining cytochrome oxidase staining and proline radioautographs in another macaque that sustained severe eye injury by [$^3$H]proline injection. In striate cortex, bands of radioactive label from the injured eye matched ocular dominance columns appearing more lightly stained by cytochrome oxidase. In the macaque tested six months after enucleation, in every other row the cytochrome oxidase patches appeared pale and shrunken. These lighter rows fit into precise register with the lighter ocular dominance columns in layer IV c, confirming the correspondence between rows of patches and ocular dominance columns demonstrated by proline injection. AChE staining of patches was similarly affected by eye removal.

The effect of visual deprivation upon cytochrome oxidase staining was tested in two monocularly sutured macaques. In the l.g.n. no effect was detected. In visual cortex wide light columns alternating with thin dark columns were observed in layer IV. In one macaque the ocular dominance columns were labelled independently by HRP injection into a deprived l.g.n. lamina. The HRP labelled ocular dominance columns fit within the pale cytochrome oxidase columns; this establishes that monocular deprivation causes a relatively greater loss of enzyme activity in ocular dominance columns belonging to the closed eye. However, there was also loss of cytochrome oxidase staining along the borders of the normal eye dominance columns, indicating that ocular dominance columns in layer IV are subdivided into core zones flanked by border strips that are susceptible to loss of cytochrome oxidase activity with suture of either eye. The core zones are the same width as the rows of cytochrome oxidase patches and correspond to the dark bands seen in Liesegang stains of normal macaque striate cortex.

In two adult cats the effect of monocular lid suture at 28 d old was assessed: no effect upon cytochrome oxidase staining in l.g.n. or cortex was observed.

The optic disc representation in visual cortex was studied by 2-deoxyglucose radioautography and cytochrome oxidase staining after eye removal or lid suture in macaque monkeys. It appeared as a pale oval, 1.65 times longer than the optic disc, a distortion probably required to maintain overall isotrophy in magnification factor. Patches were present in the disc representation although ocular dominance columns are absent: they appeared rounder and more widely separated. In the temporal cresent patches were also present. They were larger, rounder, and less densely spaced than patches in binocular cortex.

Deoxyglucose mapping in a macaque monkey monocularly stimulated with a display of parallel black and white stripes of irregular width and spacing rotated through all orientations has resulted in patches in the upper layers over ocular dominance columns corresponding to the open eye. These patches match cytochrome oxidase patches situated in every other row, thus suggesting that cells located in cytochrome oxidase patches respond to all orientations of stimulus. Macaques binocularly stimulated with vertical or horizontal stripes show a complicated pattern of deoxyglucose uptake, overlapping extensively with the pattern of cytochrome oxidase patches. In one monkey the right eye was removed and 18 d later the animal was stimulated with vertical stripes. Deoxyglucose radioautography and cytochrome oxidase staining combined in single tissue sections each revealed a matching pattern of ocular dominance columns in layer IV. In the upper layers, dots of radioautographic label were present, matching cytochrome oxidase patches in alternate rows.

In foetal monkeys at E142–144 the laminar pattern of cytochrome oxidase staining in visual cortex was remarkable for a prominent wide band of intense activity in layer IV b and upper IV $c_\alpha$, absent in mature macaques. In tangential section, patches were visible in layers II, III and in layer IV b–IV $c_\alpha$, which indicates that patches form in monkey visual cortex before birth.

The functional significance of the patches remains uncertain. It has been suggested that the visual field is analysed in visual cortex by small modules containing several hypercolumns of each stimulus variable. The cytochrome oxidase patches may constitute the anatomical correlate of these proposed modules.

## 1. Introduction

Every image that strikes the retina evokes a pattern of cellular activity in the primary visual cortex of the brain. Physiological recordings have provided some understanding of how cortical neurons responsive to visual stimulation are organized. In the macaque monkey neurons sharing common response properties are often arranged together in vertical columns that span

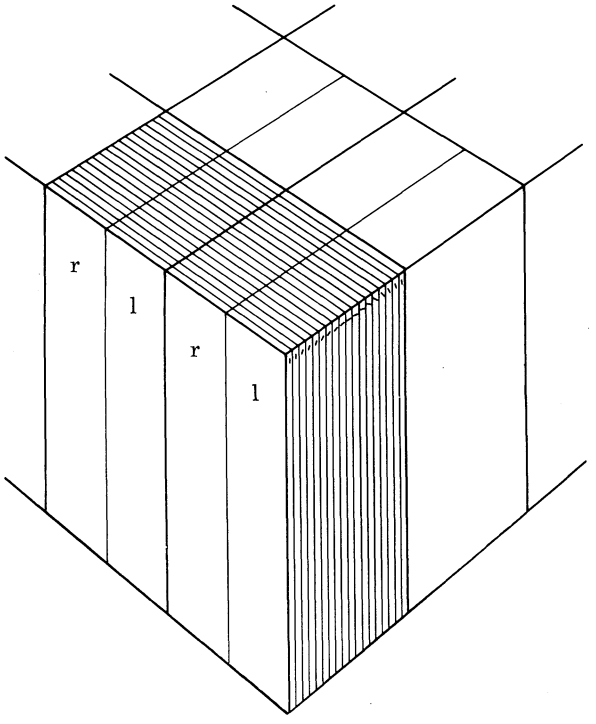


Figure 1. Diagram of the basic cortical module, from Hubel & Wiesel (1977). This unit, the boundaries of which are arbitrary, contains several intersecting orientation and ocular dominance hypercolumns. For the sake of illustration the orientation columns are shown as parallel planes crossing the ocular dominance columns at right angles, but their true relation is still unknown.

the cortex from pia to white matter. For example, cells driven most effectively by the left or right eye are grouped into 'ocular dominance' columns, and those that share a common preference for the orientation of a light–dark contour are clustered into 'orientation' columns (Hubel & Wiesel 1962, 1968, 1974*a*, *b*). Tangential microelectrode penetrations through the cortex have shown that orientation revolves through 180° every millimetre or so, and that ocular dominance shifts through both eyes over about the same distance. With approximately a 2 mm displacement through the cortex, the aggregate position of receptive fields drifts to a new, adjacent position in the visual field. This coincidence led Hubel & Wiesel (1977) to propose that macaque striate cortex consists of small identical units, each containing a few sets (hypercolumns) of each stimulus variable, devoted to analysing a given proportion of the visual

field. Such a unit is depicted schematically in figure 1. Although this model is consistent with evidence obtained by physiological recordings, it is difficult to reconstruct patterns of cellular organization over a wide area of cortex by sampling single cells in long electrode penetrations. Anatomical techniques are required to determine the exact pattern and shape of columns that make up the cortical module. For the ocular dominance columns this has been accomplished by taking advantage of the fact that left and right eye afferents from the lateral geniculate nucleus (l.g.n.) are segregated in layer IV of the cortex. Injection of a radioactive tracer into one eye (Wiesel *et al.* 1974) or placement of lesions in single lamina of the geniculate body (Hubel & Wiesel 1972) labels bands of geniculate terminals in the cortex that form the anatomical basis of the physiological eye dominance columns. They consist of parallel slabs in layer IV, about 400 μm wide, much as shown in figure 1.

Anatomical demonstration of the pattern of orientation columns has been more difficult because their structural basis is unknown. Some progress has been made by using the [$^{14}$C]2-deoxyglucose method (Kennedy *et al.* 1975, 1976) to map them. Hubel *et al.* (1978) exposed monkeys to moving vertical stripes to stimulate selectively cells tuned to vertical. The resulting radioautographs showed a puzzling, elaborate pattern of columns bearing no clear relation to the ocular dominance columns. One limitation of this experiment was that only a single orientation could be tested in a given monkey, because only a single label, carbon 14, was available. The question was left unresolved whether columns for different orientations might run parallel, as suggested in figure 1, or perhaps criss-cross, or form a more complicated mosaic. Nor was it possible, with only one label, to test how columnar systems that may exist for other stimulus variables, such as colour, spatial frequency, or directional selectivity are organized in the cortex.

After the development of the 2-deoxyglucose technique, interest turned to other methods that might be used to map metabolic activity in the brain. In 1978 Wong-Riley proposed that levels of cytochrome oxidase, a mitochondrial enzyme involved in oxidative phosphorylation, might be sensitive to long-term changes in neuronal activity. In the cat, she found that unilateral destruction of cochlear hair cells resulted in loss of cytochrome oxidase staining in ipsilateral brainstem auditory relay nuclei (Wong-Riley *et al.* 1978). In the visual system, changes were reported in the l.g.n. and cortex after monocular suture or enucleation (Wong-Riley 1979). Finally, in the somatosensory system of the mouse, the plucking of single rows of whiskers reduced cytochrome oxidase staining in corresponding rows of barrels in the posteromedial barrel subfield (Wong-Riley & Welt 1980). This work established that cytochrome oxidase levels reflect, on a more long-term basis than fluctuations in glucose uptake, relative levels of neuronal activity.

Our original purpose was to compare laminar patterns of cytochrome oxidase staining and deoxyglucose uptake in macaque striate cortex. Previous studies had shown most intense deoxyglucose uptake in cell sparse (IVb) and cell rich (IVc, VI) layers (Kennedy *et al.* 1976; Hubel *et al.* 1978). We hoped that study of the laminar distribution of cytochrome oxidase, another metabolic label, might explain why these particular cortical layers label preferentially with deoxyglucose.

In the first monkey tested for cytochrome oxidase staining we noticed that enzyme activity in the upper layers of cortex was organized into a regular pattern of patches.† This monkey was a normal animal, never exposed to any special visual pattern biased towards any particular

† While this manuscript was in preparation Dr David Hubel informed me that in 1978 he received a letter from Dr Margaret Wong-Riley describing the existence of cytochrome oxidase patches in squirrel monkey visual cortex.

orientation or eye, that might have induced a pattern of cytochrome oxidase staining to form in striate cortex. While differences in the intensity of cytochrome oxidase staining between layers was expected, a pattern within a single cortical layer was surprising. Until then, no other stain had ever revealed a pattern within a cortical layer in normal macaques, except the reduced silver Liesegang method. It showed a system of alternating dark and light bands in layer IV that were successfully correlated with the ocular dominance columns (LeVay *et al.* 1975).

We therefore set out to investigate this regular, patchy distribution of cytochrome oxidase staining in macaque striate cortex. The patches were labelled preferentially by stains for acetylcholinesterase (AChE), lactate dehydrogenase, succinate dehydrogenase, and myelin, in addition to cytochrome oxidase. The appearance of the patches was compared in a variety of primates; in non-primates they were absent. A direct input from the l.g.n. to the patches was traced by anterograde transport of horseradish peroxidase (HRP). To determine the functional significance of the patches their relation with the ocular dominance columns and orientation columns was investigated by using transneuronal [$^{3}$H]proline radioautography and [$^{14}$C]2-deoxyglucose radioautography. The effects of eye removal and eyelid suture upon cytochrome oxidase and AChE staining were compared. Patches were discovered to be present in the representation of the optic disc and temporal crescent where ocular dominance columns are absent. Finally, the appearance of the patches in foetal monkeys was studied.

Preliminary accounts pertaining to aspects of this work have been published elsewhere (Horton & Hubel 1980*a*, 1980*b*, 1981). In addition, a patchy distribution of cytochrome oxidase staining in monkey striate cortex has been reported by Humphrey & Hendrickson (1980) and Hendrickson *et al.* (1981).

## 2. Materials and methods

This report is based on studies in 20 monkeys: 15 macaques, three squirrel monkeys and two owl monkeys. To conserve, as many procedures and techniques as possible were combined in each experiment. These are summarized in table 1. The term 'juvenile' refers to monkeys aged between 1.5 and 2 years and that weighed 2–3 kg. They were essentially adult with respect to their visual system. In addition, cytochrome oxidase staining was examined in two cats monocularly sutured at 28 d and killed at 1.5 years, and in a series of normal animals: two cats, two mice and one of each of the following: rat, squirrel, rabbit, mink, tree shrew, bushbaby and baboon.

Four monkeys received horseradish peroxidase (HRP) injections into the lateral geniculate body (l.g.n.) in both hemispheres. The animals were anaesthetized and prepared for electrophysiological recordings following standard procedures. The lateral geniculate was found by recording with a tungsten electrode while stimulating with small spots of light in the visual field. A top-loading advancer was used that permits interchange of electrodes without moving the position of the guard tube in the brain. After the appropriate site in the geniculate was located, a glass micropipette containing 20% (by mass) HRP in Tris-KCl buffer solution was substituted for the tungsten electrode and the injection site verified by recording again. HRP was then delivered iontophoretically using 0.2 μA for 60–100 min. Animals were then resuscitated and allowed to survive for 36–42 h before perfusion.

Two monkeys received an eye injection under anaesthesia of 2 mCi 2,3[$^{3}$H]proline (specific activity, 23.7 Ci mmol$^{-1}$) dissolved in 20 μl of saline. The tracer was delivered into the vitreous

TABLE 1.

| | species | procedure | age at experiment | survival time | Techniques in visual cortex: cytochrome oxidase | SDH LDH | myelin | AChE | HRP | ARG | 2DG | Nissl | figures |
|---|---|---|---|---|---|---|---|---|---|---|---|---|---|
| (1) | *M. fascicularis* | normal | juvenile | — | X | | | | | | | X | 22 |
| (2) | *M. fascicularis* | normal | juvenile | — | X | | | | | | | X | 6, 7, 10 |
| (3) | *M. fascicularis* | normal | adult | — | X | X | | | | | | X | |
| (4) | *M. mulatta* | normal | adult | — | X | X | X | X | | | | X | 3, 4, 5, 8, 11 |
| (5) | *M. mulatta* | normal | adult | — | X | | | | | | | X | |
| (6) | *S. sciureus* | normal | adult | — | X | | | | | | | X | 14 |
| (7) | *S. sciureus* | normal | adult | — | X | | | | | | | X | |
| (8) | *A. trivirgatus* | normal | adult | — | X | | X | | | | | | 9 |
| (9) | *M. fascicularis* | eye injection | juvenile | 14 d | X | | | | | X | | | 23 |
| (10) | *M. mulatta*† | eye injection | adult | 7 d | X | | | | | X | | X | 27, 30, 39, 40 |
| (11) | *S. sciureus* | eye removal | adult | 48 h | X | X | | X | | | | X | |
| (12) | *M. fascicularis* | eye removal | juvenile | six months | X | | | X | | | | X | 24, 25, 26, 28, 29 |
| (13) | *A. trivirgatus* | HRP injection | adult | 40 h | X | | | | X | | | X | 16, 17, 18 |
| (14) | *M. fascicularus* | HRP injection | juvenile | 42 h | X | | X | X | X | | | | 2 |
| (15) | *M. mulatta* | lid closure HRP injection | adult | four months 36 h | X | | | X | X | | | | |
| (16) | *M. fascicularis* | lid closure HRP injection | juvenile | six months 40 h | X | | | X | X | | | | 19, 20, 21, 32, 33, 34, 35, 41, 42 |
| (17) | *M. fascicularis* | eye removal | juvenile | 18 d | X | | | | | | X | | 38, 43, 44 |
| (18) | *M. mulatta* | normal | E-144 | — | X | | | | | | | X | 45 |
| (19) | *M. mulatta* | normal | E-142 | — | X | | | | | | | X | |
| (20) | *M. mulatta* | normal | E-143 | — | X | | | | | | | X | 46, 47 |

† Right eye injured by isotope injection.

body through a 27.5 gauge needle inserted through the bluish portion of sclera posterolateral to the limbus.

Two monkeys were monocularly deprived of vision by trimming the lid margins and suturing them together under anaesthesia.

Some animals were fixed by intravascular perfusion after receiving a lethal dose of sodium pentobarbital. In other instances, specimens were donated to this study and could be fixed only by immersion. Usually a combination of aldehydes was used, 2% or 2.5% (by volume) glutaraldehyde, 1% (by volume) paraformaldehyde in 0.1 M phosphate buffer solution. If the tissue was also being processed for radioautography 10% (by volume) buffered formol-saline was preferred. Immediately after fixation the tissue was blocked and frozen, by use of a method based on the flat-mount technique of Tootell *et al.* (1981). After dissection the tissue was laid cutting surface down against a plastic coated glass slide and covered with a gently applied slurry pack of powdered dry ice and ethanol wrapped in polyethylene. This treatment tended to flatten the block so that large tangential sections were obtained, therefore patterns could be readily seen over a wide area of tissue. The number of sections that had to be cut was also greatly reduced. Furthermore, rapid freezing was usually effective in avoiding artefact that often occurs when tissue is frozen without cryoprotection. Blocks were then cut at 40 μm, unless otherwise specified, on a freezing microtome and processed for one of the following:

(1) *Cytochrome oxidase histochemistry.* Sections were air dried on gelatin-coated slides and incubated in a solution containing 50 mg diaminobenzidine, 30 mg cytochrome C (type III, Sigma), and 20 mg catalase per 100 ml of 0.1 M phosphate buffer, pH 7.4 (Seligman *et al.* 1968). Sections were usually reacted for 2–8 h, although occasionally longer times were required for well fixed tissue. Control sections incubated in the presence of sodium cyanide (0.01 M) showed complete inhibition of reaction product formation.

(2) *Succinate and lactate dehydrogenase histochemistry.* Activity of these enzymes was demonstrated by the reduction of nitrobluetetrazolium (Nachlas *et al.* 1958; Fahimi & Karnovsky 1966). Sections were reacted while floating in solution.

(3) *Acetylcholinesterase histochemistry.* Free-floating sections were reacted according to the procedure of Karnovsky & Roots (1964) by using acetylthiocholine iodide as substrate. Tetraisopropylpyrophosphoramide (iso-OMPA) was included in the incubation solution to exclude pseudocholinesterase activity. Specificity for acetylcholinesterase (AChE) activity was assured by processing control sections either in the absence of substrate or in the presence of Burroughs-Wellcome 284c51, a specific inhibitor of acetylcholinesterase (Bayliss & Todrick 1956).

(4) *Myelin stain.* The Jebb–Woolsey method (1977) was applied to mounted frozen sections. It was necessary to keep the sections in haematoxylin-$Li_2CO_3$ longer than recommended to stain the upper layers of cortex satisfactorily.

(5) *Radioautography.* Sections intended for [$^3$H]proline radioautography were cut at only 25 μm, mounted on slides, dried and defatted, coated with Kodak NTB-2 emulsion and exposed for six weeks (Cowan *et al.* 1972).

(6) *HRP histochemistry.* Free-floating tissue sections were reacted with tetramethylbenzidine (Mesulam 1978), mounted, dehydrated, coverslipped and viewed in lightfield illumination, or in a darkfield illumination through crossed polaroid filters.

(7) *2-Deoxyglucose radioautography.* For this method sections were cut on a cryostat at −25 °C and processed according to standard procedures (Kennedy *et al.* 1975) except that

overheating of coverslip mounted sections was avoided so that after radioautography tissue could be processed for cytochrome oxidase histochemistry.

In addition, occasional sections from some animals were stained with cresyl violet, sometimes after being processed first for cytochrome oxidase, HRP or AChE activity.

## 3. Results

### (*a*) *Patches: a new cytoarchitectonic feature of monkey visual cortex*

In this section the basic anatomy of the patches is described, with particular emphasis on their pattern, laminar organization, and microscopical appearance. The cytochrome oxidase stain was relied upon chiefly, but other histochemical and structural stains were also used. The material presented is based upon nine monkeys (numbers 1, 2, 3, 4, 5, 7, 8, 11 and 14).

#### (i) *The cytochrome oxidase patches in coronal and tangential section*

A coronal section through macaque striate cortex stained with cresyl violet is shown in figure 2*a*, plate 1. An adjacent section in figure 2*b* stained for cytochrome oxidase shows a distinctive laminar pattern of enzyme activity. The white matter, composed mostly of fibres poor in mitochondria, stains very weakly. Layer VI, corresponding to a cell-dense layer in the Nissl, is rich in cytochrome oxidase activity. By contrast, layer V, a relatively cell sparse zone, stains poorly for the enzyme. Layer IVc is obvious as a thick band of intense cytochrome oxidase activity running through the middle of the cortex; the lower border is sharply defined. Lund (1973) has divided layer IVc into two sublayers: IVc$_\alpha$ and IVc$_\beta$. In the cytochrome oxidase stain they can usually be distinguished in tangential section, but are more difficult to see in coronal section. The upper border of layer IVc blends into IVb, which appears as a lighter region just above. Layer IVb is separated from layer III by layer IVa, which is visible as a thin strip of dark cytochrome oxidase staining. Layers II and III, which show moderate cytochrome oxidase staining, are separated from layer I by a very narrow band of light cytochrome oxidase activity. This band, of unknown significance, is also apparent in the Liesegang and Nissl stains, where it corresponds to a thin palisade of cell bodies at the layer I–layer II interface. Layer I itself appears well stained in figure 2*b* but this is artefactual. Tissue edges tend to stain more darkly because of enhanced penetration of reagents during incubation. If one eliminates the tissue edge by embedding the block before sectioning, layer I appears pale.

Our first interest was to compare cytochrome oxidase staining with 2-deoxyglucose uptake in the cortex. According to Hubel *et al.* (1978), layer IVb labels intensely in deoxyglucose radioautographs. In the cytochrome oxidase stain layer IVb appears relatively pale, probably because of the high concentration of fibres it contains. This difference in layer IVb indicates that layers that preferentially accumulate [$^{14}$C]2-deoxyglucose-6-P are not necessarily rich in cytochrome oxidase, although both metabolic labels are thought to reflect neuronal activity.

When the geniculate projection to the cortex was examined a clue to the laminar pattern of cytochrome oxidase staining was found. Figure 2*e* contains a darkfield radioautograph of cortex made after eye injection with [$^3$H]proline. When this section is aligned with figure 2*c*, *d* it is apparent that layers IVc, IVa and VI, which receive a direct projection from the l.g.n., stain most intensely for cytochrome oxidase. Thus while relative staining of this enzyme is related to neuronal activity, it is also likely to have a direct structural basis in the wiring of striate cortex.

In figure 2*b* cytochrome oxidase staining is clumped into vertical columns, most prominent in layers II and III but also apparent in IVb. These columns could be long parallel slabs like the ocular dominance columns or a mosaic of pillars cut in cross section. To get an *en face* view of their pattern, tangential sections were cut from another normal monkey and stained for cytochrome oxidase. Figure 3, plate 2 shows a section through the right operculum passing mostly through layers II and III. A regular pattern of small patches is visible. Although there is some variety in shape, the typical patch is formed like an oval or ellipse, about 250 μm long by about 150 μm wide. Each is aligned along its major axis into rows spaced about 350 μm apart. These rows begin at right angles to the 17–18 border (vertical meridian) and curve to run roughly parallel to the horizontal meridian. Along a given row the patches are spaced about 550 μm apart, but often the end of one patch merges into the beginning of the next, forming long beaded strips. In places, the patches in adjacent rows appear to be aligned, and form a second set of crossing rows spaced about 550 μm apart. Both sets of rows show frequent breaks and irregularities, resulting in a complicated, swirling array. Given the spacing between rows, one can estimate there is about one patch per 0.2 $mm^2$ (0.550 mm by 0.350 mm) of cortex.

The cytochrome oxidase staining in figure 3 is continuous, with regular patches of higher staining density. The limits of each patch is poorly defined. As mentioned above, the patches along a given row often appear confluent, especially deep in layer III where they almost merge as background staining between patches increases. This accounts for some of the unevenness of staining in figure 3, as the section grazes through different depths in layers II and III. Neighbouring patches in adjacent rows occasionally appear paired together as doublets, with slightly darker cytochrome oxidase staining between them. Nevertheless, even without a densitometer it is possible to trace the pattern in figure 3 with reasonable accuracy, marking the shape of each cytochrome oxidase patch. The resulting sketch is shown in figure 4. There are 1917 patches in 373 $mm^2$, corresponding again to about one patch per 0.2 $mm^2$ of cortex.

The patches are seen most clearly in layers II and III, but they are also evident in layer VI. Originally they were reported only in these three layers (Horton & Hubel 1981) but with further study they have appeared faintly visible in optimally stained sections through layers V, IVb and I. Only in layers IVc and IVa do the patches seem absent. In figure 5, plate 3 a section cut slightly deeper than the section illustrated in figure 3, layer IVc is visible as a broad expanse of dense even staining, forming a crisp border with area 18. Elsewhere it is ringed by layer IVb (with faint patches), IVa and II and III, where patches are obvious. Examining a complete set of sections cut through the full cortical thickness, in every layer that contains patches (I, II, III, IVb, V, VI) their pattern matches precisely when superimposed in register. Thus in three dimensions each patch is actually a cylinder extending from the base of layer VI to the pial surface, interrupted twice, in layers IVc and IVa.

(ii) *Microscopic appearance of the cytochrome oxidase stain*

Sections were examined under the light microscope to determine what structures are preferentially labelled by the cytochrome oxidase stain, particularly in the patch regions. In coronal sections through layer IVc faint vertical striations are often visible in the cytochrome oxidase stain. When cut transversely these striations appear as a fine meshwork, seen in layer $IVc_\alpha$ at the botton of figure 7*a*, plate 4. This pattern is also seen in some fibre and myelin stains; its significance is unclear. A similar but much coarser reticular pattern is present in layer IVa. In this layer it corresponds to the 'honeycomb' pattern formed by axon terminals from the lateral geniculate (Weber *et al.* 1977*a*; Hendrickson *et al.* 1978). At the top of figure 7*a* about

six or seven patches are labelled, more darkly in layer III than layer II. They are better seen in figure 7*b*, a slightly higher power view through a tangential portion of layer III. At this magnification the pattern and shape of the patches appears quite irregular. The dark specks scattered throughout the section are diffusely labelled pyramidal cells. Cells of similar appearance are also present in IVb; in both layers they show a clear tendency to be clustered into the patches. Many diffusely filled pyramidal cells are also present in layers V and VI (figure 6) where they appear more randomly distributed; some of the largest are Meynert cells. In layer IVc stellate cell bodies show moderate cytochrome oxidase activity.

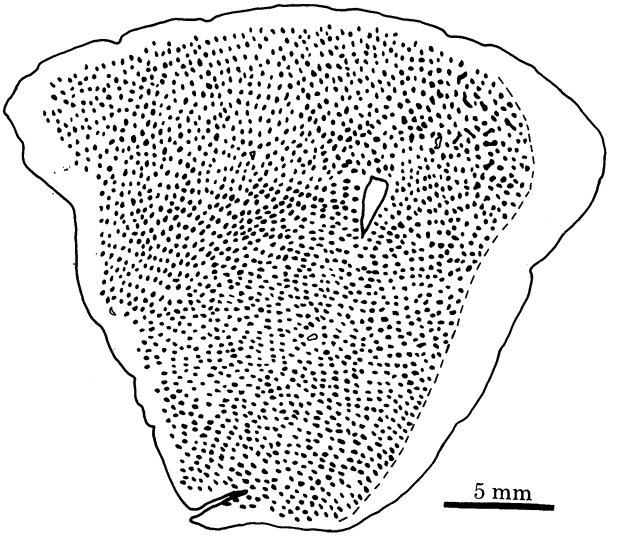


FIGURE 4. Sketch of the cytochrome oxidase patches in layers II and III from the section illustrated in figure 3. 1917 patches are present in 373 mm² (one patch per 0.2 mm²), corresponding to a total of about 6000 patches in a primary visual cortex measuring between about 1200 and 1400 mm². In fact there are probably closer to about 7000–9000 patches present, because their density is increased in peripheral binocular cortex. Although each patch in this figure is represented as a separate entity, the patches often tend to blend together, particularly along the rows spaced 350 μm apart. Dotted line at the right represents the V1–V2 border.

Although the cortex contains many cells diffusely filled with cytochrome oxidase reaction product, most of the reactive mitochondria still appear to be located in the neuropil. When the microscope condenser is racked down, cell bodies appear as pale shadows faintly silhouetted against the brown haze of labelled mitochondria. By contrast, in the l.g.n. the somata of all principal cells react intensely for cytochrome oxidase. Figure 7*c* shows the two ventral magnocellular layers and a single parvocellular layer in the l.g.n. of a normal macaque. If l.g.n. neurons have unusually high intracellular levels of cytochrome oxidase it makes sense that cortical layers receiving their axon terminals should stain darkly for the enzyme.

A view of a single cytochrome oxidase patch under oil immersion is shown in figure 7*d*. There are countless labelled mitochondria and a few diffusely filled cells, but in general rather little structural detail is visible. It is not possible to tell if labelled mitochondria are located primarily in synaptic terminals, dendrites of cortical neurons, or glia. The patches are distinguished from cortex surrounding them only by virtue of their increased density of cytochrome oxidase staining and their higher concentration of diffusely filled cells. To learn if the patches contain some special arrangement of cell bodies, synapses, or connections, other techniques must be used in conjunction with the cytochrome oxidase stain.

(iii) *Correlation with other histochemical and structural stains*

Hendrickson *et al.* (1981) have found a laminar distribution of glutamic acid decarboxylase (GAD) immunocytochemical staining in macaque striate cortex that closely parallels the laminar distribution of cytochrome oxidase activity. They also found that the cytochrome oxidase patches in layers II and III label preferentially with anti-GAD serum. This report prompted us to compare the distribution of cytochrome oxidase activity with other histochemical stains.

We began by trying stains for two other metabolic enzymes: lactate dehydrogenase (LDH) and succinate dehydrogenase (SDH). The point was to determine whether a patchy distribution is unique to cytochrome oxidase, perhaps reflecting a special arrangement of cortical processes rich in mitochondria, or whether it is a general property of enzymes involved in cellular energy production. Figure 8*a*, plate 5 shows a section stained for LDH cut slightly deeper to the cytochrome oxidase section illustrated in figure 3. Part of the section passes through layer IV where no pattern is visible; elsewhere, in layer III, patches of enzyme activity are evident. These patches of LDH staining fit in register with the cytochrome oxidase patches in figure 3; the same result was obtained in an adjacent section stained for SDH (not illustrated). This correlation between cytochrome oxidase, SDH, and LDH has been confirmed in the squirrel monkey. It is worth mentioning that LDH is a cytoplasmic enzyme, indicating that the patches consist of more than just an increased concentration of mitochondria.

---

## Description of plates 3 and 4

FIGURE 5. A tangential section cut 280 μm deep to the section illustrated in figure 3. Most of the section is occupied by layer IVc, which appears as a broad expanse of dark even staining with no patches visible. The border with V2 running between the pair of arrows appears very distinct because of the sharp drop in cytochrome oxidase activity passing from striate cortex into V2. Elsewhere, layer IVc is surrounded by layer IVb (which stains more lightly and often shows a hint of patches), layer IVa (containing the honeycomb) and layers II and III (visible at the left in this section). Layers IVc and IVa are the only two layers in which patches are not visible in normal macaque monkeys; in all other layers the patches are present and fit in register with patches in other layers. The patches are thus oval-based cylinders extending through the full thickness of the cortex, interrupted only in layers IVc and IVa. Scale = 5 mm.

FIGURE 6. In the cortex, occasional pyramidal cells react intensely for cytochrome oxidase activity; here four cells in layer V are illustrated. Numerous less strongly filled cells are visible in the background. Layers II, III, IVb, V and VI contain many diffusely filled pyramidal cells although they still constitute only a minority of the pyramidal cells in each layer. Their significance is unclear: in layers II, III, and IVb they are preferentially grouped into the patches, in layers V and VI they appear more evenly distributed. Scale = 40 μm.

FIGURE 7. (*a*) An oblique section from a normal macaque passing from layer I to layer IV$c_\alpha$. In the upper layers the cytochrome oxidase patches are visible. Just beneath, layer IVa appears as a thin strip containing a coarse weblike or honeycomb pattern. Later IVb shows weaker cytochrome oxidase activity and a few scattered densely-labelled cells. In layer IV$c_\alpha$ a fine reticular pattern is seen. Scale = 200 μm.

(*b*) Patches in layers II and III viewed at higher magnification. In the cytochrome oxidase stain they are distinguished from the surrounding cortex only by virtue of their increased enzyme activity and the greater number of diffusely labelled cells they contain. Scale ≒ 100 μm.

(*c*) View of cytochrome oxidase stained cells in the macaque lateral geniculate nucleus. The two ventral magnocellular layers and a parvocellular layer (top) are shown, separated by fibrous interlaminar zones. Principal cells in the lateral geniculate react intensely for cytochrome oxidase activity. High levels of cytochrome oxidase in geniculate neurons may account in part for the denser cytochrome oxidase staining in cortical layers receiving a direct geniculate input. Scale = 50 μm.

(*d*) A single cytochrome oxidase patch in layer III of cortex viewed under oil immersion shows numerous labelled mitochondria visible as small scattered specks. The diffuse dark background is due to labelled mitochrondria lying in different planes of focus. Little structural detail is apparent; it is not possible to determine which processes are richest in cytochrome oxidase activity. In general, cell bodies are less well labelled in the cortex than in the geniculate body. Scale = 10 μm.

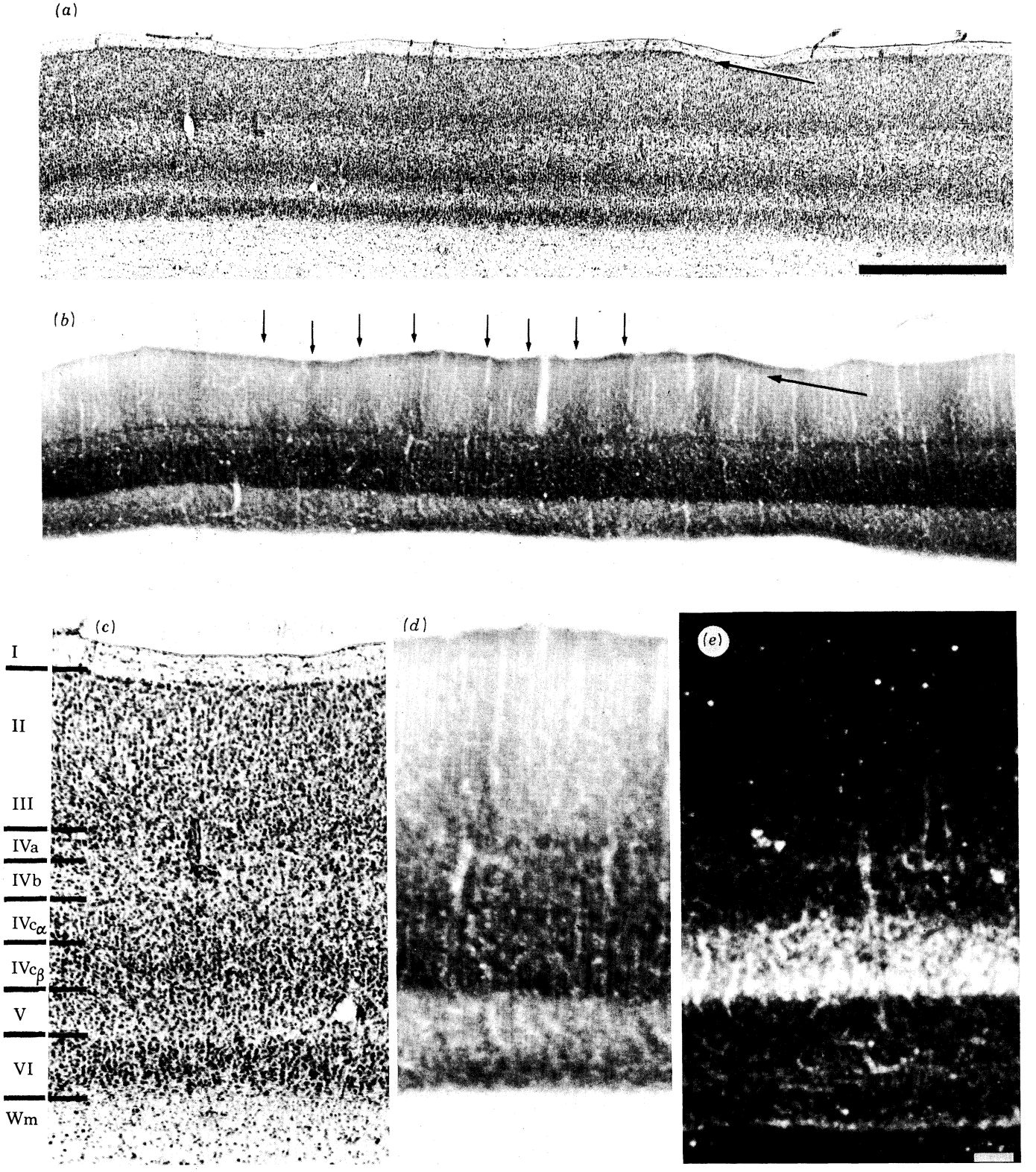


FIGURE 2. Laminar pattern of cytochrome oxidase activity compared with Nissl stain and cortical projection from lateral geniculate nucleus labelled by transneuronal radioautography.

(*a*) Coronal section through striate cortex (area 17, primary visual cortex, V1) from a normal macaque monkey stained with cresyl violet. Arrow marks a thin layer of cell bodies at interface between layers I and II which stains lightly for cytochrome oxidase activity (see corresponding arrow in *b*). Scale = 1 mm.

(*b*) An adjacent section processed for cytochrome oxidase histochemistry shows regular columns of enhanced enzyme activity spaced about 350 μm apart (arrows). Columns are most obvious in layer III, but also visible in layers II and IVb in this section. Appearance of these columns in tangential section through layer III from another macaque is shown in figure 3.

(*c*) Nissl and (*d*) cytochrome oxidase stains compared with geniculate projection to cortex labelled by eye injection with [$^3$H]proline (*e*). Darkest cytochrome oxidase staining is visible in layers VI, IVc, and IVa, all layers that receive a direct input from the lateral geniculate. Note that sharp lower border of layer IVc in the cytochrome oxidase stain matches the lower extent of proline label. Scale = 100 μm.

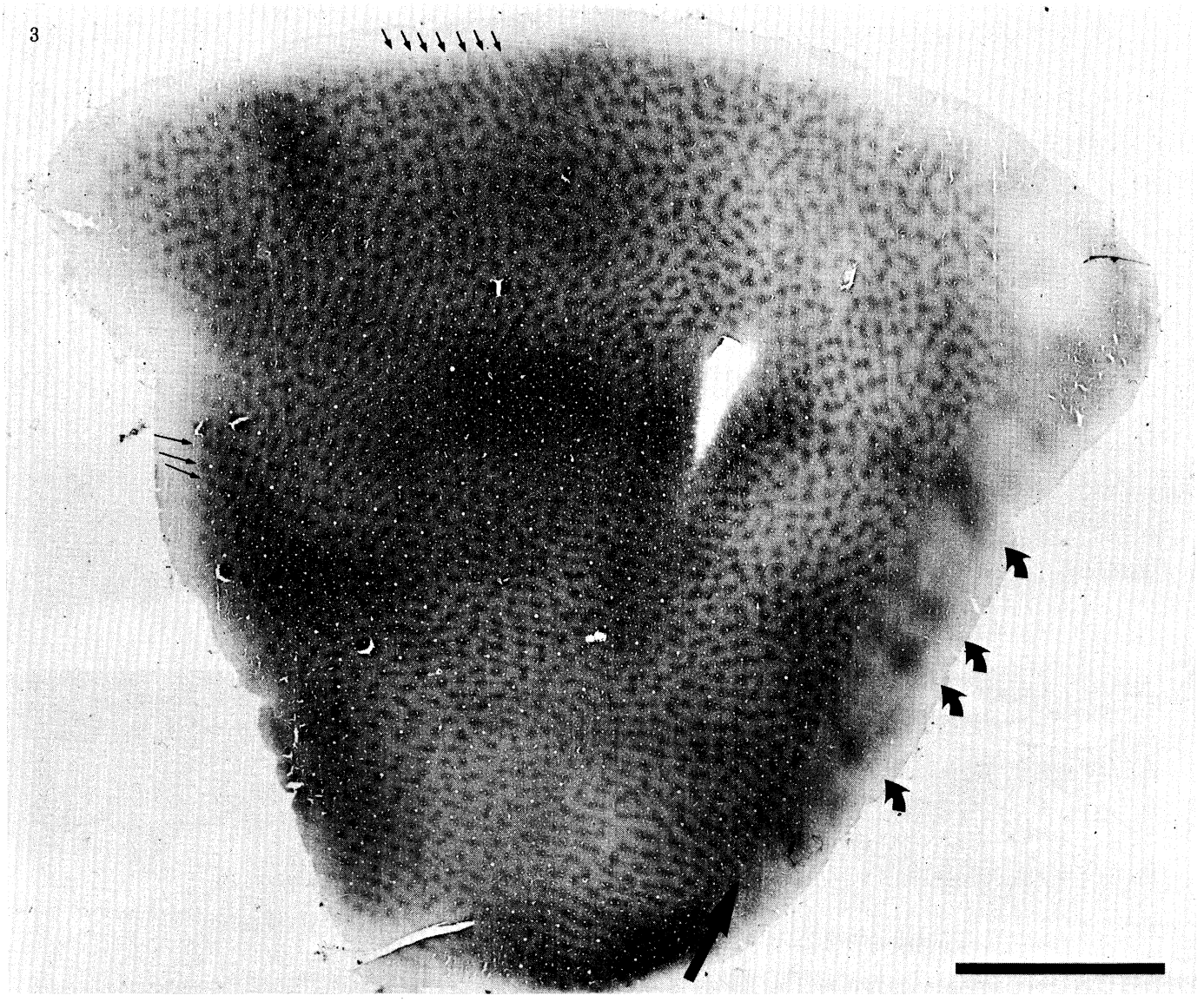


FIGURE 3. Tangential section from a normal rhesus monkey through layers II, III stained for cytochrome oxidase reveals an array of small patches, about 250 μm by 150 μm. Patches are aligned in long rows spaces about 350 μm apart which intersect the 17–18 border (small arrows) at right angles in a manner similar to the ocular dominance columns (see figure 8, LeVay *et al.* 1975). Along each row the patches partially merge, creating an impression of long beaded strips. The patches occur about every 550 μm along each row; patches in adjacent rows are often aligned, giving rise to a second set of crossing rows (three medium arrows). The V1–V2 border is clearly visible at the far right in the section, indicated by a single large arrow. In V2 patches are not present, instead there is a cruder pattern of wide slabs or stripes (four curved arrows), shown again at higher magnification in figure 11. Scale = 5 mm.

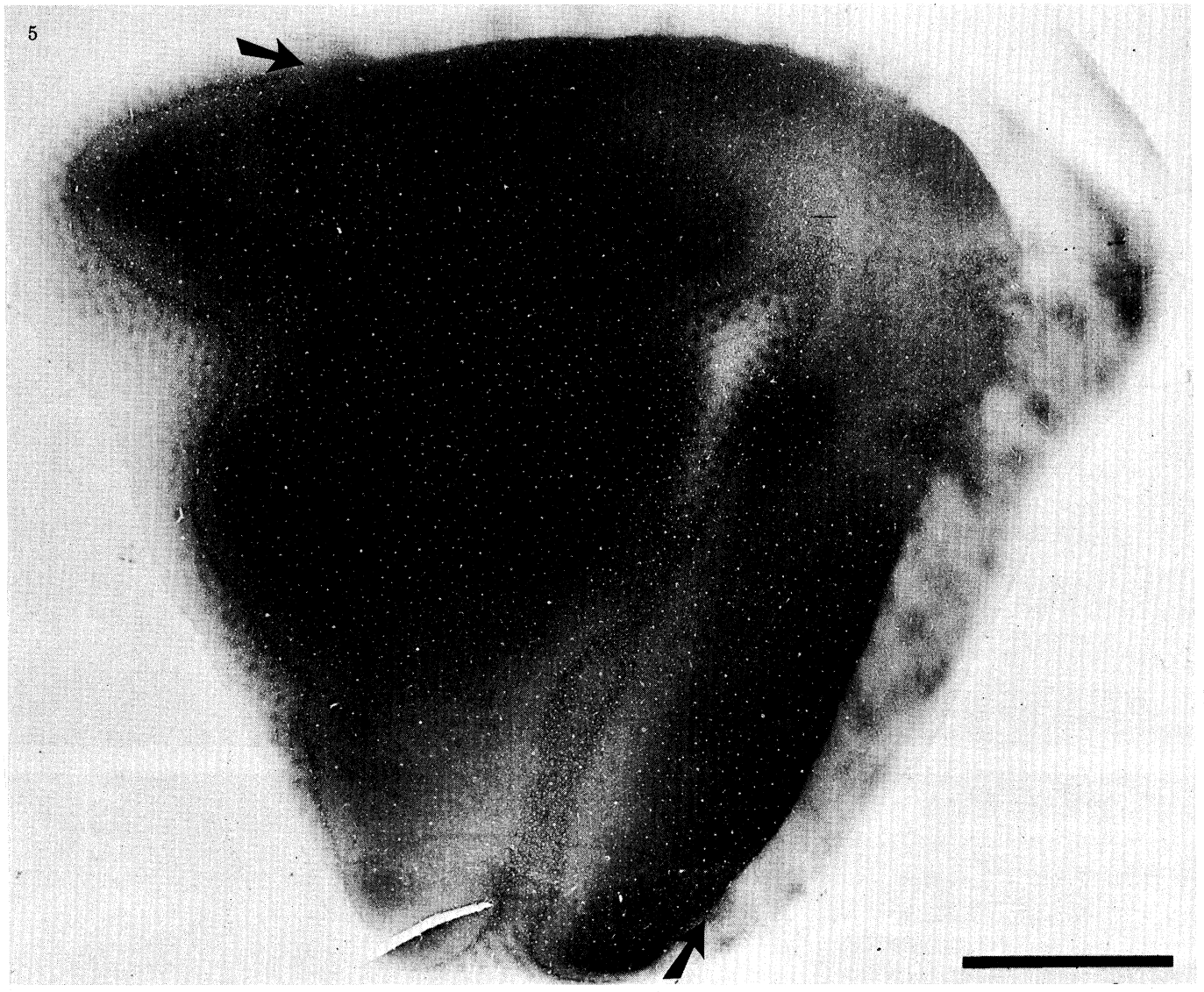


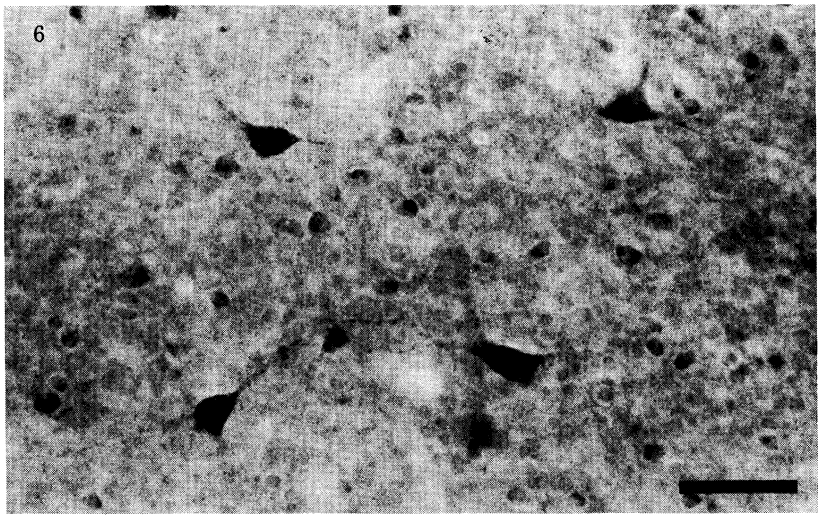


FIGURES 5 AND 6. For description see p. 210.

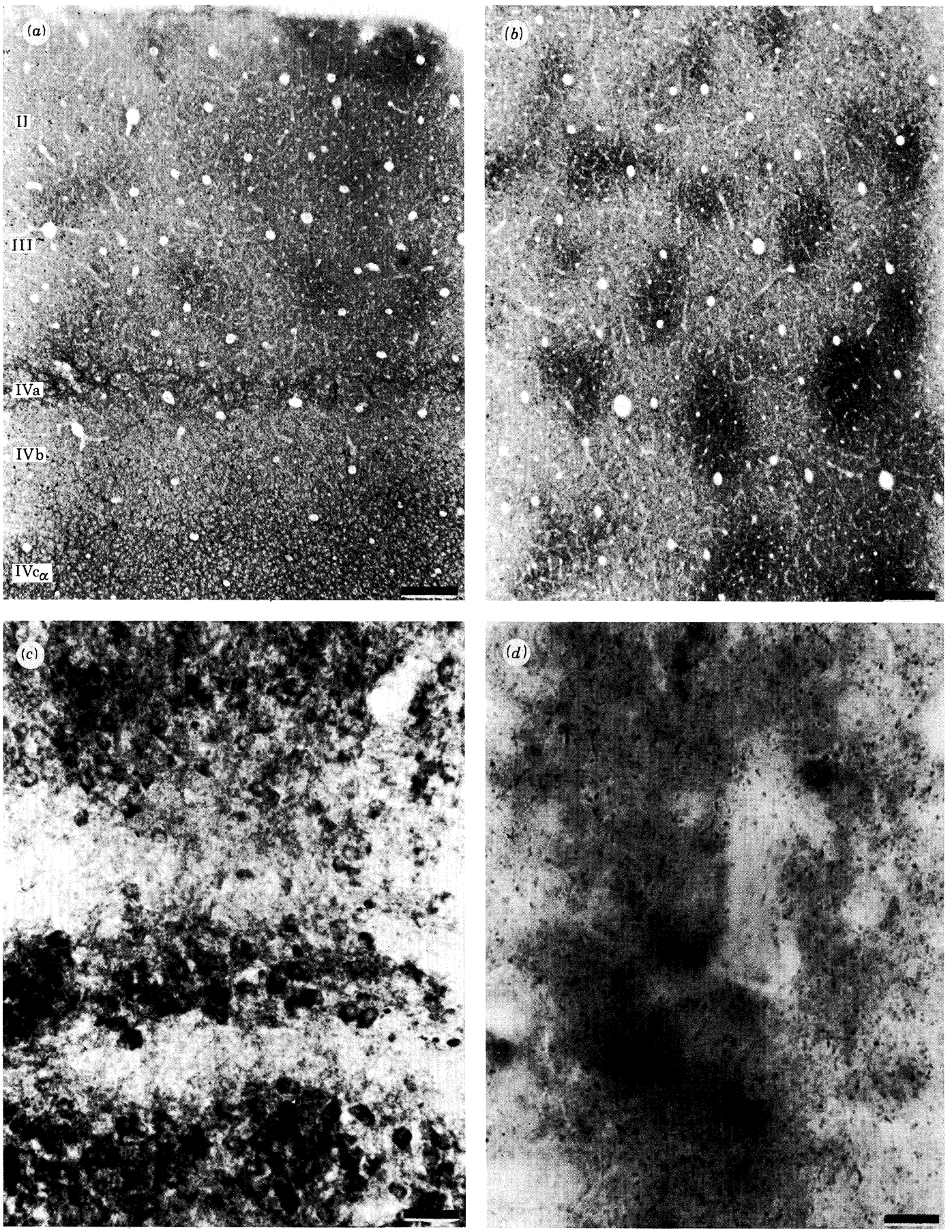


FIGURE 7. For description see p. 210.

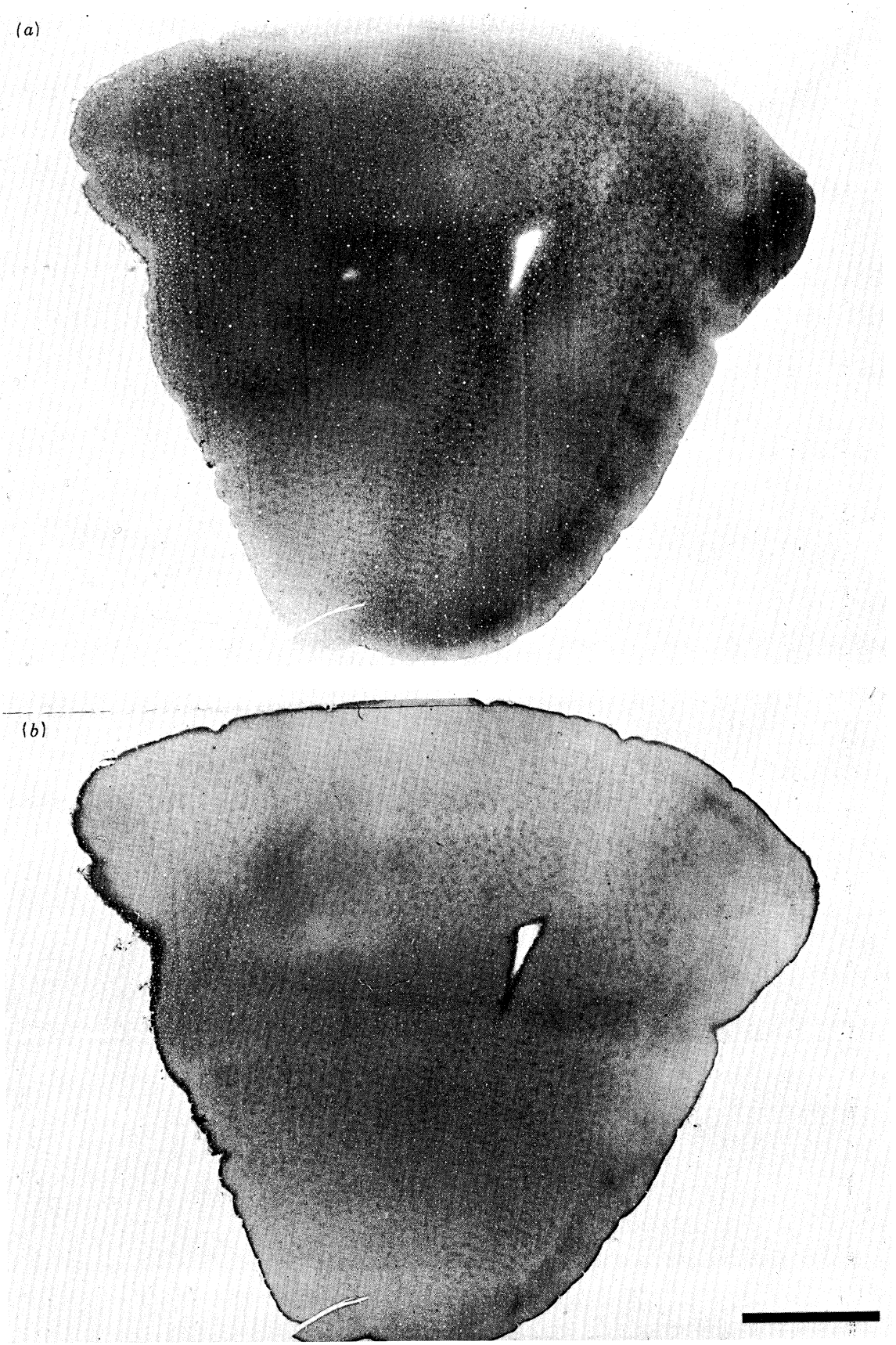


FIGURE 8. (*a*) Tangential section reacted for lactate dehydrogenase (LDH) activity from a normal macaque monkey cut from the same block as the cytochrome oxidase stained section illustrated in figure 3. Patches are visible in layers II and III; elsewhere the section passes through layer IV and no pattern is seen. Careful comparison of adjacent sections processed for cytochrome oxidase, LDH, and succinate dehydrogenase (not illustrated has demonstrated a precise match of patterns: the patches are preferentially labelled by stains for all three metabolic enzymes.

(*b*) An adjacent section cut slightly more superficially than (*a*) reacted for AChE activity shows a pattern of patches in layers II and III. These patches match exactly the patches labelled by cytochrome oxidase in figure 3. Scale = 5 mm.

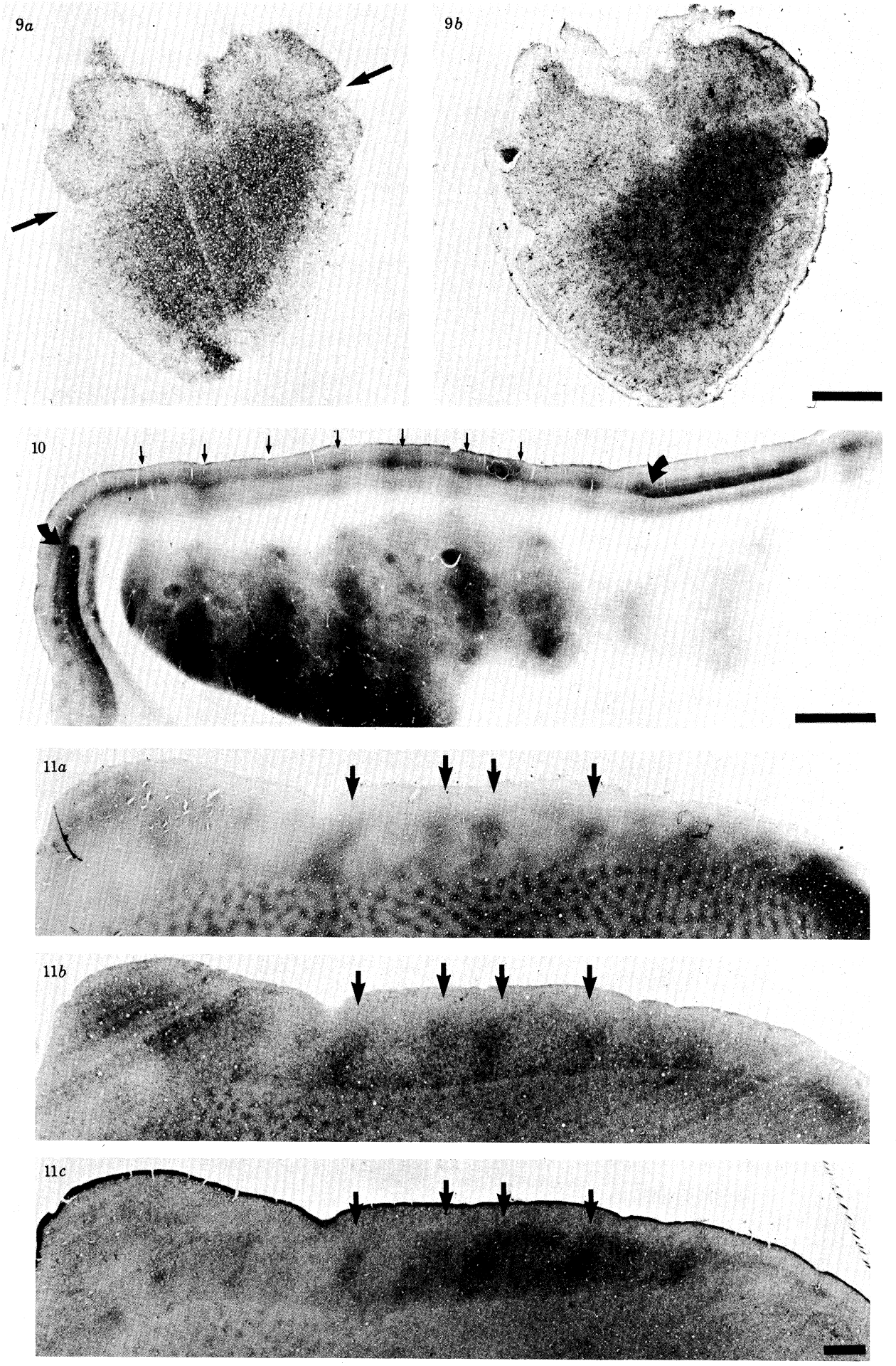


FIGURES 9–11. For description see p. 211.

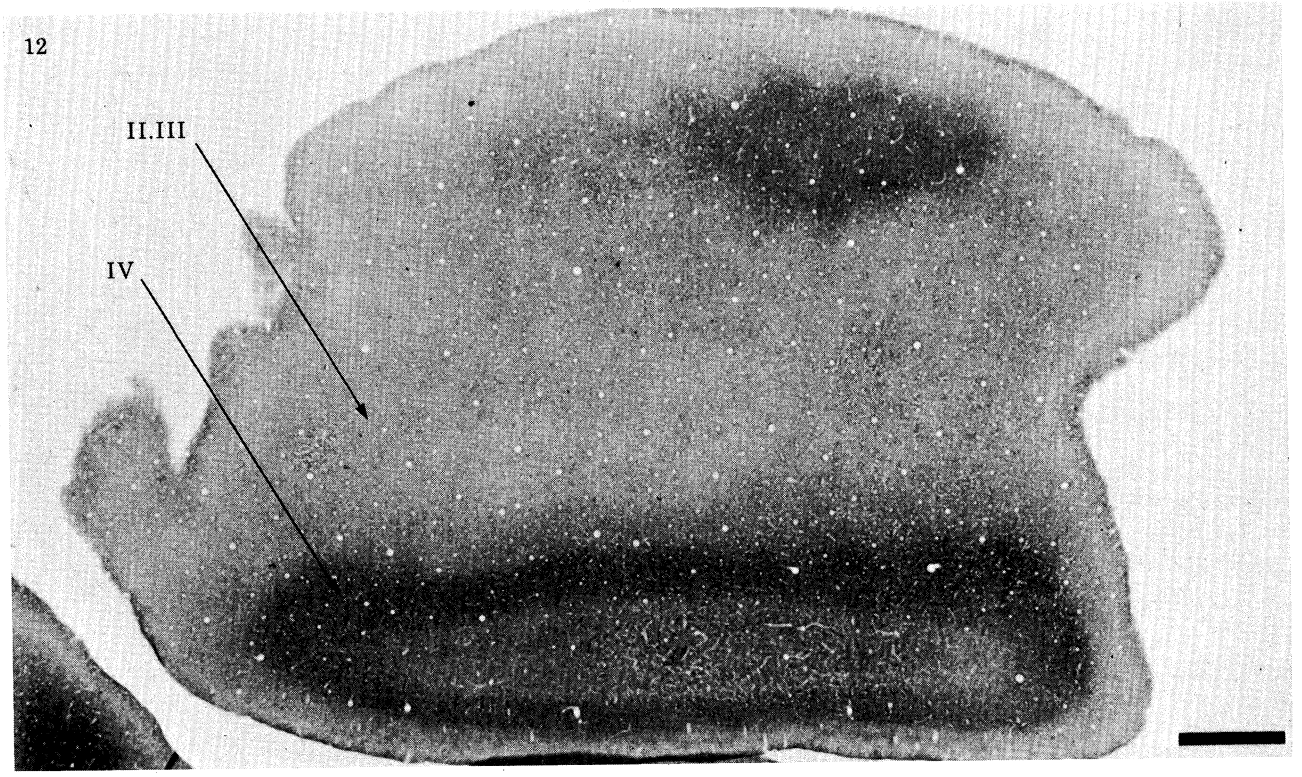


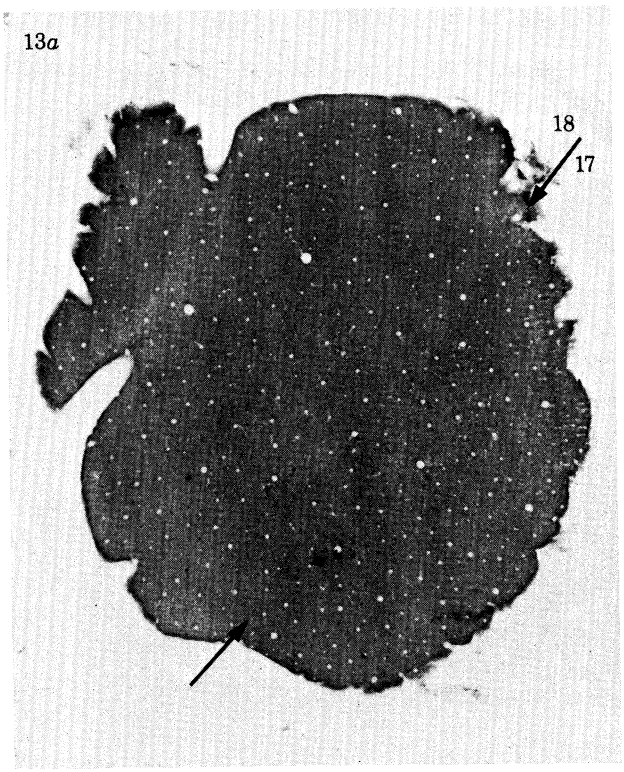


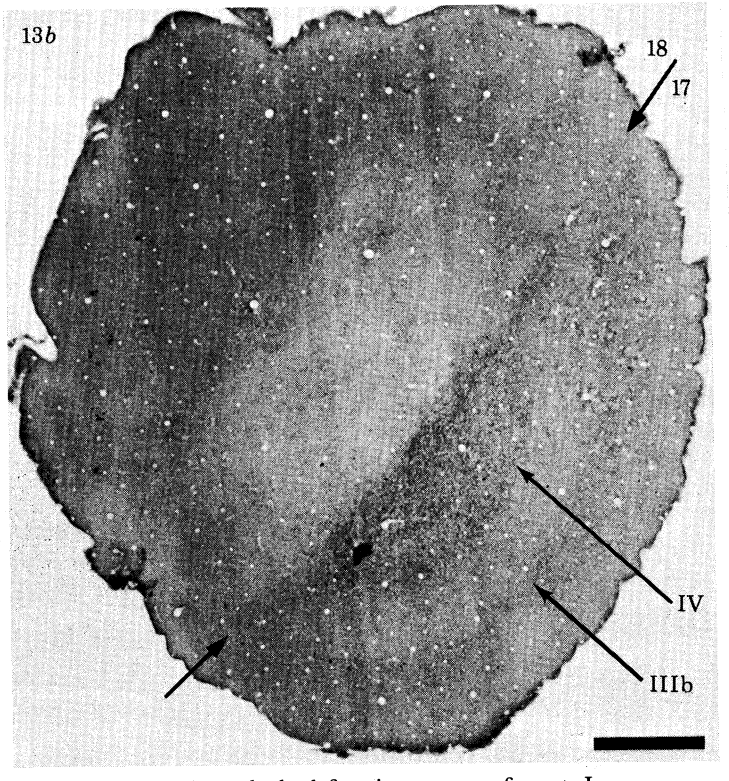


FIGURE 12. Tangential section reacted for cytochrome oxidase activity through the left striate cortex of a cat. In layers II and III no patches are present. Some faint unevenness is visible in the density of cytochrome oxidase staining, due to minor irregularities in section thickness and fixation. Scale = 1 mm.

FIGURE 13. (*a*) Cytochrome oxidase stained tangential section through the upper layers of the left occipital cortex of a normal tree shrew; medial is to the right and posterior is down. In area 17 no patches are visible.

(*b*) Another section cut 400 μm deeper from the same block. Where the section passes through layer IV the 17–18 border is easily visible. By using this section as a guide the 17–18 border was located in (*a*). So far, the cytochrome oxidase patches have not been found in a nonprimate species. Scale = 1 mm.

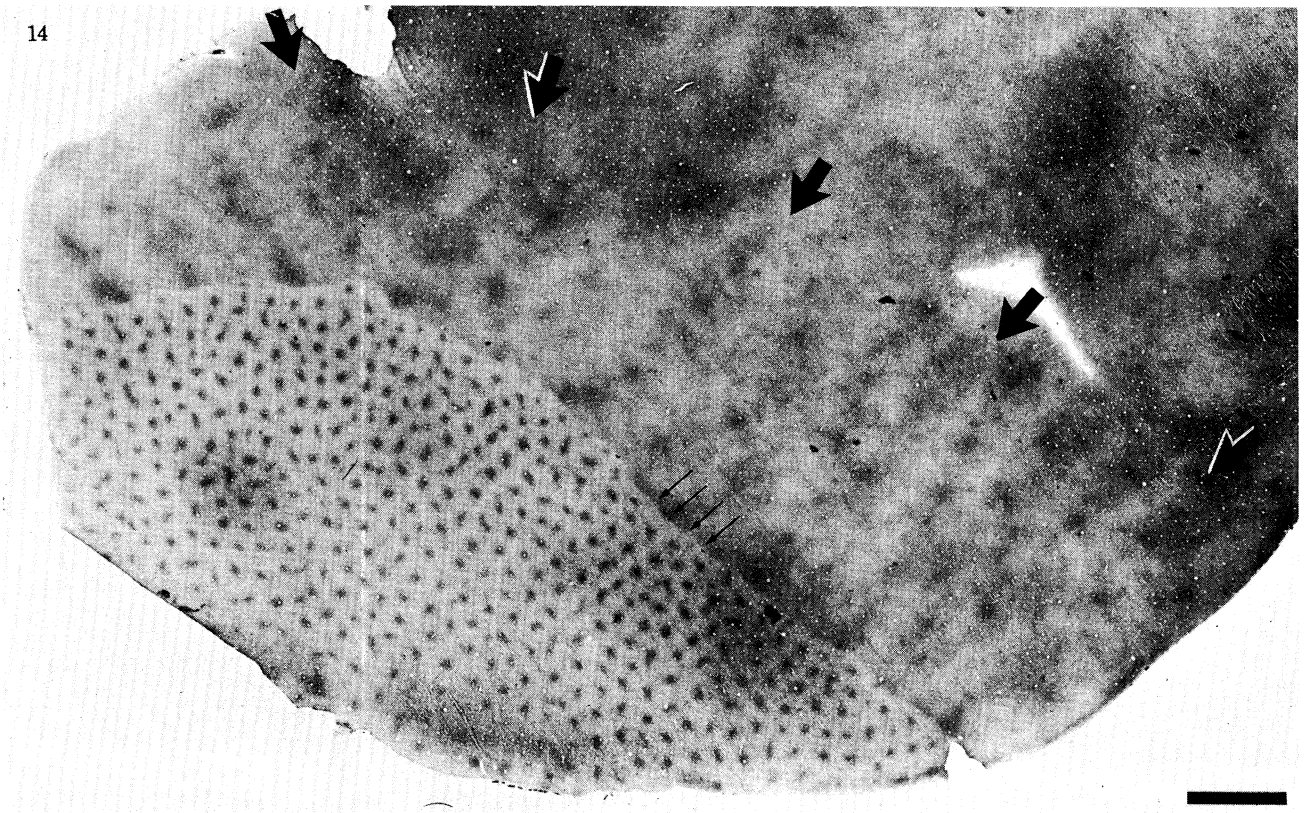


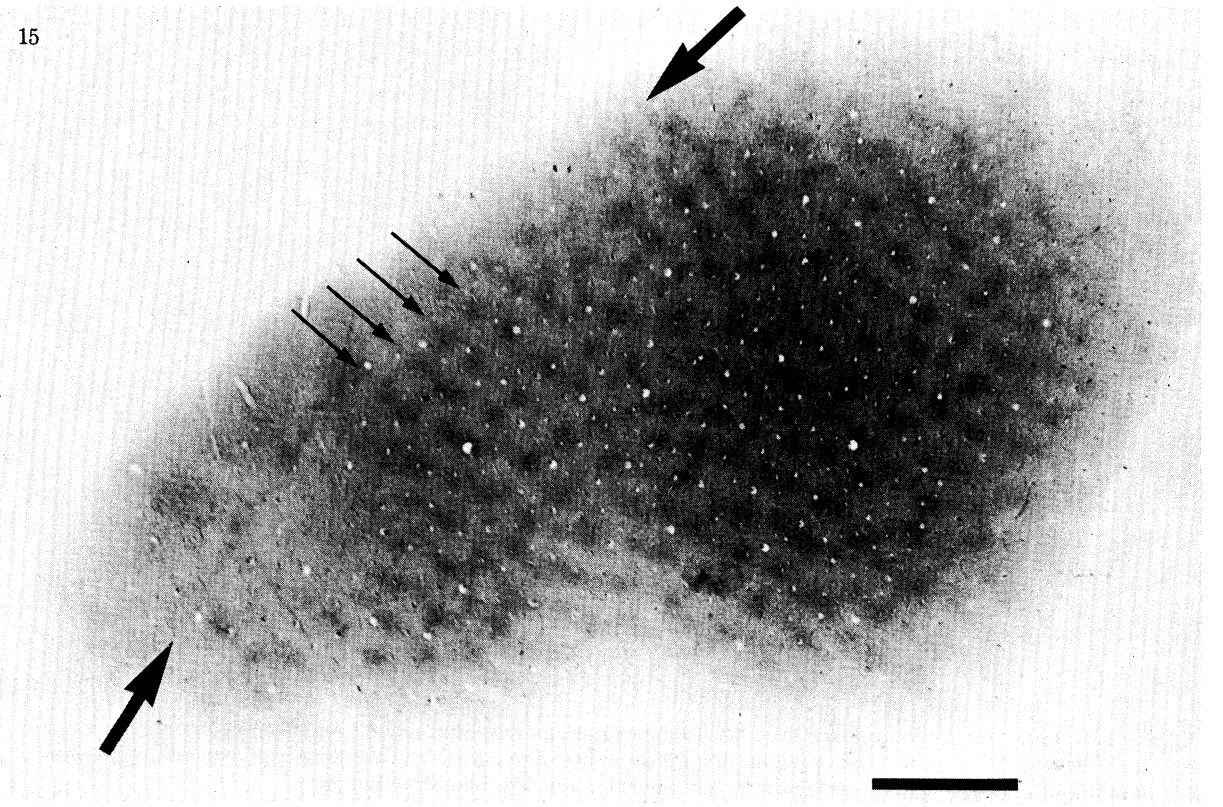


FIGURES 14 AND 15. For description see opposite.

Fitzpatrick & Diamond (1980) have studied acetylcholinesterase (AChE) staining in the geniculostriate system of the owl monkey and the bushbaby. Their published figures show a laminar distribution of AChE activity similar to the laminar pattern of cytochrome oxidase staining we have observed in these species. This suggested, as Hendrickson *et al.* (1980) found in the case of anti-GAD staining, that there might also be a correlation between cytochrome oxidase and AChE activity in tangential sections through the upper layers. Figure 8*b* shows a section stained for AChE adjacent to the section in figure 3. A distinct pattern of patches is present that matches precisely the pattern of cytochrome patches. This result has been confirmed in another normal macaque, a squirrel monkey, and the human (Horton & Hedley-Whyte 1984).

In the light microscope AChE activity in the upper layers is concentrated in fibres and beaded densities that resemble synaptic terminals. Occasionally labelled cell bodies are visible, but more often cells seem to be coated by AChE staining located either on the cell surface or in pre-synaptic processes. The source of this AChE staining is uncertain; it may arise from intracortical cholinergic neurons, or a subcortical projection. Fitzpatrick & Diamond (1980)

## Description of plates 6 and 8

FIGURE 9. (*a*) Section through the upper layers of visual cortex from a normal owl monkey treated with the Jebb–Woolsey myelin stain; the 17–18 border runs between the pair of arrows. Below, in area 17, a regular pattern of slightly darker patches of myelin staining is visible.

(*b*) An adjacent section stained for cytochrome oxidase shows patches in area 17. They appear rather faded, due to prolonged fixation of the tissue block in formalin. Despite the faint appearance of the patches in (*a*) and (*b*) it has been possible to compare their patterns to determine that they match. The patches in striate cortex are thus labelled preferentially by stains for cytochrome oxidase, LDH, SDH, AChE, and myelin. Scale = 2 mm.

FIGURE 10. Cytochrome oxidase stained section through right visual cortex of a normal macaque monkey; medial is to the left and the anterior lip of the operculum where it forms the lunate sulcus is visible above. Most of the section passes through V2 (the V1–V2 border is marked by curved arrows), tangentially grazing layers V and VI to reveal a series of regular parallel stripes of darker enzyme staining. Above, where these stripes are cut in cross-section, they are marked by small arrows. The stripes are about 0.8 mm wide, spaced about every 1.6 mm, and intersect the V1–V2 border at right angles.Within and between each strip a complicated, irregular pattern of cytochrome oxidase staining is also seen. Scale = 2 mm.

FIGURE 11. The stripes in V2 are labelled preferentially by stains for cytochrome oxidase, AChE, and LDH activity.

(*a*) Portion from the section illustrated in figure 3, oriented sideways. The cytochrome oxidase stain reveals periodic stripes in V2 cut in cross-section; the same four bands indicated in figure 3 are again marked with arrows.

(*b*) Corresponding region from the section stained for LDH activity illustrated in figure 8*a*. The same four stripes are visible, also marked by arrows.

(*c*) The same region from an adjacent section stained for AChE. Again the same four stripes are preferentially labelled (arrows). Scale = 1 mm.

FIGURE 14. Pattern of cytochrome oxidase staining in visual cortex of a normal squirrel monkey. This section was flattened while freezing to obtain a large tangential section containing a wide area of the exposed occipital cortex. In area 17, below and to the left, cytochrome oxidase patches are clearly visible. Their density is one patch per 0.22 $mm^2$ of cortex, close to the density of patches in an equivalent region of macaque striate cortex. However, patches in the squirrel monkey are smaller, rounder, more punctate and clearly separated than in the macaque; they do not form the long rows of semi-confluent patches characteristic of primates with well developed ocular dominance columns. Nevertheless, there is some suggestion that in the squirrel monkey some patches are grouped into rows (small arrows), oriented perpendicular to the 17–18 border. In V2, more widely spaced parallel stripes, also seen in the macaque, are visible. They are superimposed on a complex pattern of irregular fluctuations in cytochrome oxidase staining. The anterior border of V2 is marked by a series of large arrows. Scale = 2 mm.

FIGURE 15. Tangential section through layers II and III of striate cortex stained for cytochrome oxidase activity from a normal baboon. Patches are present, appearing quite similar to the patches in the macaque, although slightly larger. Near the 17–18 border, which passes between the pair of large arrows, rows of patches spaced about 530 μm apart can be seen; four rows are marked by small arrows. Scale = 2 mm.

report that in the l.g.n. neither enucleation nor destruction of principal cells by kainic acid injection affects AChE staining. This implies that geniculate neurons projecting to striate cortex are not associated with AChE activity.

In seeking to explain AChE activity in the cortex it is important to consider that the enzyme is not dependable evidence for cholinergic innervation. It has also been associated with neurons that use dopamine (Butcher *et al.* 1975) and noradrenaline (Palkovits & Jacobwitz 1974) as transmitters. In mapping GABAergic activity, Hendrickson *et al.* (1981) relied upon immunochemical techiques to localize GAD, the synthetic enzyme for GABA. It would be wise to repeat the present study using a monospecific antiserum for macaque choline acetyltransferase, the synthetic enzyme for acetylcholine.

The cytochrome oxidase patches have also been labelled with a stain for myelin. The first hint that this might be possible came from the animal illustrated in figure 3, a fully mature 9 kg adult rhesus monkey. It was noticed in sections dried onto slides that one could see a faint pattern of patches in the tissue even before processing for histochemistry. Because this might correspond to a special distribution of myelinated nerve fibres, the Jebb–Woolsey stain was applied to the tissue, and it yielded a faint pattern of patches (not illustrated) that matched the cytochrome oxidase patches in figure 3. The stain was repeated in another macaque, a small juvenile *Macaca fascicularis*, without success. This failure may have been because in juvenile animals, although the visual system can be considered mature in many respects, the process of myelination is not yet complete. Myelin staining was performed in a third animal, an adult owl monkey. It showed a clear pattern of patches in the upper layers (figure 9*a*, plate 6). An adjacent section (figure 9*b*) showed weak cytochrome oxidase staining because the block was post-fixed in formalin for 24 h, but it was still possible to compare the two sections and verify that the myelin patches correspond to the cytochrome oxidase patches. Finally, sections from macaque monkeys were examined with the Liesegang stain (LeVay *et al.* 1975) and faint patches, much less striking than the regular bands in layer IV, were seen in the upper layers (not illustrated).

The cytochrome oxidase, LDH, SDH, AChE, and anti-GAD stains provide evidence that the patches are richer in metabolic activity and levels of certain transmitter enzymes. Darker myelin staining suggests that the cytochrome oxidase patches have a structural basis that sets them apart from the rest of striate cortex. In a sense the prefix 'cytochrome oxidase' is misleading: one might just as well refer to 'myelin' patches or 'lactate dehydrogenase' patches. Probably in the near future the patches will be correlated with other anatomical techniques. The cytochrome oxidase stain has been relied upon principally throughout this study only because it yields such reliable results with excellent separation of absorbances. Henceforth the term 'patch' will be used without modification to refer to this structure, as yet poorly understood, that labels with each of these various methods. One hopes that as the functional significance of the patches becomes clearer, a more suitable term consistent with both their anatomical appearance and physiological properties, will be adopted.

(iv) *A pattern in V2*

In figure 3 periodic zones of darker cytochrome oxidase staining are visible in area 18 near the 17–18 border, a region corresponding to V2. In tangential sections extending further into area 18 they appear as crude parallel stripes lacking sharp boundaries, about 0.8 mm wide, spaced every 1.6 mm or so, intersecting the 17–18 border at right angles (figure 10). In the

latter respect, they are similar to the rows of patches in area 17, but overall they form a more poorly organized array. Within and between each of the stripes a complicated pattern consisting of small, irregular fluctuations in density of cytochrome oxidase activity is seen. The stripes extend through and fit in register in all layers, including layer IV, so they can be thought of as coarse slabs running through the full thickness of cortex. They also stain preferentially for LDH and AChE; in figure 11*a* the region in figure 3 that contains the slabs in V2 is shown at higher power. In adjacent sections stained for LDH (figure 11*b*) and AChE (figure 11*c*) the same slabs are visible. This pattern in V2 has also been observed by Tootell & Silverman (1981).

### (*b*) *Survey of cytochrome oxidase staining in visual cortex of non-macaque species*

Cytochrome oxidase staining in the visual cortex of a variety of species was examined to see if patches were present and how they compared in appearance with the macaque. The goal was to identify certain features shared only by species with patches, in the hope of gaining some insight into the functional role of the patches. Results are summarized in table 2.

Patches were absent in all seven non-primate species tested. A tangential section through cat striate cortex is shown in figure 12, plate 7. Layer IV appears as a prominent dark band; no patches are present in layers II and III. The animal illustrated was monocularly deprived, as discussed further in a later section, but the same finding was obtained in two normal cats.

In the tree shrew patches were also absent (figure 13). Two sections are illustrated: a tangential section through supragranular cortex (*a*) showing homogeneous staining and a deeper section (*b*) through layer IV marking the 17–18 border.

In all seven primate species tested for cytochrome oxidase staining patches were present in striate cortex. An example of the patches in the rhesus monkey was already shown in figure 3; the patches in the cynomolgus look very similar. The patches in the owl monkey are illustrated best in figure 17*b*. The squirrel monkey (figure 14, plate 8) has a very clear pattern of cytochrome oxidase patches. Compared with the macaque, they appear more punctate, slightly smaller, and generally better demarcated. The patches also tend to be rounder and more regular in shape, although many look slightly oblong or have an irregular protuberance emerging from one side. They form a highly regular square or hexagonal pattern with a remarkably constant distance between patches, about 500 μm. There is some hint that the patches are aligned in rows that approach the 17–18 border at right angles, as in the macaque. Where these rows are visible (small arrows) they curve through the patch array, an artefact caused by artificially flattening the highly curved squirrel monkey operculum. In the section illustrated, 482 patches occupy 108 $mm^2$, corresponding to one patch per 0.22 $mm^2$ of cortex, close to the density of patches in opercular cortex of the macaque. In area 18, the widely spaced parallel stripes pointed out in the macaque can be seen running perpendicular to the 17–18 border. When examined closely, the stripes and zones between are seen to contain a highly complex, irregular pattern of cytochrome oxidase staining.

In the baboon (figure 15) the patches look quite similar to the macaque except that they are slightly larger, and near the 17–18 border are organized into rows (small arrows) spaced further apart, roughly 530 μm. In the human (Horton & Hedley-Whyte 1984) the patches are very large, and less regular than in the squirrel or macaque monkey. Evidently a consistent shape or geometry is not a critical feature of the patches, because they vary considerably in appearance from species to species.

From the list of species in table 2 it is difficult to identify a single characteristic unique to the visual systems of species with patches. Species with ocular dominance columns, orientation columns, colour vision, simple and complex cells, are included on both sides of Table 2. So far the only trend to emerge is that all seven species with patches are primates. The suborder Prosimiae is represented by the galago (not illustrated). Within the suborder Simiae, patches are present in species from all three superfamilies: Ceboidea (*Saimiri*, *Aotus*), Cercopithecoidea (*Macaca*, *Papio*) and Hominoidea (*Homo*). Although 186 of 193 primate species remain untested, and more nonprimates must be screened, these results prompt me to predict that the patches will prove to be a unique, defining feature of primate striate cortex. The parallel strips of cytochrome oxidase staining in V2 also appear to be present only in primates.

TABLE 2. RESULTS OF SURVEY OF CYTOCHROME OXIDASE STAINING IN VISUAL CORTEX OF NON-MACAQUE SPECIES

| species without patches in striate cortex | number of specimens tested | species with patches in striate cortex | number of specimens tested |
|---|---|---|---|
| rat (*Rattus norvegicus*) | 2 | rhesus monkey (*Macaca mulatta*) | 3 |
| mouse (*Mus musculus*) | 2 | cynomolgus monkey (*Macaca fascicularis*) | 7 |
| ground squirrel (*Citellus tridecemlineatus*) | 1 | owl monkey (*Aotes trivirgatus*) | 2 |
| cat (*Felis catus*) | 4 | bushbaby (*Galago crassicaudatus*) | 1 |
| tree shrew (*Tupaia glis*) | 1 | baboon (*Papio papio*) | 1 |
| rabbit (*Oryctolagus cuniculus*) | 1 | squirrel monkey (*Saimiri sciureus*) | 3 |
| mink (*Mustela vison*) | 1 | human (*Homo sapiens*) | 6 |

### (*c*) *A direct projection from the lateral geniculate nucleus to the patches*

Weber *et al.* (1977*a*) were the first to report small puffs of radioautographic label in layer III of squirrel monkey cortex after injecting the l.g.n. with [$^3$H]proline. This finding was confirmed in the galago (Casagrande & Skeen 1980) and by transneuronal radioautography after eye injection in the squirrel monkey (Hubel & Wiesel 1978; Hendrickson *et al.* 1978). It has remained unclear whether this label represents a direct projection to layer III, or transneuronal transport from layer IV c to layer III, as advocated by Hendrickson *et al.* (1978). It has also remained unclear, because the cortex was cut coronally rather than tangentially in these studies, whether the puffs are long continuous bands or actually isolated patches of label. After the identification of a patchy distribution of cytochrome oxidase staining in the monkey, it seemed worthwhile to determine if these two systems, patches and puffs, might be correlated.

HRP was used as an anterograde tracer (Mesulam & Mufson 1980) because it is extremely sensitive, even superior to [$^3$H]proline, when reacted with tetramethylbenzidine (Mesulam 1978). It is also not transported transneuronally, so that distinction between a direct or transneuronal projection to the upper layers can be made. Finally, it offers the bonus of retrogradely filling the layer VI corticogeniculate projection, so that one can see whether the

labelled cells bear any special relation to the cytochrome oxidase patches in layer VI. Four monkeys were used in these experiments (numbers 13, 14, 15 and 16): one owl monkey and three macaques Two macaques were visually deprived as adults by lid suture; the effect of deprivation was not pertinent to the present results and will be treated in a later section. The peroxidase was delivered into the l.g.n. in both hemispheres of each animal using iontophoresis to achieve relatively small injections. After five of the eight injections, a pattern of patchy anterograde HRP label was seen in the upper layers of striate cortex. In the three failed cases, all macaques, the injections were too small. Two examples, one from the owl monkey and another from a macaque will be presented from the five successful cases.

(i) HRP *injection in the owl monkey*

The injection was made into the left l.g.n. straddling the border between the magnocellular layers, about 8° below the horizontal meridian at an azimuth of 6°. It was the largest injection of the series, filling most of the geniculate, with some spread of bluish reaction product into the optic radiation, perigeniculate nucleus, medial geniculate, and pulvinar (figure 16*a*, *b*, plate 9). Unlike diaminobenzidine, which usually shows a dense core of label, surrounded by a light halo, tetramethylbenzidine injection sites often appear poorly demarcated and lack a central focus. This makes it hard to be sure of the zone of actual HRP uptake and transport. In this case there was a clear possibility that structures adjacent to the geniculate were contaminated.

A clear system of patches in striate cortex is evident in figure 17*a*, a tangential section through the exposed left occipital pole processed for HRP. They are most intensely labelled in layer IV$c_\alpha$. Passing from layer IV$c_\alpha$ to IV$c_\beta$ the patches merge and labelling becomes continuous. Immediately superficial to layer IV c there is a thin label-sparse gap corresponding to layer IV b. In the owl monkey an upper tier of geniculate terminals in IV a organized into a honeycomb is absent. In layers II and III patches of label are also visible, although less clearly. In an adjacent section (figure 17*b*) stained for cytochrome oxidase the patches are obvious, particularly in layer IV$c_\alpha$. As the section passes into layer IV$c_\beta$ staining becomes more homogeneous and they appear very faint. There is a thin light gap corresponding to layer IV b; even in this layer faint patches are visible. When the patches in the two adjacent sections (figure 17*a*, *b*) were aligned and compared their patterns fitted in perfect register, both in IV$c_\alpha$ and the upper layers.

In area 18, which is coextensive with V2 in the owl monkey (Allman & Kaas 1974), HRP label is visible (figure 17*a*) and heaviest in layers III and IV. It is organized into irregular slabs running parallel across area 18. The anterior border of area 18 is well marked by a drop in label upon entering the third tier of visual areas. However, there is a weak projection to some subdivisions, particularly the middle temporal (m.t.) area where two puffs of label can be seen. Again, comparison between the pattern of cytochrome oxidase staining and the HRP label revealed an excellent match in area 18 and even within the third tier. The various subdivisions of the third tier, except m.t., are not immediately obvious in the cytochrome oxidase stain, but as their pattern of activity becomes more familiar the stain may aid in distinguishing the boundaries of these extrastriate visual areas.

A deeper HRP section passing primarily through layer VI is shown in figure 18*a*, plate 10. Layer IV c appears as a V-shaped band of intense anterograde label stopping abruptly at the 17–18 border. Anterograde label continues in area 18 more superficially but it is weaker and

less sharply restricted in laminar extent. In area 17 HRP label is present throughout layer VI, forming a clearcut border with area 18. At higher power (figure 18*b*) many retrogradely filled layer VI cells and granules of reaction product are visible. The label in the neuropil is present in the dendrites of layer VI cells and in the terminals of geniculate neurons, by anterograde transport. The position of every labelled cell in figure 18*a* was drawn at × 125 by using a microscope equipped with a camera lucida attachment. Each of the 11671 cells that were clearly labelled are indicated in figure 18*d*, plate 11, by a small dot.

In an adjacent section (figure 18*c*) stained for cytochrome oxidase, layer IVc stands out clearly as a dark band, exactly matching the band of HRP in figure 18*a*. In layer IV$c_\alpha$ patches can be seen, separated by layer IVb which stains lightly, from the tier of patches in the upper layers. In layer VI 114 patches were reliably seen; the position of each patch is marked in figure 18*d*. Occasionally it was necessary to refer to a more superficial section passing through IV$c_\alpha$ to draw the patches, but figure 18*c* was used primarily. The reconstruction in figure 18*d* shows there is no tendency for layer VI cells projecting to the l.g.n. to be clumped into the patches. It was more difficult to ascertain whether the geniculate projection to layer VI is grouped into the patches, as it is in layers IV$c_\alpha$, III, and II. The problem was that label in the distal processes of retrogradely filled cortical cells was hard to distinguish from label in geniculate terminals. While no evidence was seen for a clustered geniculate input to layer VI, it would be wise to test for this by injecting [$^3$H]proline instead of HRP into the geniculate.

(ii) HRP *injection in the macaque monkey*

The injection was centred in lamina 6 of the left l.g.n. at elevation +4°, azimuth 3° (figure 19*a*, *b*, plate 12). It was quite small, deliberately made on the lateral side of the nucleus to avoid the pulvinar. There was some diffusion of HRP into the immediately adjacent optic radiation and perigeniculate nucleus but the anterolateral border of the pulvinar, located 2 mm posterior and 3.5 mm medial to the injection site, was devoid of HRP.

In the upper layers of the cortex puffs of HRP label spaced about 350 μm apart were present (figure 20*a*). They matched precisely the position of the patches seen in an adjacent section (figure 20*b*) stained for cytochrome oxidase. Some of the cytochrome oxidase patches appear faded because this animal was visually deprived, as described in §3*f*.

In figure 20*a* beneath the puffs of labelled terminals in the upper layers a thin strip of heavy label representing the geniculate input to layer IVa is visible. It is separated from label in IVc by layer IVb which contains relatively few granules of reaction product. If this upper tier is cut tangentially (figure 21*a*) the geniculate terminals appear organized into a 'honeycomb' network, seen by Weber *et al.* (1977*a*) and Hendrickson *et al.* (1978) using radioautographic techniques. In an adjacent section (figure 21*b*), 50 μm more superficial, the honeycomb is seen in cytochrome oxidase. Unfortunately the honeycomb is so thin that in figure 21*b* it occupies the centre of the omega-shaped loop of figure 21*a*, making direct comparison between the two sections difficult. Still, it has been possible to match the inner fringe of the honeycomb in figure 21*a* with the outer fringe of the cytochrome oxidase pattern in figure 21*b* to verify that at their edges the two patterns coincide. Apparently the cytochrome oxidase stain outlines in exact detail the honeycomb formed by geniculate terminals in layer IVa. The section in figure 21*b* was counterstained with cresyl violet (not illustrated). Cell bodies were concentrated inside the hollows of the honeycomb, shunning the walls composed of l.g.n. terminals. Probably synaptic contacts between geniculate terminals and their target cells are made within

the honeycomb walls; what fraction of the heavy cytochrome oxidase staining is in geniculate terminals rather than post-synaptic dendrites of cortical neurons is unknown.

Hubel & Wiesel (1972) first identified the existence of an 'upper tier' input to layer IV by using the Fink–Heimer stain after geniculate lesions. In cresyl violet stained sections of spider monkey cortex they also noticed a cell-sparse gap in layer IV that they suggested might correlate with this geniculate input. In figures 22*a*, *b*, plate 13, adjacent sections stained for cytochrome oxidase and Nissl from a normal adult macaque are compared. In the Nissl stained section the cells at the base of layer III are more closely packed, making the cortex just above IVa appear slightly denser. The same is true of the uppermost portion of layer IVb. Layer IVa is thus flanked by two belts of enhanced cellularity. Layer IVa itself consists of three sublayers: a thin dark central strip sandwiched between a cell-sparse cleft above and below. By analogy with Lund's subdivision of layer IVc, they are labelled IVa$_\alpha$, IVa$_\beta$, and IVa$_\gamma$ in figure 22*b*. Layer IVa$_\beta$, the thin layer of cells bodies lying in the middle of IVa, actually contains the honeycomb of geniculate afferent. This division of layer IVa into three separate sublayers could be detected in five of seven normal macaque monkeys examined in tangentially cut sections.

An l.g.n. input to layer IVa has been clearly identified by radioautography in the macaque (Wiesel *et al.* 1974), squirrel monkey (Weber *et al.* 1977*a*; Hendrickson *et al.* 1978), red monkey, green vervet, baboon (Hendrickson *et al.* 1978) and marmoset (DeBruyn & Casagrande 1981). Its absence in the owl monkey therefore came as a surprise. One notable characteristic of the owl monkey is its poor colour vision; only 5% of the retinal photoreceptors are cones (Murray *et al.* 1973). Our first thought was that the honeycomb might be a specialization devoted to colour vision, which would account for its absence in the owl monkey. However this explanation seems doubtful because so far we have been unable to identify the honeycomb in the human striate cortex (Horton & Hedley-Whyte 1984) by using the cytochrome oxidase stain.

(iii) *Interpretation of the* HRP *experiments*

These experiments have established that there is a direct, rather than transneuronal, projection from the visual thalamus to the patches in the upper layers of striate cortex in new and old world monkeys. The chief question is whether this projection arises from the l.g.n. or pulvinar. Several lines of evidence suggest that the lateral geniculate is providing a direct projection to the cytochrome oxidase patches. In the macaque experiment illustrated the injection was well contained and no spillover into pulvinar was observed. In at least two other successful macaque injections there was no contamination of the pulvinar.

In the owl monkey case, spillover into the pulvinar may have occurred. Nevertheless, the geniculate still seems the likely source of the HRP label in the upper layers of cortex. Puffs of tritium label are seen in layers II and III of striate cortex after eye injection with [$^3$H]proline (Hubel & Wiesel 1978; Hendrickson *et al.* 1978); the transneuronal label must be transmitted to cortex either via the l.g.n. or the pulvinar. The retinopulvino projection in primates is weak and restricted to the ventrolateral border of the pulvinar (Campos-Ortega *et al.* 1970). It overlaps with only a subportion of the pulvinar thought to project to striate cortex. It seems doubtful that sufficient transneuronal label could reach striate cortex by this pathway. Therefore the more likely route is via the l.g.n. Of course, the pulvinar may also send a patchy projection to striate cortex, perhaps correlated with the cytochrome oxidase patches (Ogren & Hendrickson 1977; Rezak & Benevento 1979).

The presence of HRP label in V2 after l.g.n. was not unexpected since this projection has been clearly demonstrated (Wong-Riley 1976; Yukie & Iwai 1981; Fries 1981; Benevento & Yoshida 1981). However there is also ample evidence for a pulvinar projection to V2 and m.t. (Wong-Riley 1977; Ogren & Hendrickson 1977; Rezak & Benevento 1979; Lin *et al.* 1974), so that the pulvinar could account for the extrastriate label because we were not confident that HRP was confined to the l.g.n. in our owl monkey injections. In fact, label in V2 was stronger in layers III–IV than in layers IV–V, arguing in favour of a pulvinar origin (Benevento & Yoshida 1981). In either case, the HRP label does match the slabs of cytochrome oxidase label in V2.

### (*d*) *Alignment of patches and ocular dominance columns in macaque*

The rows of cytochrome oxidase patches in figure 3 were spaced about 350–375 μm apart, intersected the 17–18 border at right angles, and curved as they approached the horizontal meridian to run parallel to it. This pattern was reminiscent of the appearance of the ocular dominance columns over the operculum reconstructed by LeVay *et al.* (1975), which suggests that there may be a relation between the two systems. If so, would each row of patches lie centred within an ocular dominance column, or instead, straddle the border between a left and right eye column?

We (Horton & Hubel 1981) injected one eye of a macaque monkey (number 9) with 2 mCi [$^3$H]proline to label the ocular dominance columns in layer IVc by transneuronal radioautography. The animal was anaesthetized 14 d later, perfused with formalin, and alternate 25 μm sections were processed for cytochrome oxidase and radioautography. A tangential section through layer IVc stained for cytochrome oxidase showed no trace of any pattern (not illustrated), confirming earlier observations in other, normal monkeys (figure 5). The absence of any abnormal banding pattern in layer IVc (see §3*e*) assured us that the eye was unscathed by the isotope injection. An adjacent section processed for radioautography (figure 23*a*) showed the ocular dominance columns in darkfield illumination in layer IVc. The light bands correspond to the eye labelled with radioactive proline.

In a more superficial section from layer III of the same block stained for cytochrome oxidase (figure 23*b*) rows of patches were visible. To compare the ocular dominance columns in layer IVc with the patches in layer III a reconstruction was prepared (figure 23*c*). The borders of the eye dominance columns, marked in black, run between the rows of patches. Each row of cytochrome oxidase patches lies centred squarely within a left or right eye dominance column.

In the preceding section a direct projection from the l.g.n. to the patches was demonstrated. It was impossible to be sure whether the input was from geniculate afferents corresponding to both eyes, or strictly monocular, because the injections in the l.g.n. were not well enough confined to a single lamina. However, in the macaque, faint puffs of radioautographic label are visible in the upper layers of cortex after [$^3$H]proline eye injection (S. LeVay, personal communication). The puffs lie only over the labelled ocular dominance columns in IVc, indicating that the geniculate input to the patches is segregated by eye. As a consequence, cells within each patch will probably be strongly dominated by the same eye, corresponding to the ocular dominance column immediately underneath in layer IVc.

In the squirrel monkey the puffs seen after injecting a single eye are spaced about 500 μm apart. If only every other cytochrome oxidase patch were labelled, a spacing of every 1 mm would be expected. Therefore in the squirrel monkey, which shows continuous label in layer

IVc after injection of only one eye, each patch receives a mixed input from geniculate afferents driven by left and right eye.

### (e) *Effect of eye removal on cytochrome oxidase staining*

Transneuronal radioautography in the macaque provided evidence that each patch lies centred within an ocular dominance column and receives a direct monocular geniculate input. This anatomical correlation suggested that a functional relation might exist between the patches and the ocular dominance columns that could be demonstrated by using the cytochrome oxidase method. This possibility was explored by testing the effect of eye removal upon cytochrome oxidase staining in the l.g.n. and the striate cortex. Results are based upon four animals (numbers 10, 11, 12 and 17).

#### (i) *Effect on the lateral geniculate nucleus*

The effect of eye removal upon levels of metabolic enzymes in the l.g.n. has been studied by others and will be only briefly touched upon here. In the adult macaque 4 d after enucleation a clear drop is seen in NADH diaphorase, isocitrate, glutamate, and lactate dehydrogenase activity in denervated layers (Gay & Silverberg 1964; Cotlier *et al.* 1965). These changes slightly precede the appearance of transneuronal degeneration is Nissl stain. Similar findings have been reported for the kitten: 5 d after enucleation geniculate levels of SDH and NAD diaphorase are decreased in appropriate laminae (Kupfer & Palmer 1964). Levels of cytochrome oxidase activity are also diminished when tested 7 d after enucleation (Wong-Riley 1979).

We examined the l.g.n. after eye removal in only two monkeys. The first animal was an adult squirrel monkey perfused 48 h after enucleation (number 11). The lateral geniculate bodies appeared completely normal. Apparently more than 2 d must elapse for cytochrome oxidase levels in deafferented laminae to change appreciably. The second animal, an adult rhesus (number 10), was not actually enucleated, but suffered inadvertent eye damage in the course of injecting [$^3$H]proline into the vitreous body (*vide infra*). After one week's survival moderate loss of cytochrome oxidase staining, accompanied by mild transneuronal degeneration in the Nissl stain, was present in appropriate laminae of the l.g.n. (not illustrated). AChE staining did not appear to be affected.

In the accompanying paper (Horton & Hedley-Whyte 1984) the effect of monocular enucleation in the human followed by long term survival is illustrated. In l.g.n. laminae driven by the intact eye there is intense cytochrome oxidase activity located within principal cell bodies and in the neuropil. In denervated laminae neurons appear shrunken, pale, and stain weakly for cytochrome oxidase; there is also a dramatic drop in cytochrome oxidase activity in the neuropil.

#### (ii) *Effect on layer IVc of striate cortex*

A coronal section through the left striate cortex stained for cytochrome oxidase from a monkey whose left eye was removed six months earlier is shown in figure 24. The most striking effect of enucleation is seen in layer IVc. There is a regular, periodical alternation in the intensity of cytochrome oxidase staining, corresponding to the ocular dominance columns, most obvious in layer IV$c_\beta$. It is also visible in IV$c_\alpha$, but in this layer the transition between light and dark columns is less distinct and the fluctuation in absorbance much less pronounced. In columns

driven by the intact eye, cytochrome oxidase activity is greater in IV$c_\beta$ than in IV$c_\alpha$, while in enucleated eye columns staining is stronger in IV$c_\alpha$ than IV$c_\beta$, giving layer IVc a curious checkerboard appearance.

A feature of the laminar pattern of cytochrome oxidase activity, hidden in normal animals, is brought out by enucleation. In figure 24, at the very base of layer IV$c_\beta$, a thin dark band of staining is seen in the light columns. It is not visible in the normal eye columns because it blends in with the rest of IV$c_\beta$ lying immediately above, nor is it visible in coronal sections from normal monkeys (figure 2*b*). The significance of this sublaminae within layer IV$c_\beta$ is not known. It is apparent only because it resists the effects of enucleation more than the rest of layer IV$c_\beta$, suggesting that it may be a binocular subregion of IVc. However there is no indication from radioautographic or lesion studies of the l.g.n. projection to cortex of any mixing of left and right eye afferents at the base of layer IVc.

A tangential section through the left striate cortex from this same monkey stained for cytochrome oxidase is illustrated in figure 25*a*, plate 14. Again the ocular dominance columns are most obvious in layer IV$c_\beta$; following them into layer IV$c_\alpha$ they become less distinct. An adjacent section processed for AChE activity is shown in figure 25*b*. The ocular dominance columns are visible throughout layer IV$c_\beta$, the layer that reacts most intensely for AChE. Comparison of figures 25*a* and *b*, the dark columns of AChE activity match the light columns of cytochrome oxidase staining thought to correspond to the missing eye.

The section in figure 25*b* was specially treated to bleach out all trace of the AChE stain and then re-stained with cresyl violet, revealing a striking pattern of light and dark columns in layer IV$c_\beta$. In figure 26*a* a small region of IV$c_\beta$ from figure 25*b* is viewed at higher power. In figure 26*b* the same region of tissues is shown after re-staining for Nissl substance; the dark columns of AChE activity match the dark columns in Nissl. For comparison, the same area from the adjacent section in figure 25*a* is shown in figure 26*c*. The light columns of cytochrome oxidase activity can be seen to match the dark AChE and Nissl columns, as asserted previously.

---

## Description of plate 9

FIGURE 16. (*a*) Nissl stained left l.g.n. from a normal owl monkey. The arrow is pointing to the interlaminar zone between the right and left eye magnocellular layers where the HRP injection was made.

(*b*) A coronal section 125 μm more posterior processed for HRP activity by reacting with tetramethylbenzidine. The injection was centred at the tip of the small arrow, although a well defined focus of reaction product is not seen. This HRP injection was quite large, filling most of the geniculate, with some spillover into surrounding structures, including possibly the pulvinar. Scale = 2 mm.

FIGURE 17. (*a*) Anterograde HRP transport from the injection site in figure 16 to the visual cortex reveals a clear pattern of patches in striate cortex under darkfield illumination through crossed polaroid filters. They are most clearly seen in layer IV$c_\alpha$; to the right in layer IV$c_\beta$ labelling becomes continuous. Above, in V2, HRP label is also visible. The V2 border with V1 is obvious; the anterior border of V2 with the third tier of visual areas passes between the two large white arrows. Smaller white arrows denote three parallel slabs of HRP label in V2, oriented perpendicular to the V2 frontiers. In the middle temporal (m.t.) area, located still more anteriorly, two puffs of label are marked by short curved arrows.

(*b*) An adjacent section stained for cytochrome oxidase shows patches in IV$c_\alpha$ and in the upper layers. Layer IVb appears as a light gap, corresponding to a thin label-sparse cleft in (*a*). Comparison of the cytochrome oxidase and HRP labelled patches in adjacent sections has demonstrated that they match precisely, establishing that each patch in striate cortex receives a directly thalamic input. In V2 slabs of enhanced cytochrome oxidase activity are visible, as previously illustrated in the macaque and squirrel monkey. They match the regions of heavier HRP label in (*a*), as indicated for three slabs by small arrows. The pattern of cytochrome oxidase staining in the third tier is more complex and difficult to recognize, but within m.t. two spots of darker enzyme activity are seen (curved arrows), matching the puffs of HRP label in (*a*). Scale = 2 mm.

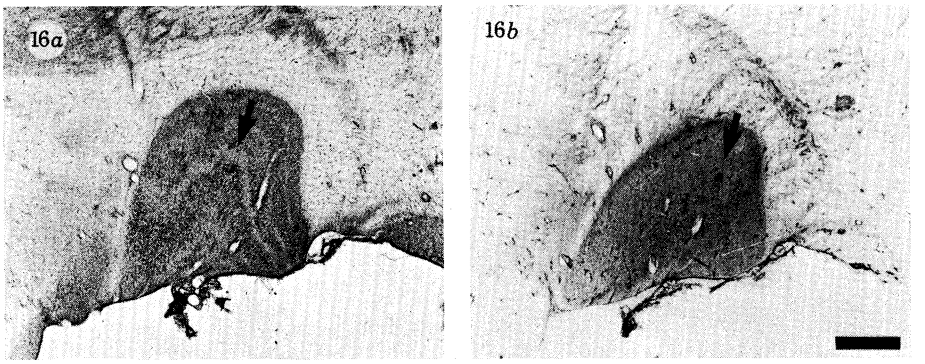


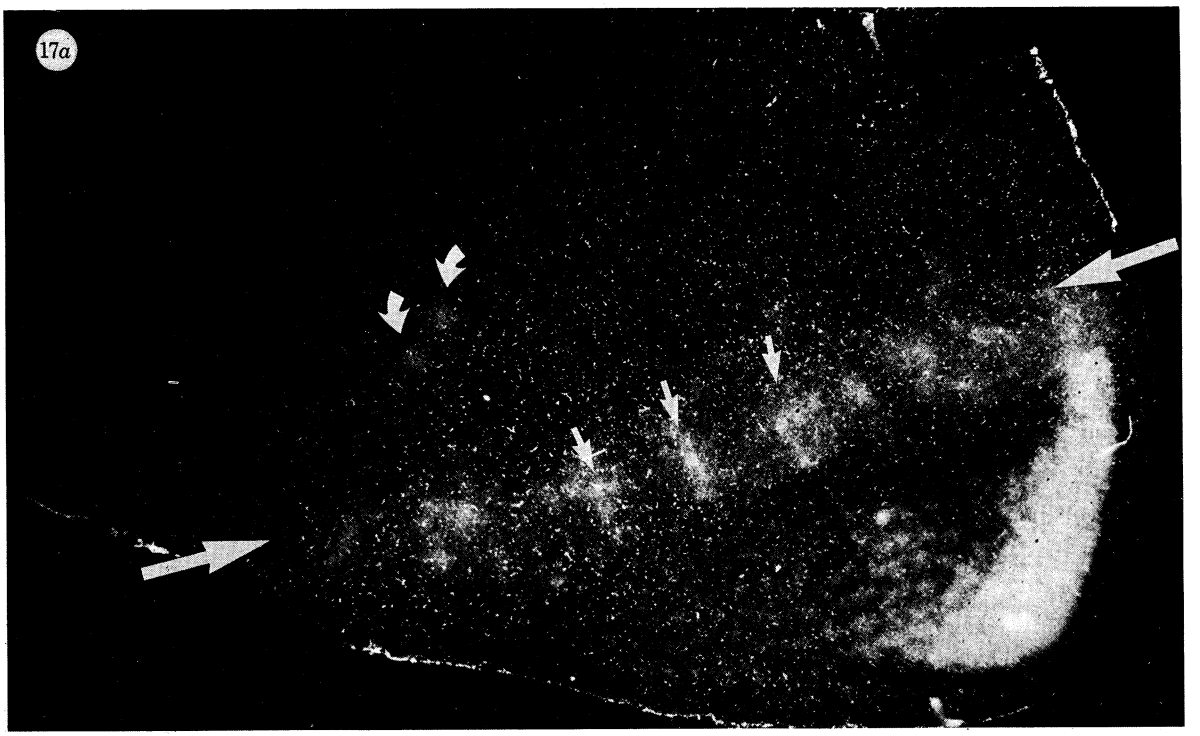


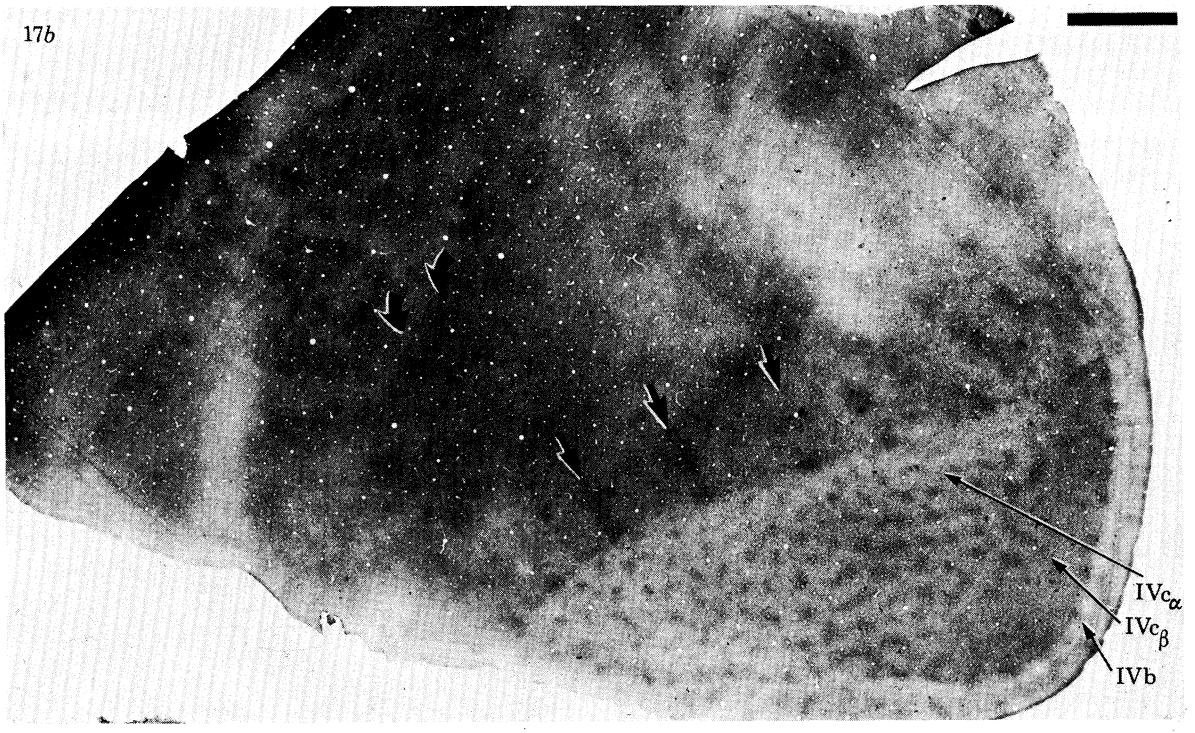


FIGURES 16 AND 17. For description see opposite.

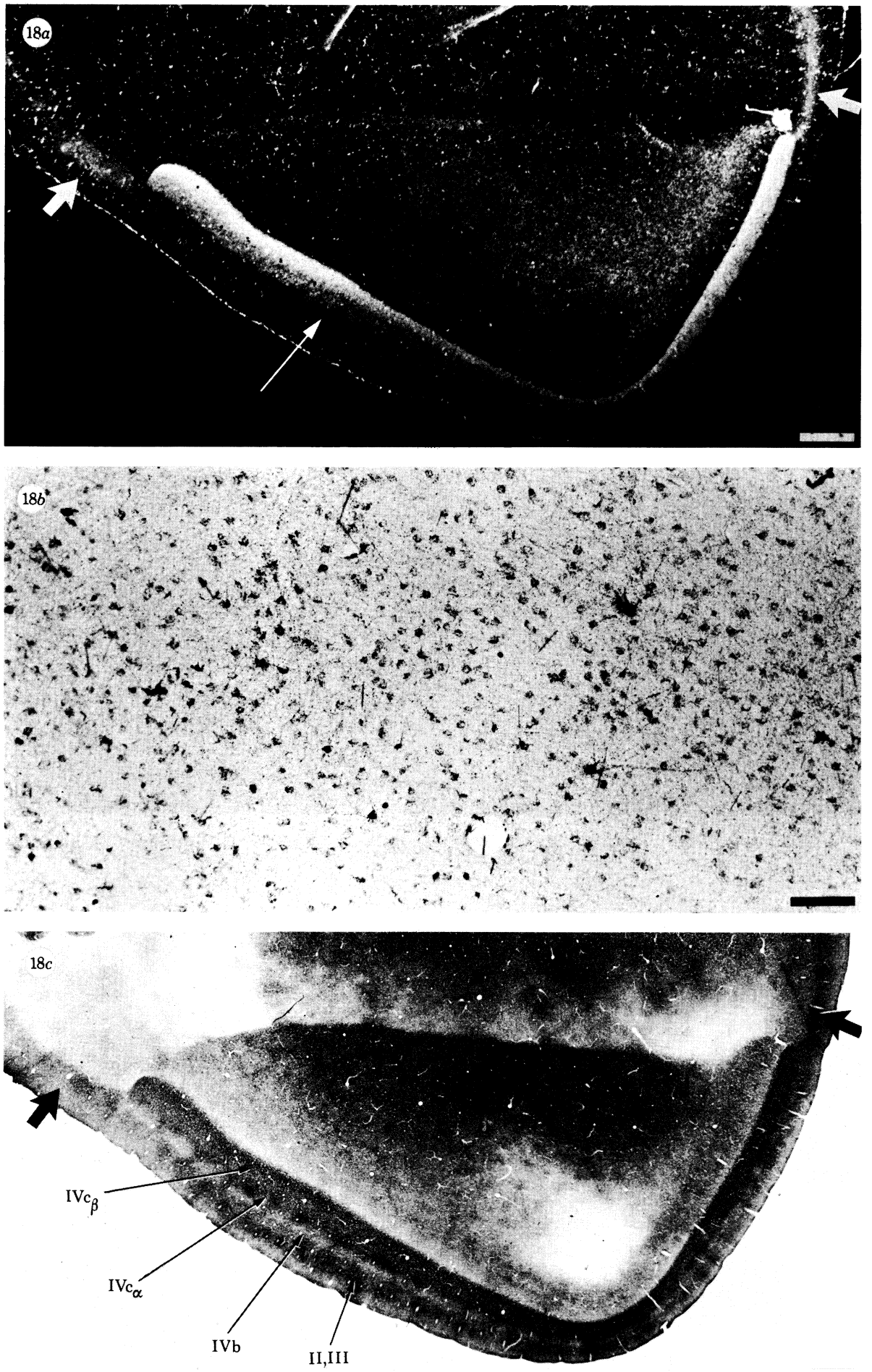


FIGURE 18*a–c*. For description see opposite.

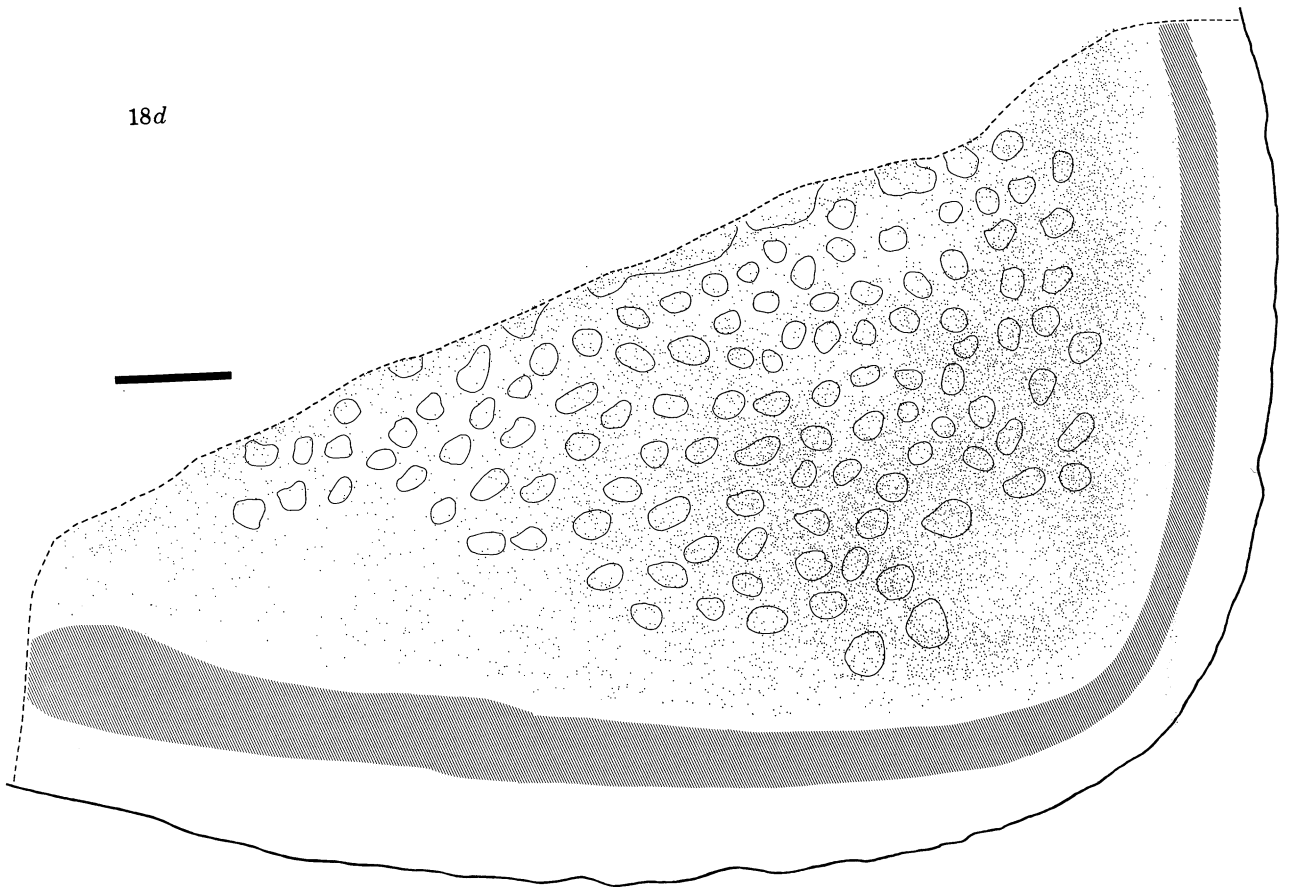


## Description of plates 10 and 11

Figure 18. (*a*) Section cut deeper to the section illustrated in figure 17 (*a*), passing primarily through layer VI. Under darkfield crossed polaroid illumination layer IVc stands out as a V-shaped band of intense HRP activity. This band stops abruptly at the 17–18 border, where it gives way to a more diffuse band of label in V2 (broad arrows). Just superficial to layer IVc in striate cortex, a label-free gap is visible, corresponding to layer IVb. It is marked by the tip of a thin arrow. Deep to layer IV a thin, relatively label-free zone is seen, corresponding to layer V. It borders layer VI which contains an even haze of faint HRP label, forming a clear border with V2 anteriorly (up). Scale = 1 mm.

(*b*) High power view of layer VI in (*a*) under brightfield illumination. Numerous cells containing retrogradely transported HRP are visible. In addition, HRP label is present, via anterograde transport, in terminals of geniculate axons projecting to layer VI. Scale = 100 μm.

(*c*) Section adjacent to (*a*) reacted for cytochrome oxidase activity. A dark V-shaped band of enzyme staining in layer IVc, corresponding to the HRP band in (*a*) is obvious. In layers IV$c_\alpha$ and II and III patches are visible, separated by the light gap characteristic of IVb. In layer VI patches are also clearly visible. The broad arrows mark the layers of heaviest cytochrome oxidase staining in V2, matching the HRP label indicated by arrows in (*a*). Scale = 1 mm.

(*d*) Reconstruction showing relationship between HRP labelled cells and cytochrome oxidase patches in layer VI of striate cortex. The dotted line indicates the 17–18 border and the band of oblique parallel lines marks HRP label in layer IVc. To prepare the reconstruction, the section in (*a*) was drawn with the aid of a camera lucida and the position of every retrogradely labelled cell marked by a small dot. A total of 11671 HRP filled cells was present in the section. Then the position of each cytochrome oxidase patch in (*c*) was indicated by drawing its borders. Alignment between (*a*) and (*c*) was achieved by careful comparison of blood vessel patterns in both sections. The reconstruction indicates that, considered as a single population, corticogeniculate projecting cells are fairly evenly distributed in layer VI, with no tendency to be clustered within the cytochrome oxidase patches. Scale = 1 mm.

## DESCRIPTION OF PLATE 12

FIGURE 19. (*a*) Nissl stained section of the left l.g.n. from a macaque; the medial geniculate body is visible to the upper left. Along the upper lateral border of the geniculate nucleus a small teardrop defect is visible, marking the HRP injection site in lamina 6.

(*b*) An adjacent section reacted with tetramethylbenzidine to demonstrate the HRP injection site. It is quite small, centred in lamina 6, with some involvement of laminae beneath and structures immediately surrounding the nucleus such as the optic radiation. There was no spillover into the pulvinar nucleus. Scale = 1 mm.

FIGURE 20. (*a*) Section of striate cortex cut in cross-section viewed under darkfield crossed polaroid illumination. Beneath, dense HRP label is seen in layer IV $c_\alpha$, separated by a thin label-sparse strip (IV b) from a dense band above corresponding to the honeycomb in IV a. Above the honeycomb, five faint puffs of HRP label in layers II and III (much stronger in layer III than layer II) are visible, marked by alternating large and small white arrows.

(*b*) Adjacent section stained for cytochrome oxidase activity. In the upper layers, five cytochrome oxidase patches are visible, marked by alternating large and small arrows. The patches under small arrows are smaller, an effect caused by visual deprivation, as described in further detail in a later section. The five cytochrome oxidase patches match the five puffs of HRP label in (*a*), demonstrating that the patches in layers II, III receive a direct input from the l.g.n. Scale = 500 μm.

FIGURE 21. (*a*) Tangential section grazing layer IV a from the experiment shown in figure 20. The loop of HRP label, representing the upper tier geniculate projection to layer IV a, contains a course reticular network termed the 'honeycomb'. Position of two obvious blood vessels is marked by curved arrows.

(*b*) An adjacent section 50 μm more superficial stained for cytochrome oxidase. The same two blood vessels are marked by curved arrows. A coarse reticular pattern of cytochrome oxidase staining is visible in IV a, which appears very similar to the honeycomb pattern of HRP label in (*a*). Careful comparison of (*a*) and (*b*) has indicated that the two patterns coincide at their fringes, i.e. the cytochrome oxidase stain labels the pattern formed by geniculate terminals in IV a. Scale = 20 μm.

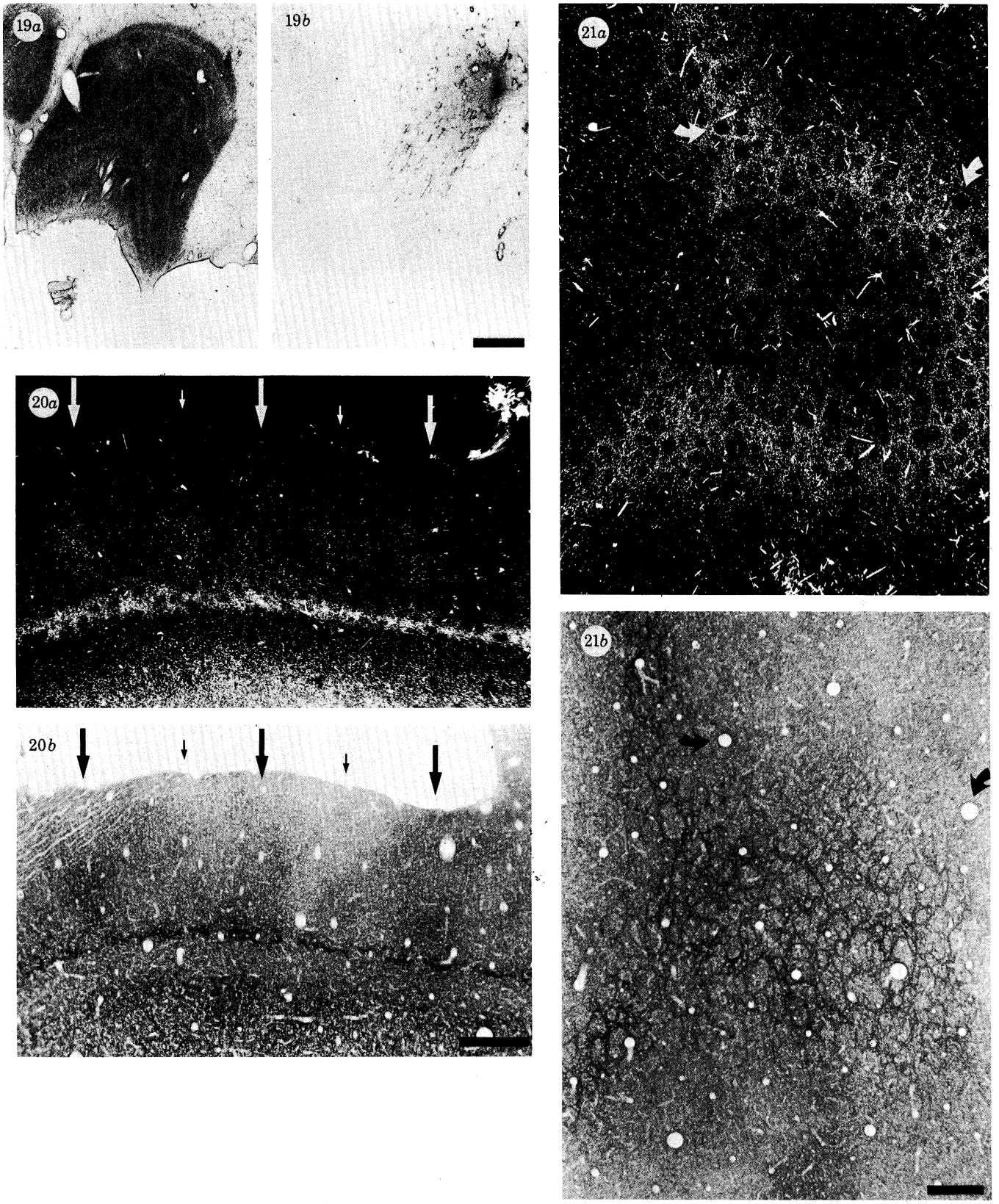


FIGURES 19–21. For description see opposite.

22*a*

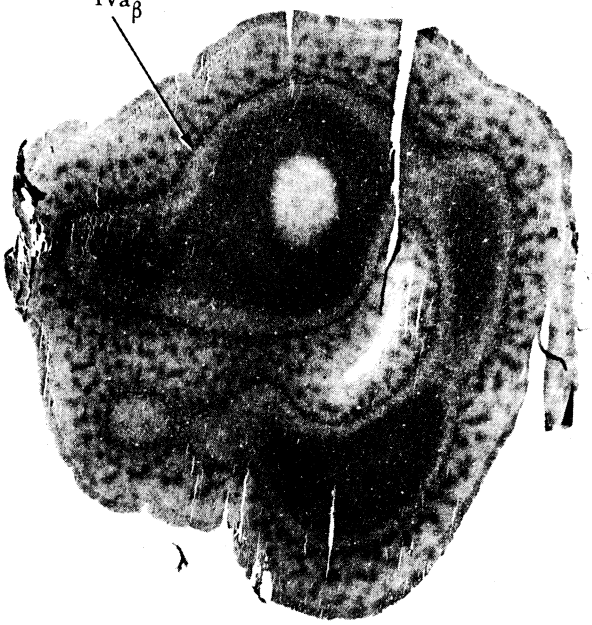


22*b*

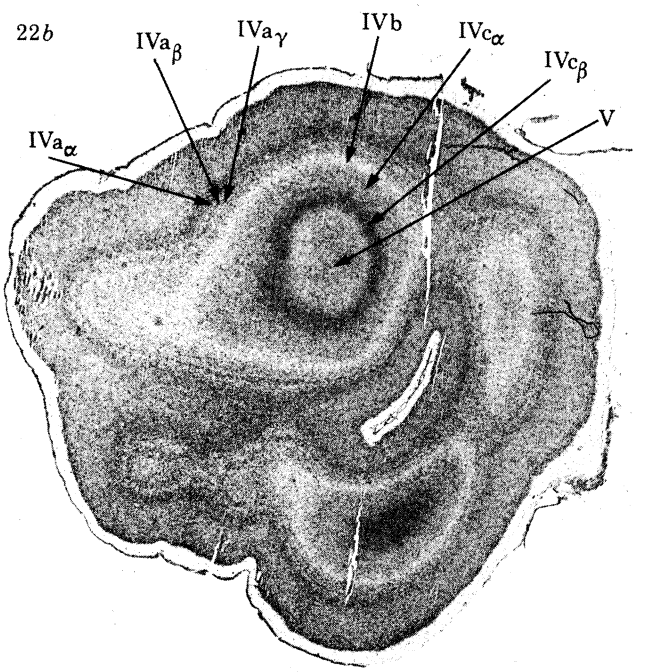


23*a*

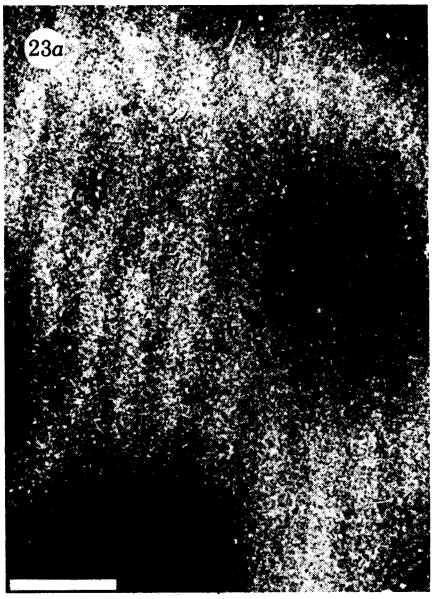

23*b*

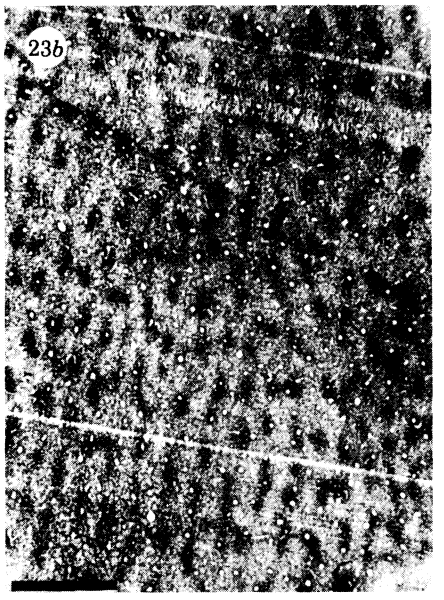

23*c*

24

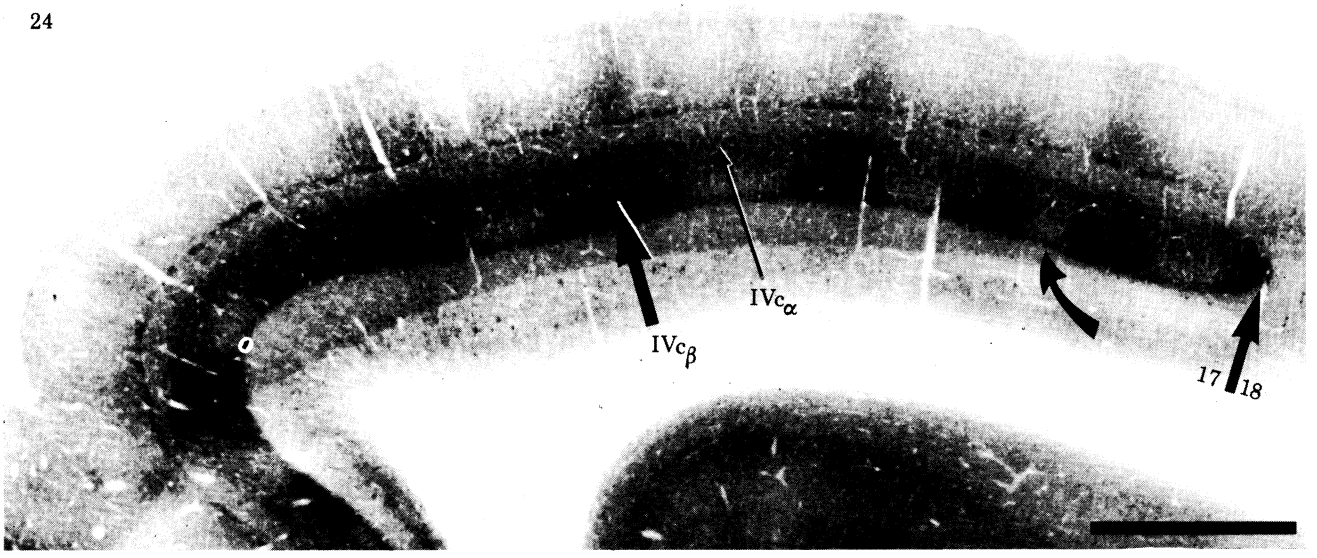


FIGURES 22–24. For description see p. 221.

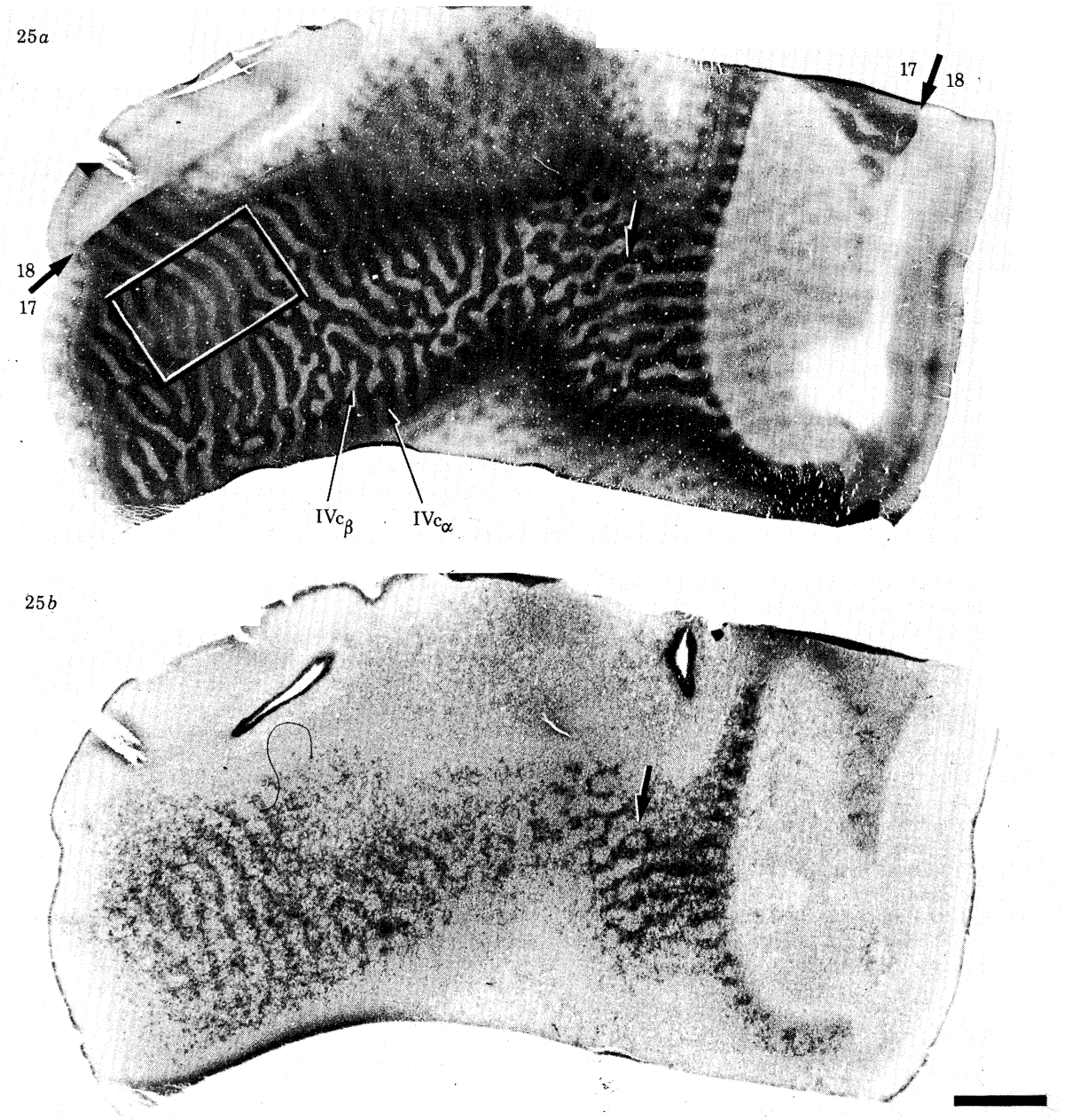


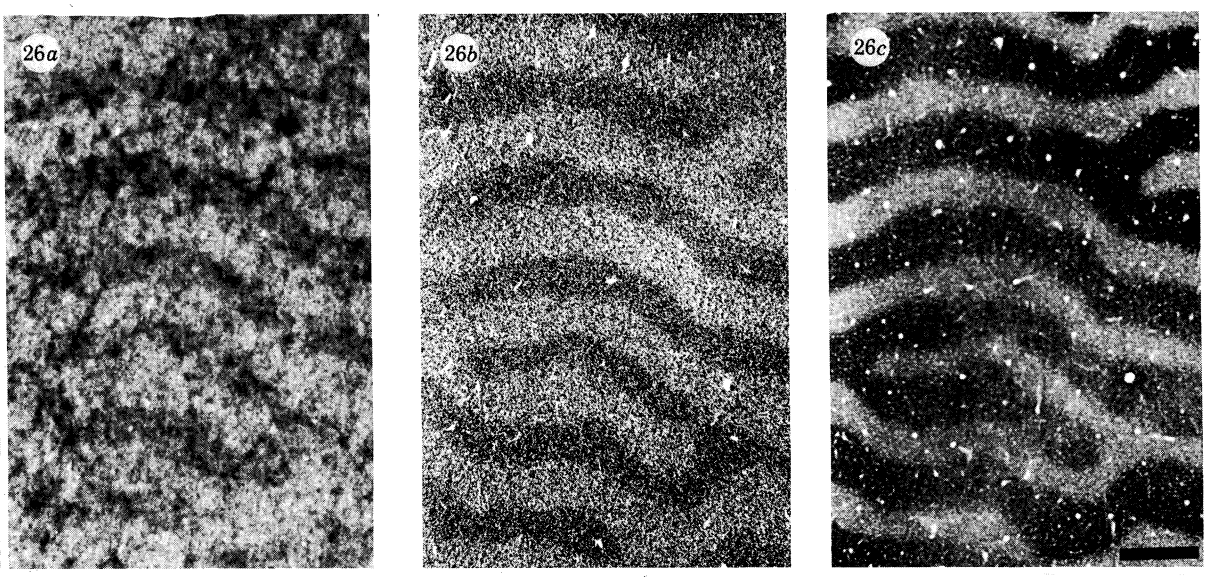


FIGURES 25 AND 26. For description see over.

## Description of plates 14 and 15

Figure 25. (*a*) Effect of eye removal upon cytochrome oxidase staining in striate cortex is shown in tangential section through left striate cortex from the same animal illustrated in figure 24. The ocular dominance columns are visible in layer IV, more clearly in IV$c_\beta$ than IV$c_\alpha$. Region enclosed in black box is shown in figure 26*c*.

(*b*) An adjacent section reacted for AChE activity shows the ocular dominance columns throughout layer IV$c_\beta$, the cortical layer containing the strongest AChE activity. The AChE stain labels the ocular dominance columns less distinctly than the cytochrome oxidase stain. Furthermore, the two enzymes preferentially label opposite sets of columns, as can be appreciated by referring to the arrow that points to a small island of light staining surrounded by darker AChE activity. An arrow in a corresponding position in (*a*) points to a dark island of cytochrome oxidase staining surrounded by light staining. The AChE stain preferentially labels the ocular dominance columns belonging to the missing eye. Scale = 2 mm.

Figure 26. (*a*) A small region from figure 25*b* shown at higher magnification. The ocular dominance columns are visible as alternating light and dark bands of AChE activity running horizontally across the figure.

(*b*) Same tissue as in (*a*) restained with cresyl violet after first bleaching out all traces of the AChE stain. In the Nissl stain the ocular dominance columns are also visible. Note that columns that appear dark in the AChE stain also stain more darkly with cresyl violet.

(*c*) The same region from the adjacent section stained for cytochrome oxidase: the area within the black box in figure 25*a* is shown, rotated 60° counterclockwise. Note that the columns which stain darkly for cytochrome oxidase match the columns in (*a*) and (*b*) that stain lightly for AChE and Nissl substance respectively. Scale = 500 μm.

ure 27. (*a*) Montage of photographs of alternate cytochrome oxidase stained sections passing through layer IV of the right striate cortex from a macaque monkey who right eye was injured by injection of [$^3$H]proline into the vitreous 7 d earlier. The ocular dominance columns, which are not visible in cytochrome oxidase stained sections through layer IV of normal monkeys (see figure 5), are seen here as a consequence of the eye injury.

(*b*) Montage of photographs of darkfield radioautographs from sections adjacent to those used to prepare montage in (*a*). Despite the eye injury, transneuronal transport of tritium to the cortex occurred, enabling one to see the ocular dominance columns corresponding to the radiolabelled eye as bright bands of tritium label against a black background.

(*c*) Reconstruction comparing the patterns of ocular dominance columns labelled by cytochrome oxidase and transneuronal radioautography. The small dots mark the set of eye dominance columns which stain darkly for cytochrome oxidase in (*a*). The set of columns indicated by parallel lines correspond to the tritium labelled ocular dominance columns in (*c*), belonging to the injected, injured eye. Referring to the construction it is evident that the tritium labelled ocular dominance columns in (*c*) match the more lightly staining columns in (*a*), establishing that ocular dominance columns belonging to the injured eye do indeed containweaker cytochrome oxidase activity. Scale = 1 mm.

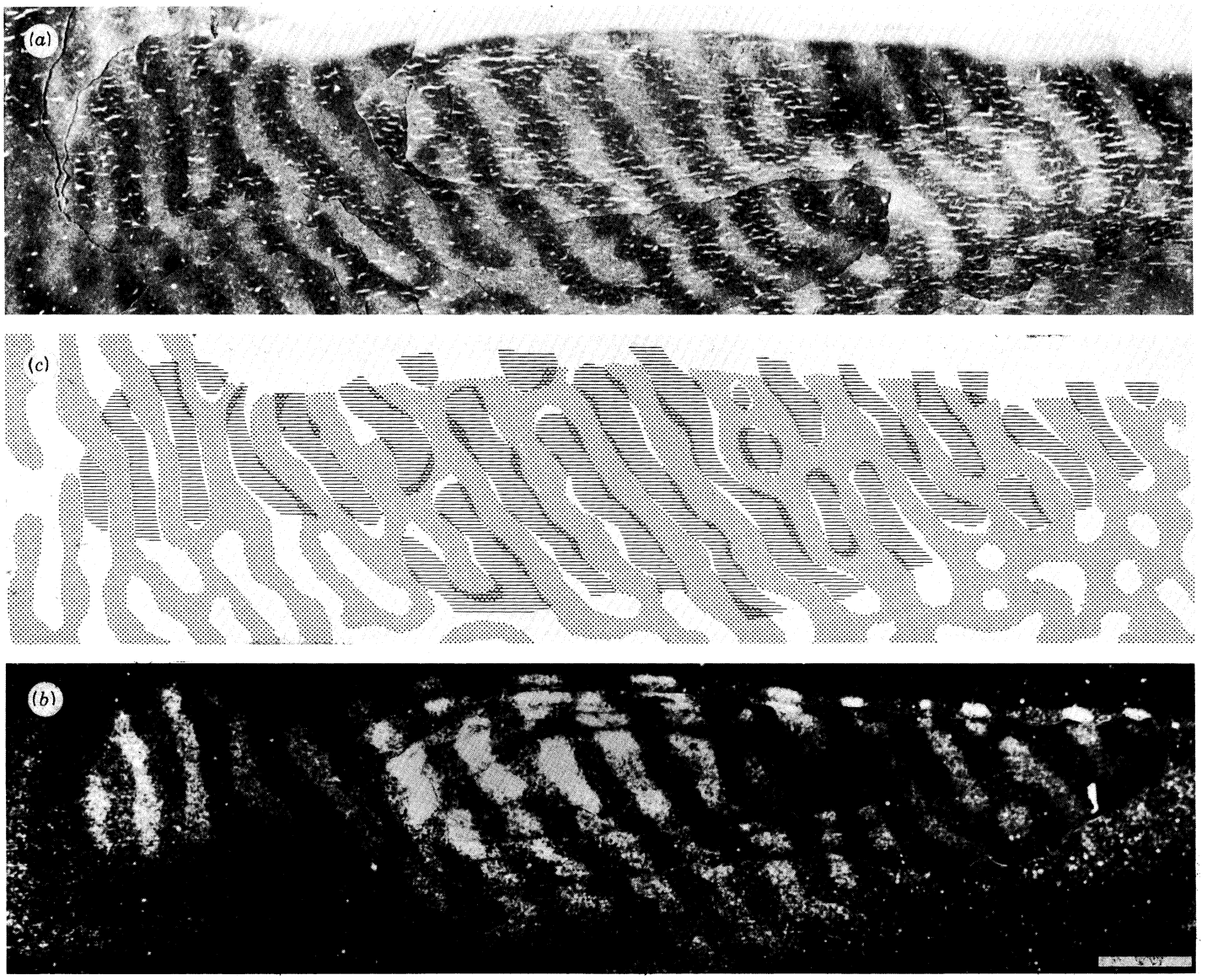


FIGURE 27. For description see opposite.

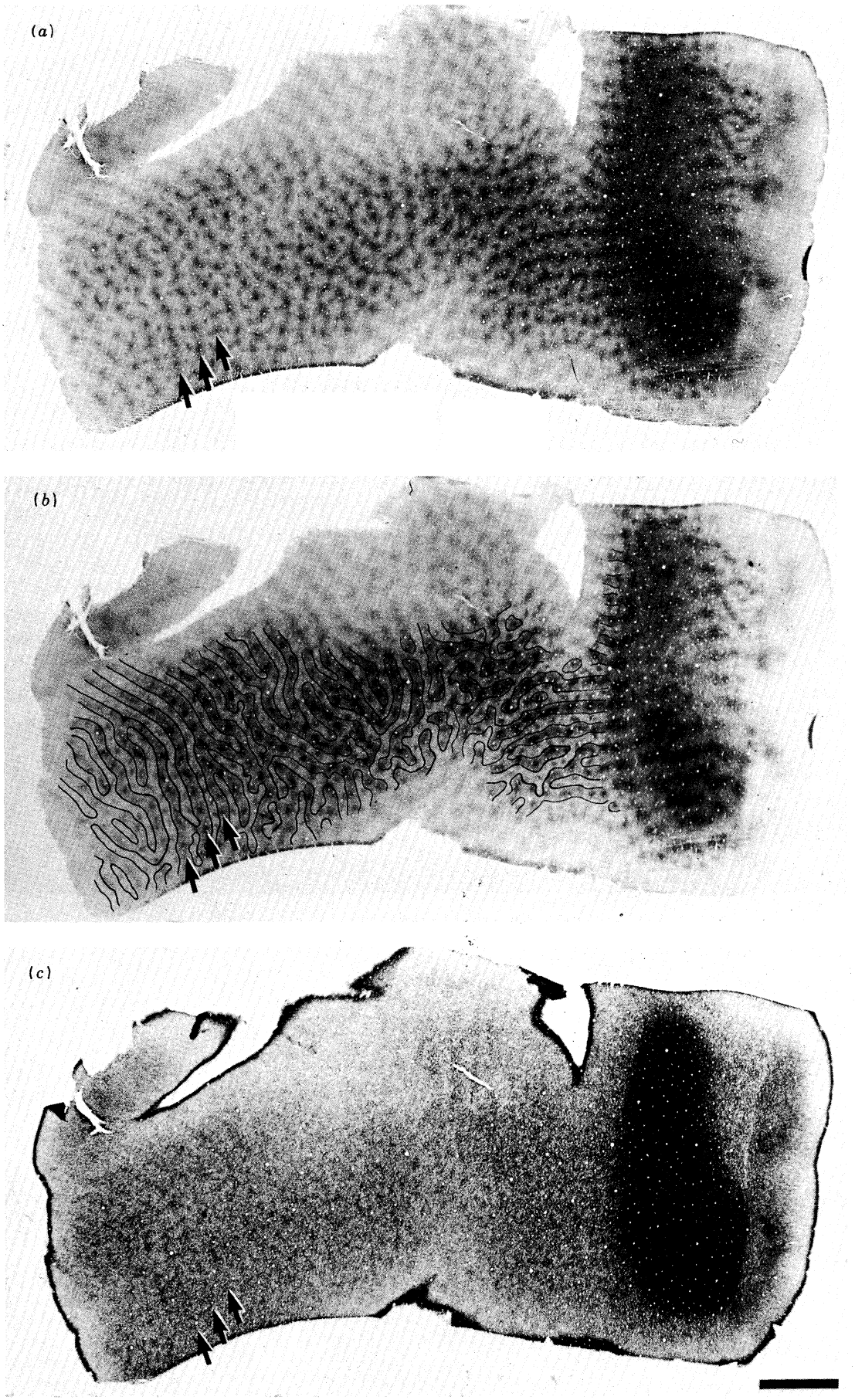


FIGURE 28. For description see opposite.

## DESCRIPTION OF PLATES 13 AND 16

FIGURE 22. (*a*) Cytochrome oxidase stained tangential section through striate cortex from a normal macaque. The honeycomb in IVa is visible as a dark band of enzyme activity, just deep to the cytochrome oxidase patches in layers II and III.

(*b*) An adjacent section stained with cresyl violet. Layer IVa is composed of several sublayers, that are clearly distinguishable. Immediately beneath layer III, which shows increased density of cell bodies at its base, there is a thin cell-sparse sublayer ($IVa_\alpha$). Just below, a thin cell-dense sublayer is visible ($IVa_\beta$), which is separated by another thin cell-sparse sublayer ($IVa_\gamma$) from the top of layer IVb. Thus IVa is composed of a thin cell-rich band ($IVa_\beta$) sandwiched between two thin cell-poor sublayers ($IVa_\alpha$ and $IVa_\gamma$). The coarse reticular pattern (honeycomb) of cytochrome oxidase staining is actually centered upon the middle, cell-rich sublayer, $IVa_\beta$. The significance of these three sublayers within IVa is unknown. Scale = 2 mm.

FIGURE 23. (*a*) Darkfield radioautograph of striate cortex from a normal macaque that received an injection of [$^3$H]proline into the right eye two weeks earlier. The section is tangential, grazing layer V (dark areas) but passing mainly through layer IVc. In layer IVc, ocular dominance columns are visible as alternating parallel light and dark slabs of label; the lighter slabs correspond to the radiolabelled eye.

(*b*) A more superficial section through layer III from the same block as (*a*), reacted for cytochrome oxidase. The cytochrome oxidase patches give the appearance of being aligned into rows that run vertically in the figure.

(*c*) Reconstruction comparing the pattern of ocular dominance columns in (*a*) with the rows of cytochrome oxidase patches in (*b*). Reconstruction was prepared by tracing the borders of the ocular dominance columns in (*a*) onto a transparent sheet of acetate. The section was then Nissl counterstained to identify prominent blood vessels that were marked on the acetate sheet. The acetate sheet was then overlaid on a print of (*b*). Correct alignment was achieved by matching blood vessels that pass radially through the cortex from pia into layer IVc. Although some blood vessels shift slightly in relative position, by referring to a matching constellation of about 20 large vessels in each section it was possible to establish a best fit. The acetate sheet was then photographed superimposed in position on (*b*) to produce (*c*). The reconstruction demonstrates that the ocular dominance column boundaries fit between each row of patches; therefore each row of cytochrome oxidase patches lies centered within a left or right eye dominance column. Scale = 1 mm.

FIGURE 24. Cytochrome oxidase stained coronal section through the left striate cortex from a monkey whose left eye was enucleated six months earlier. Layer IV is visible as a broad band of dark enzyme staining, ending sharply to the right at the 17–18 border. About a dozen ocular dominance columns are visible in layer IV as alternating light and dark zones, most obvious $IVc_\beta$. The loss of an eye has caused ocular dominance columns belonging to the missing eye to stain less intensely for cytochrome oxidase. In $IVc_\alpha$ the loss of cytochrome oxidase staining in enucleate columns is quite mild. As a consequence, in normal eye columns cytochrome oxidase staining in $IVc_\beta$ is greater than in $IVc_\alpha$; the reverse is true in enucleate eye columns. Another curious feature, not seen in normal monkeys, is the continuous narrow strip of cytochrome oxidase staining at the very base of layer $IVc_\beta$ (curved arrow). Scale = 1 mm.

FIGURE 28. (*a*) Cytochrome oxidase stained section cut 400 μm superficial to the section from the same block illustrated in figure 25*a*. To the right the section grazes layers IVa, IVb, and $IVc_\alpha$; elsewhere it passes through layers II, III where the patches are seen. They appear abnormal, in the sense that alternating rows of patches appear light or dark. Furthermore, the patches in light rows appear smaller and separated, whereas patches in dark rows appear larger and semi-confluent. Three dark rows of patches are indicated by arrows; between each dark row a lighter row can be discerned.

(*b*) Test of the relation between the light and dark rows of patches in layers II and III and the light and dark ocular dominance columns in layer IVc. The borders of the ocular dominance columns in figure 25*a* have been superimposed photographically onto (*a*); proper anatomical position was determined by close comparison of blood vessel patterns. Each row of dark patches fits within the middle of a dark ocular dominance column, and each row of light patches fits within a light ocular dominance column. This corroborates the registration between rows of patches and eye dominance columns demonstrated by eye injection with [$^3$H]proline followed by transneuronal transport. Note that not just the patches, but also surrounding cortex up to the borders of the normal eye dominance columns, stain more darkly for cytochrome oxidase. This is consistent with the view that each ocular dominance column in layer IV extends metabolically as a slab through the full thickness of cortex.

(*c*) Section adjacent to the section in (*a*) stained for AChE activity. Very faint rows of semi-confluent patches can be seen. Comparison with (*a*) has shown that these rows of AChE patches match dark rows of cytochrome oxidase patches. The three rows indicated by arrows correspond to the three rows marked by arrows in (*a*). AChE patches corresponding to the light cytochrome oxidase patches are not seen, probably because of the weak quality of the AChE staining in this section. Scale = 2 mm.

Given the surprising result that opposite sets of ocular dominance columns were labelled preferentially by the cytochrome oxidase and AChE stains, we were uncertain which set of ocular dominance columns corresponded to the missing eye. Direct evidence bearing on this point was obtained from the experiment mentioned earlier in which one eye of a rhesus monkey (number 10) was injected intravitreally with [$^3$H]proline. Although the eye appeared uninjured immediately after the injection, the next day a marked miosis was present and the direct pupillary reflex was absent. The animal was anaesthetized 7 d later and examined just before transcardial perfusion with 10% formalin. The vitreous was cloudy and the fundus could not be seen with an ophthalmoscope.

In the visual cortex the ocular dominance columns were visible, which indicates that although the eye was not removed, it was still damaged severely enough to alter cortical cytochrome oxidase activity. A montage of sections from the roof of the calcarine sulcus is shown in figure 27*a*, plate 15. In spite of the eye injury, sufficient uptake and transport of [$^3$H]proline occurred from the retina to label the ocular dominance columns transneuronally. A montage prepared from alternate sections processed for radioautography is shown in figure 27*c*. The labelled columns, which appear light under darkfield illumination, received input from geniculate laminae innervated by the damaged eye. Thus as a result of the traumatic eye injection, the ocular dominance columns were labelled by [$^3$H]proline and cytochrome oxidase in the same cortex, allowing the two techniques to be compared directly (figure 27*b*). The [$^3$H]proline labelled columns fit between the dark cytochrome oxidase columns, proving that the light cytochrome oxidase columns do indeed belong to the damaged eye.

(iii) *Effect on the patches*

A tangential section passing through layers II and III 400 μm superficial to the section in figure 25*a* is shown in figure 28*a*, plate 16. The patches are visible, as expected, but their appearance has been perturbed by eye removal. They are still organized into parallel rows, as in normal monkeys, but in every other row the patches appear paler and smaller. To compare the pattern of patches in the upper layers with the pattern of ocular dominance columns in IVc, a reconstruction (figure 28*b*) was made by following the same procedure used to prepare figure 23*c*. The rows of patches follow the pattern of the ocular dominance columns and those patches lying within in enucleate-eye columns stain more weakly. Thus the results obtained from eye enucleation confirm the alignment of patches and ocular dominance columns demonstrated in §3*d* by using transneuronal radioautography.

In figure 28*b*, within the confines of the ocular dominance columns corresponding to the intact eye, not only the patches, but also cortex immediately surrounding them appears more darkly staining. This is to be expected since all cells located above or below a column in IVc will tend to share the same eye dominance (Hubel & Wiesel 1977). Thus the ocular dominance columns in IVc extend metabolically through all layers to include both the patches and cortex immediately surrounding them. As a result there is a 'filling in' around the patches in normal-eye rows, making them appear less distinctly separated than their shrunken, pale counterparts in adjacent, enucleate-eye rows.

The effect of eye removal upon AChE staining of the patches was also tested. A section adjacent to the section in figure 28*a* reacted for AChE is shown in figure 28*c*. Regularly spaced rows of slightly darker AChE patches are visible. Comparison of this section with the adjacent cytochrome oxidase stained section demonstrated clearly that the dark rows of AChE patches

coincide with the dark rows of cytochrome oxidase patches. AChE staining in the upper layers was too weak to make out the rows of paler patches lying in between corresponding to the missing eye.

The effect of enucleation could be seen in other layers besides IVc, III and II. Figure 29*a*, plate 17 shows a tangential section, still from the same block, passing through a broad expanse of layer IVa. The honeycomb is broken into ocular dominance columns. The patches at the base of layer III appear almost confluent as they merge into the honeycomb. Finally, in figure 29*b*, a section passing primarily through layers V and VI is shown. The patches are indistinct, especially in layer V, but still present and organized into alternate light and dark rows, in register with the ocular dominance columns in IVc. The overall effect of enucleation on cytochrome oxidase staining is quite similar to the effect seen in the supragranular layers.

Cytochrome oxidase staining in V2 slabs was also examined after eye removal. No obvious effect, analogous to the dramatic changes apparent in V1, were visible. This appears to indicate a significant difference between the cytochrome oxidase patterns in V1 and V2. However, subtle alterations in staining after eye removal could escape attention because the V2 pattern tends to be less regular, especially in the macaque.

(iv) *Summary of eye removal experiments*

These experiments demonstrate that eye removal causes radical changes in levels of cytochrome oxidase activity in the l.g.n. and cortex. In the l.g.n. an appreciable drop in the levels of metabolic enzymes occurs about 3–4 d after enucleation, accompanied by early signs of pallor in the Nissl stain. Geniculate neurons are richly endowed with cytochrome oxidase activity, which accounts in part for the heavy enzyme staining in cortical layers VI, IVc, IVa, III and II, that receive geniculate terminals. After eye removal the degeneration of geniculate neurons must be accompanied by a substantial loss of cytochrome oxidase staining in their cortical terminals. This would help explain why the most dramatic effects of eye removal are seen in cortical layers that receive a direct geniculate input, and also why the ocular dominance columns appear in the cortex so soon after changes in cytochrome oxidase staining develop in the l.g.n.

The appearance of ocular dominance columns is presumably also due to a drop in cytochrome oxidase activity within cortical neurons. After enucleation the metabolic requirements of cells formerly driven by the missing eye are diminished. Consequently, their cytochrome oxidase content would be expected to fall. Atrophy of cortical neurons occurs after eye removal (Haseltine *et al.* 1979) and causes the ocular dominance columns to become visible in the Nissl stain. This should also contribute to the loss of cytochrome oxidase staining in ocular dominance columns belonging to the missing eye.

It is not clear why the ocular dominance columns in figure 25*a* appear so much less distinct in layer IVc$_\alpha$ than IVc$_\beta$. It may be relevant that magnocellular geniculate neurons are considerably more resistant to shrinkage induced by eye removal (Mathews *et al.* 1960). Another possibility is that the geniculate projection to IVc$_\alpha$ is less well segregated than to IVc$_\beta$. In figure 30 these two sublaminae of layer IVc are compared in radioautographs from the eye-damaged monkey (number 10). Certainly the borders of the ocular dominance columns in IVc$_\alpha$ look much fuzzier than in IVc$_\beta$. If segregation of magnocellular afferents in layer IVc$_\alpha$ is less strict the proportion of binocularly activated units may be higher, accounting for the milder effect of enucleation of cytochrome oxidase staining.

The results obtained with the AChE stain after eye removal are difficult to interpret. Seemingly opposite effects on the ocular dominance columns and the patches were observed, as depicted diagrammatically in figure 31. One week after eye removal we found no change in AChE staining in the l.g.n.; Fitzpatrick & Diamond (1980) report no change even three years after enucleation. Thus it seems unlikely that changes in cortical AChE staining are associated with loss of AChE activity in geniculate neurons. Certain nuclei, including the diagonal band of Broca and the basal nucleus of Meynert send a cholinergic projection to cortex (Mesulam & VanHoesen 1976). However, none of these structures receives a retinal projection, leaving no satisfactory explanation for why eye removal should alter AChE staining.

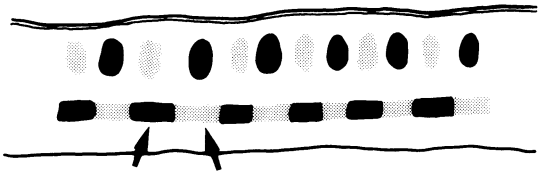


FIGURE 31. Schematic representation of AChE activity in coronal section of striate cortex after eye removal. In layer IV$c_\beta$ the ocular dominance columns are depicted as alternating light and dark columns, light (marked by small dots) columns corresponding to the remaining eye. In layers II and III alternating light and dark patches (ovals) are in register with the ocular dominance columns in layer IV. Surprisingly, light patches fit within dark ocular dominance columns.

The appearance of the ocular dominance columns in the AChE stain is probably due to secondary anterograde transneuronal degeneration. After enucleation collapse of neuropil and atrophy of layer IVc stellate cells occur (Haseltine *et al.* 1979). If AChE activity associated with afferent terminals synapsing onto layer IVc cells remains about the same after enucleation, the overall intensity of AChE staining within enucleate-eye columns will increase simply as a consequence of the increased packing density of cell bodies. If this is correct, after enucleation the ocular dominance columns should appear in the AChE stain only when they become evident in the Nissl stain. It would be interesting to verify this by testing cytochrome oxidase, AChE, and Nissl staining in a complete series of macaques at different times after enucleation.

The relative loss of AChE staining in the patches after eye removal is more difficult to explain. We have noticed degenerative changes in the upper layers in the Nissl stain (not illustrated), similar to the changes seen below in IVc, but milder. This should increase the density of AChE processes in layers II and III, and thereby cause AChE staining to darken, as in IVc. Yet eye removal decreases relative AChE activity in layers II and III of enucleate eye columns, and increases it in layer IVc. We do not understand why eye removal produces these seemingly opposite effects in layers IVc and II, III.

### (*f*) *Effect of eyelid suture on cytochrome oxidase staining*

In the case of eye removal it is difficult to distinguish changes in cytochrome oxidase staining induced by transneuronal degeneration from changes occurring as a functional consequence of neuronal inactivity. We therefore decided to test if eyelid suture, a less drastic procedure that does not result in neuronal death or atrophy in adult monkeys, produces a similar change in cytochrome oxidase levels.

In two macaque monkeys (numbers 15, 16) the lids of the right eye were sutured closed for

survival times of four and six months. As already described, these animals also received small HRP injections into the l.g.n. 1.5 d before perfusion as part of a study of the geniculate projection to the patches. The results obtained in these two animals were extremely similar despite the two month difference in the duration of eyelid suture. The monkey that lived for six months after suture will be described because it matches the six month survival time of the eye-enucleated monkey in the previous section.

(i) *Effect on the lateral geniculate nucleus*

After six months of monocular suture no effect upon cytochrome oxidase or AChE staining in the l.g.n. could be seen at the light microscopic level. This is illustrated for cytochrome oxidase staining in figure 32, plate 18. On both sides magnocellular laminae 1 and 2 and parvocellular lamina 6 appear slightly darker. The same is true of cytochrome oxidae staining in normal macaques (not illustrated) and also for LDH, SDH, citrate dehydrogenase, and NADH diaphorase as reported by Cotlier *et al.* (1965). Although functional specializations have been identified for different laminae of the macaque l.g.n. (Schiller & Malpeli 1978), it is not clear why cytochrome oxidase levels should be normally greater in this particular combination of laminae. The main point is that the l.g.n. in neither hemisphere shows any loss of cytochrome oxidase activity in laminae corresponding to the sutured eye.

(ii) *Effect on the visual cortex*

Figure 33 shows a cytochrome oxidase section through the left operculum passing through a wide area of layer IV. The ocular dominance columns are faintly visible in IV$c_\beta$, IV$c_\alpha$, and IVb. A thin, uninterrupted line of dark staining marks the base of layer IVc, as in eye-enucleated monkeys. The border between IV$c_\beta$ and IV$c_\alpha$ is also marked by a belt of slightly denser cytochrome oxidase activity; so far we have not noticed this in normal animals.

The ocular dominance columns in layer IV appear of unequal width: the light columns are much broader than the dark columns. Hubel *et al.* (1977) have reported that eyelid suture in immature monkeys causes a sprouting of geniculate terminals in layer IVc, widening normal eye columns at the expense of deprived-eye columns. However, the monkey illustrated in figure 33 was at least 1.5 years old when the lids were closed, well beyond the critical period for such changes. Furthermore, the dark columns, which presumably correspond to the open eye, are plainly thinner than the light columns, which implies if anything a contraction, rather than expansion, of geniculate terminals belonging to the normal eye.

A clue to this puzzle was provided by the HRP injections made in the l.g.n. to label the patches in the cortex. The injection site from this monkey (illustrated in figure 19) was centered in lamina 6 of the l.g.n. contralateral to the closed eye, small enough to label preferentially the deprived eye dominance columns in layer IVc. They are shown in an adjacent section under brightfield illumination in figure 34*b*, plate 19. The dark bands of HRP reaction product are the same width as the gaps between, ruling out sprouting or contraction of geniculate afferents as the cause of the unequal column sizes in figure 33.

The portion of the section in figure 33 containing the HRP labelled ocular dominance columns is shown in figure 34*a* at precisely the same magnification as figure 34*b*. To compare the cytochrome columns with the HRP columns a reconstruction was prepared, as shown in figure 34*c*. The dark cytochrome oxidase columns were filled in solidly with ink, the light columns were indicated by small dots. The columns of HRP label were represented by thin

parallel lines; two closely adjacent HRP sections were also included in making the reconstruction to widen the area available for comparison. Obviously it was critically important to achieve an accurate alignment of the adjacent cytochrome oxidase and HRP sections. Again, this was done by referring to the pattern of blood vessels in each section; a few prominent examples are marked by arrowheads.

The HRP labelled ocular dominance columns fit squarely within the light cytochrome oxidase columns, providing independent anatomical verification that ocular dominance columns corresponding to the deprived eye stain more weakly for cytochrome oxidase. Surprisingly, the dark cytochrome oxidase columns are thinner than the full width of the normal eye columns, as defined by the HRP label. In other words, the lighter cytochrome oxidase columns include the HRP labelled columns and trespass upon the borders of the open-eye columns. These fringe strips of overlap, about 75 μm across, appear in figure 34*c* as thin gaps where only small dots are visible.

In the upper layers cytochrome oxidase staining was affected severely by visual deprivation, as shown in figure 35*a*, plate 20. As in one-eyed monkeys, every other row of patches looks darker and more confluent. When the sections in figures 35*a* and 33 were aligned and compared

---

## Description of plates 17 and 18

FIGURE 29. (*a*) Cytochrome oxidase stained section cut 80 μm deep to the section illustrated in figure 28*a*. It passes primarily through layers IVa (honeycomb) and the base of layer III, except to the far right where the ocular dominance columns are obvious in layer IV$c_\alpha$. Where the section grazes layer IVa, the honeycomb appears organized into ocular dominance columns: within columns belonging to the remaining eye the reticular network of staining appears darker, whereas within columns of the missing eye it is pale. Arrows mark three well-labelled columns within the honeycomb, corresponding to arrows in figure 28*a*. Note also confluence of the patches at the bottom of layer III, as they blend into layer IV*a*.

(*b*) Deeper section from the same block passing primarily through layers V and VI, which stain rather weakly for cytochrome oxidase, compared with IVc. In layers V and VI the patches are visible, with alternating rows of patches appearing darker, according to the pattern of the ocular dominance columns. The effect of enucleation upon the patches in layers II and III and layers V and VI is quite similar, although in layers V and VI the patches are much less clearly defined. Scale = 2 mm.

FIGURE 30. (*a*) Darkfield view of a radioautograph from a macaque whose right eye was injected one week earlier with [$^3$H]proline. The ocular dominance columns are most clearly seen in layer IV$c_\beta$ where their borders appear sharp and the contrast in grain density between labelled and unlabelled columns is most striking. The labelled (light) columns appear relatively wider than the unlabelled columns because this section is located in far peripheral cortex contralateral to the injected eye.

(*b*) Radioautograph of a section cut 80 μm superficial to the section illustrated in (*a*). To the right the ocular dominance columns are again seen most clearly in layer IV$c_\beta$. As the section passes into layer IV$c_\alpha$ (large arrow) the columns become less heavily labelled and their borders appear less well defined, making them appear narrower. In the area to the left, columns are seen in layer IV$c_\alpha$; compare their appearance with the columns in layer IV$c_\beta$ shown in (*a*). Arrows at the far left in (*a*) and (*b*) mark identical points in the cortex. Scale = 1 mm.

FIGURE 32. Effect of visual deprivation on cytochrome oxidase staining in the lateral geniculate nucleus: right (*a*) and left (*b*) l.g.n.s stained for cytochrome oxidase from a monkey whose right eye was sutured closed six months previously. No loss of cytochrome oxidase staining is seen in deprived (d) laminae, compared with normal (n) laminae in either left or right geniculate body. On both sides, cytochrome oxidase staining appears slightly darker in the magnocellular laminae and in lamina 6; this pattern is also typical of cytochrome oxidase staining in geniculate bodies from normal monkeys. Scale = 500 μm.

FIGURE 33. Effect of visual deprivation on cytochrome oxidase staining in striate cortex. A single section through the left striate cortex stained for cytochrome oxidase from the monkey illustrated in figure 32 is shown. Most of the section is occupied by layer IV, although at the top and to the left two large areas of layers V and VI are seen. At the base of layer IV a continuous dark thin line of staining is visible (long curved arrow); a similar line is seen between layers IV$c_\beta$ and IV$c_\alpha$ (short curved arrow). Their significance is unknown. The most striking effect of visual deprivation is to cause the ocular dominance columns to become visible in striate cortex. They are apparent as a regular alternating pattern of light and dark bands, appearing faintly visible in layers IV$c_\beta$, IV$c_\alpha$, and IVb. Scale = 2 mm.

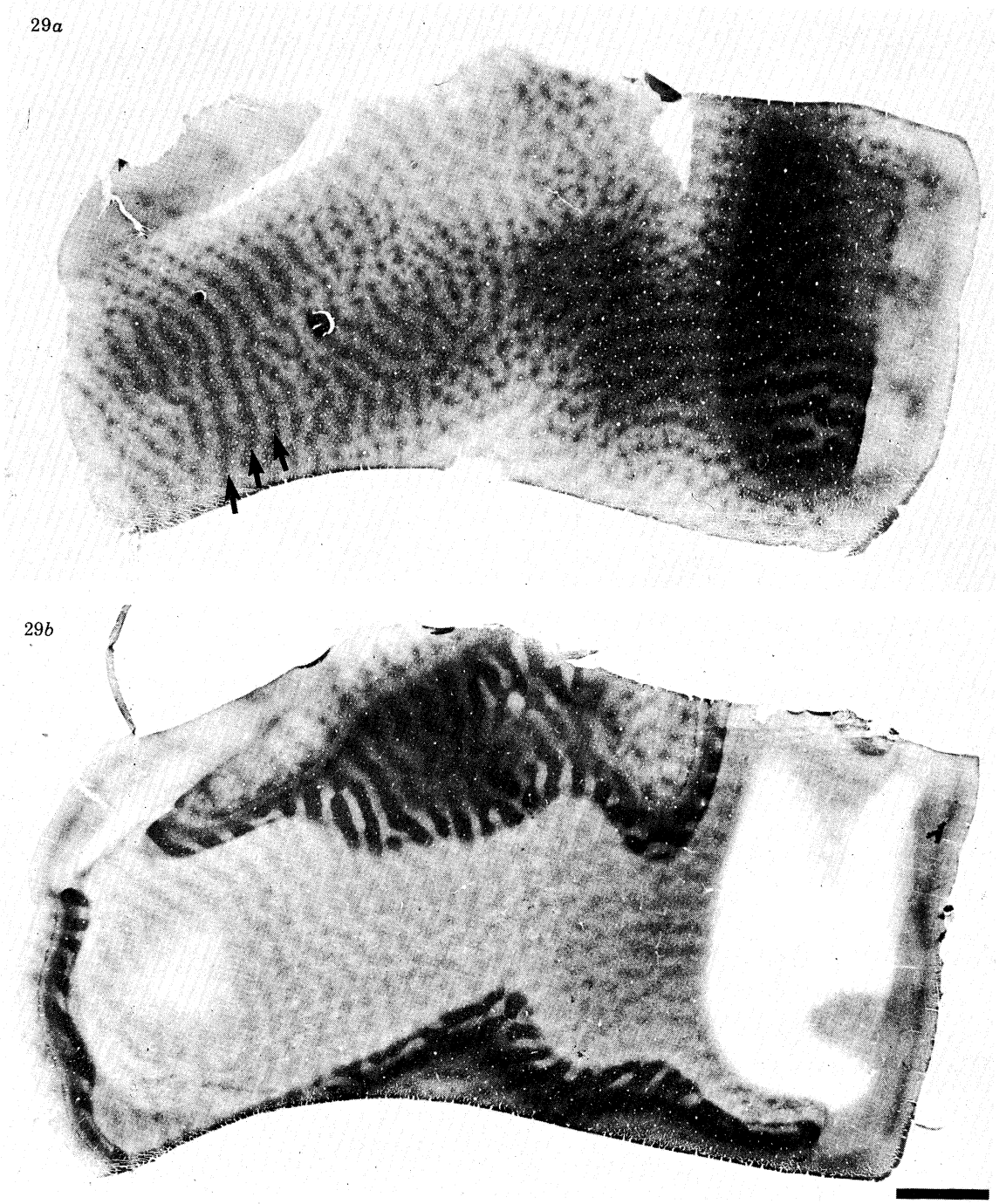


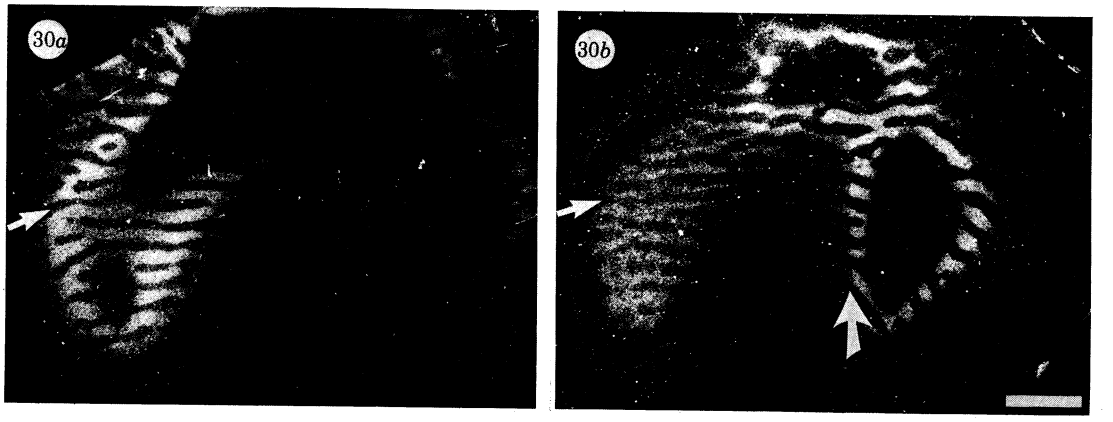


FIGURES 29 AND 30. For description see opposite.

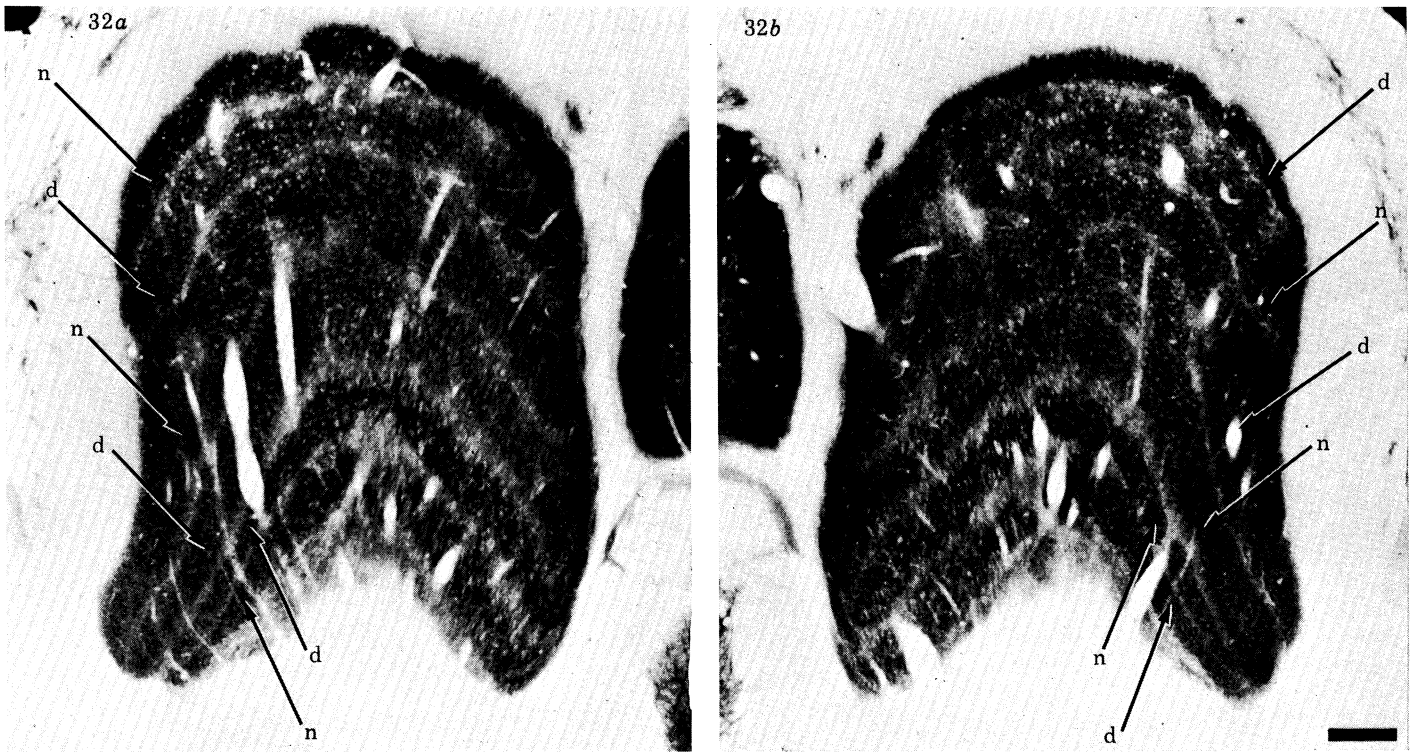


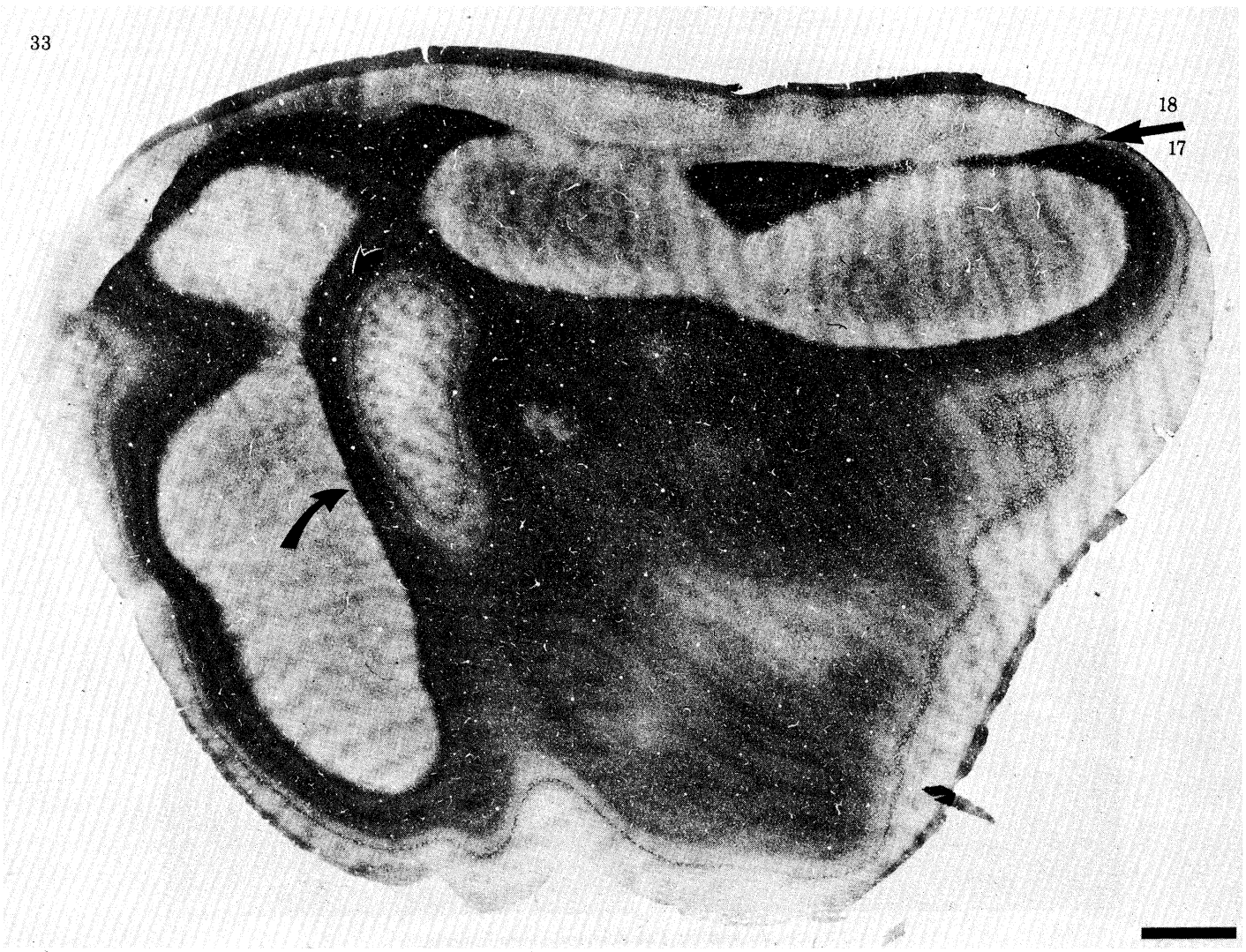


FIGURES 32 AND 33. For description see p. 226.


FIGURE 34. (*a*) Area from figure 33, illustrated at higher power to show detail of ocular dominance columns in layer IV. The dark ocular dominance columns appear thinner than the light columns. The ocular dominance columns can be followed from layer IV c to the left where they pass into layers V, VI. Arrowheads mark six blood vessels; these and numerous others were used to align the reconstruction in (*c*). Long arrows point out faint increase in density of cytochrome oxidase staining within the middle of each light ocular dominance column.

(*b*) Adjacent section showing ocular dominance columns labelled by anterograde transport of HRP from an injection made in a deprived eye laminae 6 in the l.g.n. (see figure 19). Under brightfield illumination the labelled columns appear dark. Unlike the columns visible in (*a*) the dark and light columns are of roughly equal width. Arrowheads point out a few blood vessels also visible in (*a*).

(*c*) Reconstruction comparing the ocular dominance columns visible in (*a*) and (*b*). The dark cytochrome oxidase columns in (*a*) are drawn in solidly with ink, the light columns are shown with small black dots. The labelled columns in (*b*), and from two nearly adjacent sections not illustrated, are marked with thin parallel lines. Accurate alignment of HRP and cytochrome oxidase columns was achieved by referring to position of blood vessels in adjacent sections. Reconstruction demonstrates that the lighter cytochrome oxidase columns match the ocular dominance columns corresponding to the deprived eye, although they actually extend beyond boundaries of HRP labelled columns to infringe upon open-eye columns. Scale = 1 mm.

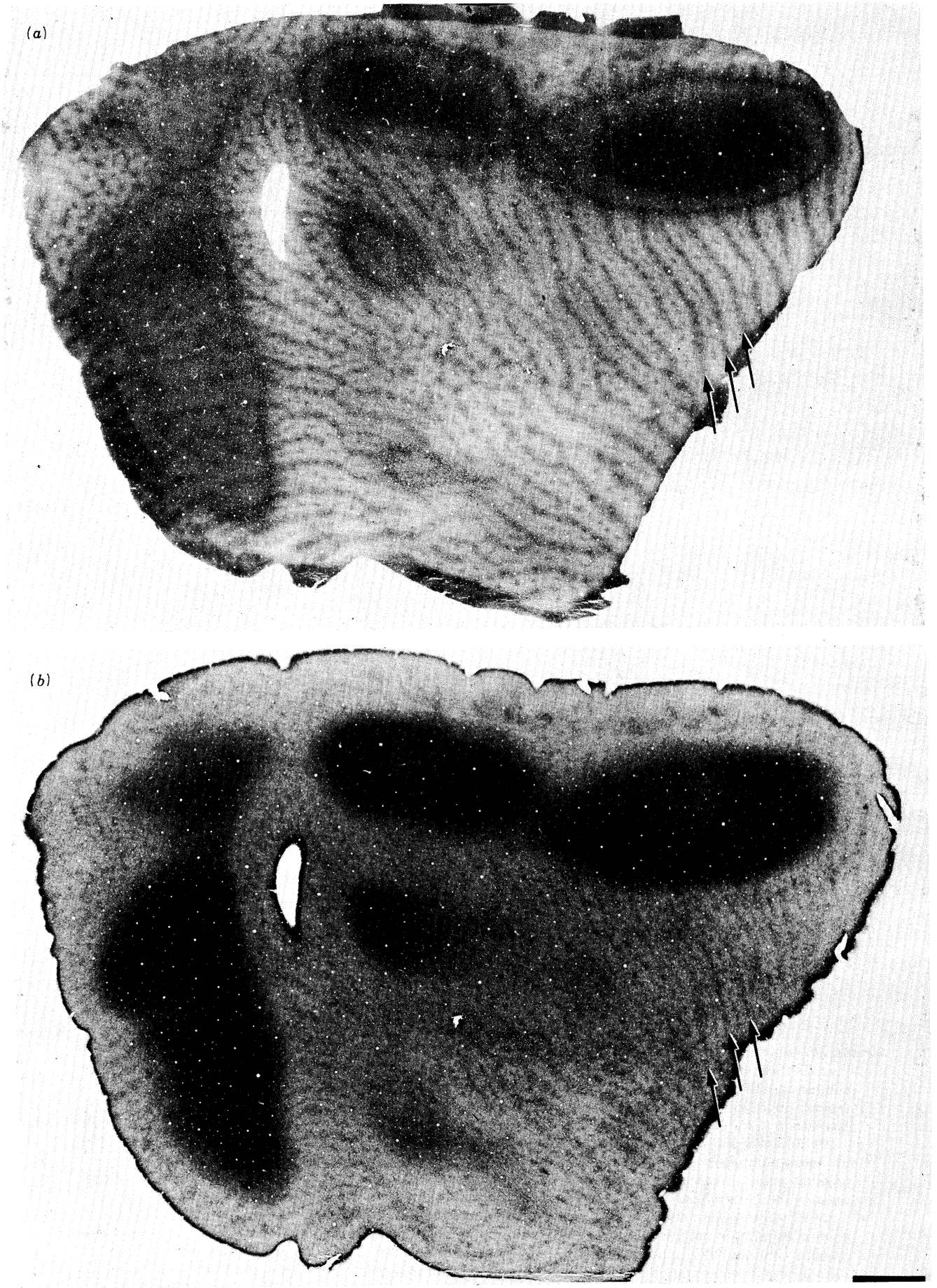


FIGURE 35. For description see opposite.

it was found that the light rows of patches lie centred within the light cytochrome oxidase columns in layer IV. However, the rows of patches are much thinner, roughly 200 μm wide, than the light columns in layer IV, which are about 500 μm wide. At the same time, the dark rows of patches fit in perfect register with the dark columns in layer IV and are of exactly the same width. This can be appreciated by referring to figure 33 or 35*a* and following rows of light and dark patches from the upper layers into IVc where they join the cytochrome columns. The same is true of the light and dark rows of patches in layer V and VI (figure 33).

Finally, AChE staining was also affected by visual deprivation. Figure 35*b* shows a section adjacent to the section in figure 35*a*. Although the patches stain more weakly for AChE than cytochrome oxidase, they are clearly organized into light and dark rows. The patterns in figure 35*a*, *b* coincide: the dark rows of cytochrome oxidase patches match the dark rows of AChE patches. A few corresponding rows are marked with arrows in both figures. Notice that the honeycomb in IVa does not stain with a fine reticular pattern in the AChE stain, as it does with cytochrome oxidase.

The effects of visual deprivation were not tested in newborn monkeys. However, there was an opportunity to examine two cats monocularly sutured at 28 d. Eyelid suture at this age causes atrophy of geniculate neurons in deprived laminae and shrinkage of the fraction of layer IV occupied by their terminals in the cortex. In addition, the number of cells in layer IV that can be driven through the deprived eye becomes sharply reduced (Wiesel & Hubel 1963*a*, *b*, 1965; Shatz & Stryker 1978).

Both cats were perfused 18 months after lid suture and alternate sections from the l.g.n. and cortex on each side were stained for cytochrome oxidase and Nissl. In the l.g.n. mild atrophy of neurons in deprived laminae was visible in Nissl sections, as expected. Nevertheless, there was no convincing loss of cytochrome oxidase activity, when compared with adjacent laminae of the normal eye. This corroborates a report by Kupfer & Palmer (1964) that NADH diaphorase levels appear undiminished by monocular suture performed in kittens at 4 and 35 d old, followed by 28 d survival.

In the cortex, no clearcut effect of visual deprivation on cytochrome oxidase staining was seen. In figure 36, plate 21 the cortex contralateral to the closed eye is illustrated. There is some faint mottling in layer IV that might correspond to the ocular dominance columns, but without verification by another technique it is not possible to be sure. In normal animals often some fluctuation in density of cytochrome oxidase staining is visible, probably because of slight unevenness in section thickness and subtle changes in depth in the cortex. Considering that layer IV in the cat is more binocular than in the macaque it is not surprising that the ocular

---

DESCRIPTION OF PLATE 20

FIGURE 35. (*a*). Cytochrome oxidase section superficial to the section from the same block illustrated in figure 33. Most of the section passes through layers II and III and the severe effect of visual deprivation upon the patches is apparent: in every other row the patches appear darker and more confluent. Three dark rows are marked by arrows. Careful comparison with figure 33 has shown that the dark rows of patches fit in register with the dark cytochrome oxidase columns in layer IV. This can also be appreciated by following dark rows of patches from layers II and III into layer IV (at top or left) where they merge with dark columns of the same width.

(*b*) An adjacent section stained for AChE activity. The effect of visual deprivation upon AChE staining is quite similar to the effect seen in (*a*) upon cytochrome oxidase staining: the patches lying in every other row appear more darkly labelled and confluent. Comparison of (*a*) and (*b*) has confirmed that the dark rows of cytochrome oxidase patches match the dark rows of AChE patches. Three arrows indicating dark rows of AChE patches correspond in position to three arrows in (*a*). Scale = 2 mm.

dominance columns are not clearly visible. Even in the macaque they appear faint in layer IV after visual deprivation.

The upper layers from this same cat were illustrated in figure 12. No patches were visible, nor was any abnormality that could be ascribed to the effects of monocular suture. The section looks identical to sections obtained from two normal cats.

Wong-Riley (1979) has demonstrated rather different effects of visual deprivation in kittens upon cytochrome oxidase staining in the l.g.n. and cortex. However, timing of lid suture and survival schedules were different from those followed in our experiments, and those of Kupfer & Palmer (1964), which makes comparison difficult.

(iii) *Comparison of the effects of eye removal and eyelid suture*

In layer IV columns appear after eyelid suture, but they appear relatively much fainter than the columns produced by eye removal. There is no striking difference between the effect on cytochrome oxidase levels in IV$c_\beta$ and IV$c_\alpha$, as there is with enucleation. Most importantly, the columns induced by monocular deprivation are unequal in width. The dark columns are much thinner than the light columns, in fact, they are the same width as the rows of dark patches in layers VI, V, III and II. In normal animals the cytochrome oxidase pillars are interrupted in layer IVc, so that no pattern is visible in tangential sections. Visual deprivation seems to reveal a hidden core structure centred within each ocular dominance column in layers IVc and IVb that matches in width the rows of patches above and below.

One is reminded of the pattern of Liesegang bands discovered by LeVay *et al.* (1975) in layer IV of normal animals. This pattern consists of wide dark bands that fit within each ocular dominance column, separated by thin light strips that straddle the boundaries between columns. This pattern has always lacked a satisfactory explanation; it is tempting to draw a connection between it and the rows of cytochrome oxidase patches. The dark bands may reflect an increased density of fibres within layer IV, connecting the patches in layer VI and V with those in layers III and II to form a single continuous pillar. The light bands may represent the space separating each row of pillars.

LeVay *et al.* (1980) have studied the effect of visual deprivation on the pattern of Liesegang staining in two macaques monocularly sutured at 12 and 14 months old. There was no expansion or shrinkage of l.g.n. afferents in layer IV as shown by radioautography, nor was there any decrease in geniculate cell size. However the Liesegang pattern was grossly distorted: the dark bands belonging to deprived eye columns appeared very pale, causing them to blend with the thin light border strips, creating a pattern of abnormally wide light bands alternating with shrunken dark bands. The overall appearance (see figure 24, LeVay *et al.* 1980) was extremely similar to the appearance of cytochrome oxidase staining in layer IV in visual deprivation (figure 33). To summarize these points, the light and dark columns in the Liesegang and cytochrome oxidase stains are compared in a scheme in figure 37.

Why should visual deprivation cause a Liesegang pattern of alternating fat light bands and thin dark bands to develop in layer IV? Apparently visual deprivation causes structural changes in the density or composition of cortical fibres that reduces their affinity for silver, thereby obliterating the distinction between the dark bands centred within the deprived eye columns and the pale border bands. In the cytochrome oxidase stain, levels of activity fall in deprived eye columns. The decrease is slightly less in the core zone of each deprived eye column than in the border strip. This can be appreciated in figure 34*a*: the core zone of each deprived eye

column is just visible as a slightly more dense, dot-like region in the middle of each light column (long arrows). The fact that the dark cytochrome oxidase columns in figure 34*a* are thinner than the full width of the non-deprived eye dominance columns (as defined by the size of the gaps in the HRP label in figure 34*b*) leads inescapably to the conclusion that visual deprivation affects cytochrome oxidase staining in non-deprived eye columns too, though less severely than in deprived ocular dominance columns. The effect is similar; cytochrome oxidase levels are depressed more in the border strips than in the core zones. The net result is that the non-deprived-eye border strips merge with the border strips and core zones of the deprived eye, producing a single fat pale band.

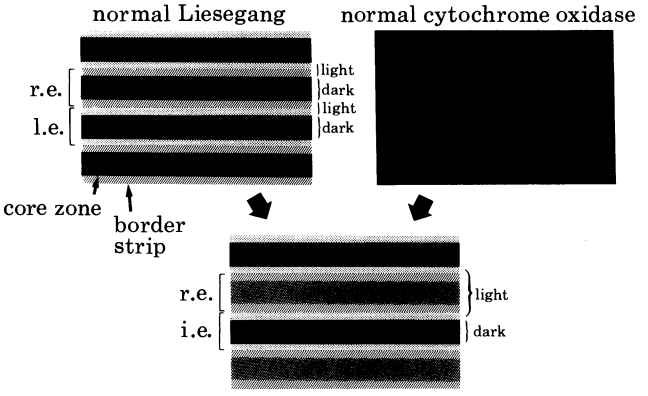


FIGURE 37. Schematic representation of the effect of visual deprivation on Liesegang and cytochrome oxidase staining in layer IV. In normal macaques no pattern is seen in layer IVc in the cytochrome oxidase stain. In the Liesegang stain a pattern of alternating wide dark bands and thin pale bands is present normally. The dark bands are proposed to correspond to the 'core zones' of the ocular dominance columns; the pale bands consist of combined 'border strips' of adjacent ocular dominance columns. The square brackets marked 'r.e.' and 'l.e.' denote the boundaries of the ocular dominance columns occupied by geniculate terminals driven by the right eye and left eye respectively. If the right eye is deprived, Liesegang staining in core zones of the r.e. weakens, causing a pattern of alternating wide light bands and thin dark bands to emerge. Cytochrome oxidase staining also decreases in the r.e. core zones. However, it falls in l.e. and r.e. border strips too, causing a pattern to develop which appears similar to the pattern of Liesegang staining. The loss of cytochrome oxidase activity is slightly greater in the l.e. and r.e. border strips than the r.e. core zones, causing the r.e. core zones to appear faintly visible (diamond hatching) as indicated in figure 34*a* (long arrows).

In layers VI, V, III and II, visual deprivation causes alternate rows of patches to appear darker. These rows of dark patches lie in register with the core zones in layer IV. The most pronounced effects of visual deprivation are seen outside layer IV, in fact, they appear almost as severe as the effects of enucleation.

### (*g*) *Pattern of patches in optic disc and monocular crescent regions of macaque striate cortex*

The evidence from [$^3$H]proline eye injection, eye removal, and eyelid suture indicates that patches in macaque striate cortex are organized into rows that lie in register with the ocular dominance columns in layer IV. In two regions of cortex, containing the representation of the optic disc and the temporal crescent, ocular dominance columns are absent. Are patches still present in these regions and, if so, what pattern do they form?

#### (i) *Optic disc*

The location of the optic disc representation in striate cortex has been located by [$^3$H]proline

transneuronal radioautography in the roof of the calcarine fissue, about 6–10 mm from the midline. Ipsilateral to the injected eye it appears as a large oval of continuous label embedded within a surrounding pattern of ocular dominance columns; contralaterally it is devoid of label (LeVay *et al.* 1980; Swindale *et al.* 1981). This anatomical evidence proves that in layer IV there is no geniculate substrate for the presence of ocular dominance columns. Conceivably, however, by some 'fill-in' mechanism from cortex surrounding the optic disc representation the layers outside layer IV might be organized into 'physiological' ocular dominance columns. This hypothetical scheme could allow a normal pattern of cytochrome oxidase patches in the disc area, organized into alternating rows corresponding to each eye.

Evidence from 2-deoxyglucose experiments militates against this notion. Kennedy *et al.* (1976) have shown in coronal radioautographs from a monocularly occluded macaque that ocular dominance columns appear absent in the optic disc representation. We have studied the deoxyglucose appearance of the optic disc in one monkey (number 17) whose right eye was removed. [$^{14}$C]2-Deoxyglucose was administered 18 days later while the left eye was stimulated with moving vertical stripes of irregular width and spacing. The resulting pattern of 2-deoxyglucose uptake is shown in the roof of the calcarine sulcus in the right striate cortex (figure 38). A pale oval is visible, corresponding to the expected shape and location of the optic disc representation of the left eye. Within this oval, which passes obliquely through layers IV, III and II, no pattern is present. When 80 consecutive serial sections were searched, from white matter to layer I, no trace of any pattern was seen within the optic disc representation. Therefore, to the extent that the 2-deoxyglucose technique accurately reflects local neuronal activity, the optic disc representation in all layers is purely monocular, metabolically and physiologically. This means that if patches are present within the disc area, they must all be dominated by the ipsilateral eye.

To determine if patches are indeed present within the optic disk representation, a proline eye injection was performed, hoping to mark the disk area in layer IVc, with the intention of then examining cytochrome oxidase stained sections from the cortex above. Unfortunately, the eye in this monkey (number 10) was damaged by the injection, as already described (see figure 27). In the cortex the cytochrome oxidase stain showed the ocular dominance columns clearly in layer IVc. A montage of sections from the roof of the right calcarine fissue, ipsilateral to the damaged eye, is illustrated in figure 39*a*, plate 22. The representation of the left optic disc appears as a pale oval, amid surrounding ocular dominance columns that match the pallor of injured-eye columns. The ratio of the major to minor axis of the optic disc oval is 2.3:1. Notice that the oval is aligned with its major axis running parallel with the general flow of the ocular dominance column pattern in surrounding cortex.

The fundus of the right eye from this monkey is pictured in figure 39*b*. The optic disc appears as a white egg-shaped structure with large blood vessels emanating from the rim. It appears more nearly circular than the representation of the optic disc in the cortex: the ratio of the major to minor axis is 1.4:1. Thus while both the optic disc and its cortical representation are oval, the major axis of the cortical representation is relatively more elongated, by a factor of 1.65:1 (2.3/1.4:1).

When more superficial sections were examined from this monkey, alternate rows of light and dark patches were seen (figure 40*a*). In an oval shaped region, located roughly where the optic disc representation appeared in layer IV, the patches did not seem to be organized in a light and dark pattern. To see if these patches might lie within the confines of the disc area a

reconstruction was prepared (figure 40*b*). The section in figure 40*a* actually passes through several layers (II, III, IV) which accounts for the unevenness of staining in some areas. Where it passes through layers II and III light and dark rows of patches fit in register with the light and dark ocular dominance columns in IVc. In the disc representation, where ocular dominance columns are absent, patches are nonetheless clearly visible. They appear more widely spaced and better separated. Cytochrome oxidase patches were also present in the representations of the optic discs of the monkey studied six months after eye removal.

We have also examined the disc area in both hemispheres in the two visually deprived monkeys (numbers 15, 16). Similar findings were present in both animals, an example is illustrated in figure 41*a*, plate 23 a section through the roof of the right calcarine sulcus, ipsilateral to the sutured eye. Again, the patches are grouped into alternate light and dark rows following the course of the ocular dominance columns in IV, except in one region, presumably the optic disk representation of the contralateral eye, where this pattern breaks down and isolated patches appear. This is drawn schematically in figure 41*b*; because the patches in dark rows appear so confluent, making it hard to draw them accurately, they are represented as continuous columns. In the optic disc area, where these continuous columns are absent, the patches appear larger, rounder, more widely spaced, and organized into a more nearly square array compared with patches in surrounding cortex. Their density has been measured in disc representations from two animals and is about 3.1 patches per $mm^2$. The density of patches in immediately adjacent binocular cortex is higher, about 5.6 patches per $mm^2$. Therefore it seems that in the optic disc region, where only one eye is represented, the density of patches falls by almost, but not quite half, rather as if the rows of patches corresponding to the contralateral eye simply drop out.

In one normal macaque we examined the roof of the calcarine sulcus, but could not recognize a region of lowered patch density that might correspond to the disc representation. This may have been because of variability in position of the disc area from animal to animal. Obviously the location of the optic disc area in normal animals must be marked by some anatomical technique. We attempted to do this by transneuronal radioautography, but damaged the eye in making the injection, thereby perturbing cytochrome oxidase staining in the cortex (figure 39*a*). Because there is always a risk of eye injury with isotope injection it would probably be better to use 2-deoxyglucose in a monocularly stimulated monkey to identify the disc representation. This approach has the additional advantage of labelling the optic disc representation in all layers, not just IVc.

It is still possible to extrapolate from the cases involving eye-removal and eyelid closure. The evidence from the 2-deoxyglucose experiment (figure 38) indicates that the optic disc representation is entirely monocular through all layers. Therefore, while suturing or removing the ipsilateral eye will cause all the patches in the disc area to fade, it should not alter their overall pattern, as it does in binocular regions. Probably it is safe to infer that in normal animals the patches are larger, rounder, and more widely spaced in the disc representation.

(ii) *Monocular crescent*

In the cortex ocular dominance columns are also absent in the far periphery of the visual field, where only the extreme nasal retina of the contralateral eye is represented (Wiesel *et al.* 1974). We have examined cytochrome oxidase staining in flat-mounted sections containing this 'monocular crescent' in both hemispheres of the eye-damaged monkey (number 10), both

visually deprived monkeys (numbers 15 and 16), and one normal monkey (number 4). In the normal monkey a region was visible in the extreme periphery where the patches looked rounder and larger, and the spacing between patches suddenly increased. This transition probably marked the beginning of the monocular crescent representation, although no independent evidence was available. In the eye-removal or eye-closure cases the border line between monocular and binocular cortex is clearly marked because the pattern of alternating rows of light and dark patches ceases abruptly. An example is shown in figure 42*a*, *b*, two sections 75 μm apart from the same block containing peripheral cortex contralateral to the sutured right eye. Alternating rows of light and dark patches, about 250 μm apart, are visible streaming at right angles to the 17–18 border; here the density of patches is about nine patches per $mm^2$. Lower in each section this pattern of alternating rows breaks up and isolated patches are seen, generally appearing larger and rounder than patches in binocular cortex. They are spaced about 400 μm apart with a density of 5.5 $mm^{-2}$. There is some suggestion that the patches in this area, the monocular crescent, are still organized into a regular array, more square than in binocular cortex, with some rows approaching the 17–18 border at right angles. The monocular crescent ipsilateral to the closed eye from this same animal is illustrated in figure 42*c*; the same effects can be seen although a smaller region of monocular crescent is included in this section.

### (*h*) *Correlation between cytochrome oxidase staining and 2-deoxyglucose uptake*

We originally became interested in the cytochrome oxidase stain to compare its laminar distribution with the laminar distribution of 2-deoxyglucose in macaque striate cortex. After

---

## Description of plates 21 and 22

Figure 36. Tangential section through the left striate cortex from a cat whose right eye was sutured closed 18 months earlier at four weeks old. In layer IV some faint irregularity in cytochrome oxidase staining is visible, but ocular dominance columns are not seen. A more superficial section from this cat was illustrated in figure 12. Scale = 1 mm.

Figure 38. Deoxyglucose appearance of the optic disc representation in monkey whose right eye was removed 18 d before experiment; left eye was stimulated with moving vertical stripes of irregular width and spacing. In roof of right calcarine sulcus, encircled by a band of white matter (w.m.), a pale oval is visible, corresponding to the expected shape and location of disk representation of the left eye. In 80 serial sections from white matter to layer I, no pattern of deoxyglucose uptake was present within the disk area. To the left (anterior) a coarse pattern of spots is seen in V2. Scale = 2 mm.

Figure 39. (*a*) Montage of cytochrome oxidase stained sections in layer IV of right striate cortex from a rhesus monkey whose right eye was damaged during intravitreal injection of [$^3$H]proline. Region shown is from the roof of the calcarine sulcus; anterior is up and medial to the left. Representation of the left optic disc appears as a pale oval with a ratio of major to minor axis of 2.3:1. The major axis of the oval is oriented parallel to the general flow of the ocular dominance column pattern in surrounding cortex. Scale = 1 mm.

(*b*) Fundus of the injured right eye: the optic disc appears as a white oval (ratio of major: minor axis = 1.4:1) structure with large blood vesssels emanating from the rim. Fovea is visible to the left as a dark spot. The cortical representation of the optic disc is elongated by 1.65 times (2.3/1.4). Scale = 1 mm.

Figure 40. (*a*) Single section superficial to montage of layer IV illustrated in figure 39*a*. Where section passes through layers II and III rows of light and dark patches are present, except in an oval region located approximately where optic disc representation appeared in layer IV. In this area, patches are present but not organized into an alternating light and dark pattern.

(*b*) Reconstruction prepared by transferring the pattern of ocular dominance columns from figure 39 onto the section illustrated in (*a*), according to procedure employed to prepare reconstructions in figures 23 and 28. As expected, light and dark rows of patches in upper layers fit in register with ocular dominance column pattern. In region corresponding to the disc representation where ocular dominance columns are absent, patches are present but appear more widely spaced and separated. Scale = 1 mm.

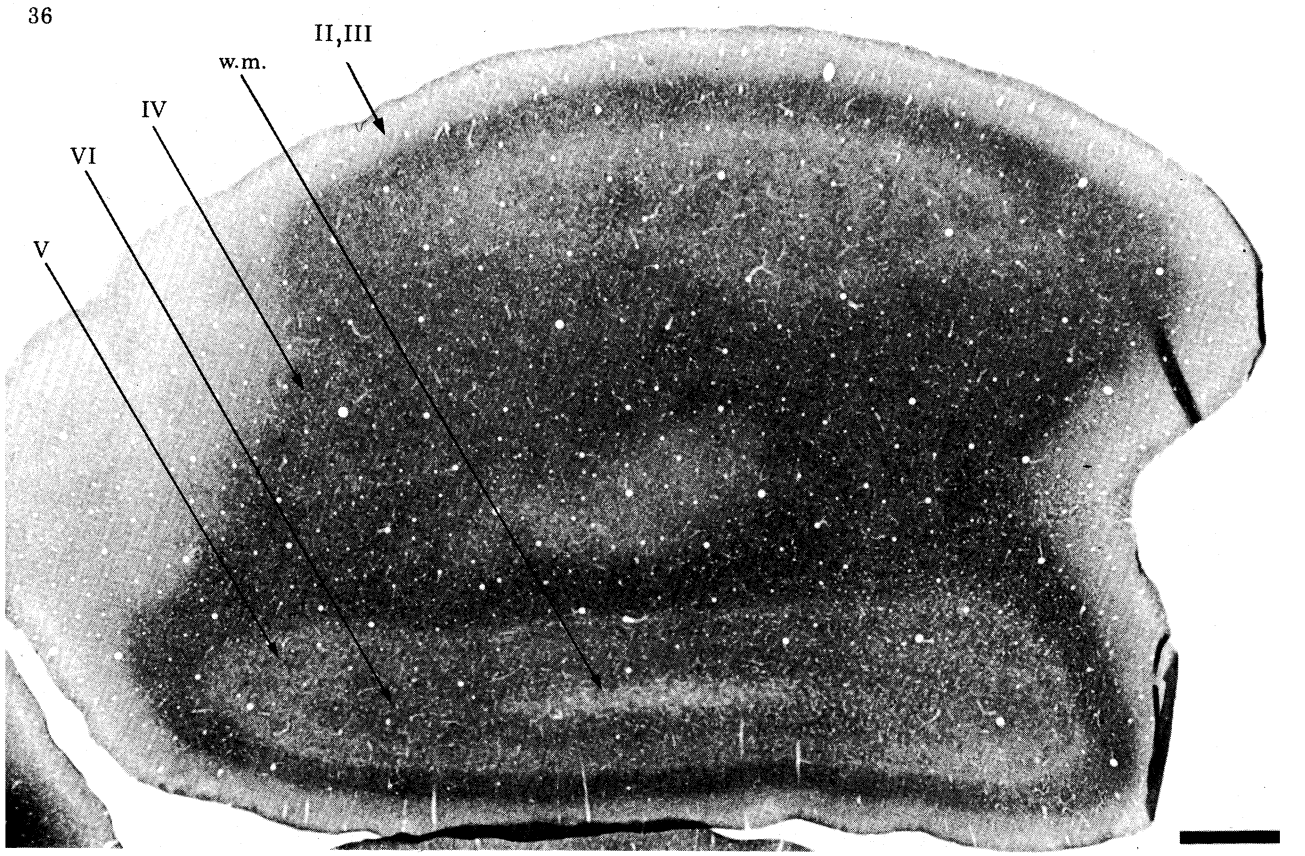



FIGURES 36 AND 38. For description see opposite.

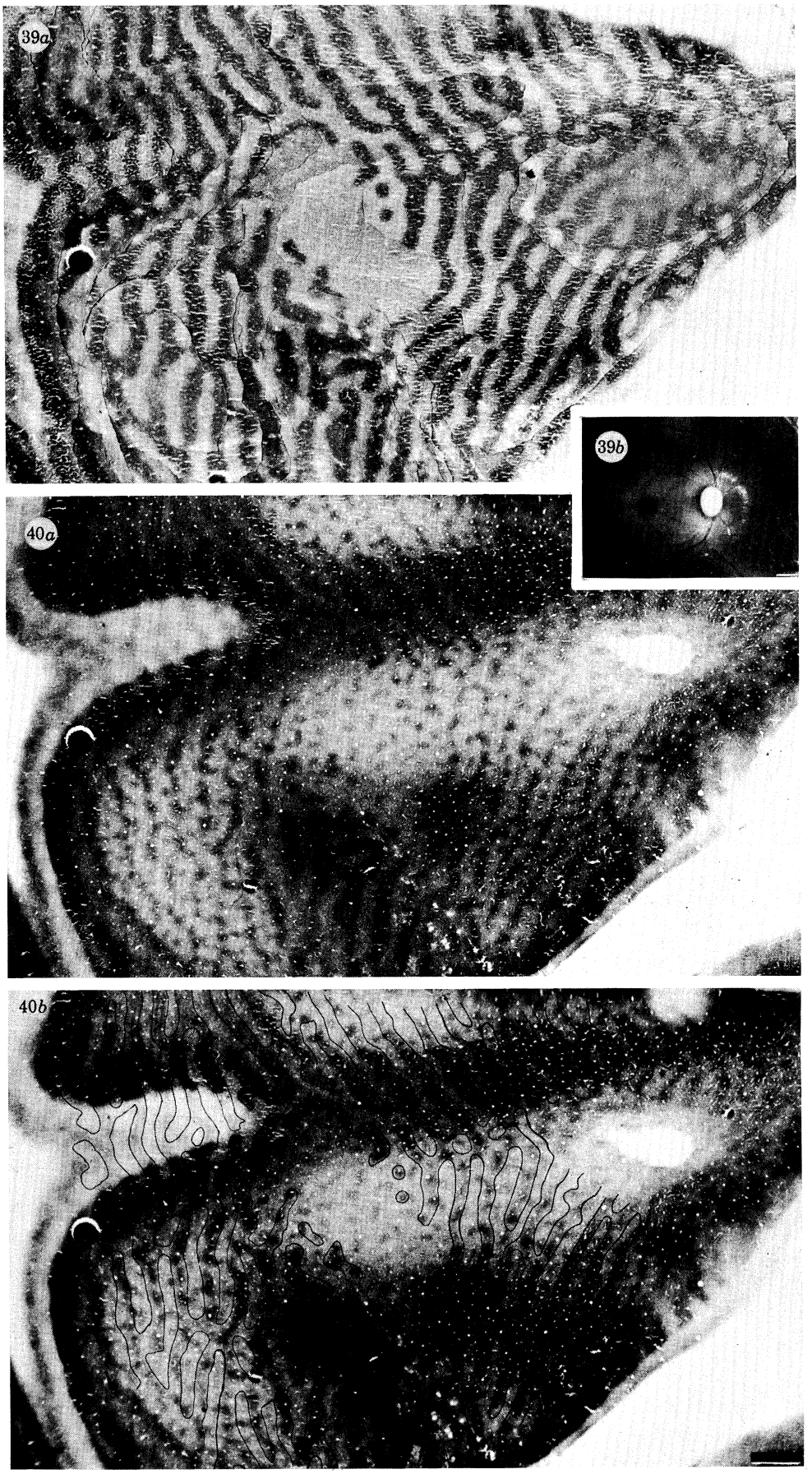


FIGURES 39 AND 40. For description see p. 232.

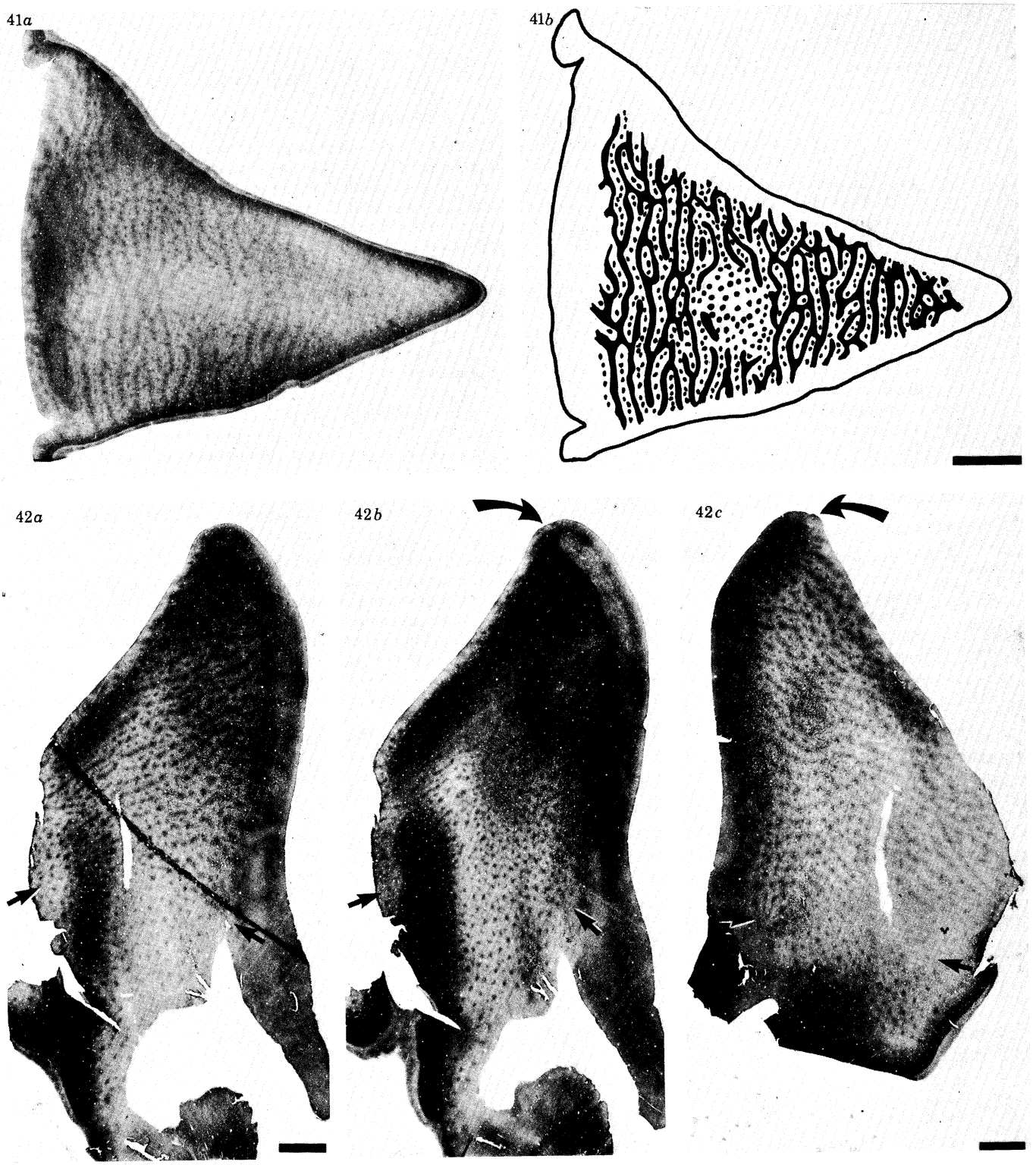


FIGURES 41 AND 42. For description see over.

## Description of plates 23 and 24

Figure 41. (*a*) Cytochrome oxidase stained section through the roof of right calcarine sulcus from macaque whose right eyelid was closed for six months: medial is to left, anterior is up. Patches are organized into light and dark rows, except in an oval region representing the optic disc of the contralateral eye.

(*b*) Drawing of section illustrated in (*a*). Patches along dark rows tend to coalesce, making them difficult to draw accurately, so they have been represented as continuous columns. In optic disc area, where continuous columns are absent, patches appear larger and rounder. Their density (3.1 $mm^2$) is about half their density (5.6 $mm^2$) in surrounding binocular cortex. Scale = 5 mm.

Figure 42. (*a*) Section through left striate cortex along the stem of the calcarine sulcus containing representation of extreme periphery of the visual field; same monkey as illustrated in figure 41. Alternating light and dark rows of patches in layers II and III are seen running perpendicular to the 17–18 border that lies at the right edge of the section. The border between monocular and binocular cortex passes between the pair of arrows; below the pattern of alternating light and dark rows is replaced by an array of evenly staining patches, appearing larger and rounder.

(*b*) Slightly deeper section from the same block, curved arrow points to the 17–18 border and pair of arrows marks transition between binocular and monocular cortex. Top of section in binocular cortex has passed into layer IV and patches are not visible. Below in monocular cortex, section passes through base of layer III and patches are clearly seen.

(*c*) Corresponding region of right striate cortex from the same monkey. The 17–18 border is indicated at left edge of section by curved arrow. Below pair of arrows, in monocular crescent representation, patches are visible. Scale = 2 mm.

Figure 43. (*a*) 2-Deoxyglucose radioautograph from the one-eyed monkey illustrated in figure 38. In tangential section through striate cortex from the right operculum ocular dominance columns appear as light and dark bands in layer IV. The three arrows mark several dark ocular dominance columns.

(*b*) Section used to prepare the radioautograph in (*a*) after processing for cytochrome oxidase activity. Enzyme activity is richest in layer IV, where ocular dominance columns are visible. The three arrows are placed in exactly the same location as in (*a*). Note that dark columns of cytochrome oxidase activity match dark columns in the 2-deoxyglucose radioautograph. Scale = 2 mm.

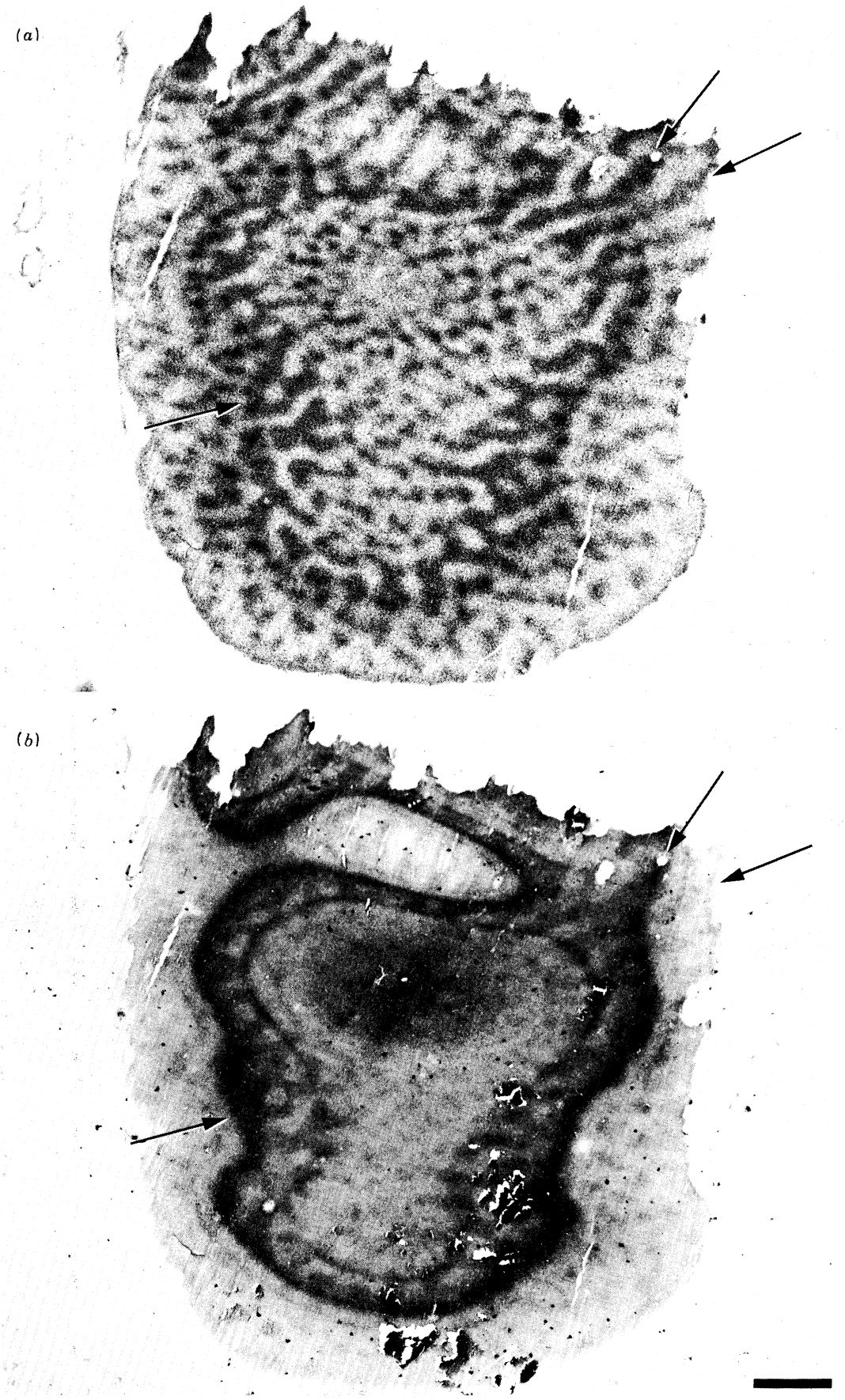


FIGURE 43. For description see opposite.

44*a*

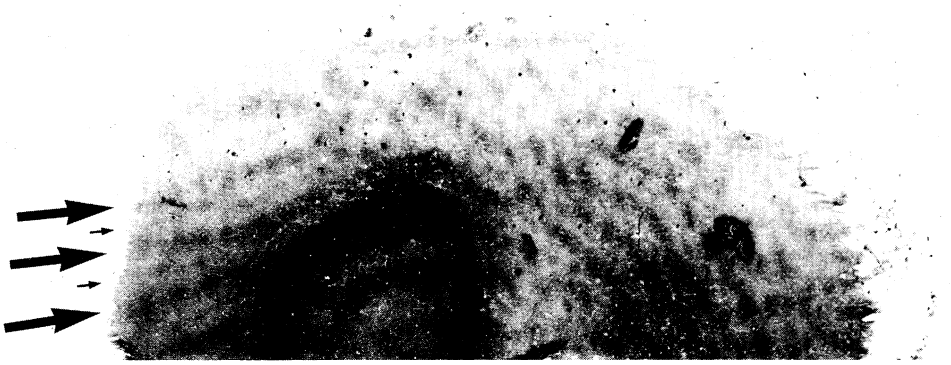

44*b*

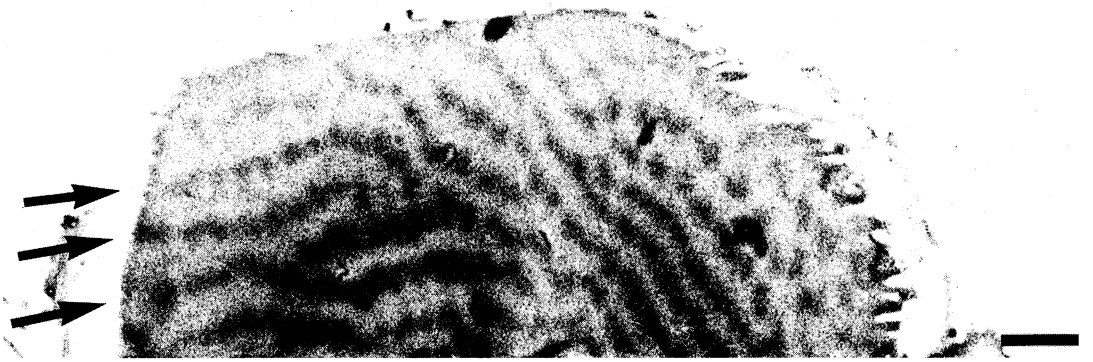

45

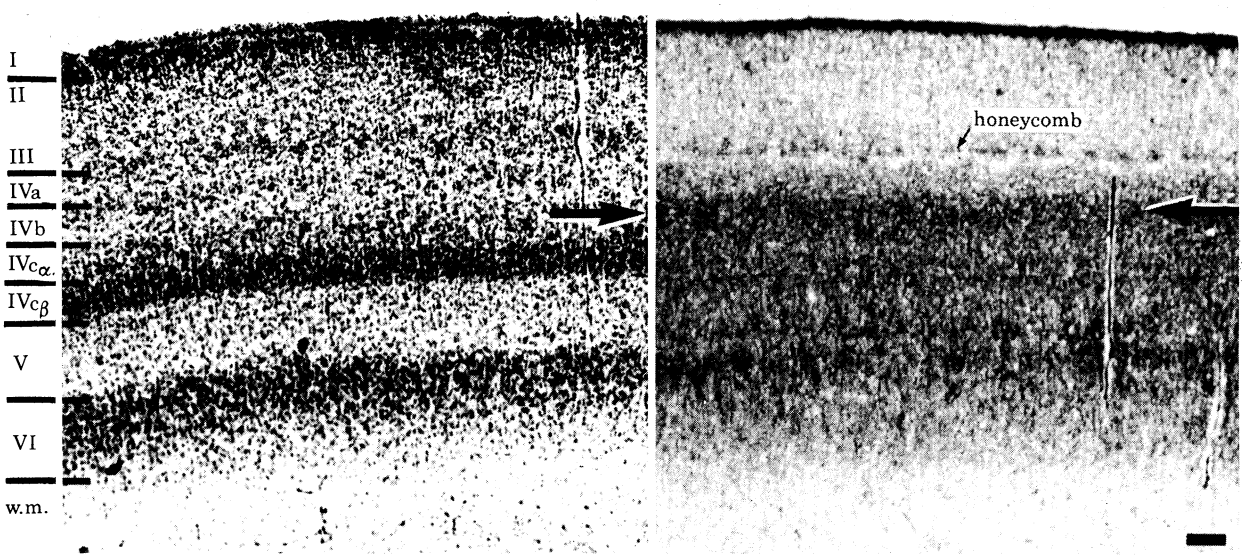


FIGURES 44 AND 45. For description see opposite.

## Description of plates 25 and 26

Figure 44. (*a*) More superficial section through right striate cortex from the one-eyed monkey illustrated in figures 43 and 38. In layers II and III cytochrome oxidase stain shows alternating rows of dark (large arrows) and light (small arrows) patches as a result of eye removal. Along each row the patches partially merge, forming almost continuous bands.

(*b*) 2-Deoxyglucose radioautograph of the section in (*a*) prepared before processing for cytochrome oxidase activity. Rows of patches are present (large arrows) that match the dark rows of patches labelled by cytochrome oxidase in (*a*). These rows correspond to the remaining eye which was stimulated by vertical stripes during the administration of deoxyglucose. Scale = 2 mm.

Figure 45. Comparison of Nissl and cytochrome oxidase staining in coronal section through striate cortex of a normal macaque foetus at E-144. In the Nissl stain the cortex appears similar to adult cortex; all the major cell layers are formed, as indicated to the left. In the cytochrome oxidase stain the cortex appears less mature compared with the adult (see figure 2). More layers are present, some lacking a clearly defined counterpart in the Nissl stain. Pair of arrows mark a prominent band of dark cytochrome oxidase activity, corresponding to layer IVb and the upper portion of IV$c_{\alpha}$, not present in the adult. Scale = 100 μm.

Figure 46. (*a*) Tangential section through the left operculum of an E-143 foetus. Cytochrome oxidase stain shows patches, more clearly in layer III than layer II. At lower right, the dark ring labelled 'IV' marks the dark band of cytochrome oxidase staining present in layer IVb–IV$c_{\alpha}$.

(*b*) A slightly deeper section from the same block, again showing patches in the upper layers. In layer IVb–IV$c_{\alpha}$, which stains darkly for cytochrome oxidase, patchess are also seen. When compared, the pattern of patches in layer IV matches exactly the pattern in the upper layers. Scale = 2 mm.

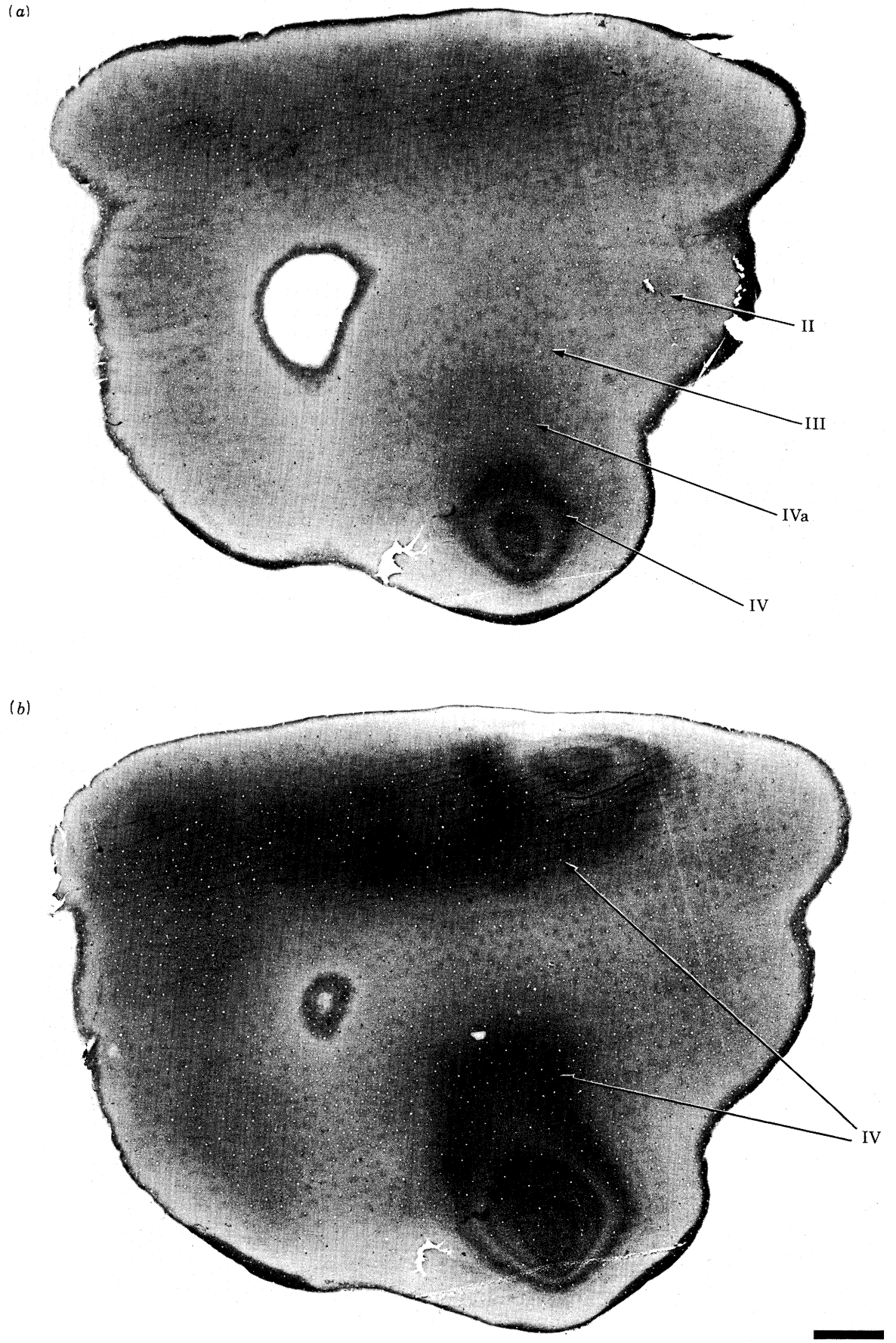


FIGURE 46. For description see previous page.

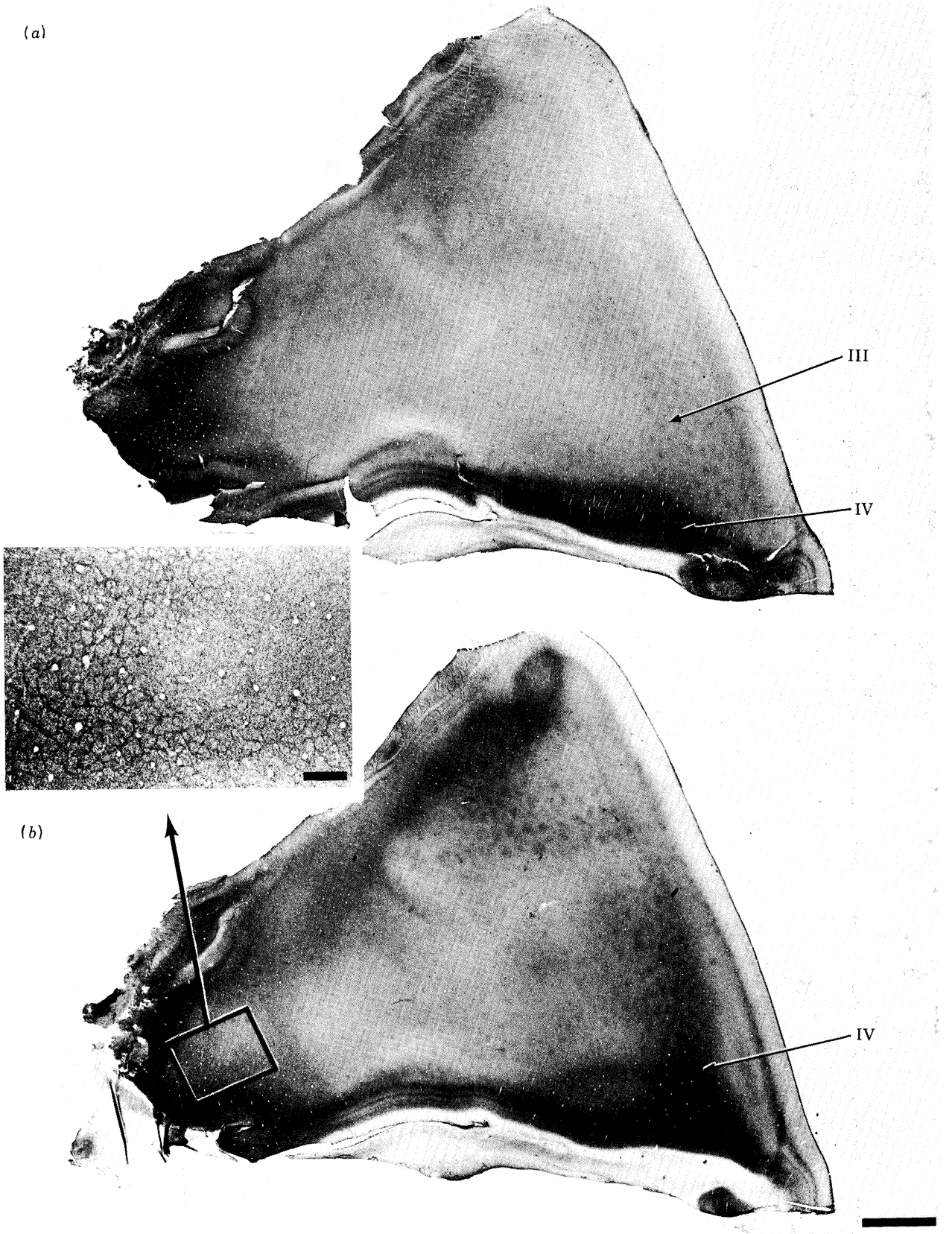


FIGURE 47. (*a*) Section from the roof of the left calcarine sulcus from the monkey illustrated in figure 46, showing patches in the upper layers.

(*b*) A deeper section from the same block grazing the dark band in layer IV, showing the patches more clearly. Scale = 2 mm. Inset: coarse pattern of cytochrome oxidase staining in layer IV a which closely resembles adult honeycomb pattern characteristic of layer IV a. Scale = 200 μm.

discovering that cytochrome oxidase has a non-homogeneous distribution in tangential sections within a single layer, we attempted to correlate the cytochrome oxidase stain with patterns of 2-deoxyglucose uptake elicited by different patterns of visual stimulation.

(i) *Stimulation with all orientations*

In particular, we hoped to shed light on a puzzling finding described by Kennedy *et al.* (1976) in their pioneering 2-deoxyglucose mapping study of macaque striate cortex. In a monkey monocularly stimulated with a complex geometric pattern, or by viewing the surrounding laboratory, ocular dominance columns were visible in layer IV, as anticipated. But in the upper layers, 'the columns appeared in cross section as dots arranged in parallel rows that seem to merge in layer IV' (see their figure 5). According to the model of striate cortex prevailing at that time (figure 1), monocular stimulation with a pattern containing essentially all orientations should have resulted in ocular dominance slabs running through all layers. While outside layer IV the borders of these slabs might be expected to appear blurred by the presence of binocularly responsive cells, the existence of a dot-like pattern outside layer IV was unexpected. Surprisingly, this discrepancy received little notice until several years later when Hendrickson & Wilson (1979) called attention to it. In their experiments, monocularly occluded macaque and squirrel monkeys viewing a laboratory scene showed a 2-deoxyglucose pattern of dots in the upper layers of striate cortex. In the macaque the dots were arranged in rows 700 μm apart, in the squirrel monkey the dots were not organized into obvious rows; average spacing was 478 μm. Hendrickson & Wilson (1979) concluded that perhaps the dots were 'due to some other as yet unknown aspect of cortical organization or function'. After the discovery of the cytochrome oxidase patches it seemed possible that they might also represent this unknown aspect of cortical organization. Accordingly we set out to correlate the patches with 2-deoxyglucose uptake produced by monocular stimulation with all orientations.

In an experiment illustrated elsewhere (Horton & Hubel 1981) we exposed a monocularly occluded macaque to a display of parallel black and white stripes of irregular width (0.5–1.5°) and spacing (1.5–2°) moved slowly back and forth (2–4° $s^{-1}$) in a direction perpendicular to the stripe's orientation. The pattern was rotated steadily to expose the animal to all orientations at least once every minute. In 2-deoxyglucose radioautographs through the superficial layers of cortex rows of dots were visible, confirming the reports of Kennedy *et al.* (1976) and Hendrickson & Wilson (1979). The dots tended to be larger than the patches seen in adjacent sections stained for cytochrome oxidase. When the cytochrome oxidase and 2-deoxyglucose dot patterns were compared, the patches lying in every other row, corresponding to the eye open during visual stimulation, fell within the dots of 2-deoxyglucose uptake. A similar correlation between deoxyglucose dots and cytochrome oxidase patches has been reported by Humphrey & Hendrickson (1980) in the squirrel monkey. There are at least three plausible (not mutually exclusive) interpretations of this result: (1) cells within cytochrome oxidase patches have weak or no orientation selectivity; (2) cells lying within patches are well oriented, but a mix of cells tuned to all orientations is present; (3) when the visual stimulus consists of all orientations, cells in all orientation columns are activated about equally, neutralizing orientation selectivity as a factor in determining the resulting pattern of 2-deoxyglucose uptake. Therefore only the patches, inherently richer in 2-deoxyglucose uptake and cytochrome oxidase activity, are visible.

(ii) *Stimulation with a single orientation*

Cytochrome oxidase patches in adjacent rows 350 μm apart are often aligned, forming a second set of crossing rows spaced roughly 550 μm apart. Hubel & Wiesel (1974*a*) have estimated on the basis of physiological mapping experiments that each orientation hypercolumn is about 640 μm wide. If two regular repeating patterns have the same periodicity they must intersect in some systematic fashion. The coincidence between the estimates for the dimensions of an orientation hypercolumn and the second dimension of the patch array led us to explore their relationship using the 2-deoxyglucose technique (Horton & Hubel 1981).

Macaque monkeys were binocularly stimulated with a display of parallel stripes in a similar manner to the monocular case described above. No attempt was made to align the eyes that diverged by 3–6° after induction and paralysis with succinylcholine. Similar findings were obtained in four experiments, two involving stimulation with vertical stripes and two with horizontal stripes. The resulting 2-deoxyglucose uptake patterns in the upper layers appeared as complicated, swirling lattices of beaded columns. The patches in adjacent sections stained for cytochrome oxidase tended to fall within labelled portions of the 2-deoxyglucose lattice. However, the deoxyglucose pattern was more extensive so that labelled regions of cortex were visible around and between the cytochrome oxidase patches. We concluded that either portions of the 2-deoxyglucose lattice were not labelling orientation columns, or that the orientation columns coalesce at the patches, intersecting and intermingling or giving way to unoriented cells.

One serious shortcoming of these experiments is that 2-deoxyglucose patterns were compared with cytochrome oxidase patterns in adjacent, not identical sections. In dehydrating the 2-deoxyglucose sections on a slide warmer at 98 °C to avoid diffusion, cytochrome oxidase activity was destroyed. Although adjacent sections are adequate for matching cytochrome oxidase patches with relatively coarse patterns like the pattern of ocular dominance columns, for intricate, irregular 2-deoxyglucose patterns, obviously comparison within the same tissue section is preferable. Eventually we noticed that cytochrome oxidase activity was preserved in occasional 2-deoxyglucose sections that were spared extreme heat. Since then we have found that if sections are heated to only 60 °C, dehydration will proceed rapidly enough to avoid deoxyglucose diffusion without harming cytochrome oxidase reactivity. Results from these experiments are more compelling because alignment between the cytochrome oxidase and 2-deoxyglucose patterns is perfect.

An example will be illustrated from one monkey (number 17) whose right eye was removed 18 d before the 2-deoxyglucose experiment.The animal was stimulated with a display of vertical stripes of irregular width (0.5–1.5°) and spacing (1.5–2°) moved slowly back and forth (2–4° $s^{-1}$). The optic disc representation in the right cortex from this animal was shown in figure 38.

Sections were exposed against X-ray film to prepare radioautographs and then processed for cytochrome oxidase activity. In a radioautograph through the right operculum (figure 43*a*, plate 24) faintly connected dots of 2-deoxyglucose uptake were visible in all layers except IV, where the ocular dominance columns were seen. The patches in the cytochrome oxidase stain (figure 43*b*) were rather faint, because some enzyme activity was lost in processing, although the ocular dominance columns in layer IV were clear. Comparing figure 43*a*, *b* we have verified that in layer IV the dark cytochrome oxidase columns match the dark columns in the

2-deoxyglucose radioautograph, confirming that ocular dominance columns corresponding to the remaining eye label more intensely with both techniques.

A more superficial section from the right cortex just grazing layer IVc processed for cytochrome oxidase and 2-deoxyglucose is shown in figure 44 *a*, *b*, plate 25. In the radioautograph dots of label are present in layers II and III, merging as they pass into layer IV. In the cytochrome oxidase stain, alternating rows of dark and light patches are visible, as expected after enucleation. The dark patches fit precisely within the dots of 2-deoxyglucose uptake visible in the radioautographs. Thus it appears that under some conditions with either binocular or monocular stimulation it is possible to generate 2-deoxyglucose patterns, using a stimulus confined to a single orientation, that include regions of cortex containing the cytochrome oxidase patches.

### (*i*) *Cytochrome oxidase staining in foetal macaques*

The findings presented in earlier sections demonstrate that the cytochrome oxidase patches are organized into rows that lie in register with the ocular dominance columns in layer IV. It was therefore natural to inquire how this special inter-relationship between patches and ocular dominance columns forms during the development of the visual cortex. The cells in the upper layers of the cortex are born around E-90, about 10–15 d later than cells in layer IV (Rakic 1977). They also remain vulnerable to the effects of monocular deprivation up to one year after birth, much longer than cells in IVc, which lose their sensitivity to deprivation at only ten weeks. If the maturation of the upper layers lags behind layer IV, one might suppose that after the ocular dominance columns form in IVc they determine the pattern of patches. While this might be true in binocular regions of cortex, certainly in monocular cortex the patches develop and organize into an array without any guidance from ocular dominance columns. Perhaps this is also true in binocular cortex; if so, how do the two systems end up in alignment?

Interpretation of the results presented below depends on an accurate knowledge of the timing of the development of the ocular dominance columns. Rakic (1977) has shown by transneuronal radioautography, after eye injection of [$^3$H]proline and fucose in a foetal rhesus monkey, that at E-144 labelled geniculocortical axons form a continuous sheet in layer IV. However, grain counts disclosed a faint periodic fluctuation in density, indicating that geniculate afferents were just beginning to segregate. Thus it is probably fair to take E-144 as around the starting date of ocular dominance formation. This is three weeks before birth at E-165. Three weeks after birth, LeVay *et al.* (1980) report that ocular dominance columns are nearly adult in appearance. So, apparently the geniculocortical afferents for the left and right eyes segregate over a period of six weeks. To judge from more detailed studies in the cat (Shatz & Stryker 1978; LeVay *et al.* 1978), this process occurs gradually, although it has not been well examined in the monkey. Only one monkey has been tested by eye injection in the three weeks before and after birth: an animal injected by Hubel *et al.* (1977) 1 d after birth. Transneuronal radioautography after 5 d survival revealed a clear suggestion of ocular dominance columns in ipsilateral visual cortex. Probably the ocular dominance columns are better developed at 6 d than this experiment implies. Physiological recordings (Hubel *et al.* 1977) in an 8 d old monkey have shown a clear grouping of cells in layer IVc according to eye preference. Finally, Des Rosiers *et al.* (1978) have applied the 2-deoxyglucose technique to a monocularly stimulated newborn monkey and find a well developed pattern of light and dark bands in layer IV.

In this present study cytochrome oxidase staining was examined in striate cortex of both hemispheres in three foetal monkeys at gestational ages E-142, E-143, E-144 from timed pregnancies. Foetuses were delivered by hysterotomy, decapitated and the head submerged immediately in ice-cold 2% (by volume) glutaraldehyde. The anterior fontanelle was incised, the soft cartilaginous skull opened, and the brain immersed in fixative. After about 10 h fixation, just adequate to allow sectioning, the tissue was blocked, rapidly frozen against a brass plate cooled to −70 °C, and cut at 50 μm. Sections were then routinely processed for cytochrome oxidase histochemistry, with occasional sections stained for Nissl substance. Similar results were obtained in all three monkeys; material will be illustrated from the two specimens with the best staining.

A coronal section from the E-144 foetus processed for cytochrome oxidase is compared with an adjacent section stained with cresyl violet in figure 45. In the Nissl stain the cortex looks well developed, with the principal cell layers such as VI and IVc clearly identifiable. By contrast, the laminar pattern of cytochrome oxidase activity is quite different from the pattern seen in the adult macaque. It appears surprisingly complex, containing at least 14 separate laminae, many without an obvious counterpart in the Nissl stain. The most remarkable feature is a prominent wide band of intense cytochrome oxidase activity occupying layer IVb and the upper portion of layer IV$c_\alpha$; a more lightly staining gap above separates it from layer IVa. This dark band is absent in the adult macaque, where layer IVb stands out as a single light band sandwiched between IVc and IVa. In both foetus and adult, layer IVb appears relatively cell-sparse and lightly staining in cresyl violet. Thus in the foetus there is a sharp contrast between the appearance of IVb stained by cytochrome oxidase and cresyl violet.

A tangential section through layers II and III stained for cytochrome oxidase from the left operculum of an E-143 is shown in figure 46*a*, plate 26. The patches are readily visible, particularly where the section passes through layer III. Figure 46*b* shows another section from the same block, cut 250 μm deeper. In addition to the patches in layers II and III, one has the impression that the dark band of cytochrome oxidase staining that characterizes IVb in the foetus is also organized into patches. This was confirmed by exploring other regions of striate cortex, namely the roof (figure 47*a*, *b*, plate 27) and stem (not illustrated) of the calcarine fissure in the same hemisphere. In the deeper section of each pair, patches were visible in tangentially sectioned portions of layer IVb. In fact, in layer IVb the patches were more obvious and intensely labelled than in the upper layers. When the pattern of patches in each pair of sections is compared (figures 46, 47), we have verified that the patches in layers II and III lie in perfect register with the patches in layer IVb. They also lie in register with an extremely faint pattern in layer VI (not illustrated). In layers V and I the patches are not visible in the three animals tested so far, but this is not surprising since the patches are altogether fainter in foetal tissue, compared with adult specimens. In figure 47 (inset) layer IVa can be recognized by its characteristic honeycomb pattern which appears almost as well formed at E-144 as in the adult

One reason for sectioning as much cortex as possible from each hemisphere was to see if the patches might show some gradient in development, from central to peripheral cortex, for example. However, at E-142 to E-144 patches appear present and about equally well developed in all regions of striate cortex. In some areas the patches seemed to be organized into rows following the general pattern typical for that particular region of cortex in the adult. Finally, the patches were present in cortex that, at least in adult monkeys, contains the representation of the monocular crescent.

The evidence obtained from these three monkeys indicates that the patches are present remarkably early in development: by E-142 to E-144, at a time when the ocular dominance columns in IVc are apparently just beginning to form. It would be tempting to conclude that the patches precede the ocular dominance columns in development and perhaps guide their formation. However, the ocular dominance columns may actually be better developed at E-144 than they appear by transneuronal radioautography. After eye injection with a radioactive tracer, there is inevitably leakage of label into laminae corresponding to the uninjected eye, particularly in younger animals. This spillover tends to obscure the segregation of geniculate afferents in the cortex. For now, one is probably safe in concluding only that development of the patches in layers II, III, and VI does not occur after the segregation of geniculate terminals in IVc.

## 4. Discussion

### (*a*) *The geniculate projection to the patches*

The HRP injections provided evidence that each patch in the upper layers of striate cortex receives a direct projection from the lateral geniculate body. This finding, in addition to the cytochrome oxidase myelin staining correlation, indicates that the patches are structurally distinct regions. They are not merely areas in an otherwise homogeneous cortex where levels of various enzymes such as cytochrome oxidase, AChE, LDH, or SDH are elevated as a simple consequence of enhanced physiological activity. Rather, the patches are discrete anatomical structures, fixed in position, that receive a special input in layers II and III not shared by surrounding cortex. Compared with the massive geniculate input to layer IVc this projection is weak, especially to layer II. Probably only a subpopulation of cells in each patch receives geniculate contacts, or each cell receives a relatively sparse input. Thus cells in the patches are less likely, compared with cells in layer IVc, to be dominated by their geniculate input, especially if located at the fringe of a patch.

We did not make small enough HRP injections to determine which layers of the geniculate body project to the patches. Recently G. G. Blasdel and J. S. Lund (personal communication) have reconstructed the axonal arbourizations of single geniculate fibres in macaque striate cortex filled by HRP injection. In their sample of 20 fibres projecting to layer IVc, none sent collaterals into the upper layers. Of six fibres ramifying in layer IVa three sent branches into layers II, III, thus suggesting that some fraction of the neurons projecting to the honeycomb account for the projection to the patches. While this may be true in the macaque, in the owl monkey a honeycomb in IVa is lacking and the input to IV$c_\alpha$ is patchy. This indicates that the details of the organization of the geniculate projection to striate cortex will probably prove quite different in various species. Fitzpatrick *et al.* (1983) have recently done HRP studies on the geniculate projection to the squirrel monkey visual cortex. They concur that the patches receive a direct geniculate input and suggest that this projection arises from the small intercalated layers of the geniculate body. Whether the patches receive an exclusive input from a specific subclass of neurons, or share collaterals from a projection to other layers, it will be important to learn more about the receptive field properties of the geniculate cells of origin.

In the macaque, cytochrome oxidase patches are not visible in IV$c_\alpha$ and the magnocellular input to this layer is organized into ocular dominance slabs, not patches. By contrast, in owl monkey cytochrome oxidase patches are present in layer IV$c_\alpha$, and the geniculate input to IV$c_\alpha$ is patchy. In the owl monkey, Rowe *et al.* (1978) have reported patches in IV$c_\alpha$ in coronal

sections after [$^3$H]proline eye injection, that they suggested might be ocular dominance columns. However, it is also possible the patches they observed may have corresponded to the cytochrome oxidase patches in layer IV$c_\alpha$.

If projections to layer VI and the honeycomb are ignored, the existence of segregated, distinct geniculate inputs to layers IV$c_\beta$, IV$c_\alpha$, and II, III means that there are at least three parallel channels conveying geniculate information to striate cortex. Our knowledge of the receptive field properties of cells in these different cortical layers is limited. Cells in both layer IV$c_\alpha$ and IV$c_\beta$ are thought to have centre-surround receptive field organization.Absence of orientation specificity has been defended for many years as a unique feature of cells in layer IVc, whereas layers II, III have been regarded as the exclusive domain of complex cells (Hubel & Wiesel 1968). The discovery of a geniculate projection to the upper layers means that, at the very least, unoriented fibres can be recorded from in these layers. It is also tempting, particularly with our deoxyglucose results in mind, to conclude that cells in the upper layers within the patches may be unoriented. This would be consistent with the fact that cells in layer IVc, which receive a direct geniculate input, lack orientation specificity. However, it does not follow automatically that cortical layers receiving a direct geniculate input contain unoriented cells: there is no evidence for unoriented cells in layer VI of monkey striate cortex, or layer IV of cat cortex, for that matter. In any case, while some geniculate information is transmitted to supragranular cortex via layer IV, there is also clearly direct geniculate access to layers II and III. This means that either some complex cells receive direct geniculate input or that other species of cells are present in the upper layers. A recent report describes cells lacking orientation selectivity in layers II and III in the vicinity of the cytochrome oxidase patches (Hubel & Livingstone 1981).

In this paper we have stressed that the patches are really oval-based pillars or cylinders extending from pia to white matter. Vertical connections will bestow upon cells in each pillar certain common receptive field properties. For example, cells in the upper layers within a pillar will derive their input preferentially from the core zone of the ocular dominance column situated directly below in layer IVc. Consequently, most of the upper layer cells in patches will tend to be monocular, not only because they receive a direct monocular geniculate input and are located as far as possible from the borders between left and right eye dominance slabs, but as a specific result of vertical processing within each pillar. By the same token, if cells in the upper layers have special receptive field properties, this will be reflected in the properties of other cells in different layers within the same pillar. For instance, layer V cells lying within a pillar will get their strongest input from cells situated above in layers III and II.

Just as the patches in the upper layers receive a clustered input from the l.g.n., and perhaps from other sources, they may also give rise to parcelled efferent projections, although this was not true for the corticogeniculate projection in the owl monkey. After HRP injection into the l.g.n. retrogradely filled cells were scattered evenly in layer VI without preferential clumping into the patches. However, this does not rule out the possibility that some retrogradely filled cells in the patches may form a special subclass, or project back only to certain laminae of the l.g.n. The other major subcortical projection, from layer V to the superior colliculus, has not yet been tested.

There are widespread interleaving columnar connections between various visual cortical areas in the monkey (Wong-Riley 1979; Montero 1980; Gilbert & Wiesel 1980) whose relationship with the patches has yet to be tested. It seems hard to imagine that this elaborate

array of patches we have uncovered in striate cortex will not figure prominently in the pattern of connections that unites striate cortex with the rest of the brain.

Recently Rockland *et al.* (1982) have reported the existence of widespread periodical connections within the striate cortex of tree shrews and squirrel monkeys. The fact that these connections are present in the tree shrew, a nonprimate, indicates that they serve a functional role unrelated to the cytochrome oxidase patches. Nevertheless, in primates such as the squirrel monkey, they may maintain a regular, stereotypic relationship to the patches; a definitive answer on this point is not yet available.

### (*b*) *Eye removal and eyelid suture experiments*

Eye removal and eyelid suture produced very different effects in the l.g.n. and the striate cortex. Eye removal caused massive neuronal degeneration in the l.g.n. and a precipitous drop in cytochrome oxidase levels within 3–4 d, whereas no effect of eyelid suture on either cytochrome oxidase or cresyl violet staining was found even after six months. In the case of eye removal, spontaneous activity in denervated geniculate laminae falls virtually to zero (Hubel *et al.* 1977). Furthermore, if retinal ganglion cells provide any sort of trophic factors required for the sustenance of geniculate neurons, these are lost after severing the optic nerve. By contrast, with eyelid suture no lesion is inflicted and the optic pathway remains anatomically intact. Spontaneous activity in the l.g.n. is maintained and neurons continue to respond to diffuse light; during recording sessions we found that vigorous discharges were evoked by shining a flashlight through the closed lids.

Still, it was surprising to find no loss of cytochrome oxidase activity in the l.g.n. after eyelid suture. Perhaps the balance of excitation and suppression of on- and off-centre geniculate neurons by normal light patterns is roughly equivalent in terms of metabolic requirements to the maintenance of the spontaneous discharge rate. It may also be that cytochrome oxidase levels within certain terminals and processes in the l.g.n. do change slightly with deprivation, but the net effect is too subtle to be appreciated in stained histological sections.

In the cortex the ocular dominance columns become visible in layer IVc after enucleation. They resemble the appearance of ocular dominance columns seen radioautographically with [$^3$H]proline (figure 27). To judge from the severe atrophy of l.g.n. neurons caused by eye removal, the altered staining in layer IVc is due in part to loss of cytochrome oxidase activity in geniculate axon terminals. Moreover, there is probably a generalized diminution of cytochrome oxidase staining in the somata and processes of all cortical neurons that receive a driving input, direct or multi-synaptic, from geniculate cells formerly innervated by the missing eye. This presumably occurs as a result of diminished metabolic requirements secondary to functional inactivity and of transneuronal degeneration of cortical cells.

With eyelid suture, because cytochrome oxidase staining in l.g.n. cells is basically unaffected, we see the isolated effects of functional inactivity upon enzyme levels in cortical cells and processes. Pale columns appear in layer IV, but they are wider than the ocular dominance columns seen with 2-deoxyglucose after acute monocular deprivation (Kennedy *et al.* 1976). It appears that cytochrome oxidase activity falls in both deprived eye columns and along the fringes of normal eye columns. We are puzzled that eyelid suture should influence cytochrome oxidase staining within the boundaries of the open eye dominance columns in layer IVc. This effect reveals, along with the banding pattern seen in the Liesegang stain, that the ocular dominance columns contain two subdivisions: central core zones (in register with the patches)

flanked by border strips. For some reason, cytochrome oxidase activity in these two separate domains is affected differently by visual deprivation. The simplest guess is that core zones are more monocular than border strips.

Our results confirm the original report of Wong & Riley *et al.* (1978) that the cytochrome oxidase stain can be used to map alterations in enzymes levels induced by changes in neural activity. In this respect the cytochrome oxidase technique is analogous to the 2-deoxyglucose method of mapping functional activity, except that it reflects changes in protein levels occurring over days or weeks, rather than changes in glucose uptake over a period of minutes. However, the two techniques show certain discrepancies. After monocular deprivation in adult macaques we found no effect upon cytochrome oxidase staining in the l.g.n. Results obtained with the 2-deoxyglucose technique show a clearcut difference in labelling of normal and deprived geniculate laminae after acute monocular deprivation (Kennedy *et al.* 1976). It remains to be seen if any difference would be found if the monkey were monocularly sutured for several months before performing the deoxyglucose experiment. Perhaps long-term compensatory changes might nullify the differences in 2-deoxyglucose uptake seen after acute monocular exposure.

After eye removal the ocular dominance columns in the macaque appear very similar in cytochrome oxidase stained sections and 2-deoxyglucose radioautographs (figure 43). Des Rosiers *et al.* (1978) have examined 2-deoxyglucose uptake in mature macaques after three months of monocular deprivation. They report that a thin band of labelling emerges at the base of layer IV which is not seen in cases of acute monocular deprivation. This band may be related to the cytochrome oxidase band we find at the base of layer IV after four to six months of visual deprivation. In their radioautographs (see figure 1*c*, Des Rosiers *et al.* 1978) deprived eye dominance columns also appear wider than normal eye columns, but it is difficult to judge because the tissue is cut coronally. Obviously it would be interesting to combine both 2-deoxyglucose and cytochrome oxidase mapping in a macaque subjected to long-term monocular deprivation.

The changes we saw in AChE staining demonstrate that levels of cortical enzymes besides cytochrome oxidase are sensitive to effects of eye removal and eyelid suture. Probably levels of GAD, which also correlated with cytochrome oxidase levels (Hendrickson *et al.* 1981), would show a similar response to enucleation or deprivation. It is widely believed that levels of enzymes associated with neurotransmission in the central nervous system fluctuate with changes in functional activity, but surprisingly few examples of this effect have been clearly demonstrated.

If eventually we can associate certain neurotransmitter enzymes with particular receptive field properties of cells in striate cortex it may be possible to manipulate the intensity or pattern of various enzyme stains by exposing animals to appropriate chronic stimulus conditions. To take a simple example: if cells devoted to processing colour information use a given transmitter, housing monkeys under monochromatic lighting conditions might induce characteristic patterns of enzyme activity to change in the cortex. In fact, this would almost certainly occur; the real question is whether we would be able to detect and recognize it. In adult macaques, monocular deprivation induces clear changes in cytochrome oxidase, AChE, and Liesegang staining in the visual cortex. Evidently there is substantial potential for plasticity, both chemical and structural, even beyond the age when rearrangement of geniculate afferents in IVc can occur in response to deprivation. This plasticity is apparent only because we have identified an obvious enzyme pattern associated with a well segregated ocular dominance system that

can be easily altered by suturing closed an eyelid. The same experiment conducted in the squirrel monkey would show no discernable effect upon AChE or cytochrome oxidase patterns in the cortex, because the ocular dominance columns are poorly developed in this species. Yet changes would probably be occurring in the cortex, undetected by our present techniques.

### (*c*) *Findings in optic disc and monocular crescent regions*

The optic disc representation is elongated by a factor of 1.65 in the cortex. The explanation for this distortion presumably lies with the problem of maintaining overall isotropy in the magnification factor in a cortex that is diced into ocular dominance columns. Their presence in layer IVc requires that the visual field be represented twice, once for each eye. As a consequence, moving through the cortex in a direction that regularly crosses column boundaries, progression through the visual field occurs in an interlacing manner (Hubel *et al.* 1974). If the local magnification factor within each ocular dominance column were isotropic, the results would be a distortion of a circular object in the visual field into an oval in the cortex, with the major axis of the oval oriented perpendicular to the flow of the ocular dominance columns. LeVay *et al.* (1975) have suggested that this distortion is avoided by the presence of a local anisotropy in the cortex, such that the magnification factor is twice as great when moving along the ocular dominance columns, rather than across them.

In the optic disc region only one eye is represented. If it is assumed that a local 2:1 anisotropy is nevertheless maintained, the representation of the disc should be elongated by a 2:1 factor, with the major axis parallel to the surrounding ocular dominance columns. Otherwise, if the optic disc were represented exactly as it appears in figure 39*b*, it would not 'fit' within the overall retinotopy, resulting either in a frank discontinuity or an idiosyncratic distortion of the visual field map at the edge of the disk representation, where the ocular dominance columns take up again. Actually, as mentioned above, the ratio of the major axis of the disc representation to the major axis of the disc is only 1.65:1, not 2:1. This means that either the local anisotropy is relaxed slightly in the disc area, or elsewhere it is actually a bit less than 2:1. Strong evidence favouring the latter possibility has recently emerged from some elegant deoxyglucose experiments by Tootell *et al.* (1982) analysing the retinotopic map in macaque striate cortex.

The finding that patches are present in both monocular and binocular regions of cortex means that whatever functions are served by the patches, these functions are required and expressed everywhere in macaque striate cortex. Some interesting clues are afforded by the fact that the patches appear different in binocular and monocular cortex, as illustrated diagrammatically in figure 48. Their decreased density in monocular regions is probably because duplication of the patches, required in binocular cortex because the visual field must be represented twice, is unnecessary. The shape of the patches in monocular cortex is also different: they are rounder and larger. In binocular cortex, because of the 2:1 (or 1.65:1) anisotropy in the local magnification factor, the patches tend to be stretched along the length of the ocular dominance columns, resulting in an oval shape. This anisotropy is present to a significant extent in monocular cortex, as evidenced by the distorted shape of the optic disc representation. One might therefore expect patches in monocular cortex also to appear oval. That they tend to look rounder is because they are larger, merging what would be a pair of oval patches in binocular cortex, into one large monocular patch governing a wider area of tissue. In a sense, the patches

in monocular macaque cortex resemble the more circular patches of binocular squirrel monkey cortex, where ocular dominance columns are nearly absent.

The measurements provided on the density of patches in binocular cortex on the operculum (5.1 $mm^{-2}$), near the optic disc (5.6 $mm^{-2}$), and near the monocular crescent (9 $mm^{-2}$) indicate an increased density of patches in the representation of the peripheral visual field. This effect is explained by some recent findings of Connolly *et al.* (1982). They report that the width of an ocular dominance hypercolumn is roughly half as great in the far periphery as in the central

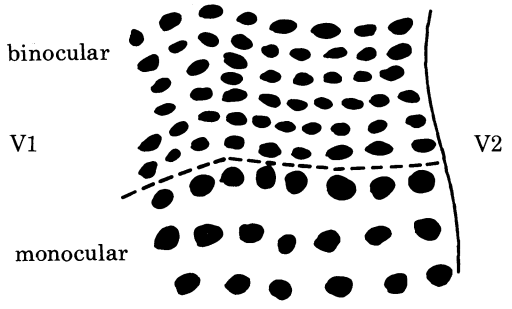


FIGURE 48. Schematic diagram showing difference between appearance of cytochrome oxidase patches in binocular and monocular cortex: dotted line marks border of temporal crescent representation. In binocular cortex rows of patches are oriented perpendicular to the V1–V2 border. In monocular cortex patches are also arranged in a regular system of rows, but their density is only about half the density of patches in binocular cortex. In addition, the patches are larger and rounder rather than oval.

visual field. Since the ocular dominance columns and patches lie in register, an increase in patch density is required, along with a small diminution in their size, to maintain this relation.

Repeatedly in this paper we have said that the cytochrome oxidase patches follow the pattern of the ocular dominance columns. Perhaps, since the patches form a pattern present throughout striate cortex, it would be more logical to say the reverse, namely that the ocular dominance columns follow the pattern of the patches. According to this view, the patches provide the fundamental organizing pattern within striate cortex, onto which the ocular dominance columns are engrafted wherever the cortex is binocular. In these regions each patch is split, as it were, into two smaller oval patches, to provide a patch for each eye's representation of the visual field. This might explain why occasionally we see patches in adjacent ocular dominance columns that give a strong impression of being paired as doublets.

### (*d*) *Development of patches in the foetal monkey*

Our cytochrome oxidase experiments in foetal macaques have shown that the patches are present and well developed at least three weeks before birth. Too little is known about the process of cortical development in the foetus to decided whether the patches precede, and perhaps guide, the segregation of the ocular dominance columns, or whether the two systems form on a parallel timetable. Whatever the case, clearly the critical events in the development of the visual cortex are occurring prenatally, and an extensive series of experimental studies in the foetus will be necessary to describe them more completely.

The cytochrome oxidase stain revealed a surprisingly complex, poorly understood laminar pattern of activity in the foetal striate cortex. Of particular interest was a prominent band of

intense staining located approximately in layer IVb. In the adult we have established that those layers that stain most intensely for cytochrome oxidase receive a direct projection from the l.g.n. The dark band in IVb suggests that this layer receives a direct geniculate input in the foetus. So far we have not confirmed this by combining cytochrome oxidase histochemistry with any of the various techniques available for labelling geniculate afferents to the foetal cortex. However, published radioautographs of striate cortex at E-144 (see figure 7*c* inset, Rakic 1977) show a strong band of label in IVb, separated by clear gaps from label in IVa and IVc. This layer also contains a striking pattern of cytochrome oxidase patches matching the patches in the upper layers.

In adult monkeys, layer IVb lacks direct geniculate input and cytochrome oxidase staining is weak; the patches appear exceeding faint, though visible. Apparently the maturation of the geniculate projection to the foetal cortex involves not only segregation of afferents in IVc, but also a loss of input to IVb, where the patches are so strikingly developed at E-143. The significance of this transient projection to IVb is unclear. We need to know more about the geniculate projection to the upper layers at various foetal ages. Is there initially intermingling of afferents driven by the left and right eyes, as in layer IVc, followed by selective dying back to leave just a patchy monocular projection to each patch? Or, quite the opposite: is the projection to the upper layers patchy from the very beginning? In that case it might be initially monocular, or binocular with eventual loss of one eye's input to alternate rows of patches. Is the geniculate input to layer IVb patchy, and does it precede the input to the upper layers? These problems could be addressed by making HRP injections into the foetal lateral geniculate body and using the tetramethylbenzidine reaction to reveal tracer transported orthogradely to the cortex. Intravitreal injection of HRP-wheatgerm agglutinin (Itaya & Van Hoesen 1982) or 2-deoxyglucose radioautography could be used to study the development of the foetal ocular dominance columns in closer detail.

If future studies show that patches form before segregation of ocular dominance columns in layer IVc, it will seem unlikely that patches take their cue from ocular dominance columns in forming their pattern in striate cortex. Further evidence could be obtained by examining cytochrome oxidase activity in an adult monkey monocularly enucleated at two to three months gestation. Such animals show a normal laminar projection from geniculate to cortex, but no grouping of terminals driven by the surviving eye into ocular dominance columns (Rakic 1981). If these animals show a pattern of cytochrome oxidase patches throughout the cortex, it will be established beyond dispute that ocular dominance columns are not necessary for patch formation in the macaque. The pattern of patches in these one-eyed monkeys may resemble the pattern and spacing seen in the temporal crescent and optic disc areas of normal animals, indicating that the development of ocular dominance columns induces certain modifications of the patches in binocular cortex. Alternatively, the pattern of patches might resemble the pattern seen in normal monkeys, in both binocular and monocular cortex, which implies that development and expression of the pattern is completely independent of ocular dominance column formation. This would not mean, of course, that patches are not susceptible to binocular interactions. Eyelid suture performed at term or in the first weeks of postnatal life causes severe contraction of ocular dominance columns driven by the deprived eye (Hubel *et al.* 1977). The Liesegang pattern is also severely corrupted (LeVay *et al.* 1980), showing abnormally thin dark bands (deprived eye's core zones) alternating with extra wide dark bands (normal eye's core

zones). One might predict that cytochrome oxidase staining in such deprived animals would show narrowed patches sitting over shrunken dominance columns belonging to the closed eye, and unusually wide patches over the expanded ocular dominance columns. In radioautographs from eye-sutured animals, the deprived ocular dominance columns in IVc often appear broken into chains of islands; perhaps each of these islands with be centred within a deprived cytochrome oxidase pillar. It will also be interesting to learn how the geniculate projection to the patches is affected by visual deprivation: will it result in alternate rows of shrunken and enlarged clusters of geniculate terminals in layers III and II? Will the timing of the critical period be different in the upper layers than in layer IV?

Finally, if patches in adult monkeys contain cells lacking orientation selectivity, or cells tuned to a mixture of orientations, they will tend on the average to be unusually active, since they will be driven effectively by any light–dark contour, regardless of orientation. This enhanced neuronal activity in turn might induce the intense cytochrome oxidase activity that is characteristic of the patches. This argument has some appeal, in the sense that cytochrome oxidase levels do reflect chronic levels of physiological stimulation, as attested to by our monocular lid suture experiments. However, the presence of the patches *in utero*, before any visual stimulation, indicates that they are an inherent feature of macaque striate cortex. Like the monkey ocular dominance columns and orientation columns, they do not depend on visual experience for their appearance early in life (Hubel & Wiesel 1977).

### (*e*) *Lessons from comparative anatomical studies*

We examined cytochrome oxidase staining in the striate cortex of 14 different species in an effort to determine if patches might prove to be associated with the presence or absence of certain cardinal features of the visual system. The patches fit in register with ocular dominance columns in the rhesus monkey, but in monocular cortex where ocular dominance columns are absent, patches are still present. In owl monkey and squirrel monkey ocular dominance columns are weakly developed, yet a beautiful pattern of patches is seen. The cat has reasonably formed ocular dominance columns but no trace of patches. These observations indicate that although patches and ocular dominance columns are aligned in some primates, ocular dominance columns are irrelevant to the basic functional role served by the patches.

Orientation columns are highly organized in cat, tree shrew, squirrel monkey, and macaque, yet only the latter two species have patches. Clearly the presence of orientation columns does not allow one to predict if patches will be present in the cortex. Neither does the existence of unoriented cells, either in layer IV or the upper layers. Such units are a notable feature of macaque striate cortex (Hubel & Wiesel 1968) but they are also common in the mouse and tree shrew (Drager 1975; Humphrey & Norton 1980).

In this paper we have identified a geniculate projection to the patches in the upper layers of new and old world primates. However, a geniculate projection to the upper layers, broken into patches or columns, is also seen in the cat (LeVay & Gilbert 1975) although the cytochrome oxidase stain reveals no patches.

A more elaborate functional architecture is often considered an adaption necessary in brains with a large cortical surface area, the thought being that detailed parcelling is required for organization and economy of connections in a large sheet of tissue. Most of the species found to have patches do indeed have a large surface area of striate cortex. But *Galago crassicaudatus*

has a relatively small visual cortex, about the same in surface area as the cat's. It would be interesting to examine cytochrome oxidase staining in *Galago senegalensis*, a prosimian with a tiny striate cortex estimated by von Bonin to measure only 58 $mm^2$, about one sixth the area of cat striate cortex and only one 20th the area of macaque striate cortex. If this diminutive primate has patches, which seems most likely, will they be scaled down in size, compared with the greater galagos, or similar in size but less numerous? At any rate, areal extent of cortical surface area is probably not a decisive factor in considering whether cytochrome oxidase patches are present.

Colour vision is generally regarded as a characteristic feature of the primate visual system. However the owl monkey, a nocturnal primate, has few retinal cones and a very weak capacity to distinguish wavelengths (Jacobs 1977). For this reason we deliberately chose to test cytochrome oxidase staining in this animal. Compared with the macaque it showed some intriguing differences in laminar activity referred to previously, but nonetheless a clear pattern of patches present in tangential sections. On the other hand, animals like the ground squirrel, with excellent colour vision and a retina dominated by cones, showed no patches. The conclusion must follow that although colour coded units may turn out to have a good relation to be patches in some species of monkeys, the patches should not be viewed as a specialization developed for colour vision.

So far we have failed to uncover an obvious association between the patches and any particular visual system feature. At this point we can say only that patches appear to be unique to primates. We have not been able to identify any distinctive aspect of vision in primates, absent in other species, that is served by the patches.

### (*f*) *Interpretation of 2-deoxyglucose results*

Early 2-deoxyglucose studies in monkeys (Kennedy *et al.* 1976; Hubel *et al.* 1978) assumed an inherent metabolic homogeniety within single layers of the striate cortex. In cat and tree shrew, species lacking cytochrome oxidase patches, this seems to be the case. In these animals, binocular stimulation with a display of irregular stripes at all orientations yields no 2-deoxyglucose pattern in the visual cortex (Humphrey *et al.* 1980; Schoppmann & Stryker 1981). Excellent evidence is available, from experiments combining physiological mapping with 2-deoxyglucose radioautography, that patterns produced by stimulation with stripes of a single orientation truly reflect the disposition of the corresponding orientation columns in the cortex (Schoppmann & Stryker 1981).

The discovery of patches of chronically elevated metabolic activity in primates using the cytochrome oxidase stain raises the possibility of a non-homogeneous baseline for 2-deoxyglucose uptake in the visual cortex. This notion is reinforced by the finding that in the squirrel monkey binocular stimulation with diffuse light in a ganzfeld results in faint dots of 2-deoxyglucose label matching the cytochrome oxidase patches (Humphrey & Hendrickson 1980). If the patches take up 2-deoxyglucose more avidly than surrounding cortex, regardless of the pattern of visual stimulation, this would seriously complicate the interpretation of radioautographs and perhaps limit the usefulness of the technique in primate visual cortex. It would always be necessary to subtract out the non-specific contribution of uptake in the patch zones in order to see the pattern actually due to the visual stimulus. Since this non-specific factor would probably vary with different stimulus patterns it would be a difficult variable to control.

Concern over this point has been allayed in part by some recent experiments of Tootell *et al.* (1981, 1982; R. B. H. Tootell, personal communication). They have provided convincing evidence that with appropriate stimuli, 2-deoxyglucose patterns can be generated in striate cortex that skirt the patches entirely. This is true even for some visual patterns confined to a single orientation. The key is that, in addition to orientation, one must manipulate other parameters such as spatial frequency and colour of the stimulus pattern. Furthermore, they find that in parts of macaque cortex stimulated by diffuse light, 2-deoxyglucose uptake within the patches is only slightly greater than in surrounding tissue. In macaques binocularly stimulated with a pattern incorporating a wide range of spatial frequencies, displayed at all orientations, a relatively flat 2-deoxyglucose pattern is seen in the cortex. Therefore it is clear that although metabolic activity may be chronically higher in the patches, as reflected by cytochrome oxidase, 2-deoxyglucose patterns can be obtained without contamination from the patches.

This conclusion casts new light on the interpretation of the 2-deoxyglycose experiment involving monocular stimulation with all orientations. If we can safely reject the argument that the cytochrome oxidase patches were labelled preferentially merely because they take up 2-deoxyglucose more avidly under any conditions, it then seems most likely that the patches contain unoriented cells, or cells tuned to a mix of orientations. If so, it is hard to understand why such vigorous uptake occurred in the patch regions in the experiment involving monocular stimulation with vertical stripes (figure 44). We would have predicted some deoxyglucose labelling in the patches because of unoriented or vertically tuned cells, and some labelling outside the patches, in vertical orientation columns. Instead it seemed to be concentrated exclusively in the vicinity of the cytochrome oxidase patches. Perhaps the key factor is that this experiment involved *monocular* stimulation. So far we have ignored the question of stereopsis and the contribution of cells, probably organized into columns, that might be sensitive to different retinal disparities. Perhaps such cells are relatively scarce in the patch regions.

The cortex is probably comprised of many dovetailed columnar systems: for colour, orientation, retinal disparity, ocular dominance, spatial frequency, and directionality, just to name a few. Sorting these out using the 2-deoxyglucose technique will require a comprehensive series of experiments, systematically controlling for and isolating each stimulus variable. The cytochrome oxidase stain will be helpful in these experiments. A critical shortcoming of the 2-deoxyglucose technique is that it is a single label, making it difficult to test how two different columnar systems are interrelated in the same cortex. The two dimensional array formed by the cytochrome oxidase patches can serve as a template, facilitating the comparison of 2-deoxyglucose patterns obtained using different stimuli in different experiments.

### (*g*) *Patches as the fundamental cytoarchitectonic unit of primate striate cortex*

The patches in primate striate cortex are reminiscent of the barrels present in mouse somatosensory cortex. The barrels have also been labelled preferentially by stains for SDH (Labedsky & Lierse 1968), AChE (Kristt & Waldman 1981), cytochrome oxidase (Wong-Riley & Welt 1980), and GABA transaminase (Kristt & Waldman 1981). They are also visible in Nissl stain; so far we have not convinced ourselves of this for the patches in monkey striate cortex, although hints have been seen. Both patches and barrels can be seen in unstained tissue sections (personal observations; Tootell *et al.* 1983; Dietrich *et al.* 1981). Like the patches, each

mouse barrel receives a discrete cluster of thalamic axon terminals (Lorente de No 1922; Killackey & Leshin 1975). The barrels also show diminished activity of metaboic enzymes after cautery of facial whiskers (Wong-Riley 1980; Dietrich *et al.* 1981), an effect similar to the loss of activity seen in patches following enucleation. The barrels are preferentially labelled by deoxyglucose (Durham & Woolsey 1978), also true for the patches under some conditions of visual stimulation. It should be noted that there are differences between barrels and patches, particularly in the details of their internal structure. The barrel is composed of a cell dense wall enclosing a 'hollow' centre receiving thalamic input. At this point we have a poorer understanding of the anatomy of the patches, but cell bodies and geniculate terminals seem to be freely intermingled. These sorts of differences between the organization of patches and barrels should probably be viewed as variations on a common theme: the modular construction of cerebral cortex.

Woolsey & Van der Loos (1970) have suggested that the barrels in rodents constitute the fundamental cytoarchitectonic unit of the Sm1 face area, responsible for processing sensory input from the whiskers. According to their model, there is a special correspondence between each barrel and a given mystacial vibrissa. It seems credible that a sensory surface composed of discrete entities – whiskers – should be mapped onto discrete units in the cortex.

Hubel & Wiesel (1977) have suggested a similar subdivision of macaque striate cortex into individual elementary units (figure 1), each containing several hypercolumns of every stimulus variable, devoted to analysing a particular portion of the visual field. Since the visual field constitutes a continuous sensory surface their hypothetical units were imagined, unlike the mouse barrels, to have arbitrary boundaries. At the time there was no suspicion that any macroscopic inhomogeneity might be present in tangential sections through the cortex, except for the Liesegang bands in IV that were attributed simply to the presence of ocular dominance columns. The discovery of the cytochrome oxidase patches has changed our perspective on this point. It seems possible that the patches will prove to be the fundamental cytoarchitectonic unit of primate striate cortex. If so, this would mean that the module originally conceived by Hubel & Wiesel (1977) does actually have a definite size, shape, and boundary. It comes as a surprise that a sheet of tissue like the visual cortex, processing information about a continuous sensory surface, should be carved piecemeal into structurally distinct units. Apparently, regardless of the nature of the surface being mapped, the cortex may be constructed on a modular plan. Why this should be so, and what advantages such a system confers, has remained an unanswered riddle since Mountcastle first identified columns in cerebral cortex more than 20 years ago. It also remains unclear why various types of modules or columns should be present in only certain cortical areas of certain species. Comparative studies by Woolsey *et al.* (1975) have shown that barrels are characteristic of rodents with vibrissae. However they are absent in beavers, rodents with an enviable set of whiskers, and present in some whiskered non-rodents like rabbits and porcupines. By the same token, we lack insight into why only primates seem to have patches, or, for that matter, why ocular dominance columns are present in only some species.

Believing that the cytochrome oxidase patches perhaps represent the fundamental modular unit of primate striate cortex, one of my foremost aims in this paper has been to relate the patches to other elements of the cortical architecture. With regard to the ocular dominance columns, several independent lines of anatomical evidence have demonstrated that each patch

sits squarely within a left or right eye column. This result implies that the basic module in striate cortex does not necessarily contain a complete hypercolumn of each stimulus parameter, as predicted by Hubel & Wiesel's model. For example, in the macaque, a doublet of patches is required to house each ocular dominance hypercolumn. Consequently, moving from module to module, roughly 0.5 mm apart, there will be an obvious displacement of aggregate receptive field position in layer IVc (Hubel *et al.* 1974), but not in the upper layers where a longer traverse, about 2 mm, is required (Hubel & Wiesel 1974*b*). Therefore, outside layer IV, the aggregate receptive field of each patch will overlap extensively with the aggregate fields of neighbouring patches. An analogous situation holds in the mouse barrelfield: in layer IV the majority of cells will respond to stimulation of only a single 'principal' whisker, whereas in other layers units activated by several different whiskers are common (Simons 1978).

Attempts to relate the patches to the orientation columns have met with less success. The coincidence between the spacing of the patches and the dimensions of an orientation hypercolumn, estimated at 640 μm (Hubel & Wiesel 1974*a*), makes some sort of regular, systematic relationships very likely. At this stage we are uncertain whether the orientation columns form a continuous, global pattern within striate cortex, rather as the ocular dominance columns do (Connolly *et al.* 1982), or whether they will turn out to be organized on a local basis in conjunction with each patch module. This latter possibility was envisaged by Braitenberg & Braitenberg (1979) several years before the discovery of the cytochrome oxidase patches. Reconsidering Hubel & Wiesel's original physiological data they suggested that the orientation columns might be radially organized around local 'centres' spaced evenly throughout striate cortex. A separation of about 0.5 mm between 'centres' was determined to be most compatible with Hubel & Wiesel's plots of optimal orientation versus distance along electrode penetration. This figure of 0.5 mm is remarkably close to the spacing between cytochrome oxidase patches. In figure 49, a block of striate cortex is depicted schematically, showing the cytochrome oxidase patches, ocular dominance columns, and orientation columns as they might be arranged according to the Braitenberg's concept. In this scheme the patches represent the 'centres', around which the orientation columns are distributed in a semi-regular radial mosaic. If the columns converge as they approach the patches, the rate of change in orientation with electrode advance will increase as the penetration passes close to a cytochrome oxidase patch. In addition, occasional regions of rapidly changing orientation or abrupt fracture will be present at the interfaces between adjacent patches. This seems to be required if one abandons the notion of the orientation columns as long continuous, locally parallel slabs. At the same time, long traverses of systematically changing orientation without interruption are possible, especially if the electrode follows a fortuitous path. In their recordings, Hubel & Wiesel (1974*a*) found evidence for long sequences of regularly changing orientation and for regions of unexpected reversal or jump in orientation. There is no reason why discontinuities should not be present in the pattern of orientation columns: discontinuities are also seen in the pattern of ocular dominance columns, in the retinotopic map in layer IVc, and in the geniculate projection to the upper layers.

If the orientation columns lie outside the patches, what about the patches themselves? The Braitenbergs suggested that their hypothetical 'centres' might be special anatomical structures responsible for generating orientation selectivity in surrounding cortex. The evidence obtained from deoxyglucose experiments indicates that the patches contain collections of unoriented cells.

While there are grounds for caution in interpreting the deoxyglucose data, certainly if any clusters of cells lacking orientation selectivity are present in supragranular cortex, they are likely to correspond in position to the patches of geniculate input.

For the present, the general model of figure 49 is consistent with the physiological and anatomical evidence at our disposal. As more evidence becomes available, it will be refined

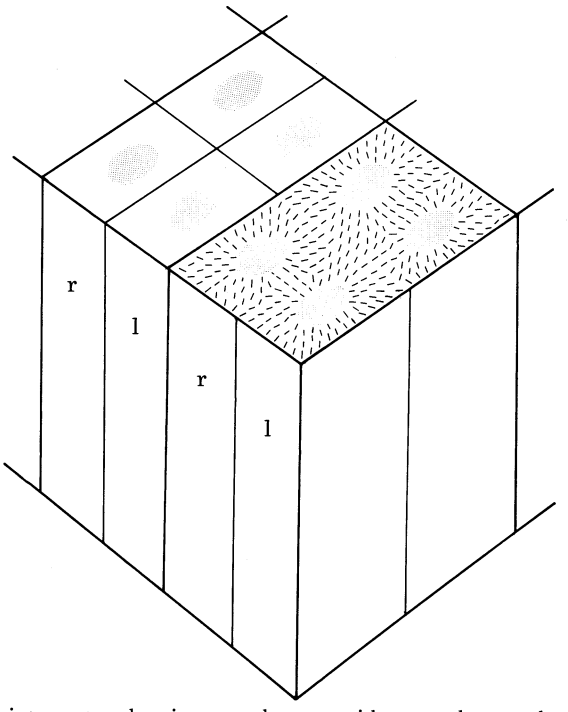


FIGURE 49. Model of macaque striate cortex showing cytochrome oxidase patches, ocular dominance columns, and orientation columns. Each patch fits within an ocular dominance column, with its long axis oriented parallel to the length of the column. The orientation columns are shown arranged in a radial fashion around each patch, as they might be according to the scheme of Braitenberg & Braitenberg (1979). An electrode passing tangentially through the cortex would encounter long sequences of regular orientation shifts interrupted occasionally by abrupt discontinuities. Deoxyglucose evidence suggests that the patches may contain cells lacking orientation selectivity.

and modified, or discarded. Just a few years ago, optimists were willing to venture that we had a clear understanding of primate striate cortex. Whether or not the cytochrome oxidase patches turn out to be the fundamental structural unit of primate striate cortex, the mere fact that such a basic issue remains unsettled indicates that our understanding is still quite rudimentary.

I am deeply indebted to Torsten N. Wiesel and Simon LeVay for their valuable help and guidance. Many useful conversations with Helen Sherk, Paul Desan, Eric Frank, and Roger Tootell are gratefully acknowledged. David Miller aided with the intraocular injections. Photographic assistance was provided by Marc Peloquin and Joe Gagliardi. The foetal monkey tissue was donated by Benjamin Jackson and George Piasecki whose work is supported by P.H.S. Grant HD15892-01. My funding was received from U.S.P.H.S. Medical Scientist Training Grant GM07753 and N.I.H. Grant EY00606 to Torsten Wiesel.

## References


Allman, J. M. & Kaas, J. H. 1974 The organization of the second visual area (VII) in the owl monkey: a second order transformation of the visual hemifield. *Brain Res*, **76**, 247–265.

Bayliss, B. J. & Todrick, A. 1956 The use of a selective acetylcholineresterase inhibitor in the estimation of pseudocholinesterase activity in rat brain. *Biochem. J.* **62**, 62–67.

Benevento, L. A. & Yoshida, K. 1981 The afferent and efferent organization of the lateral geniculo-prestriate pathways in the macaque monkey. *J. comp. Neurol.* **203**, 455–474.

Braitenberg, B. & Braitenberg, C. 1979 Geometry of orientation columns in the visual cortex. *Biol. Cybernetics* **33**, 179–186.

Butcher, L. L., Talbut, K. & Bilezikjian, L. 1975 Acetylcholinesterase neurons in dopamine-containing regions of the brain. *J. neurol. Trans.* **38**, 137–153.

Campos-Ortega, J. A., Hayhow, W. R. & de V. Cluver, P. F. 1970 A note on the problem of retinal projections to the inferior pulvinar nucleus of primates. *Brain Res.* **22**, 126–130.

Casagrande, V. A. & Skeen, L. C. 1980 Organization of ocular dominance columns in galago demonstrated by autoradiographic and deoxyglucose methods. *Soc. Neurosci.* **6**, 113.7.

Connolly, M., LeVay, S. & Van Essen, D. C. 1982 The complete pattern of ocular dominance stripes in macaque striate cortex. *Soc. Neurosci.* **8**, 192.4.

Cotlier, E., Lieberman, T. W. & Gay, A. J. 1965 Dehydrogenases and diaphorases in monkey lateral geniculate body. *Arch. Neurol.* **12**, 295–299.

Cowan, W. M., Gottlieb, D. I., Hendrickson, A. E., Price, J. L. & Woolsey, T. A. 1972 The autoradiographic demonstration of axonal connections in the central nervous system. *Brain Res.* **37**, 21–51.

DeBruyn, E. J. & Casagrande, V. A. 1981 Demonstration of ocular dominance columns in a New World primate by means of monocular deprivation. *Brain Res.* **207**, 453–458.

Des Rosiers, M. H., Saurada, O., Jehle, J., Shinohara, M., Kennedy, C. & Sokoloff, L. 1978 Functional plasticity in the immature striate cortex of the monkey shown by the [$^{14}$C]deoxyglucose method. *Science, N.Y.* **200**, 447–449.

Dietrich, W. D., Durham, D., Lowry, O. H. & Woolsey, T. A. 1981 Quantitative histochemical effects of whisker damage on single identified cortical barrels in the adult mouse. *J. Neurosci.* **1**, 929–935.

Drager, U. C. 1975 Receptive fields of single cells and topography in mouse visual cortex. *J. comp. Neurol.* **160**, 269–290.

Durham, D. & Woolsey, T. A. 1978 Acute whisker removal reduces neuronal activity in barrels of mouse Sm1 cortex. *J. comp. Neurol.* **178**, 629–644.

Fahimi, H. D. & Karnovsky, M. J. 1966 Cytochemical localization of two glycolytic dehydrogenases in white skeletal muscle. *J. Cell Biol.* **29**, 113–128.

Fitzpatrick, D. & Diamond, I. T. 1980 Distribution of acetylcholinesterase in the geniculostriate system of galago senegalensis and aotus trivirgatus: evidence for the origin of the reaction product in the lateral geniculate body. *J. comp. Neurol.* **194**, 703–719.

Fitzpatrick, D., Itoh, K. & Diamond, I. T. 1983 The laminar organization of the lateral geniculate body and the striate cortex in the squirrel monkey (*Saimiri sciureus*). *J. Neurosci.* (In the press.)

Fries, W. 1981 The projection from the lateral geniculate nucleus to the prestriate cortex of the macaque monkey. *Proc. R. Soc. Lond.* B, **213**, 73–80.

Gay, A. L. & Silberberg, D. H. 1964 Histochemical correlates of transynaptic degeneration. *Arch. Neurol.* **10**, 85–90.

Gilbert, C. D. & Wiesel, T. N. 1980 Interleaving projection bands in cortico-cortical connections, *Soc. Neurosci.* **6**, 113.8.

Haseltine, E. C., DeBruyn, E. J. & Casagrande, V. A. 1979 Demonstration of ocular dominance columns in Nissl-stained sections of monkey visual cortex following enucleation. *Brain Res.* **176**, 153–158.

Hendrickson, A. E., Hunt, S. P. & Wu, J. Y. 1981 Immunocytochemical localization of glutamic acid decarboxylase in monkey striate cortex. *Nature, Lond.* **292**, 605–607.

Hendrickson, A. E. & Wilson, J. R. 1979 A difference in [$^{14}$C]deoxyglucose autoradiographic patterns in striate cortex between Macaca and Saimiri monkeys following monocular stimulation. *Brain Res.* **170**, 353–358.

Hendrickson, A. E., Wilson, J. R. & Ogren, M. P. 1978 The neuroanatomical organization of pathways between the dorsal lateral geniculate nucleus and visual cortex in old World and New World primates. *J. comp. Neurol.* **182**, 123–136.

Horton, J. C. & Hedley-Whyte, E. T. 1984 Mapping of cytochrome oxidase patches and ocular dominance columns in human visual cortex. *Phil. Trans. R. Soc. Lond.* B **304**, 255–272.

Horton, J. C. & Hubel, D. H. 1980*a* Correlation of cytochrome oxidase staining with 2-deoxyglucose uptake in monkey visual cortex. *Arch. Biol. Med. Exp.* **13**, 12.

Horton, J. C. & Hubel, D. H. 1980*b* Cytochrome oxidase stain preferentially labels intersection of ocular dominance and vertical orientation columns in macaque striate cortex. *Soc. Neurosci.* **6**, 113.5.

Horton, J. C. & Hubel, D. H. 1981 Regular patchy distribution of cytochrome oxidase staining in primary visual cortex of macaque monkey. *Nature Lond.* **292**, 762–764.

Hubel, D. H. & Livingstone, M. S. 1981 Regions of poor orientation tuning coincide with patches of cytochrome oxidase staining in monkey striate cortex. *Soc. Neurosci.* **7**, 118.12.

Hubel, D. H. & Wiesel, T. N. 1962 Receptive fields, binocular interaction and functional architecture in the cat's visual cortex. *J. Physiol., Lond.* **160**, 106–154.

Hubel, D. H. & Wiesel, T. N. 1968 Receptive fields and functional architecture of monkey striate cortex. *J. Physiol., Lond.* **195**, 215–243.

Hubel, D. H. & Wiesel, T. N. 1972 Laminar and columnar distribution of geniculo-cortical fibres in the macaque monkey. *J. comp. Neurol.* **1972**, 421–450.

Hubel, D. H. & Wiesel, T. N. 1974*a* Sequence regularity and geometry of orientation columns in the monkey striate cortex. *J. Comp. neurol.* **158**, 267–294.

Hubel, D. H. & Wiesel, T. N. 1974*b* Uniformity of monkey striate cortex: a parallel relationship between field size, scatter, and magnification factor. *J. comp. Neurol.* **158**, 295–306.

Hubel, D. H. & Wiesel, T. N. 1977 Functional architecture of macaque monkey visual cortex. *Proc. R. Soc. Lond.* B **198**, 1–59.

Hubel, D. H. & Wiesel, T. N. 1978 Distribution of inputs from the two eyes to striate cortex of squirrel monkeys. *Soc. Neurosci.* **4**, 632.

Hubel, D. H., Wiesel, T. N. & LeVay, S. 1974 Visual representation in layer IVc of monkey striate cortex. *Soc. Neurosci.* 4th annual meeting, p. 311.

Hubel, D. H., Wiesel, T. N. & LeVay, S. 1977 Plasticity of ocular dominance columns in monkey striate cortex. *Phil. Trans. R. Soc. Lond.* B **278**, 377–409.

Hubel, D. H., Wiesel, T. N. & Stryker, M. P. 1978 Anatomical demonstration of orientation columns in macaque monkey. *J. comp. Neurol.* **177**, 361–380.

Humphrey, A. L. & Hendrickson, A. E. 1980 Radial zones of high metabolic activity in squirrel monkey striate cortex. *Soc. Neurosci.* **6**, 113.6.

Humphrey, A. L. & Norton, T. T. 1980 Topographic organization of the orientation column system in the striate cortex of the tree shrew (*Tupaia glis*). I. Microelectrode recording. *J. comp. Neurol.* **192**, 531–547.

Humphrey, A. L., Skeen, L. C. & Norton, T. T. 1980 Topographic organization of the orientation column system in the striate cortex of the tree shrew (*Tupaia glis*). II. Deoxyglucose mapping. *J. comp. Neurol.* **192**, 549–566.

Itaya, S. K. & Van Hoesen, G. W. 1982 WGA-HRP as a transneuronal marker in the visual pathways of monkey and rat. *Brain Res.* **236**, 199–204.

Jacobs, G. H. 1977 Visual capacities of the owl monkey (*Aotus trivirgatus*). I. Spectral sensitivity and colour vision. *Vision Res.* **17**, 811–820.

Jebb, A. H. & Woolsey, T. A. 1977 A simple stain for myelin in frozen sections: a modification of Mahon's method. *Stain Tech.* **52**, 315–318.

Karnovsky, M. J. & Roots, L. 1964 A 'direct coloring' thiocholine method for cholinesterases. *J. Histochem. Cytochem.* **12**, 219–221.

Kennedy, C., Des Rosiers, M. H., Reivich, M., Sharpe, F. & Sokoloff, L. 1975 Mapping of functional neural pathways by autoradiographic survey of local metabolic rate with [$^{14}$C]deoxyglucose. *Science, N.Y.*, **187**, 850–853.

Kennedy, C., Des Rosiers, M. H., Sakurada, O., Shinohara, O., Reivich, M., Jehle, J. W. & Sokoloff, L. 1976 Metabolic mapping of the primary visual system of the monkey by means of the autoradiographic [$^{14}$C]deoxyglucose technique. *Proc. natn. Acad. Sci. U.S.A.* **73**, 4230–4234.

Killackey, H. P. & Leshin, S. 1975 The organization of specific thalamocortical projections to the posteromedial barrel subfield of the rat somatic sensory cortex. *Brain Res.* **86**, 469–472.

Kristt, D. A. & Waldman, J. V. 1981 Development of neocortical circuitry: Gaba-transaminase replaces AChE in the barrel centres. *Soc. Neurosci.* **7**, 247.5.

Kupfer, C. & Palmer, P. 1964 Lateral geniculate nucleus: histological and cytochemical changes following afferent denervation and visual deprivation. *Exp. Neurol.* **9**, 400–409.

Labedsky, L. & Lierse, W. 1968 Die Entwicklung der Succinodehydrogenaseaktivatat im Gehirn der Maus wahrend per Postnatalzeit. *Histochemie* **12**, 130–151.

LeVay, S. & Gilbert, C. D. 1976 Laminar patterns of geniculocortical projection in the cat. *Brain Res.* **113**, 1–19.

LeVay, S., Hubel, D. H. & Wiesel, T. N. 1975 The pattern of ocular dominance columns in macaque visual cortex revealed by a reduced silver stain. *J. comp. Neurol.* **159**, 559–576.

LeVay, S., Stryker, M. P. & Shatz, C. J. 1978 Ocular dominance columns and their development in layer IV of the cat's visual cortex: a quantitative study. *J. comp. Neurol.* **179**, 223–244.

LeVay, S., Weisel, T. N. & Hubel, D. H. 1980 The development of ocular dominance columns in normal and visually deprived monkeys. *J. comp. Neurol.* **191**, 1–51.

Lin, C. S., Wagor, E. & Kaas, J. H. 1974 Projections from the pulvinar to the middle temporal visual area (m.t.) in the owl monkey, *Aotus trivirgatus*. *Brain Res.* **76**, 145–149.

Lorente de No, R. 1922 La corteza cerebral del raton. *Trab. Lab. Invest. Biol.* (*Madrid*), **20**, 41–78.

Lund, J. S. 1973 Organization of neurons in the visual cortex, area 17, of the monkey (*Macaca mulatta*). *J. comp. Neurol.* **147**, 455–496.

Matthews, M. R., Cowan, W. M. & Powell, T. P. S. 1960 Transneuronal cell degeneration in the lateral geniculate nucleus of the macaque monkey. *J. Anat.* **94**, 145–169.

Mesulam, M. M. 1978 Tetramethyl benzidine for horseradish peroxidase neurohistochemistry: a non-carcinogenic blue reaction-produce with superior sensitivity for visualizing neural afferents and efferents. *J. Histochem. Cytochem.* **26**, 106–117.

Mesulam, M. M. & Mufson, E. J. 1980 The rapid anterograde transport of horseradish peroxidase. *Neuroscience* **5**, 1277–1286.

Mesulam, M. M. & Van Hoesen, G. W. 1976 Acetylcholinesterase-rich projections from the basal forebrain of the rhesus monkey to neocortex. *Brain Res.* **109**, 152–157.

Montero, V. M. 1980 Patterns of connections from the striate to cortical visual areas in superior temporal sulcus of macaque and middle temporal gyrus of owl monkey. *J. comp. Neurol.* **189**, 45–59.

Murray, R. G., Jones, A. E. & Murray, A. 1973 Fine structure of photoreceptors in owl monkey. *Anat. Rec.* **175**, 673–696.

Nachlas, M. M., Tsou, K. C., De Souza, E., Cheng, C. S. & Seligman, A. M. 1957 Cytochemical demonstration of succinic dehydrogenase by the use of a new p-nitrophenyl substituted ditetrazole. *J. Histochem. Cytochem.* **5**, 420–436.

Ogran, M. & Hendrickson, A. E. 1977 The distribution of pulvinar terminals in visual areas 17 and 18 of the monkey. *Brain Res.* **137**, 343–350.

Palkovits, M. & Jacobwitz, D. 1974 Topographic atlas of catecholamine and acetylcholinesterase-containing neurons in the rat brain. II. Hindbrain (Mesencephalon, Rhombencephalon). *J. comp. Neurol.* **157**, 29–42.

Rakic, P. 1977 Prenatal development of the visual system in rhesus monkey. *Phil. Trans. R. Soc. Lond.* B **278**, 245–260.

Rakic, P. 1981 Development of visual centers in the primate brain depends on binocular competition before birth. *Science, N.Y.* **214**, 928–931.

Rezak, M. & Benevento, L. A. 1979 A comparison of the organization of the projections of the dorsal lateral geniculate nucleus, the inferior pulvinar and adjacent lateral pulvinar to primary visual cortex (area 17) in the macaque monkey. *Brain Res.* **167**, 19–40.

Rockland, K. S., Lund, J. S. & Humphrey, A. L. 1982 Anatomical banding of intrinsic connections in striate cortex of the tree shrews (*Tupaia glis*). *J. comp. Neurol.* **209**, 41–58.

Rowe, M. H., Benevento, L. A. & Rezak, M. 1978 Some observations on the patterns of segregated geniculate inputs to the visual cortex in New World primates: an autoradiographic study. *Brain Res.* **159**, 371–378.

Schiller, P. H. & Malpeli, J. G. 1978 Functional specificity of lateral geniculate nucleus laminae of the rhesus monkey. *J. Neurophysiol.* **41**, 788–797.

Schoppmann, A. & Stryker, M. P. 1981 Physiological evidence that the 2-deoxyglucose method reveals orientation columns in cat visual cortex. *Nature, Lond.* **293**, 574–576.

Seligman, A. M., Karnovsky, M. J., Wasserkrug, H. L. & Hanker, J. S. 1968 Nondroplet ultrastructural demonstration of cytochrome oxidase activity with a polymerizing osmiophilic reagent, diaminobenzidine (DAB). *J. Cell Biol.* **38**, 1–14.

Shatz, C. J. & Stryker, M. P. 1978 Ocular dominance in layer IV of the cat's visual cortex and the effects of monocular deprivation. *J. Physiol., Lond.* **281**, 267–283.

Simons, D. J. 1978 Response properties of vibrissa units in rat SI somatosensory neocortex. *J. Neurophysiol.* **41**, 798–820.

Swindale, N. V., Vital-Durand, F. & Blackmore, C. 1981 Recovery from monocular deprivation in the monkey. III. Reversal of anatomical effects in the visual cortex. *Proc. R. Soc. Lond.* B **213**, 435–450.

Tootell, R. B. H. & Silverman, M. S. 1981 A comparison of cytochrome oxidase and deoxyglucose patterns in macaque visual cortex. *Soc. Neurosci.* **7**, 118.6.

Tootell, R. B., Silverman, M. S. & De Valois, R. L. 1981 Spatial frequency columns in primary visual cortex. *Science, N.Y.* **214**, 813–815.

Tootell, R. B. H., Silverman, M. S., De Valois, R. L. & Jacobs, G. H. 1983 Functional organization of the second cortical visual area in primates. *Science, N.Y.* **220**, 737–739.

Tootell, R. B. H., Silverman, M. S., Switkes, E. & De Valois, R. L. 1982 Deoxyglucose analysis of retinotopic organization in primate striate cortex. *Science, N.Y.* **218**, 902–904.

Weber, J. T., Kaas, J. H., Huerta, M. F. & Harting, J. K. 1977 Connections of the lateral geniculate nucleus (l.g.n.) of the squirrel monkey. *Soc. Neurosci.* **3**, 1860.

Wiesel, T. N. & Hubel, D. H. 1963*a* Effects of visual deprivation on morphology and physiology of cells in the cat's lateral geniculate body. *J. Neurophysiol.* **26**, 978–993.

Wiesel, T. N. & Hubel, D. H. 1963*b* Single-cell responses in striate cortex of kittens deprived of vision in one eye. *J. Neurophysiol.* **26**, 1003–1017.

Wiesel, T. N. & Hubel, D. H. 1965 Comparison of the effects of unilateral and bilateral eye closure on cortical unit responses in kittens. *J. Neurophysiol.* **28**, 1029–1040.

Wiesel, T. N., Hubel, D. H. & Lam, D. M. K. 1974 Autoradiographic demonstration of ocular dominance columns in the monkey striate cortex by means of transneuronal transport. *Brain Res.* **79**, 273–279.

Wong-Riley, W. T. T. 1976 Projections from the dorsal geniculate nucleus to prestriate cortex in the squirrel monkey as demonstrated by retrograde transport of horseradish peroxidase. *Brain Res.* **109**, 595–600.

Wong-Riley, M. T. T. 1977 Connections between the pulvinar nucleus and the prestriate cortex in the squirrel monkey as revealed by peroxidase histochemistry and autoradiography. *Brain Res.* **134**, 225–236.

Wong-Riley, M. T. T. 1979*a* Columnar cortico-cortical interconnections within the visual system of the squirrel and macaque monkeys. *Brain Res.* **162**, 201–217.

Wong-Riley, M. T. T. 1979*b* Changes in the visual system of monocularly sutured or enucleated kittens demonstrable with cytochrome oxidase histochemistry. *Brain Res.* **171**, 11–28.

Wong-Riley, M. T. T., Merzenich, M. M. & Leake, P. A. 1978 Changes in endogenous enzymatic reactivity to DAB induced by neuronal inactivity. *Brain Res.* **141**, 185–192.

Wong-Riley, M. T. T. & Welt, C. 1980 Histochemical changes in cytochrome oxidase of cortical barrels after vibrissal removal in neonatal and adult mice. *Proc. natn. Acad. Sci. U.S.A.* **77**, 2333–2337.

Woolsey, T. A. & Van Der Loos, H. 1970 The structural organization of layer IV in the somatosensory region (SI) of mouse cerebral cortex. *Brain Res.* **17**, 205–242.

Woolsey, T. A., Welker, C. & Schwartz, R. H. 1975 Comparative anatomical studies of the sml face cortex with special reference to the occurrence of 'barrels' in layer IV. *J. comp. Neurol.* **164**, 79–94.

Yukie, M. & Iwai, E. 1981 Direct projection from the dorsal lateral geniculate nucleus to the prestriate cortex in macaque monkeys. *J. comp. Neurol.* **201**, 81–97.

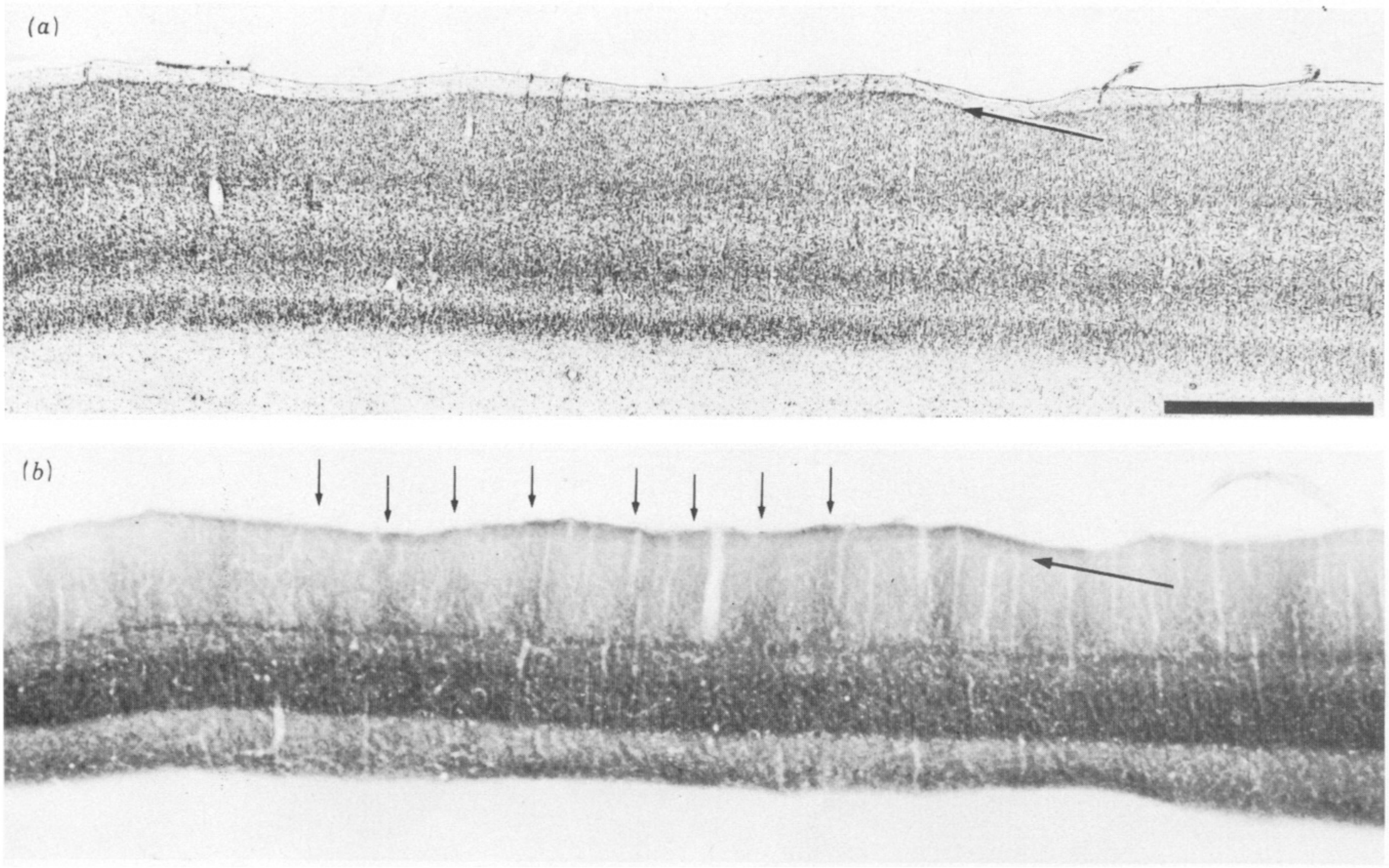


FIGURE 2. Laminar pattern of cytochrome oxidase activity compared with Nissl stain and cortical projection from lateral geniculate nucleus labelled by transneuronal radioautography.

(*a*) Coronal section through striate cortex (area 17, primary visual cortex, V1) from a normal macaque monkey stained with cresyl violet. Arrow marks a thin layer of cell bodies at interface between layers I and II which stains lightly for cytochrome oxidase activity (see corresponding arrow in *b*). Scale = 1 mm.

(*b*) An adjacent section processed for cytochrome oxidase histochemistry shows regular columns of enhanced enzyme activity spaced about 350 μm apart (arrows). Columns are most obvious in layer III, but also visible in layers II and IVb in this section. Appearance of these columns in tangential section through layer III from another macaque is shown in figure 3.

(*c*) Nissl and (*d*) cytochrome oxidase stains compared with geniculate projection to cortex labelled by eye injection with [$^3$H]proline (*e*). Darkest cytochrome oxidase staining is visible in layers VI, IVc, and IVa, all layers that receive a direct input from the lateral geniculate. Note that sharp lower border of layer IVc in the cytochrome oxidase stain matches the lower extent of proline label. Scale = 100 μm.

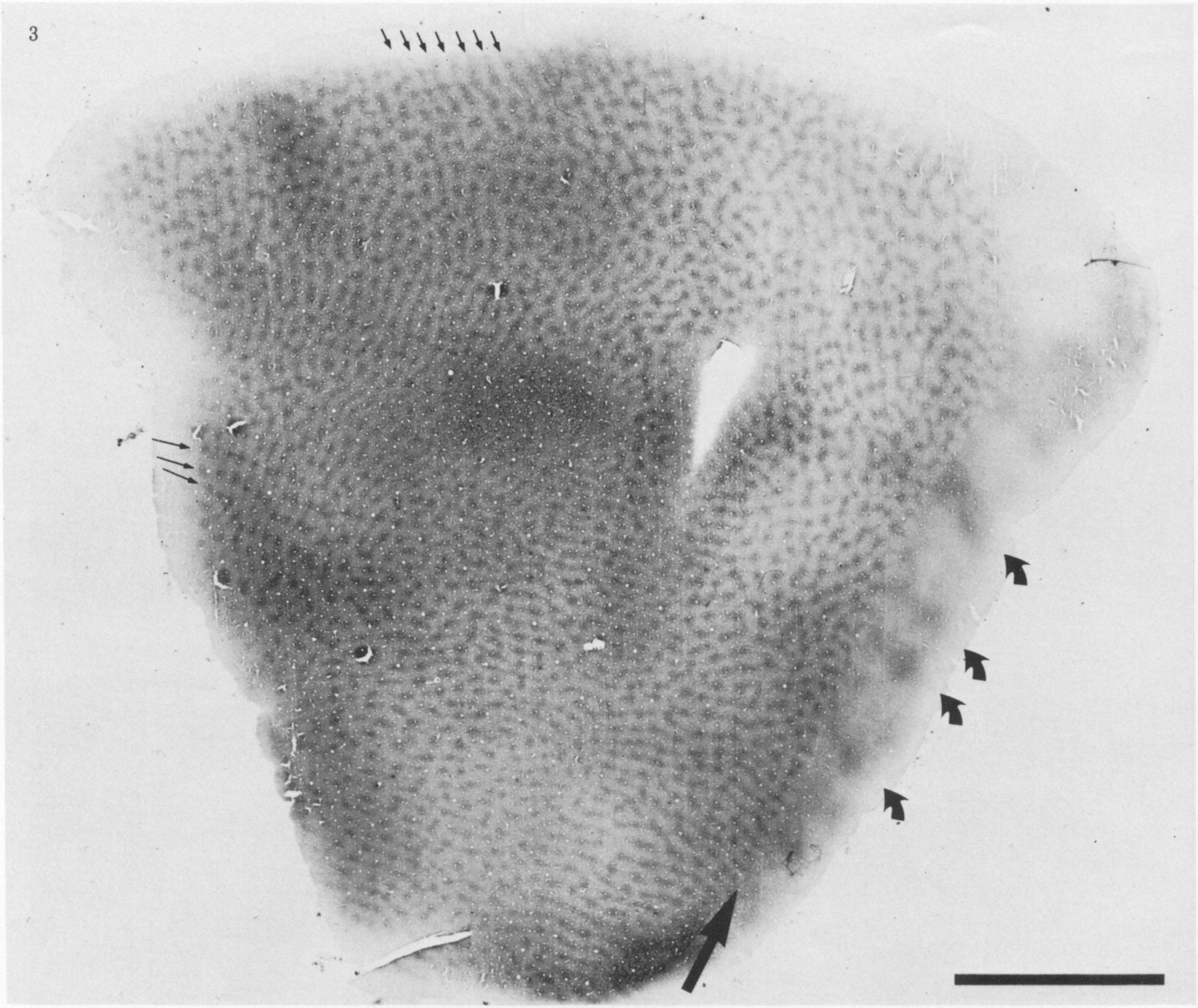

FIGURE 3. Tangential section from a normal rhesus monkey through layers II, III stained for cytochrome oxidase reveals an array of small patches, about 250 μm by 150 μm. Patches are aligned in long rows spaces about 350 μm apart which intersect the 17–18 border (small arrows) at right angles in a manner similar to the ocular dominance columns (see figure 8, LeVay *et al.* 1975). Along each row the patches partially merge, creating an impression of long beaded strips. The patches occur about every 550 μm along each row; patches in adjacent rows are often aligned, giving rise to a second set of crossing rows (three medium arrows). The V1–V2 border is clearly visible at the far right in the section, indicated by a single large arrow. In V2 patches are not present, instead there is a cruder pattern of wide slabs or stripes (four curved arrows), shown again at higher magnification in figure 11. Scale = 5 mm.

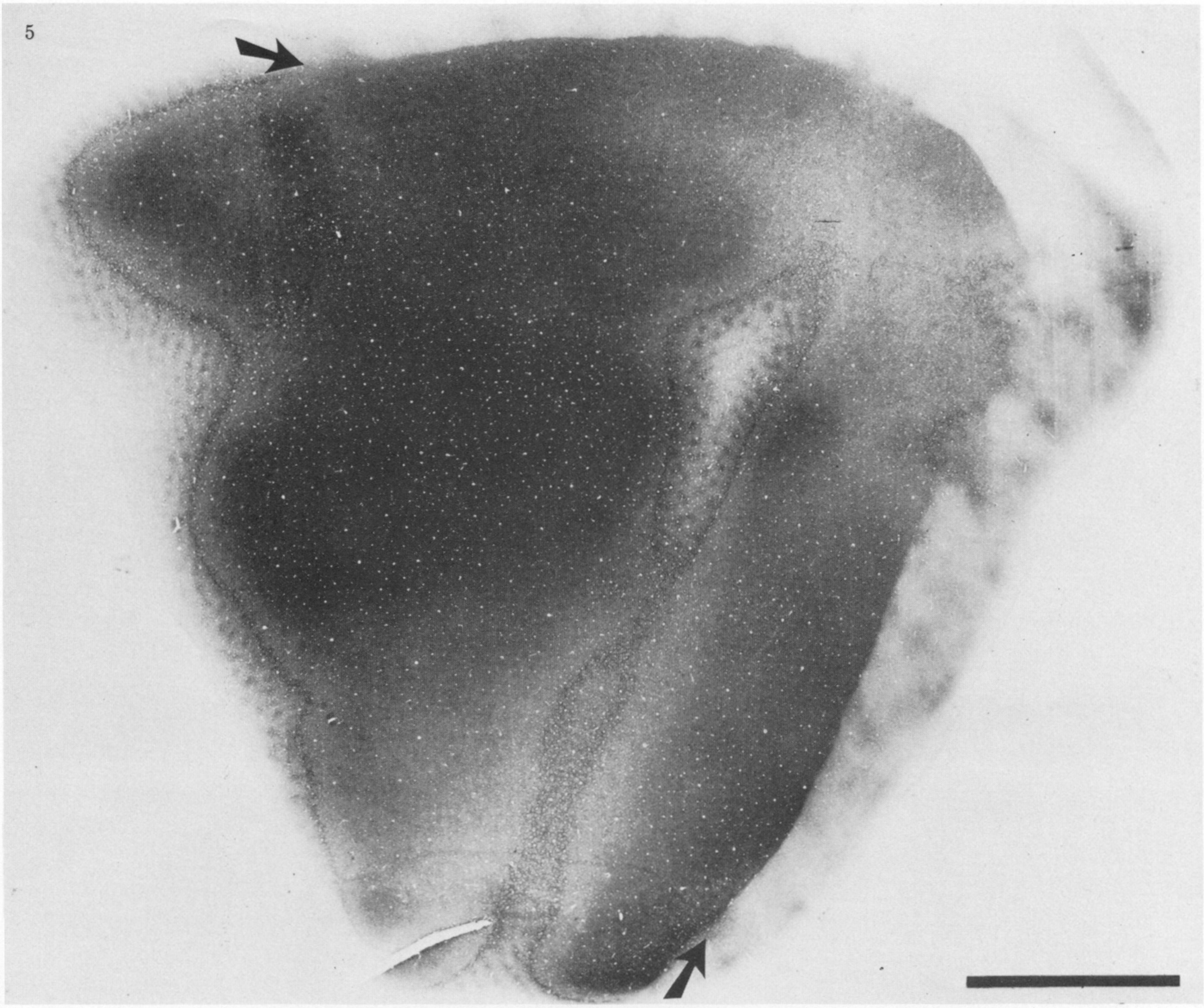


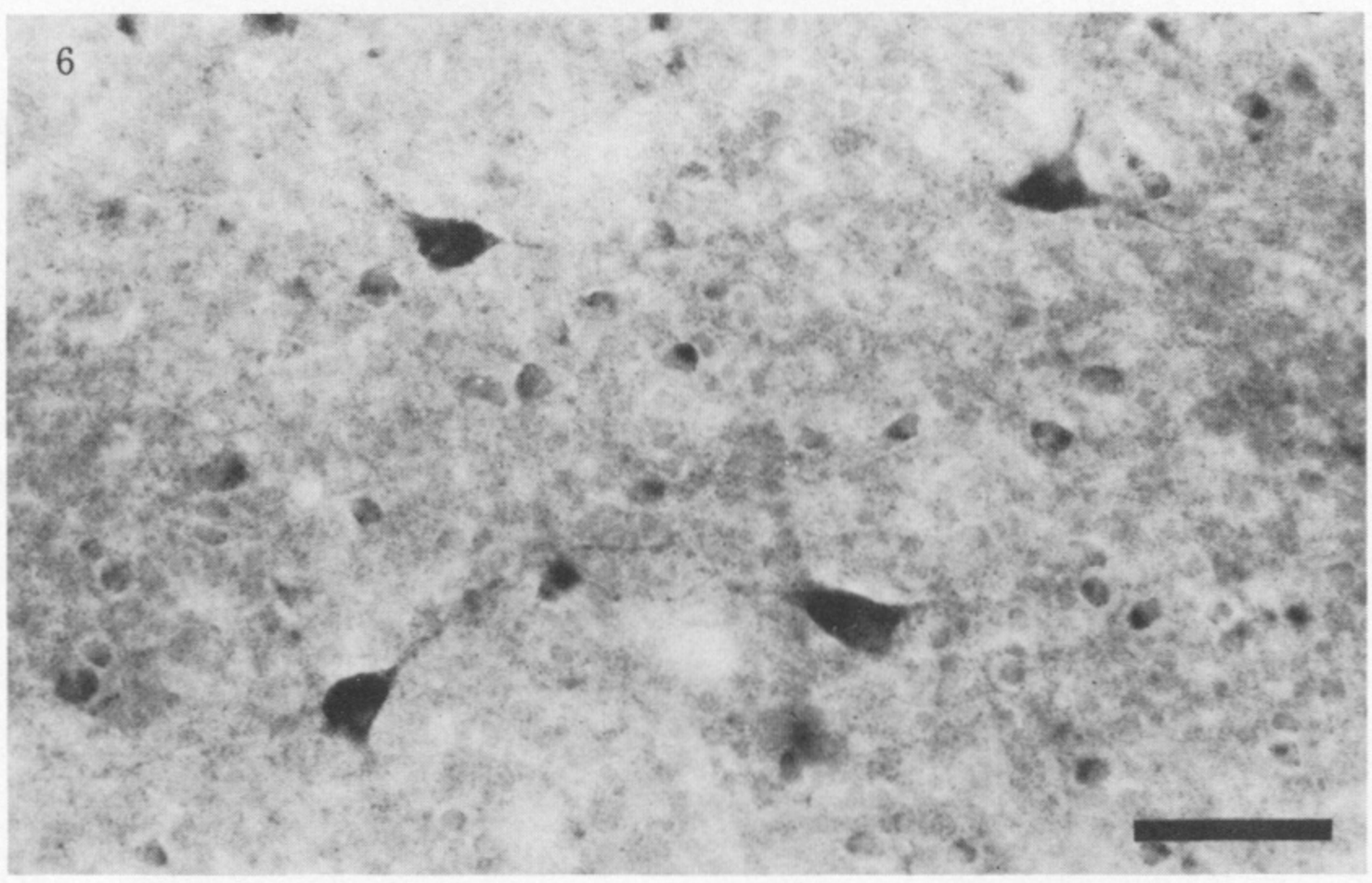


FIGURES 5 AND 6. For description see p. 210.

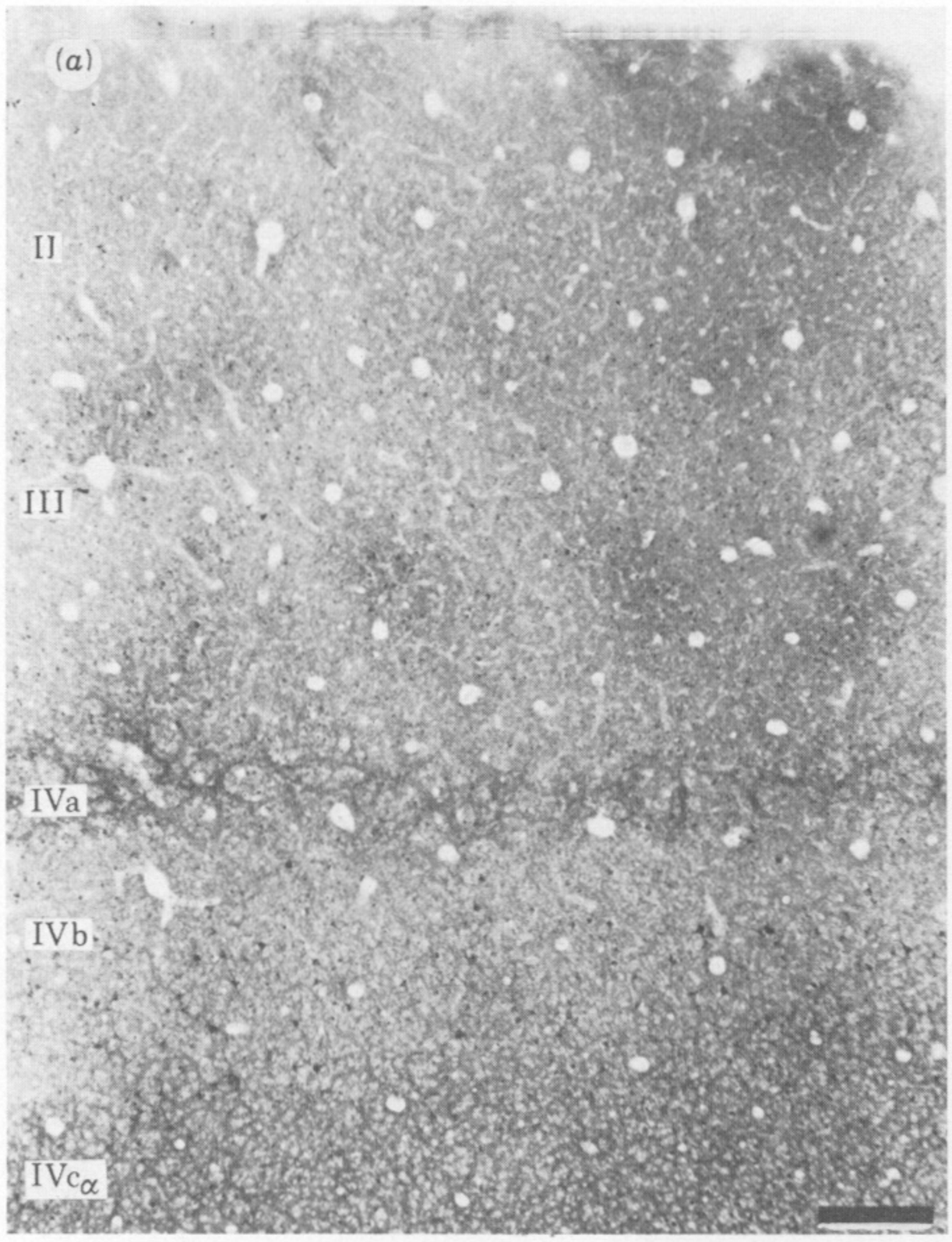



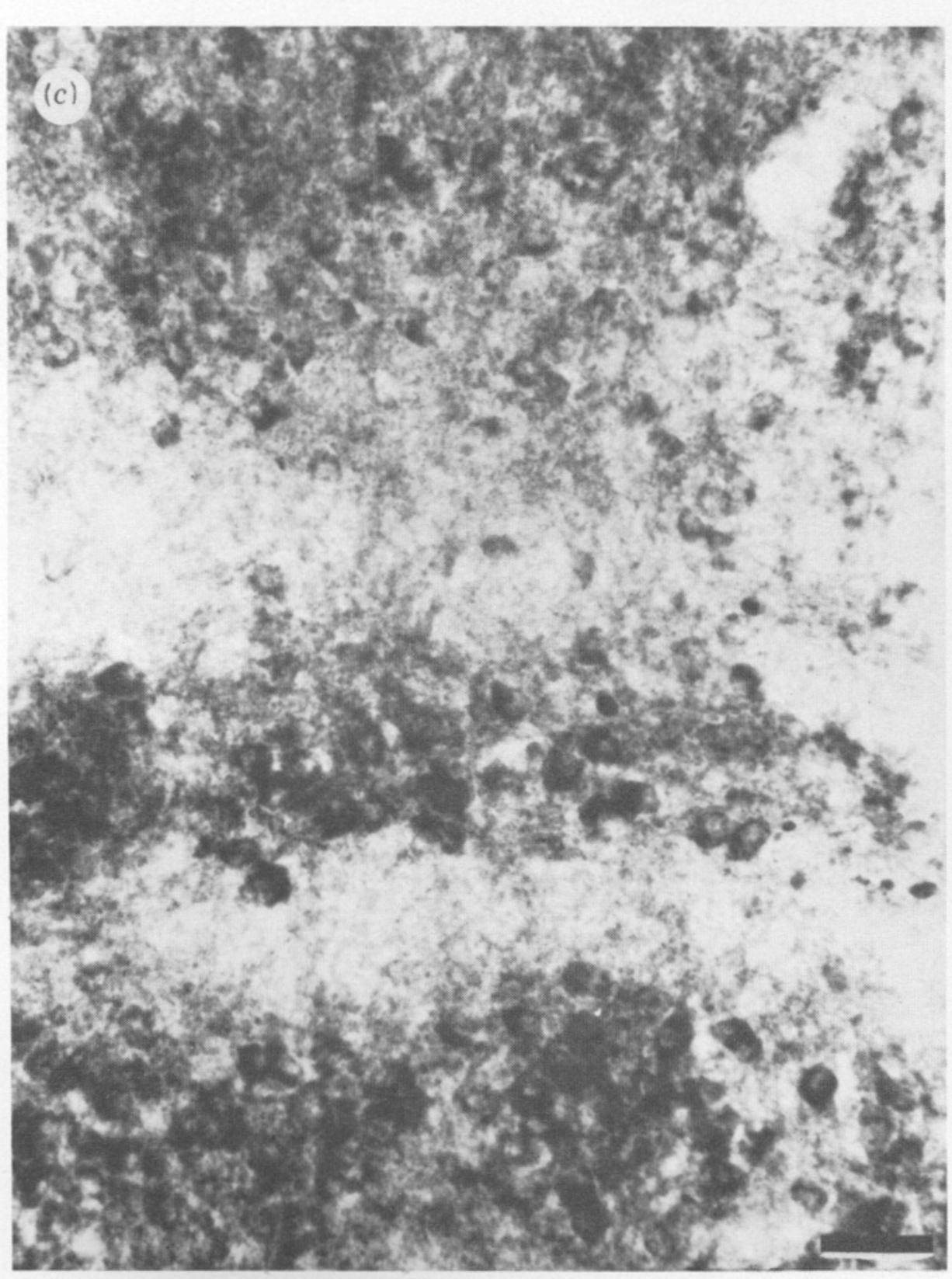



FIGURE 7. For description see p. 210.

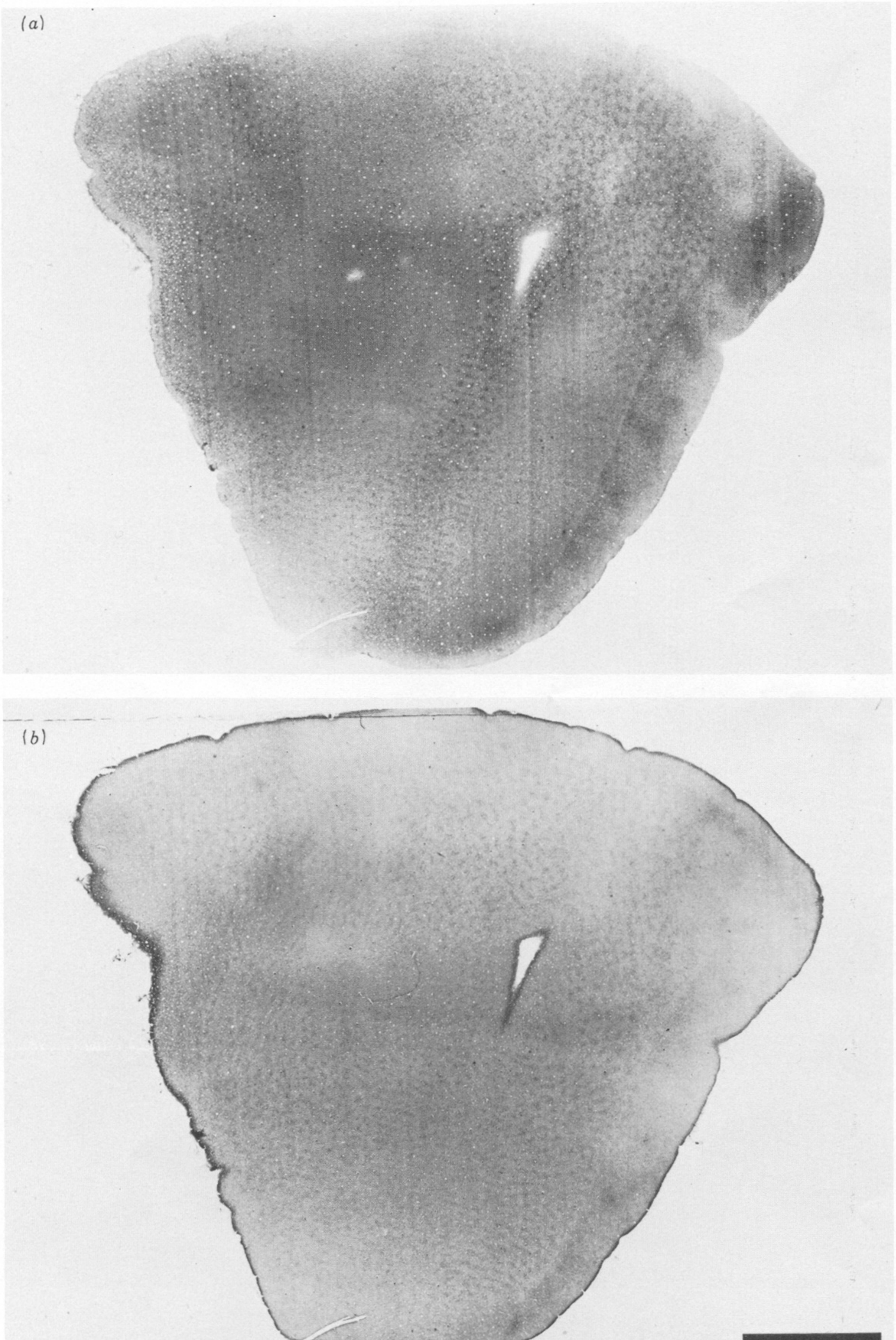


FIGURE 8. (*a*) Tangential section reacted for lactate dehydrogenase (LDH) activity from a normal macaque monkey cut from the same block as the cytochrome oxidase stained section illustrated in figure 3. Patches are visible in layers II and III; elsewhere the section passes through layer IV and no pattern is seen. Careful comparison of adjacent sections processed for cytochrome oxidase, LDH, and succinate dehydrogenase (not illustrated has demonstrated a precise match of patterns: the patches are preferentially labelled by stains for all three metabolic enzymes.

(*b*) An adjacent section cut slightly more superficially than (*a*) reacted for AChE activity shows a pattern of patches in layers II and III. These patches match exactly the patches labelled by cytochrome oxidase in figure 3. Scale = 5 mm.

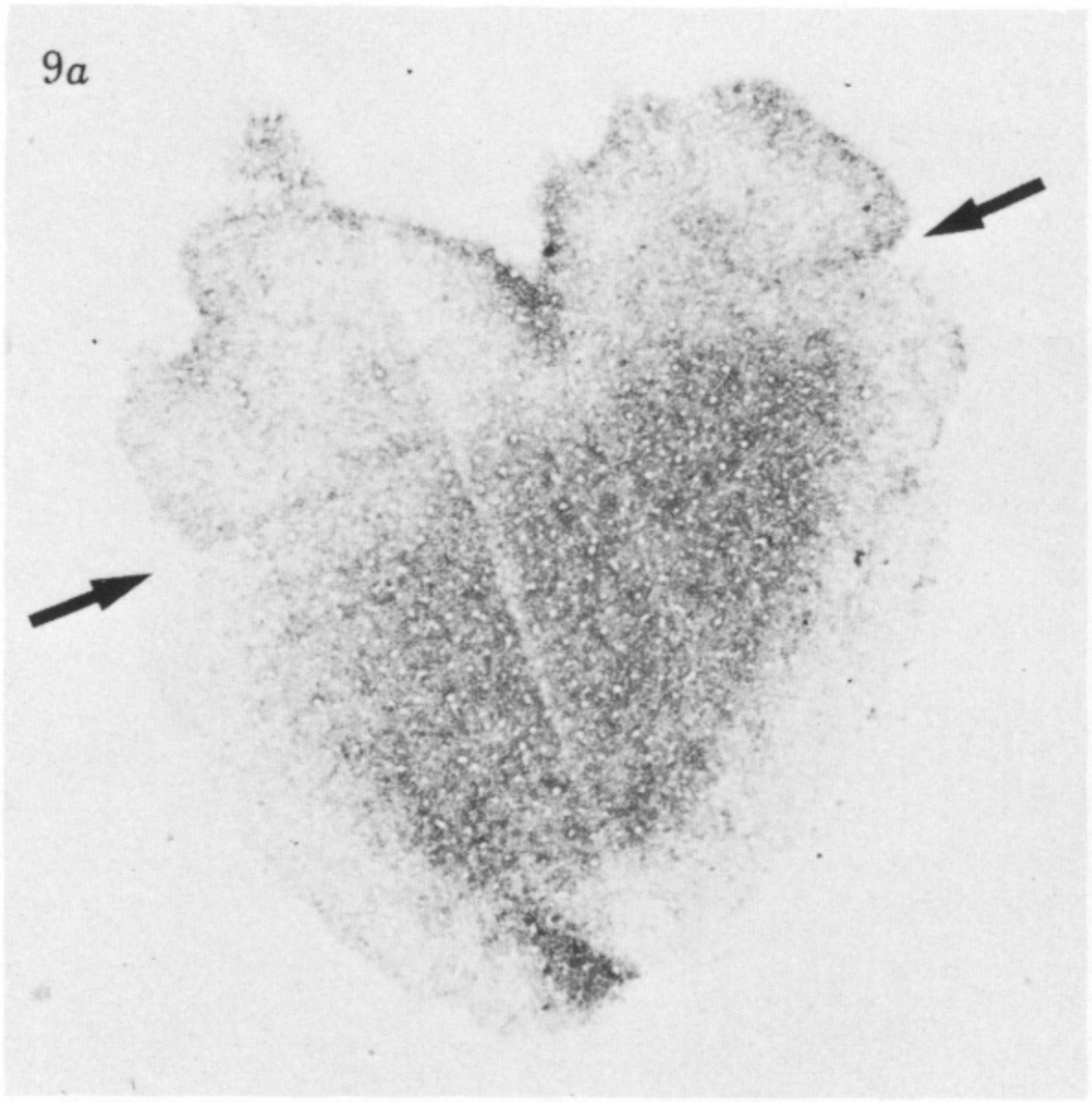


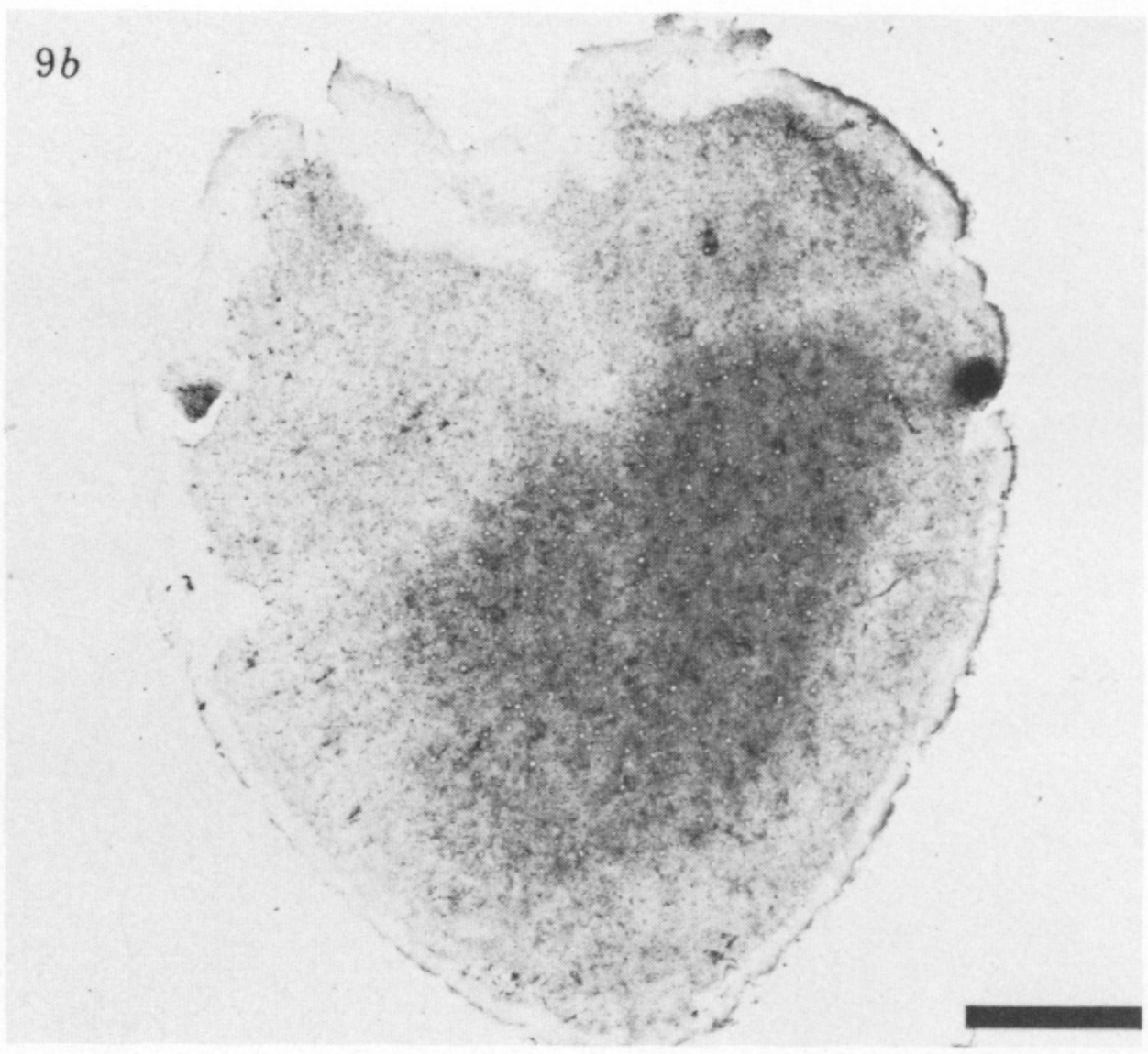


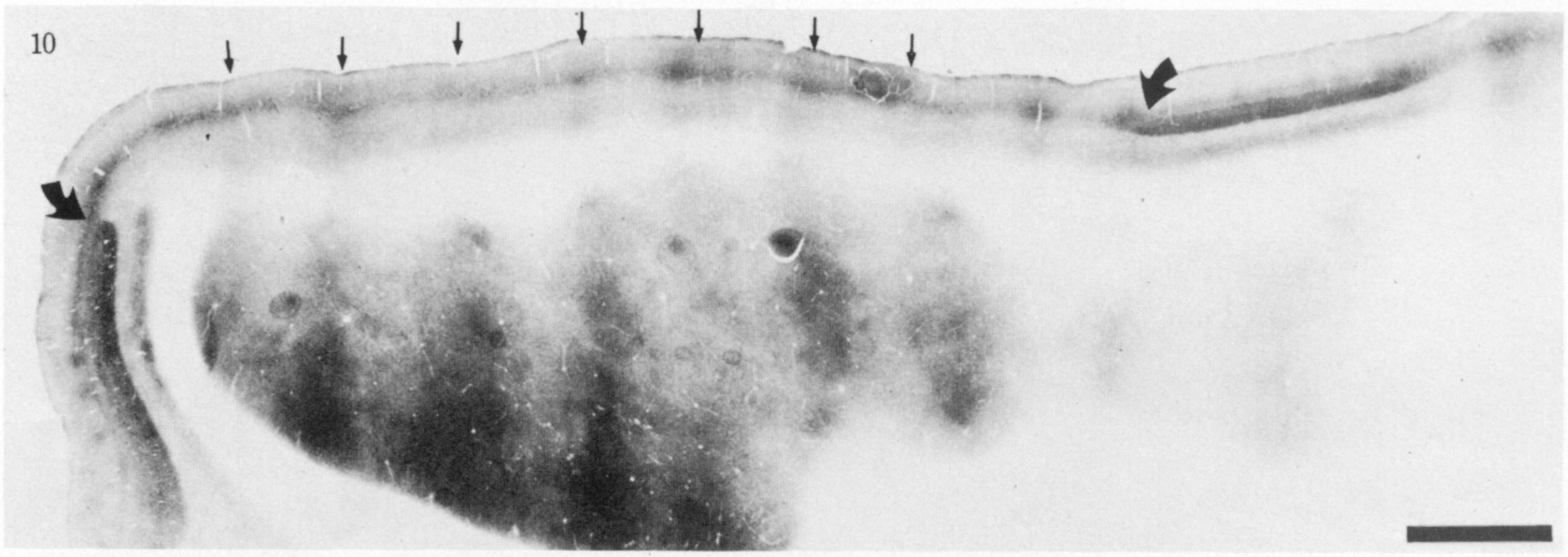


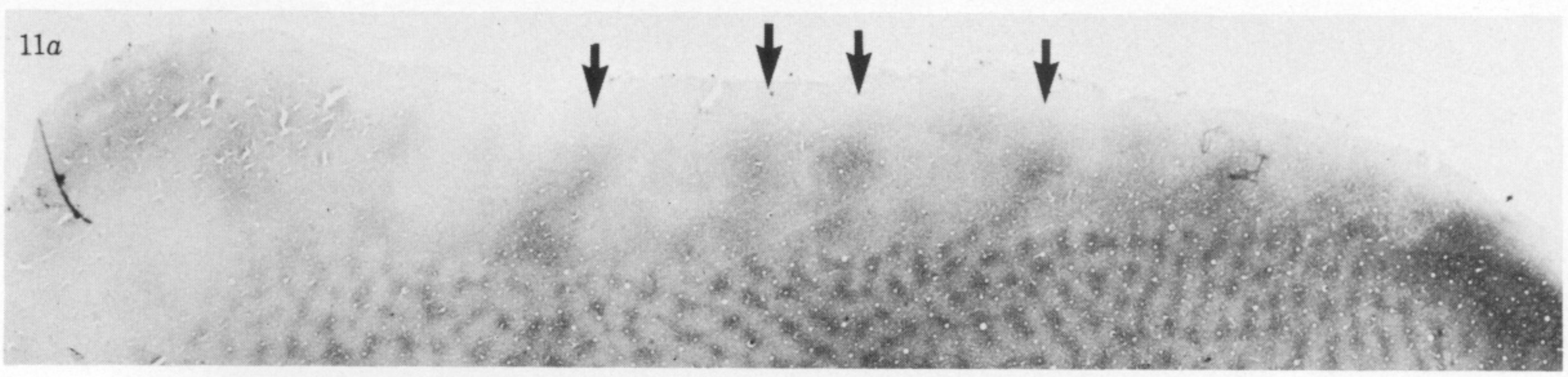


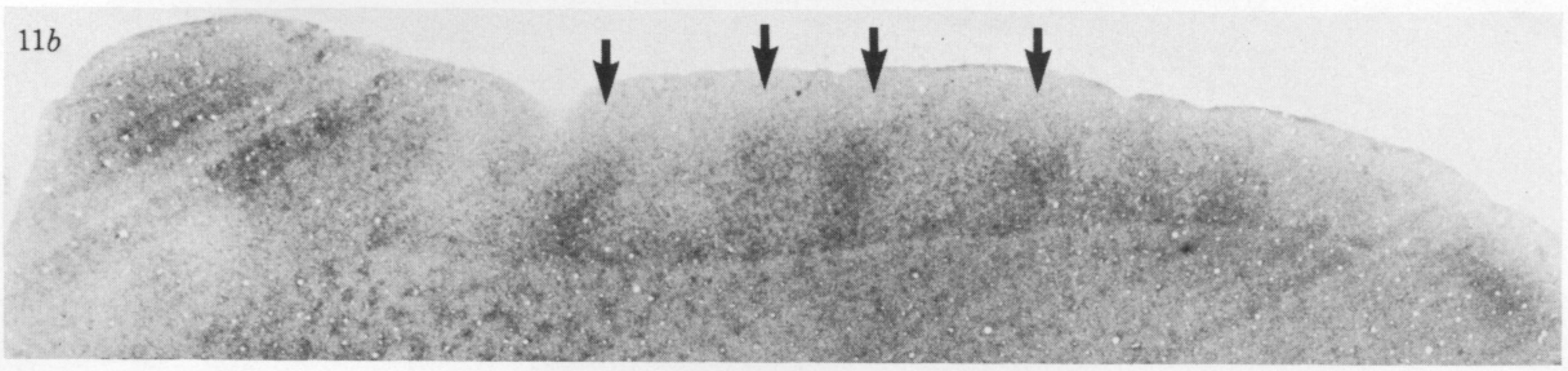


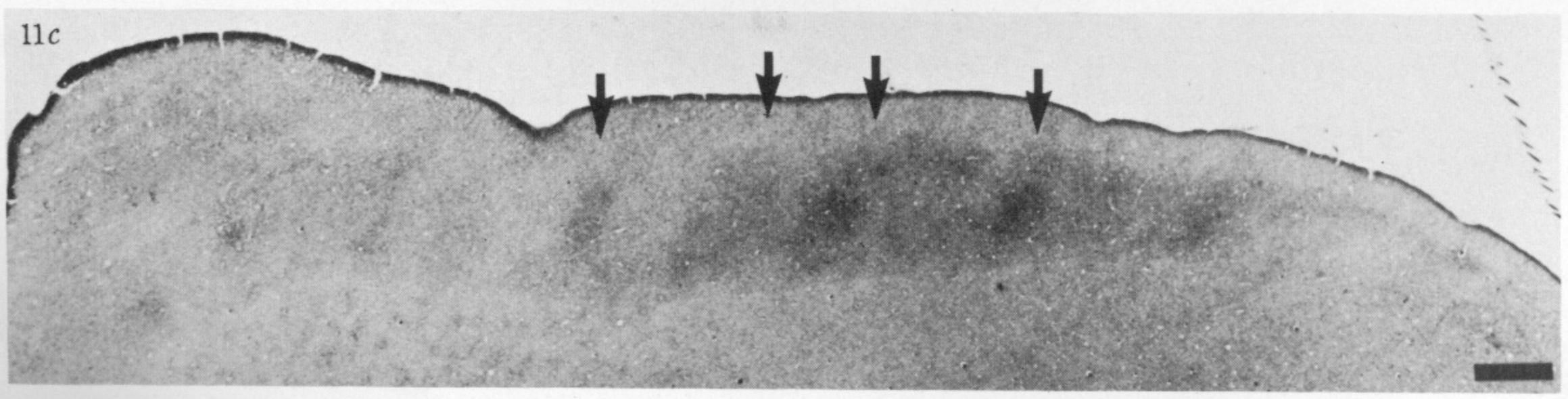


FIGURES 9–11. For description see p. 211.

12

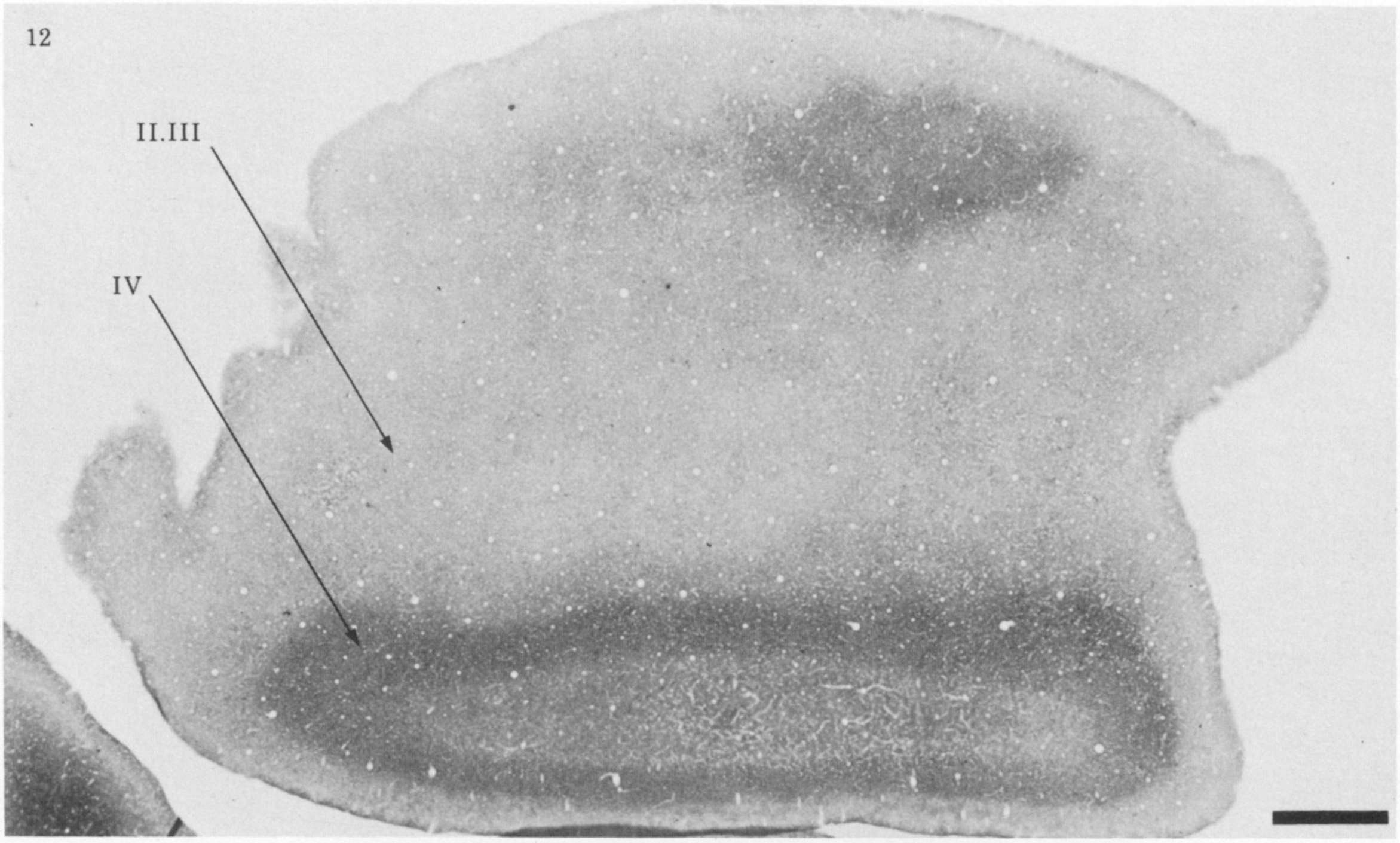


13*a*

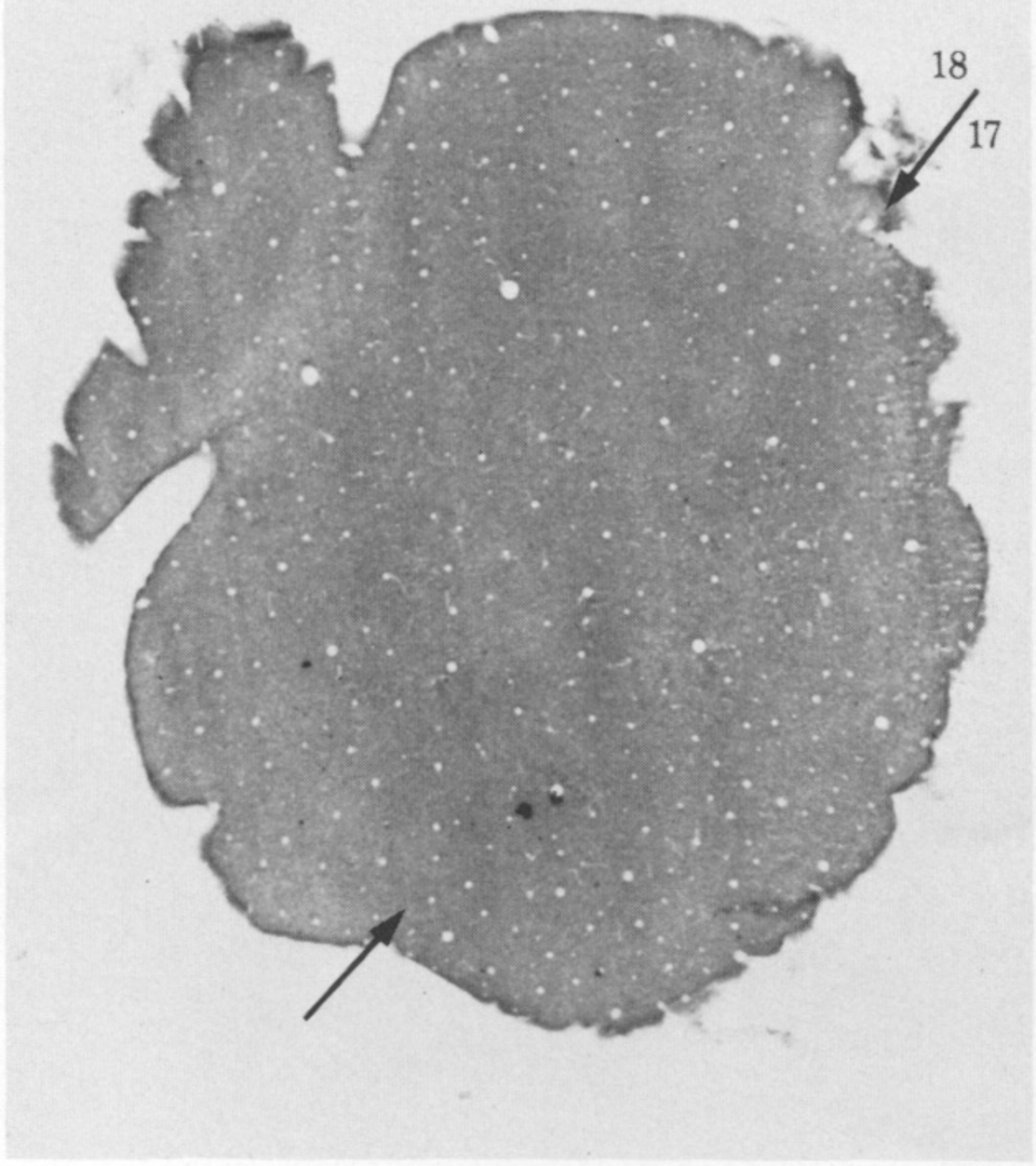


13*b*

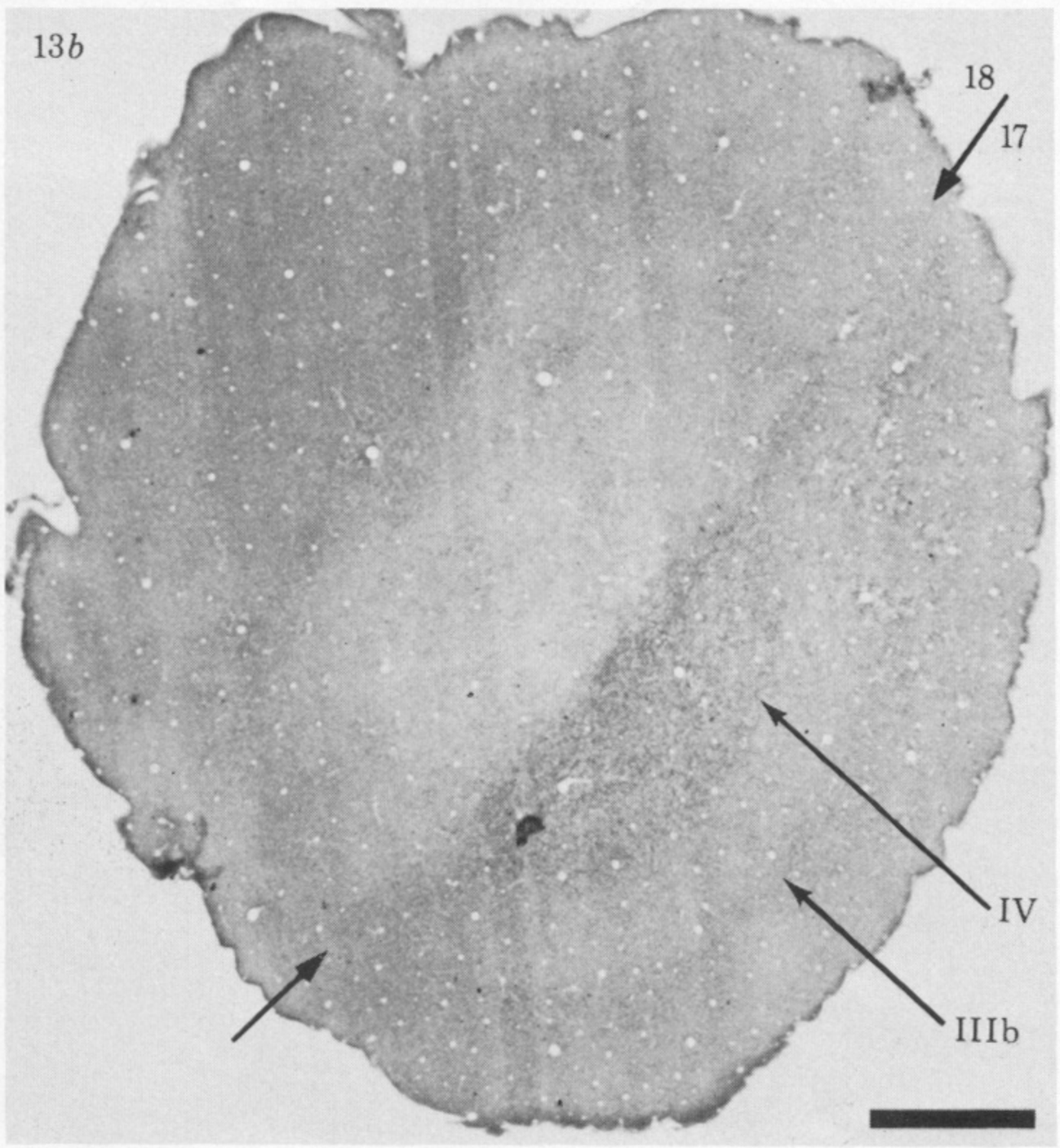


FIGURE 12. Tangential section reacted for cytochrome oxidase activity through the left striate cortex of a cat. In layers II and III no patches are present. Some faint unevenness is visible in the density of cytochrome oxidase staining, due to minor irregularities in section thickness and fixation. Scale = 1 mm.

FIGURE 13. (*a*) Cytochrome oxidase stained tangential section through the upper layers of the left occipital cortex of a normal tree shrew; medial is to the right and posterior is down. In area 17 no patches are visible.

(*b*) Another section cut 400 μm deeper from the same block. Where the section passes through layer IV the 17–18 border is easily visible. By using this section as a guide the 17–18 border was located in (*a*). So far, the cytochrome oxidase patches have not been found in a nonprimate species. Scale = 1 mm.

14

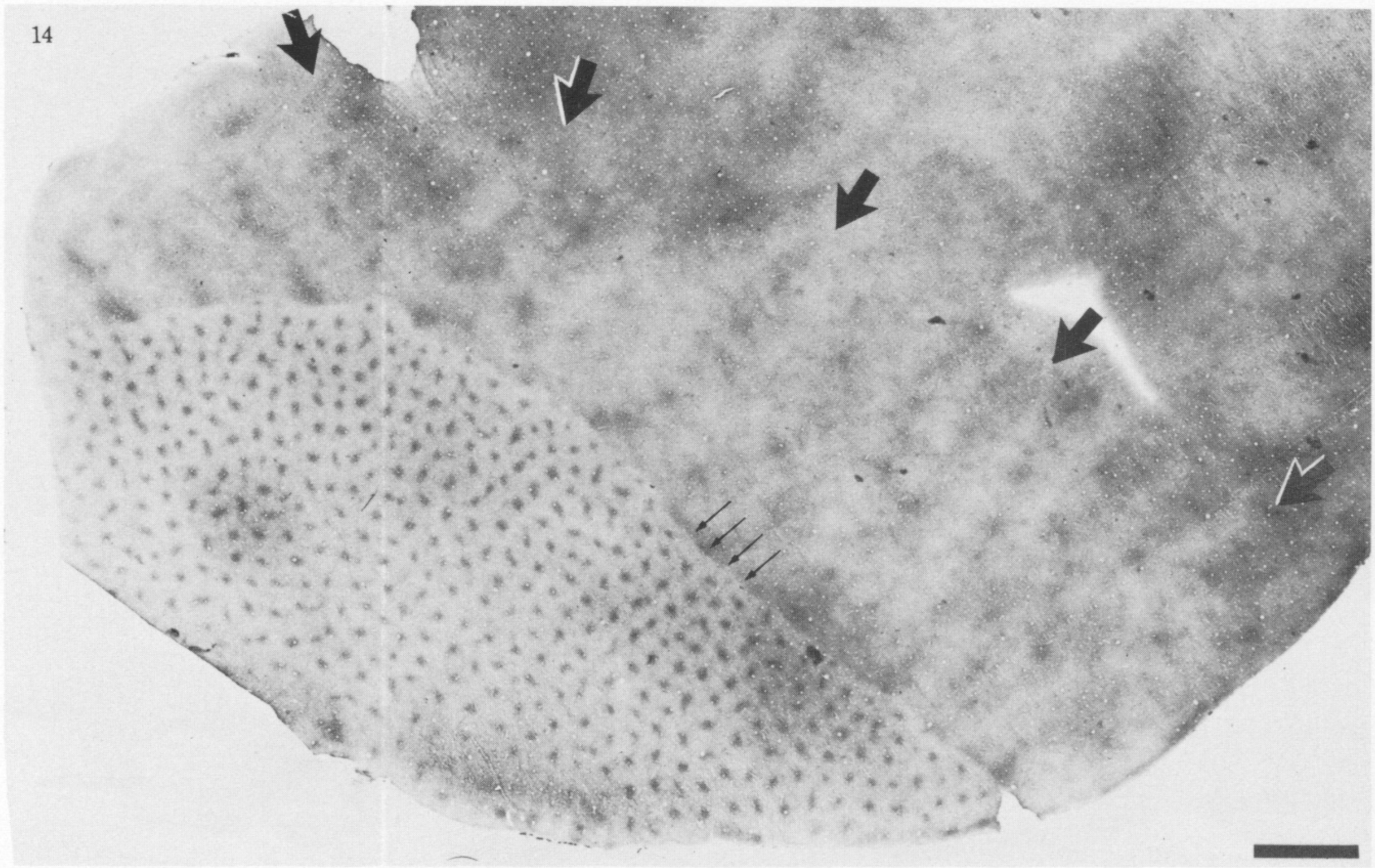

15

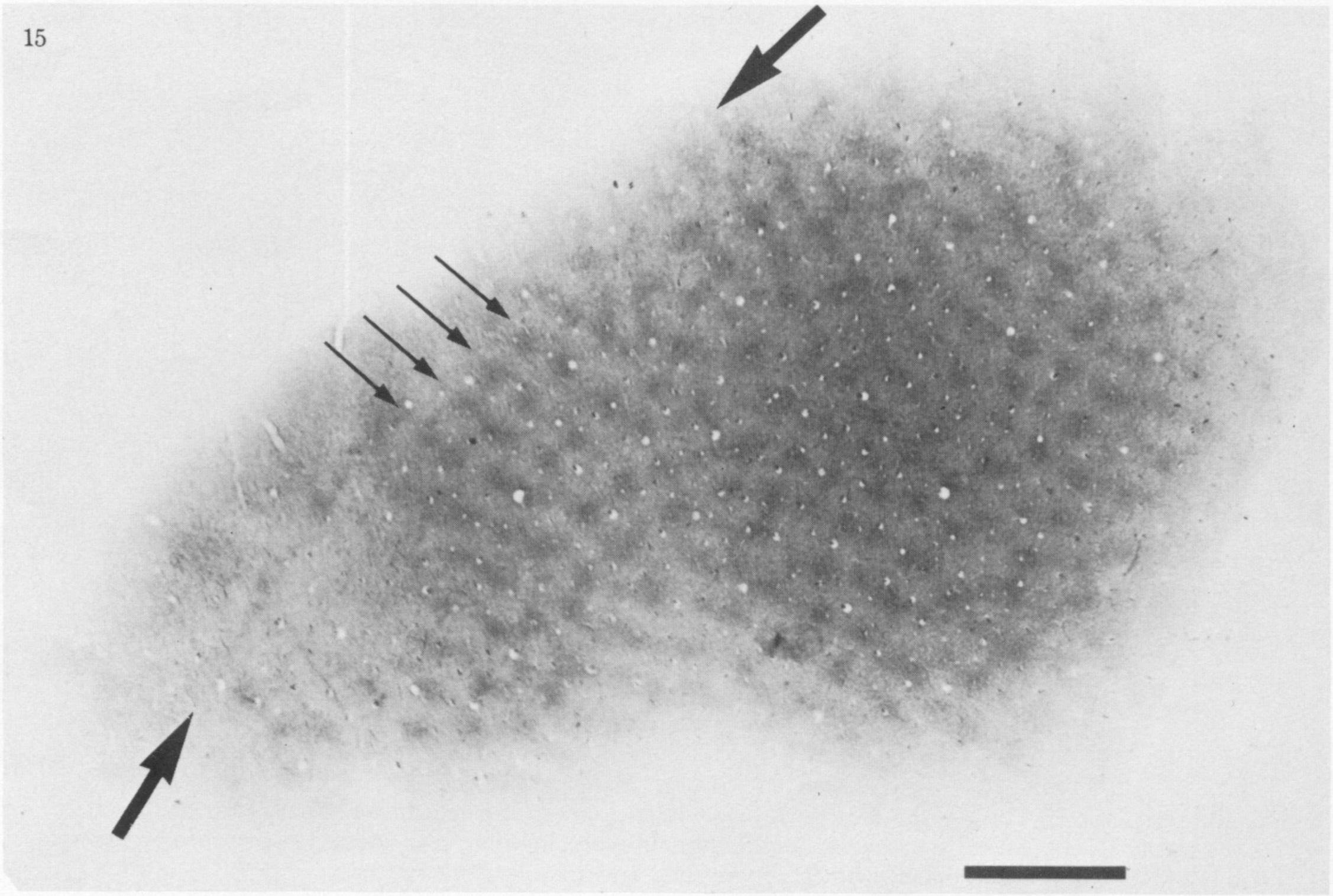

FIGURES 14 AND 15. For description see opposite.

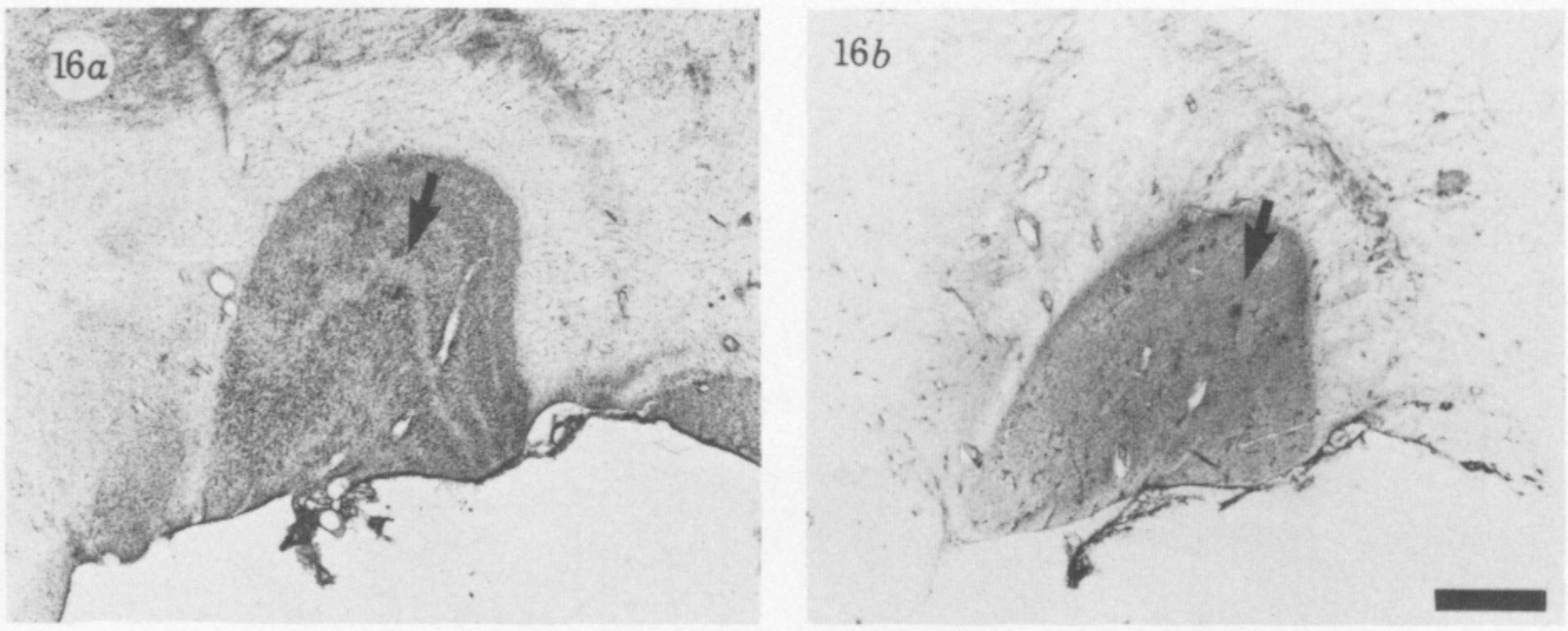



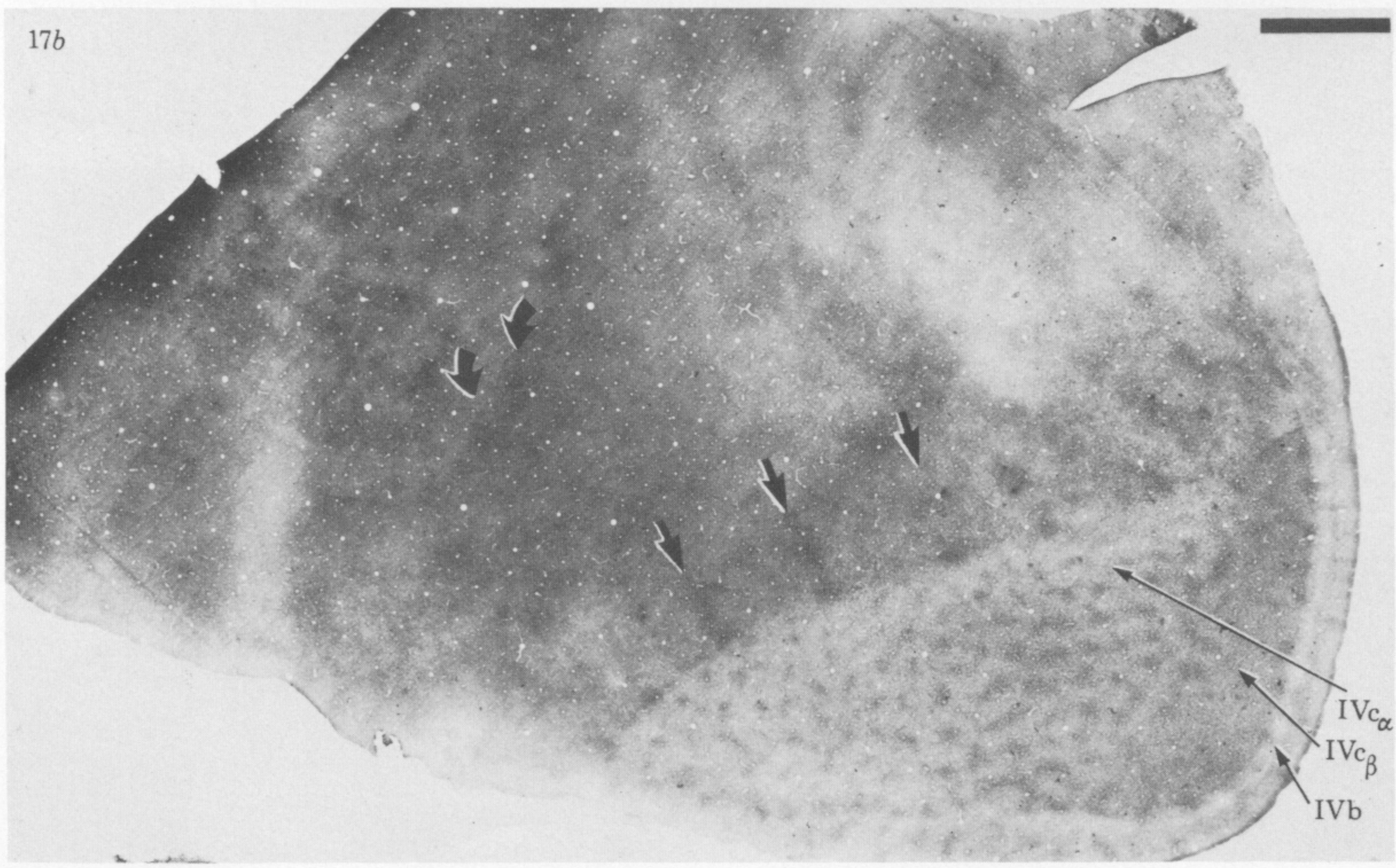


FIGURES 16 AND 17. For description see opposite.

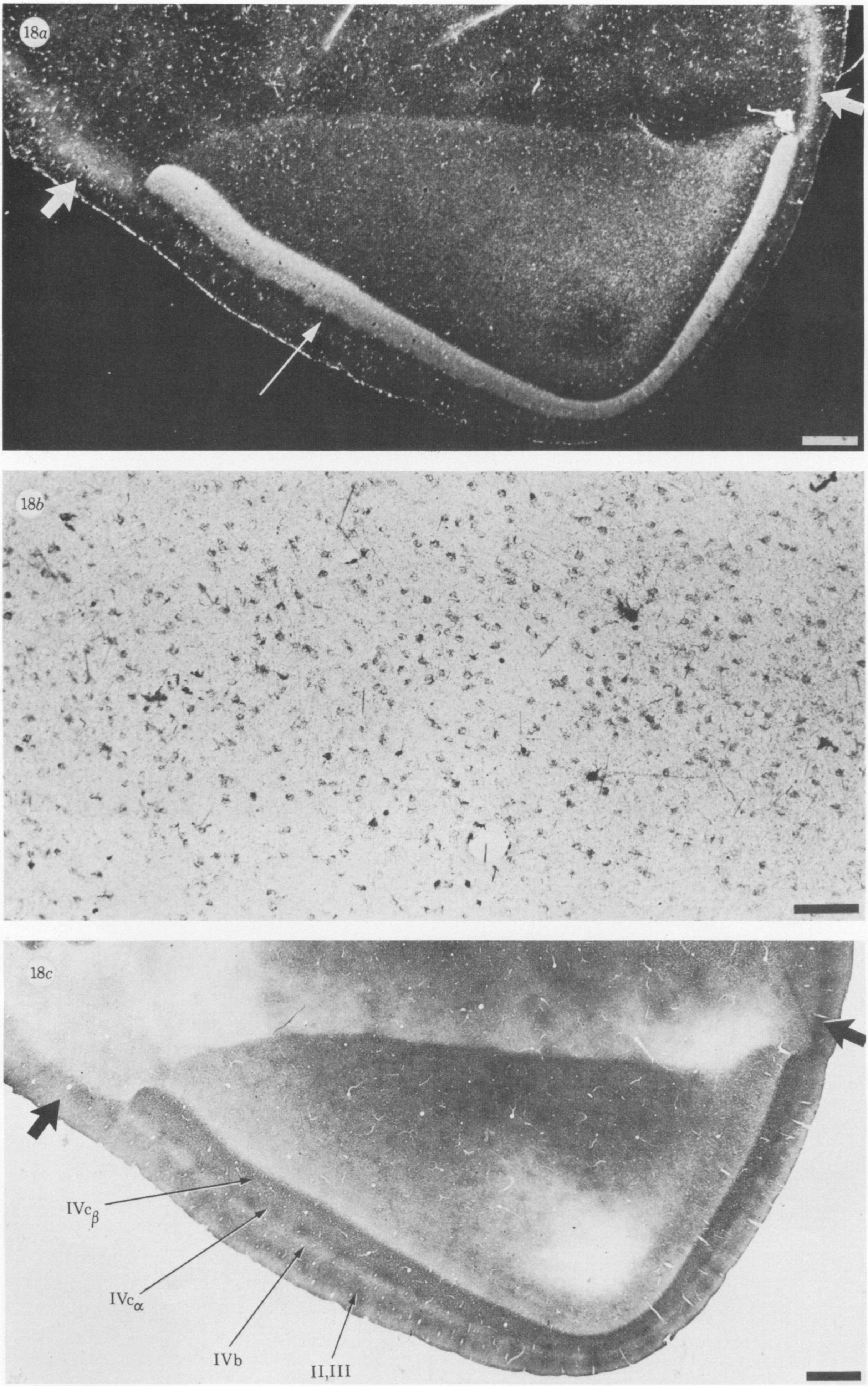


FIGURE 18*a–c*. For description see opposite.

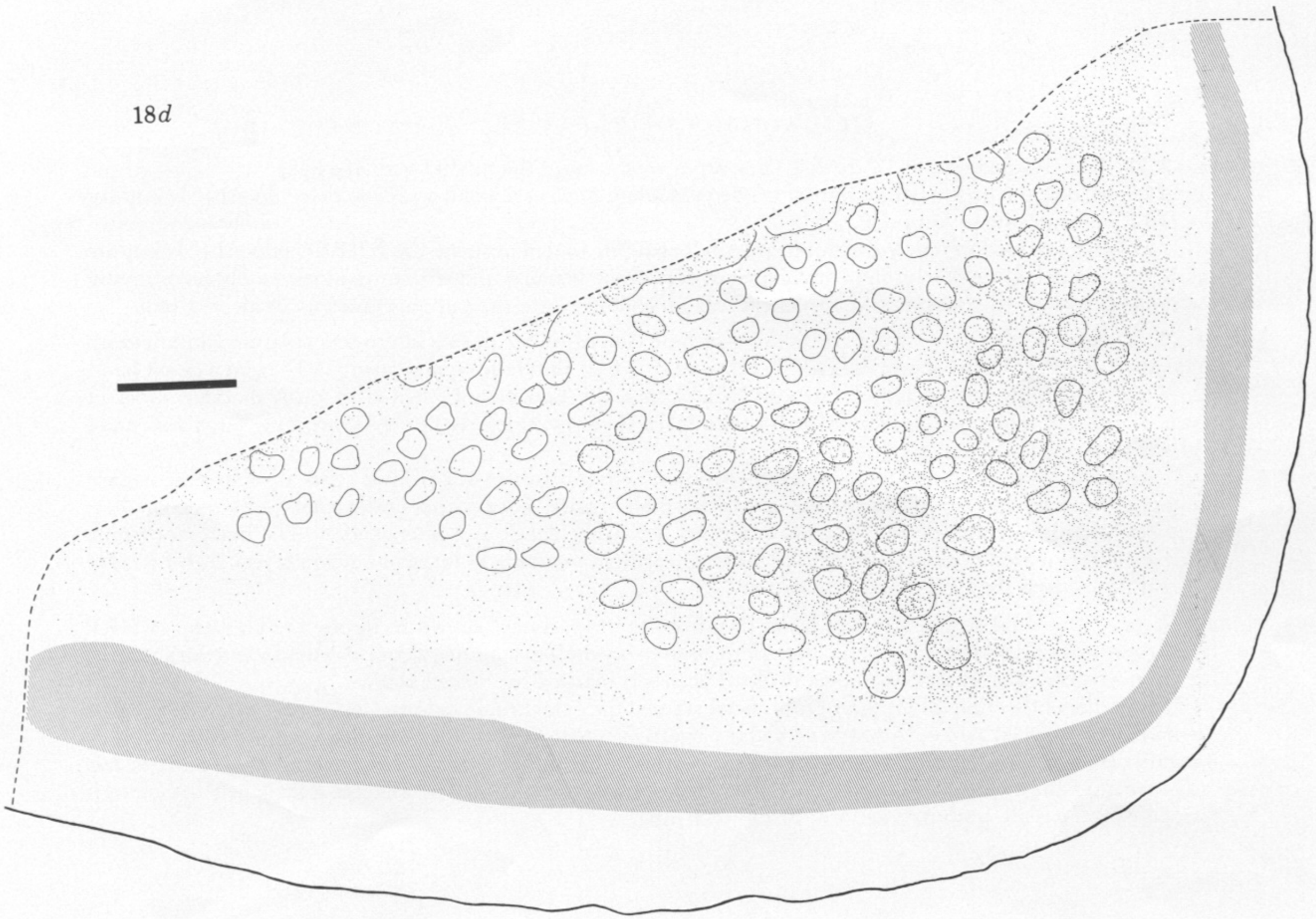


## Description of plates 10 and 11

Figure 18. (*a*) Section cut deeper to the section illustrated in figure 17 (*a*), passing primarily through layer VI. Under darkfield crossed polaroid illumination layer IV c stands out as a V-shaped band of intense HRP activity. This band stops abruptly at the 17–18 border, where it gives way to a more diffuse band of label in V2 (broad arrows). Just superficial to layer IV c in striate cortex, a label-free gap is visible, corresponding to layer IV b. It is marked by the tip of a thin arrow. Deep to layer IV a thin, relatively label-free zone is seen, corresponding to layer V. It borders layer VI which contains an even haze of faint HRP label, forming a clear border with V2 anteriorly (up). Scale = 1 mm.

(*b*) High power view of layer VI in (*a*) under brightfield illumination. Numerous cells containing retrogradely transported HRP are visible. In addition, HRP label is present, via anterograde transport, in terminals of geniculate axons projecting to layer VI. Scale = 100 μm.

(*c*) Section adjacent to (*a*) reacted for cytochrome oxidase activity. A dark V-shaped band of enzyme staining in layer IV c, corresponding to the HRP band in (*a*) is obvious. In layers IV $c_\alpha$ and II and III patches are visible, separated by the light gap characteristic of IV b. In layer VI patches are also clearly visible. The broad arrows mark the layers of heaviest cytochrome oxidase staining in V2, matching the HRP label indicated by arrows in (*a*). Scale = 1 mm.

(*d*) Reconstruction showing relationship between HRP labelled cells and cytochrome oxidase patches in layer VI of striate cortex. The dotted line indicates the 17–18 border and the band of oblique parallel lines marks HRP label in layer IV c. To prepare the reconstruction, the section in (*a*) was drawn with the aid of a camera lucida and the position of every retrogradely labelled cell marked by a small dot. A total of 11671 HRP filled cells was present in the section. Then the position of each cytochrome oxidase patch in (*c*) was indicated by drawing its borders. Alignment between (*a*) and (*c*) was achieved by careful comparison of blood vessel patterns in both sections. The reconstruction indicates that, considered as a single population, corticogeniculate projecting cells are fairly evenly distributed in layer VI, with no tendency to be clustered within the cytochrome oxidase patches. Scale = 1 mm.


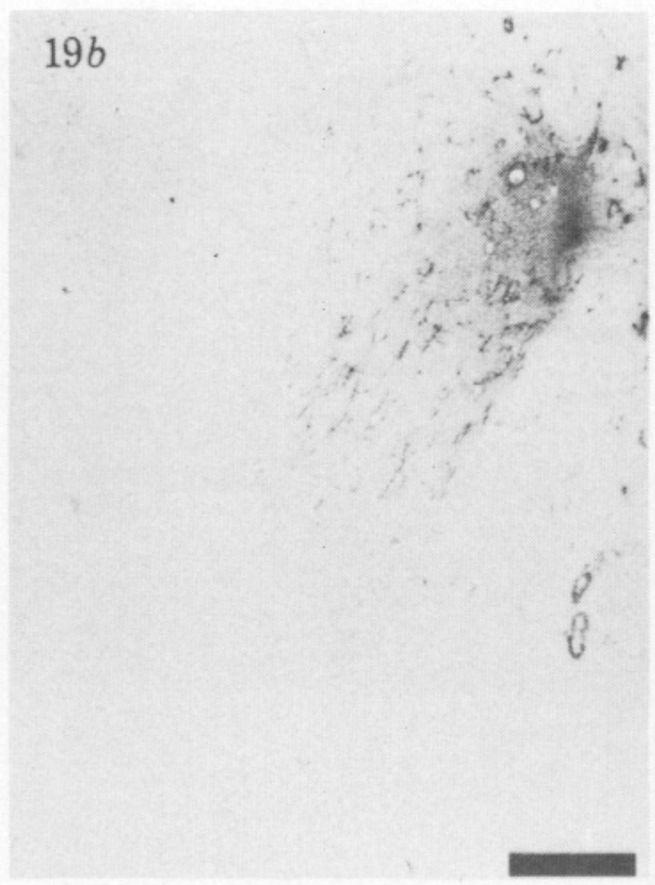


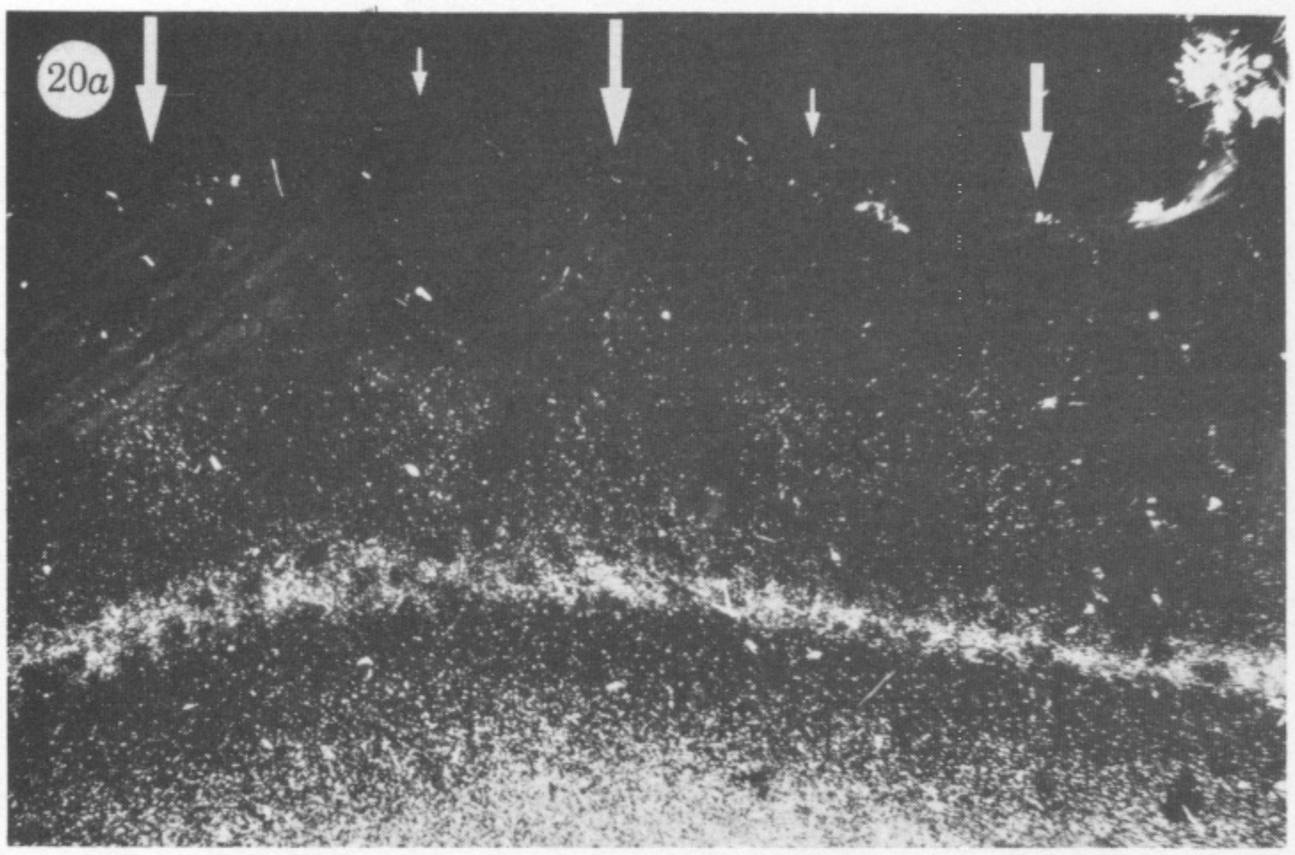


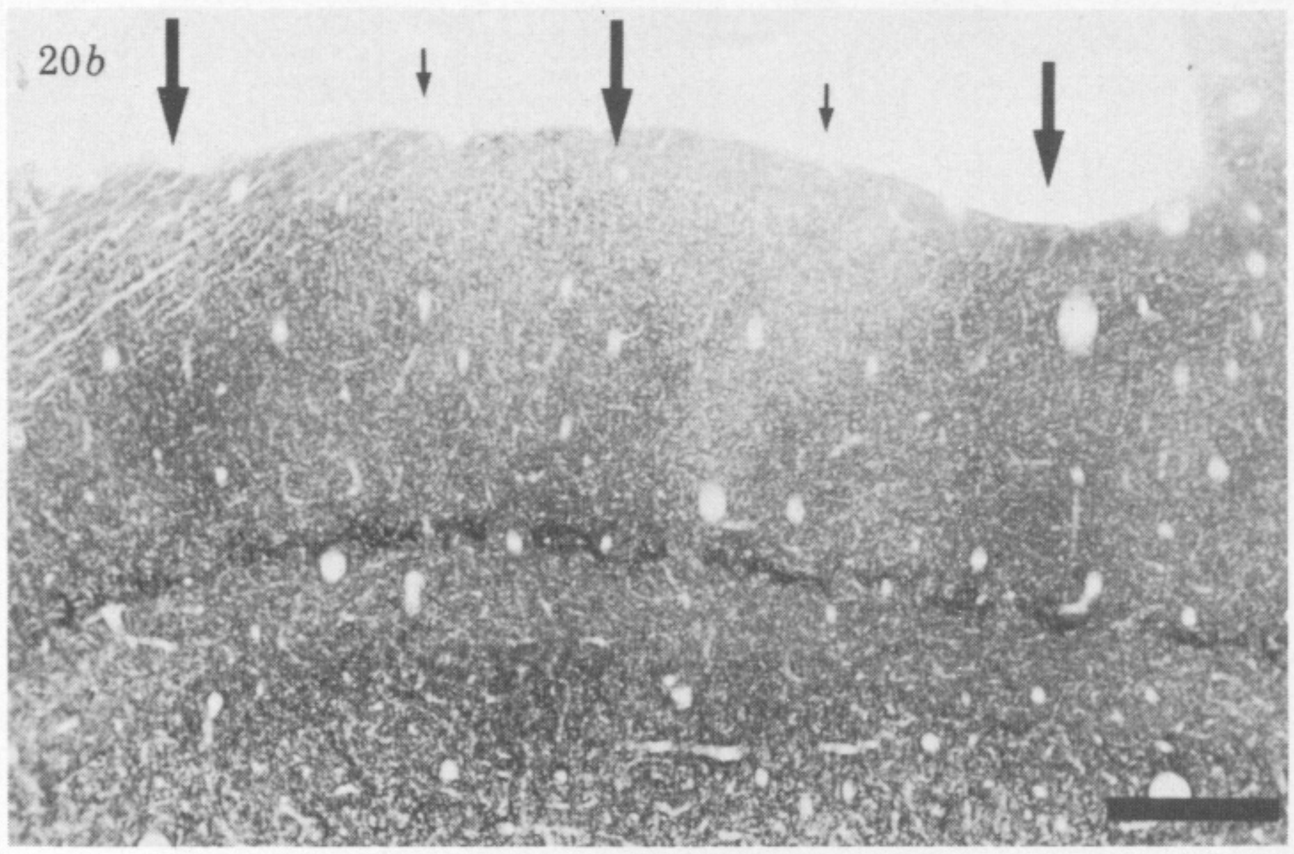


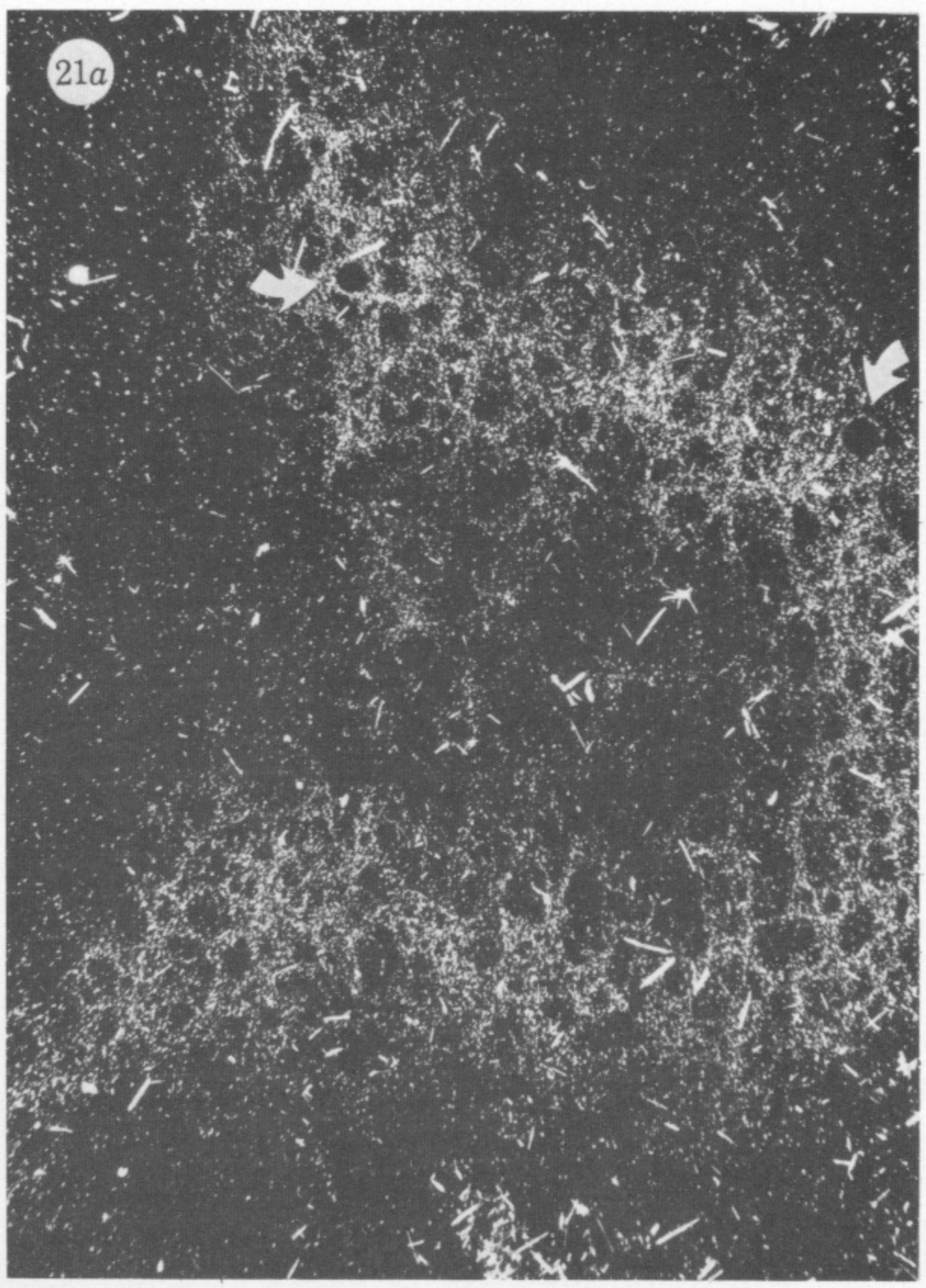


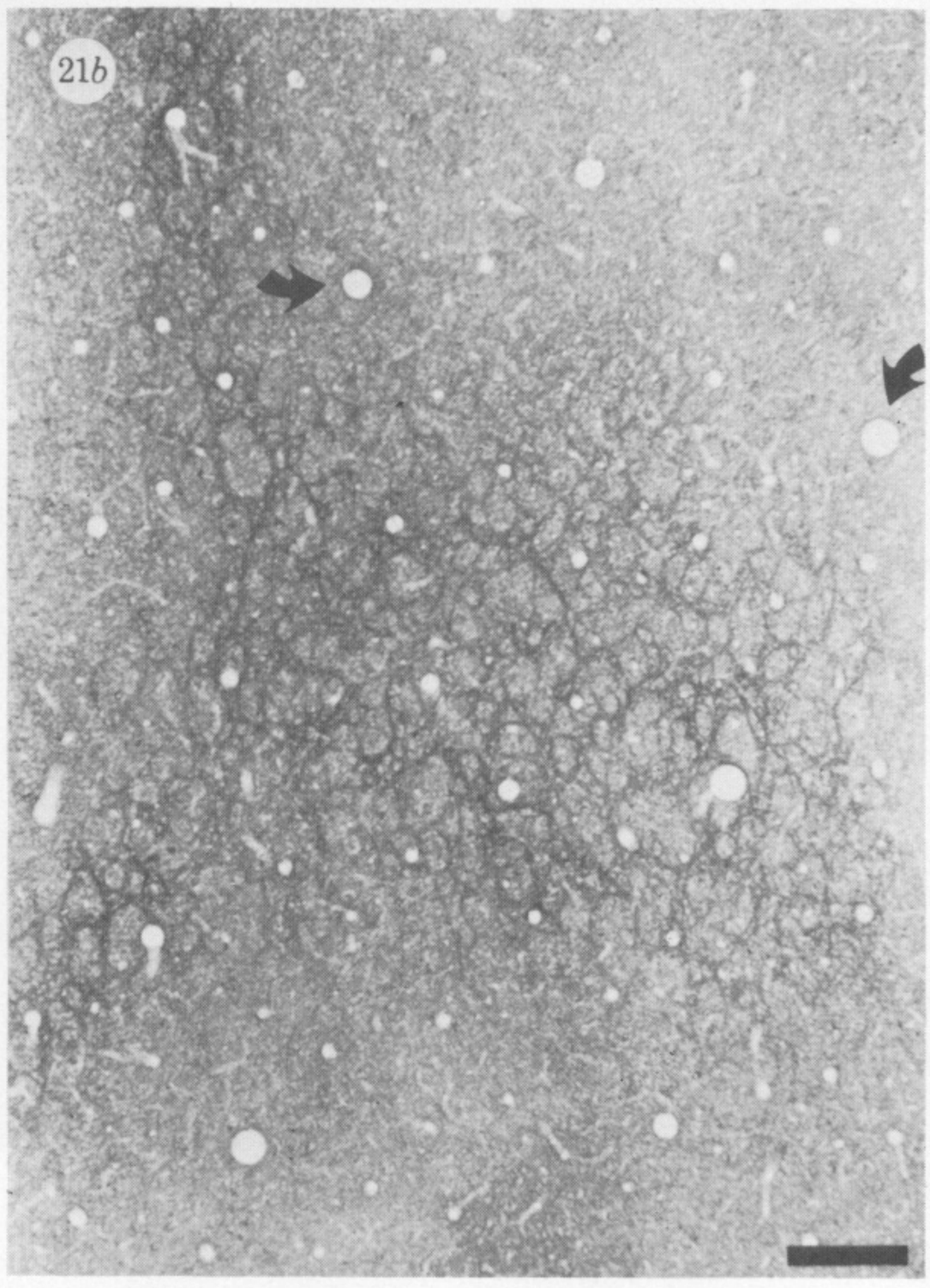


FIGURES 19–21. For description see opposite.

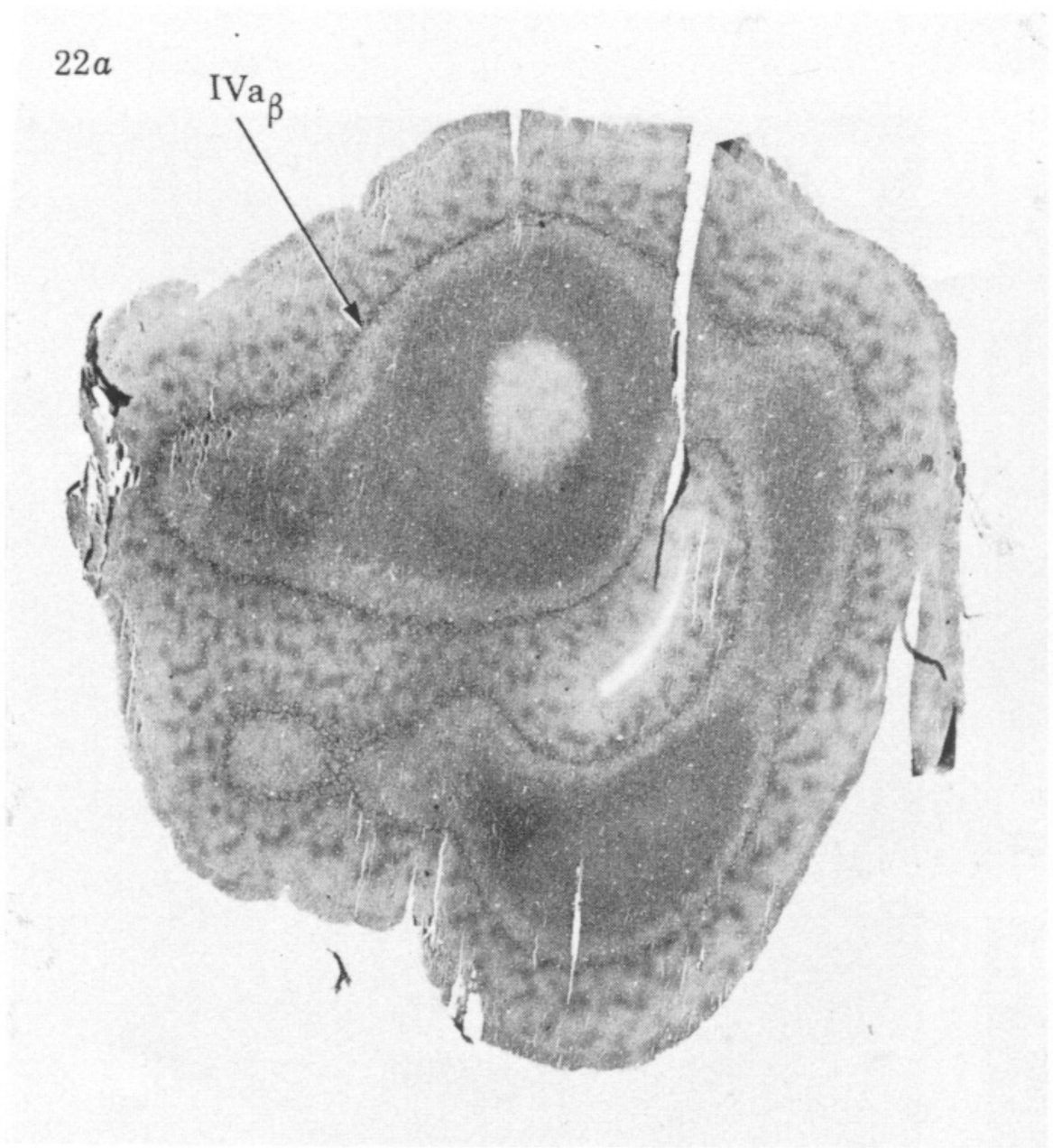


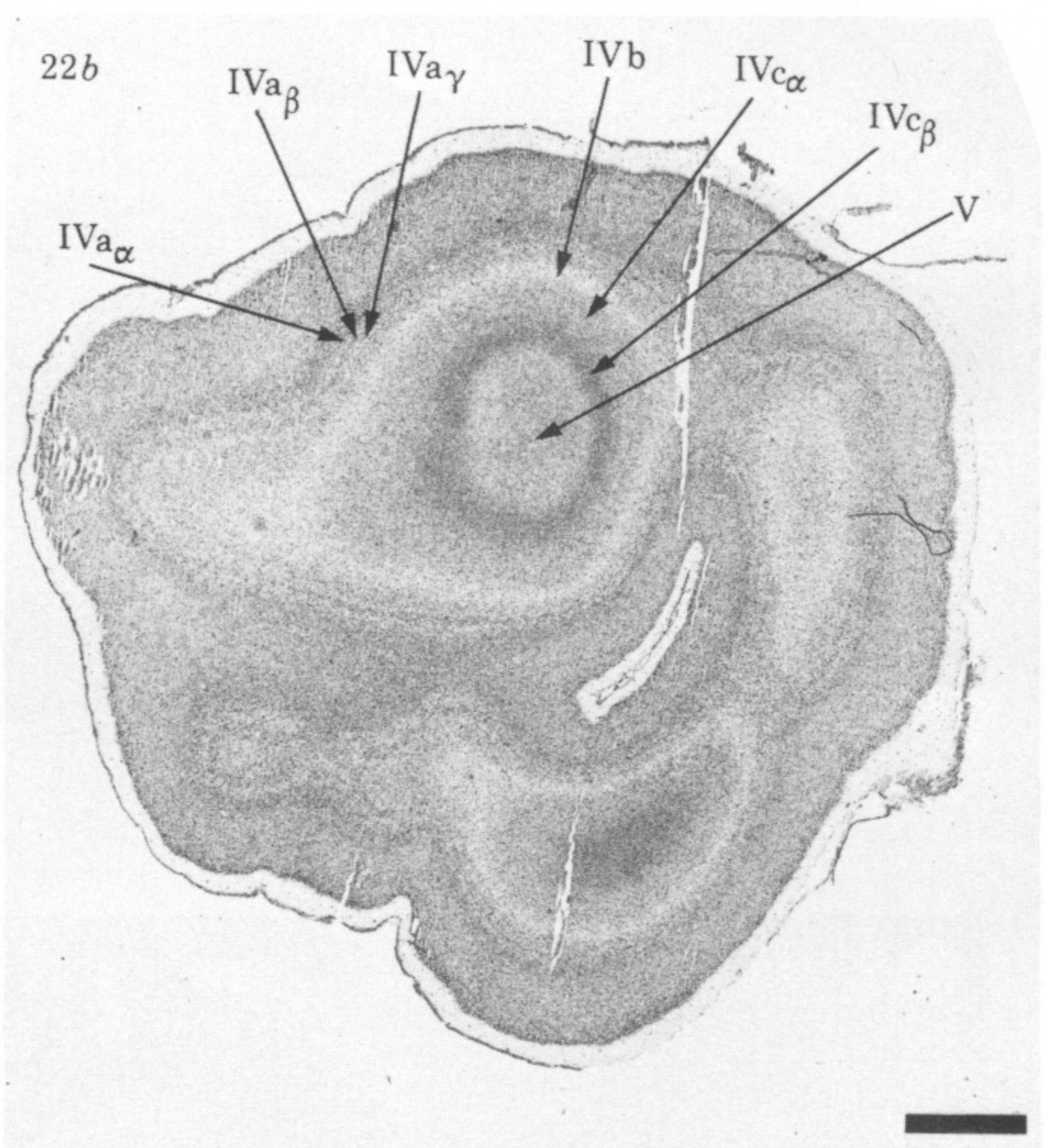


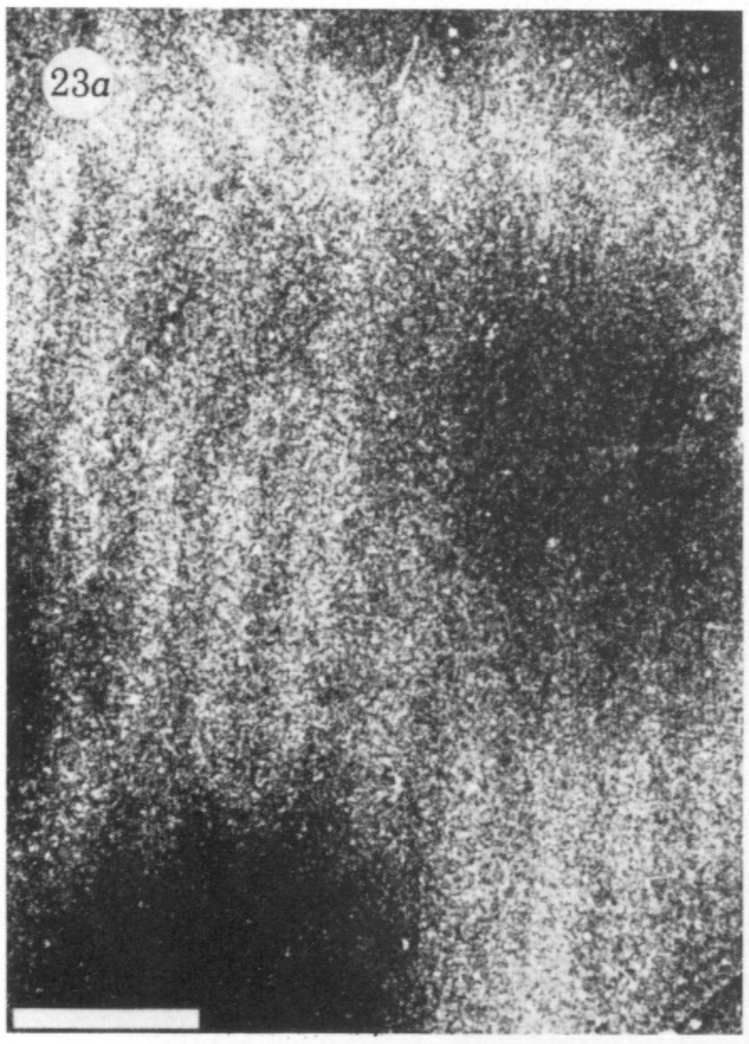


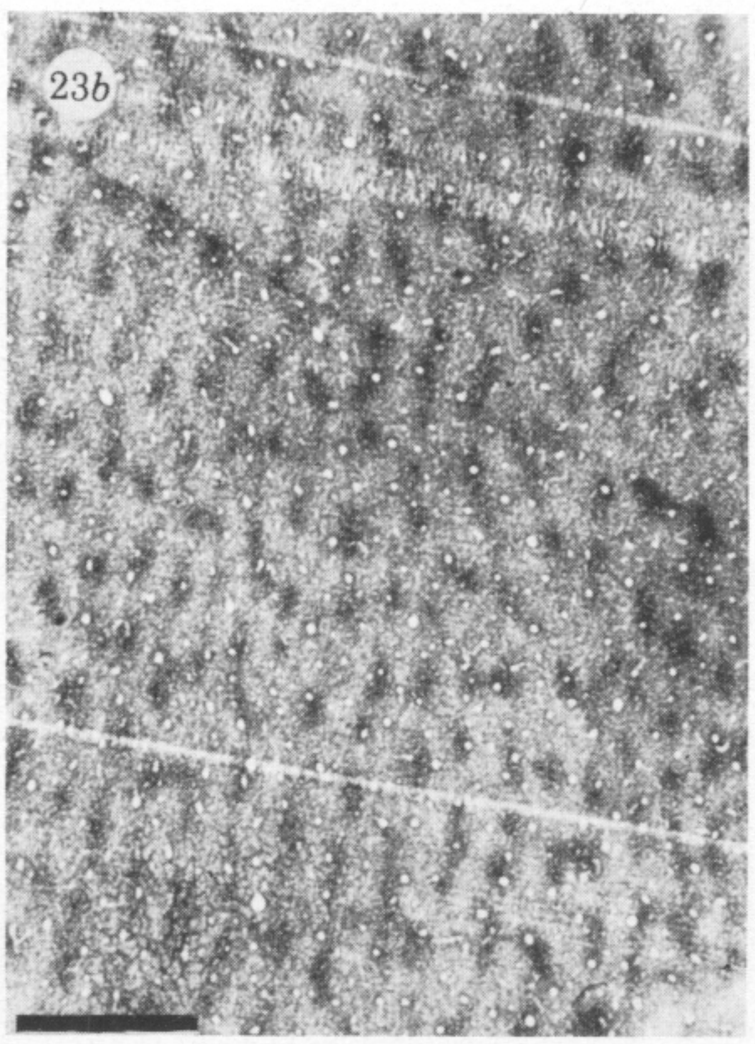


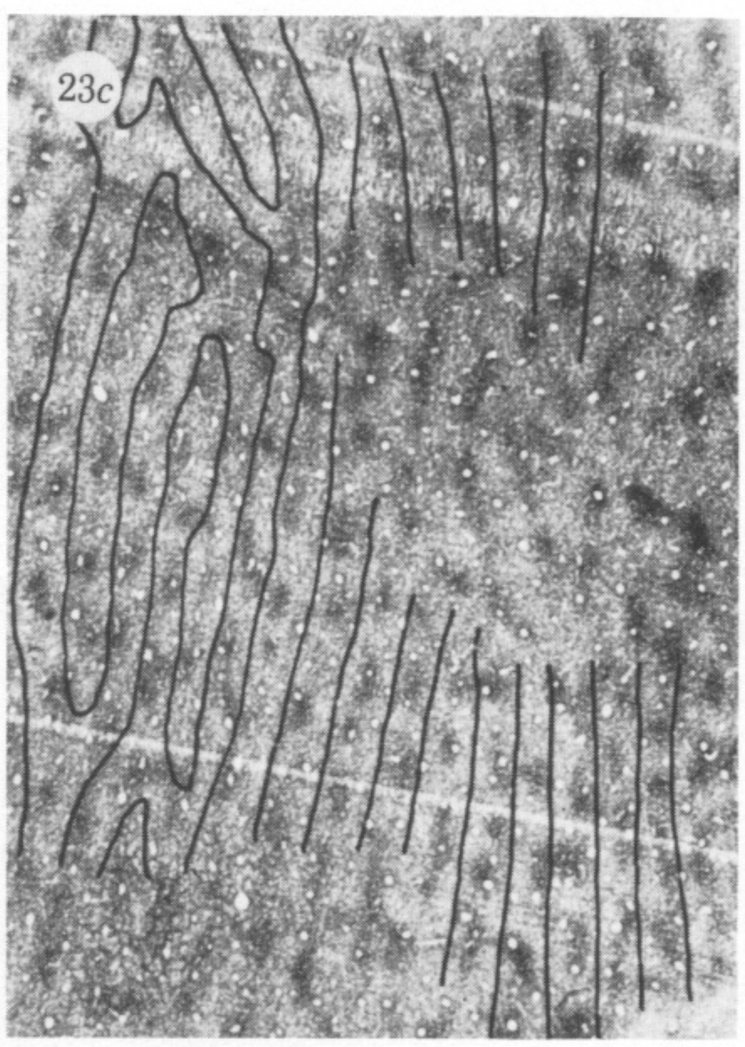


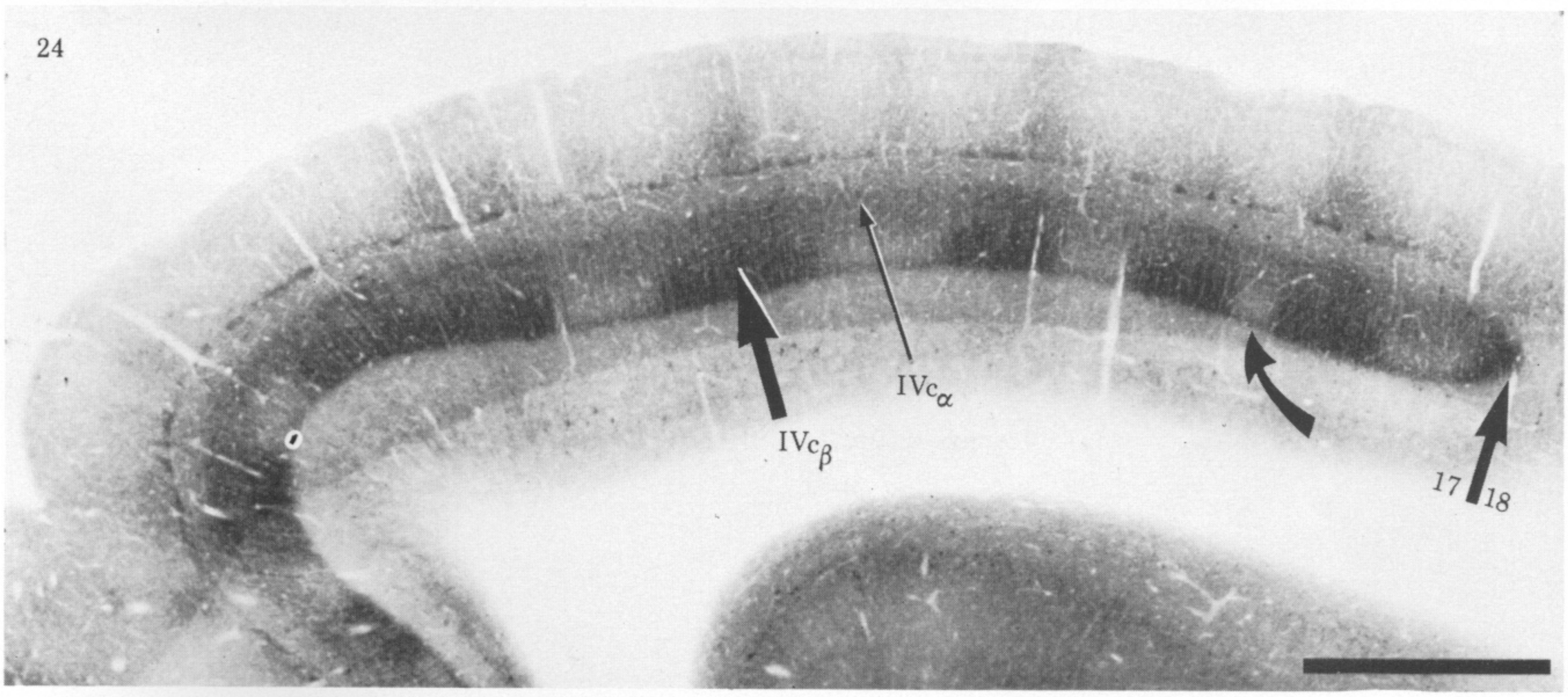


FIGURES 22–24. For description see p. 221.

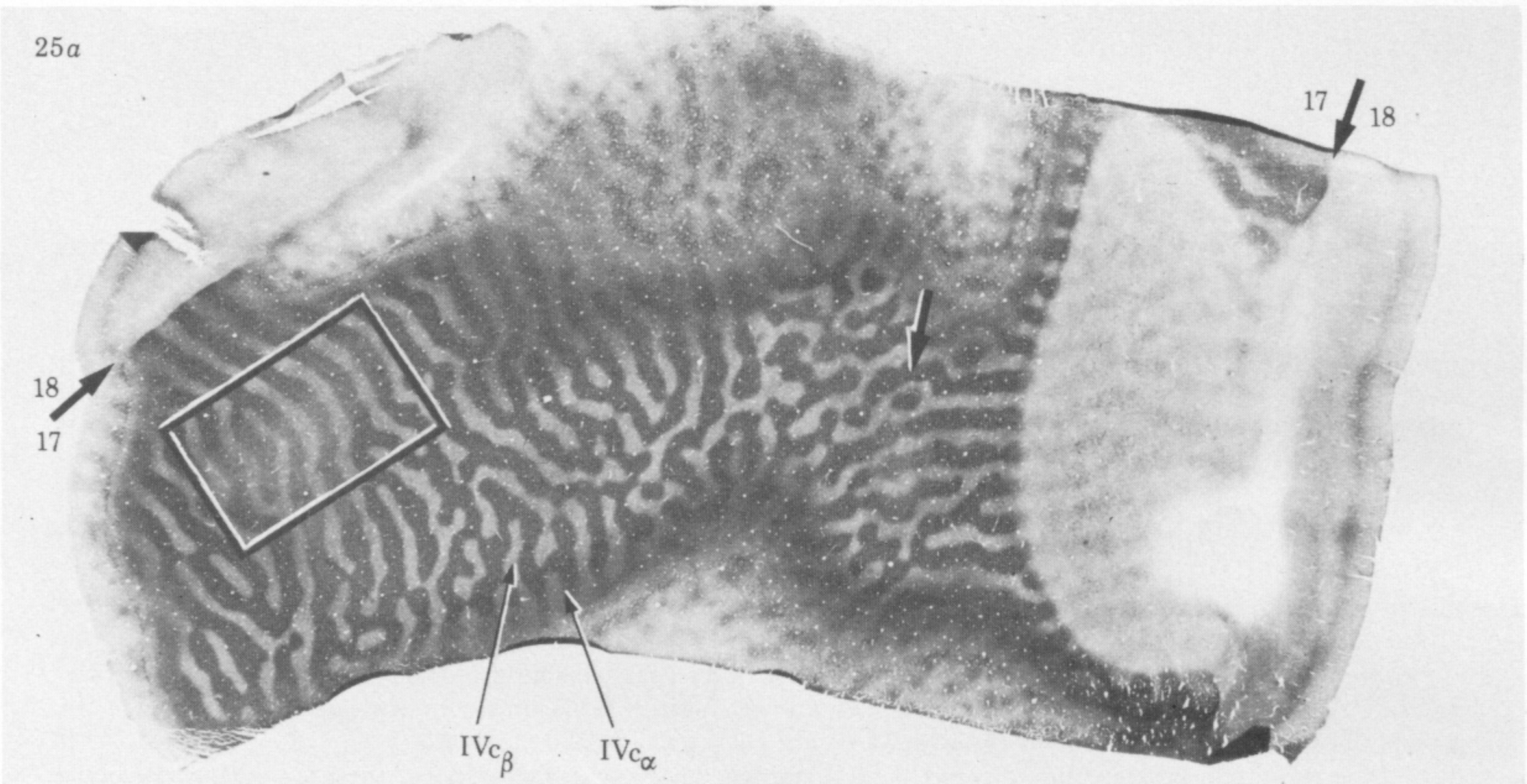



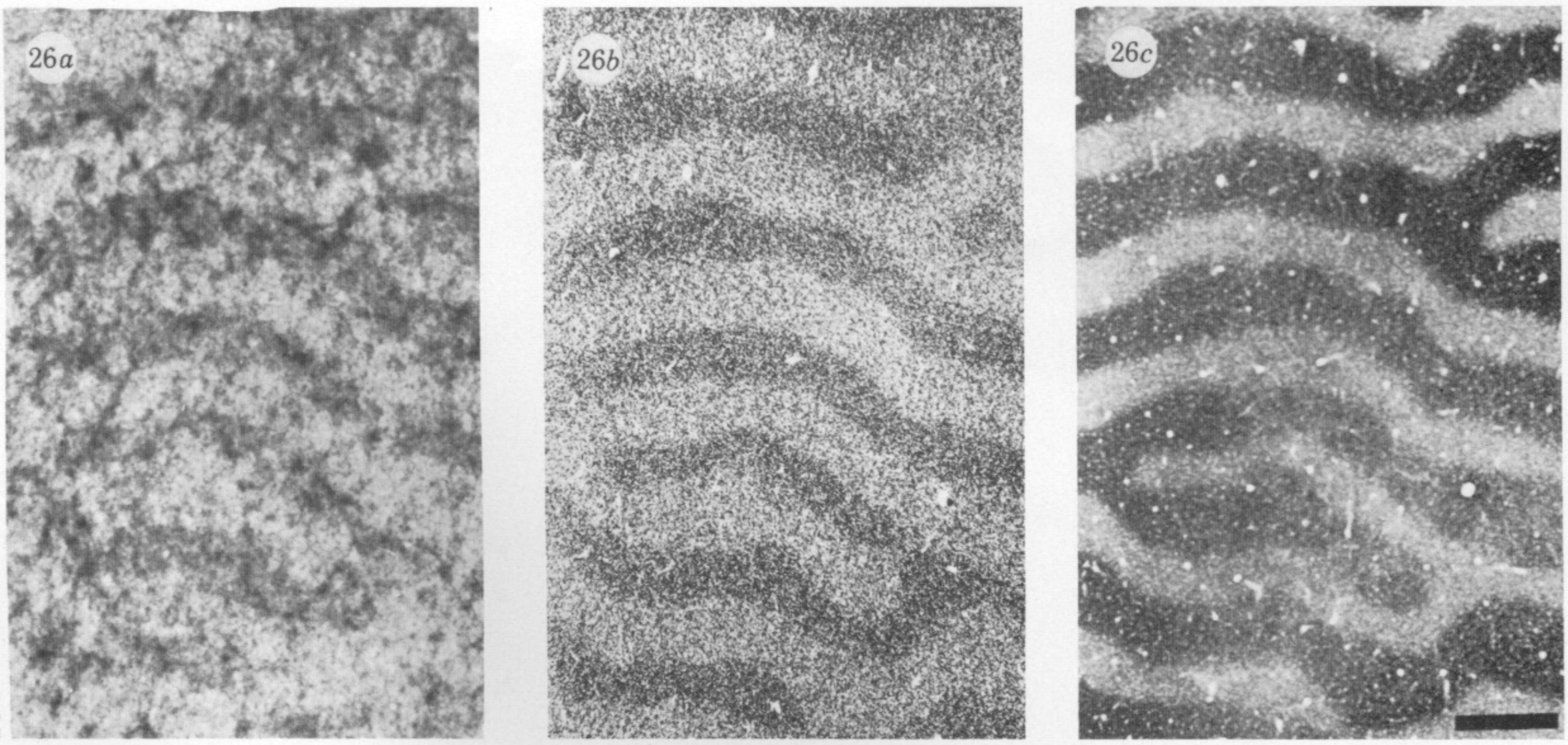


FIGURES 25 AND 26. For description see over.

FIGURE 27. For description see opposite.

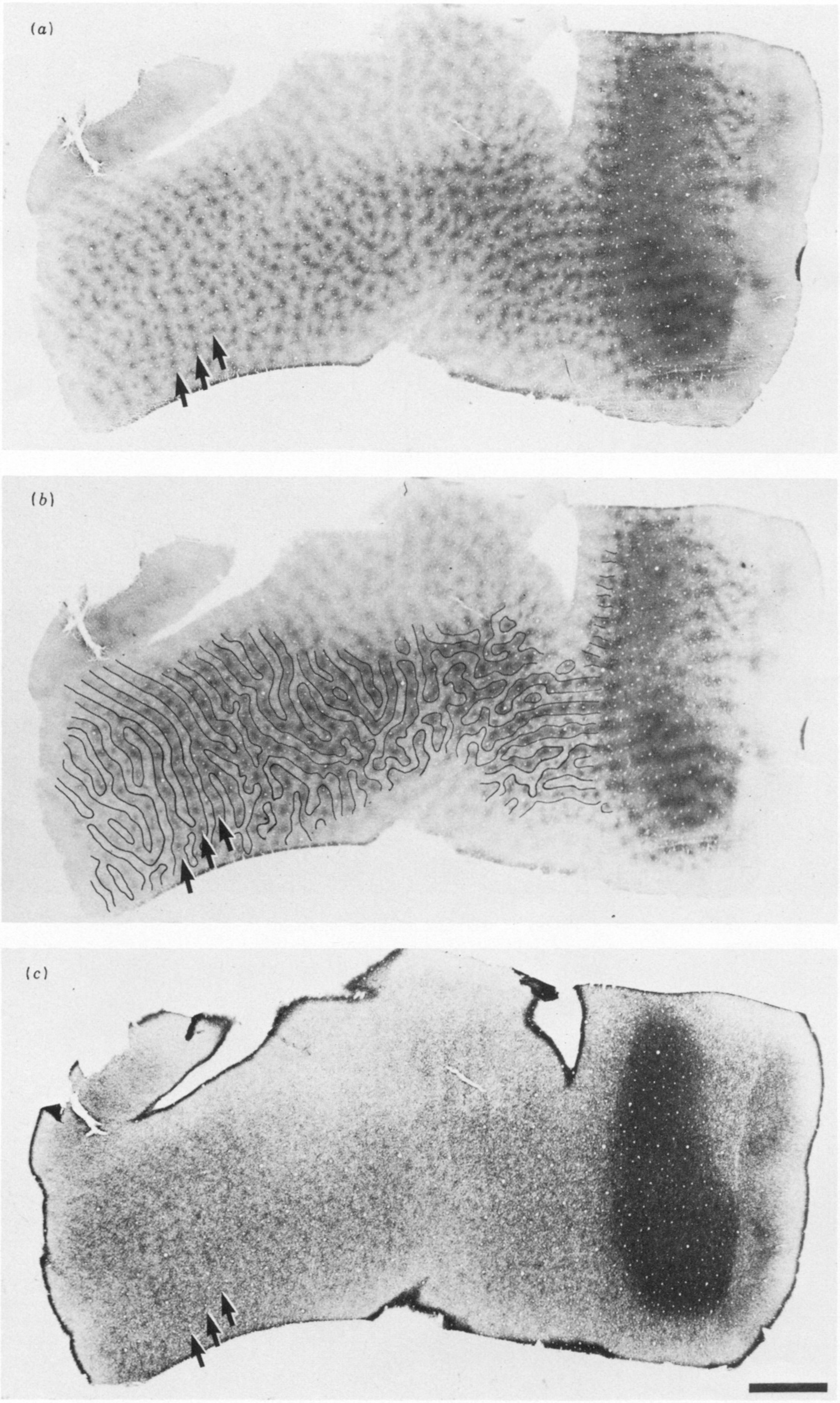


FIGURE 28. For description see opposite.

29*a*

29*b*

30*a*

30*b*

FIGURES 29 AND 30. For description see opposite.

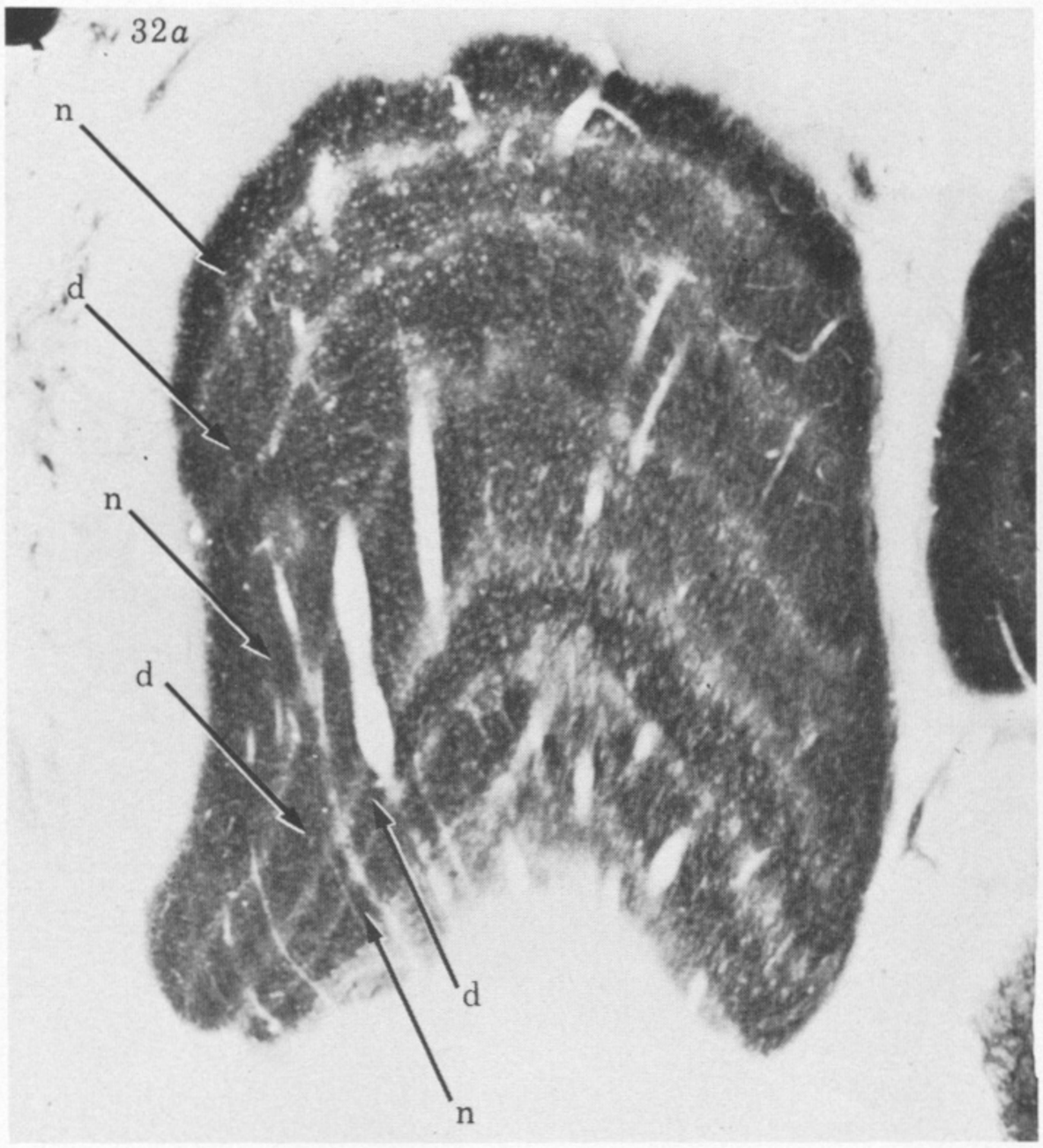


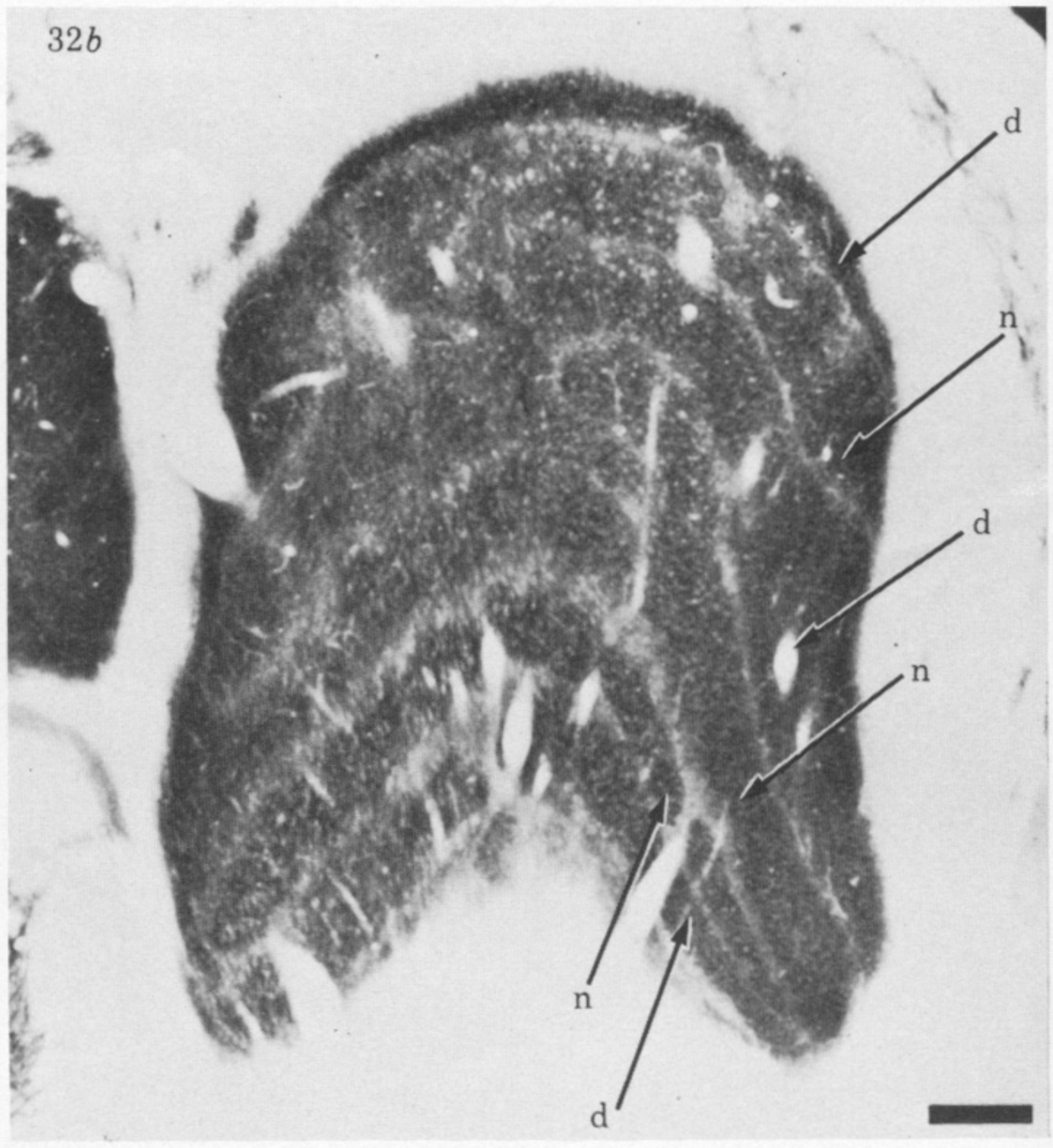


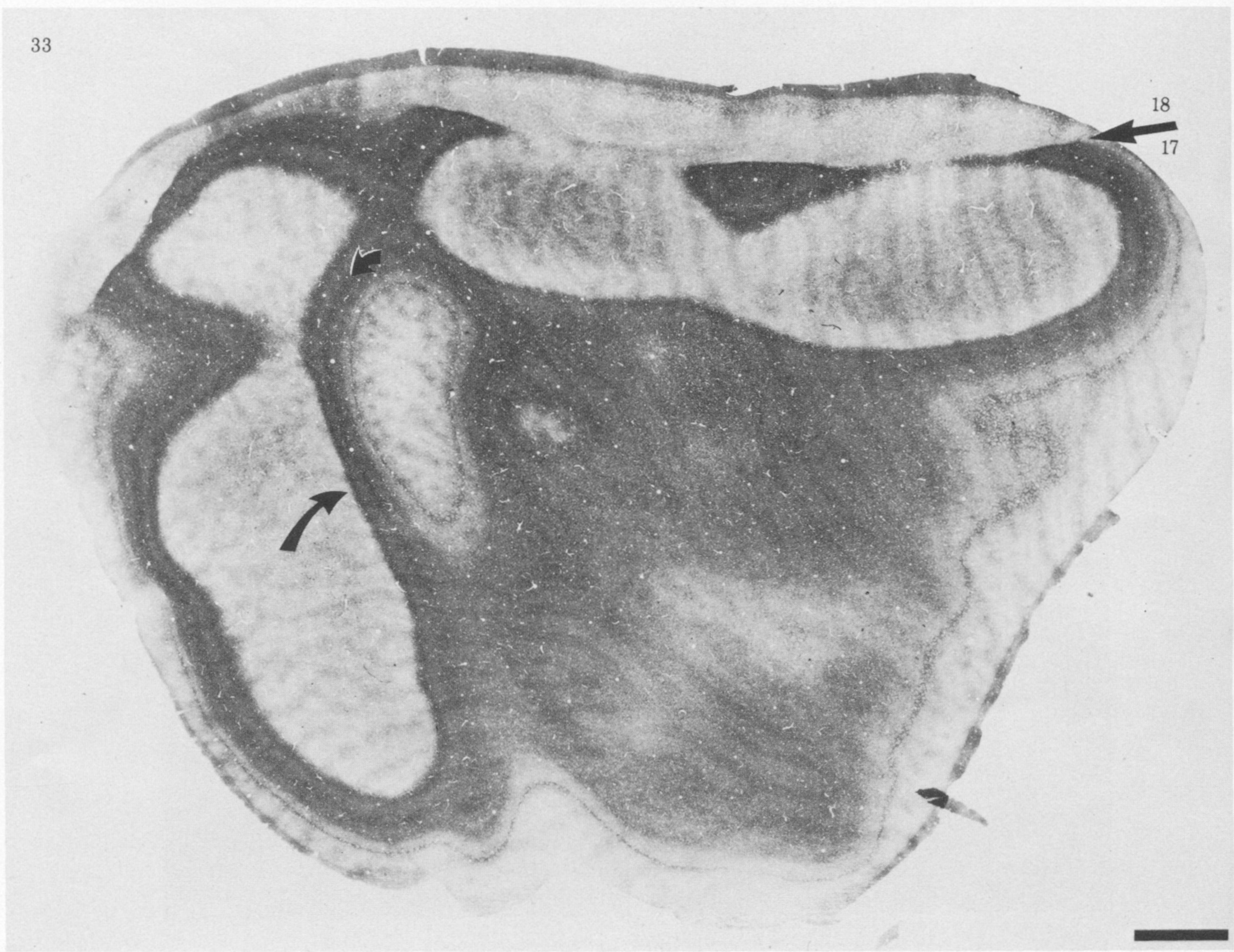


FIGURES 32 AND 33. For description see p. 226.

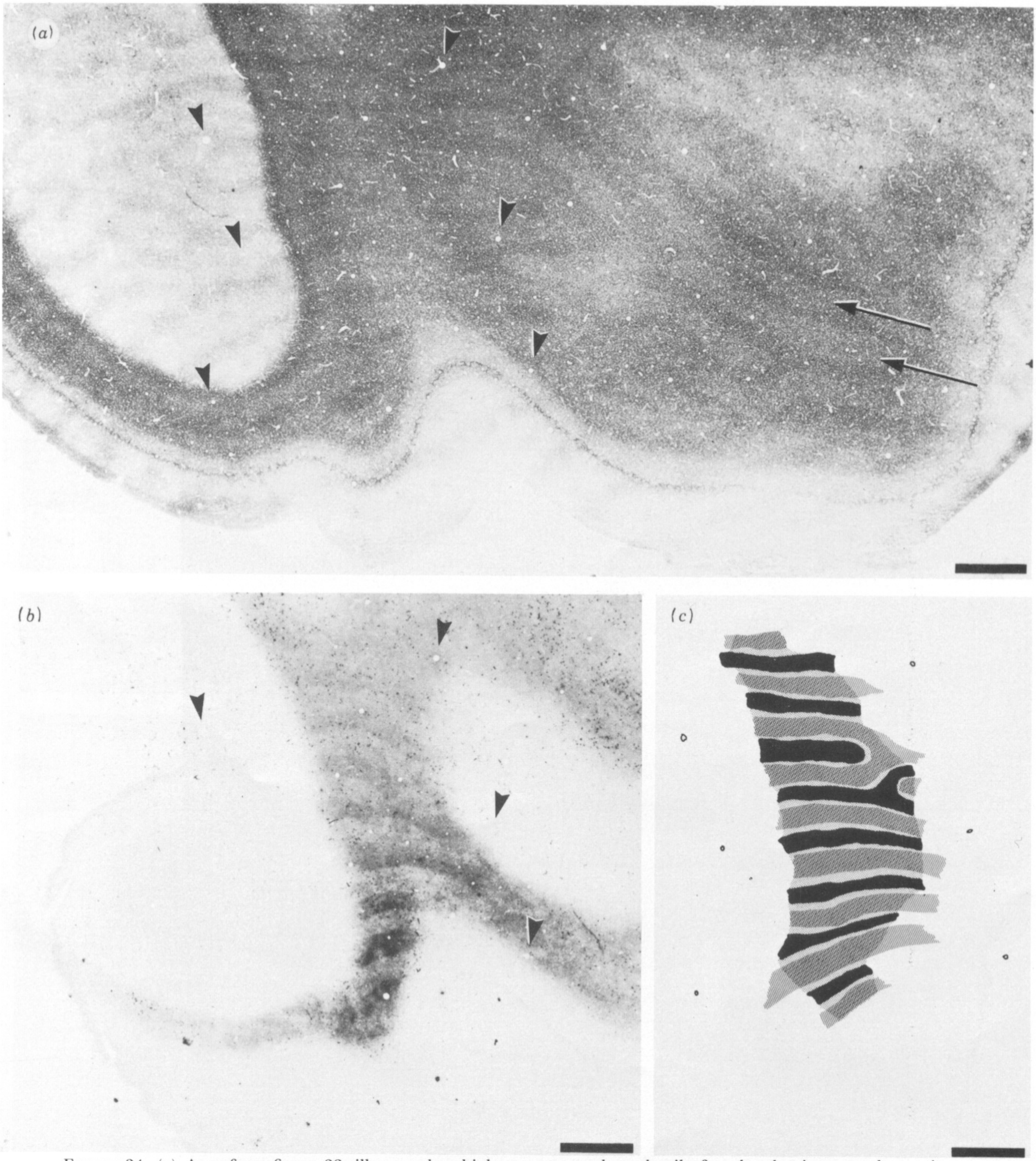


FIGURE 34. (*a*) Area from figure 33, illustrated at higher power to show detail of ocular dominance columns in layer IV. The dark ocular dominance columns appear thinner than the light columns. The ocular dominance columns can be followed from layer IV c to the left where they pass into layers V, VI. Arrowheads mark six blood vessels; these and numerous others were used to align the reconstruction in (*c*). Long arrows point out faint increase in density of cytochrome oxidase staining within the middle of each light ocular dominance column.

(*b*) Adjacent section showing ocular dominance columns labelled by anterograde transport of HRP from an injection made in a deprived eye laminae 6 in the l.g.n. (see figure 19). Under brightfield illumination the labelled columns appear dark. Unlike the columns visible in (*a*) the dark and light columns are of roughly equal width. Arrowheads point out a few blood vessels also visible in (*a*).

(*c*) Reconstruction comparing the ocular dominance columns visible in (*a*) and (*b*). The dark cytochrome oxidase columns in (*a*) are drawn in solidly with ink, the light columns are shown with small black dots. The labelled columns in (*b*), and from two nearly adjacent sections not illustrated, are marked with thin parallel lines. Accurate alignment of HRP and cytochrome oxidase columns was achieved by referring to position of blood vessels in adjacent sections. Reconstruction demonstrates that the lighter cytochrome oxidase columns match the ocular dominance columns corresponding to the deprived eye, although they actually extend beyond boundaries of HRP labelled columns to infringe upon open-eye columns. Scale = 1 mm.

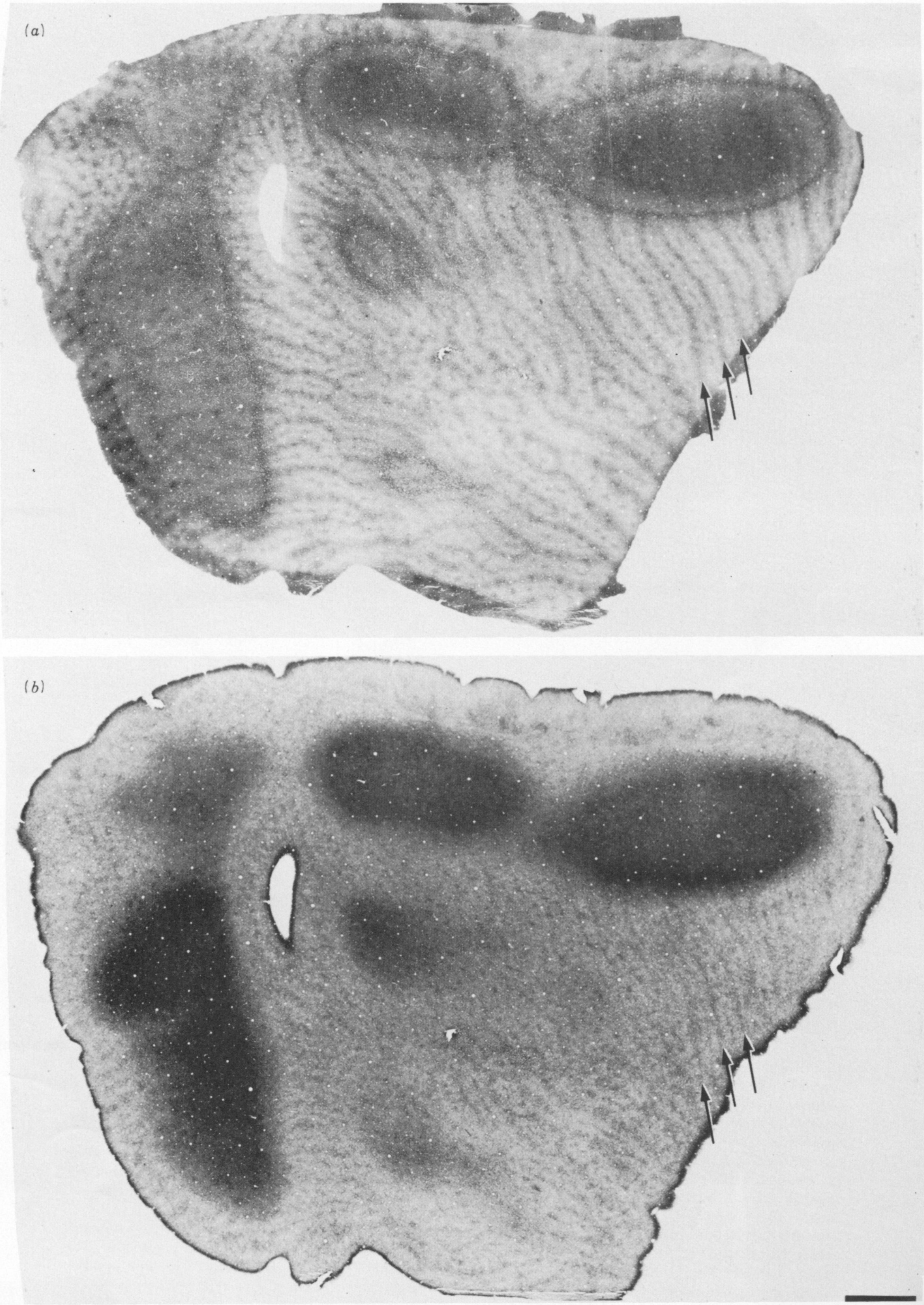


FIGURE 35. For description see opposite.

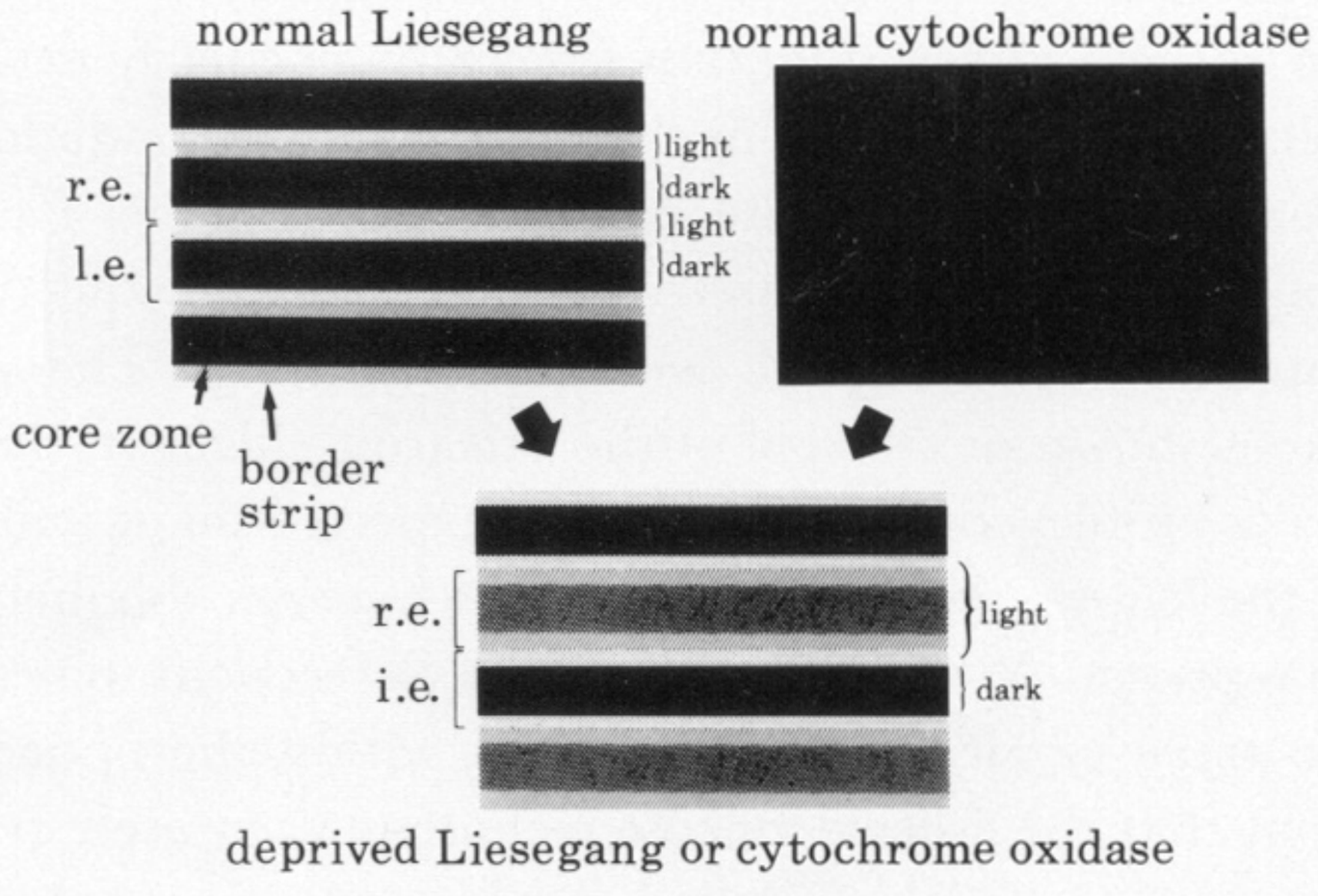


FIGURE 37. Schematic representation of the effect of visual deprivation on Liesegang and cytochrome oxidase staining in layer IV. In normal macaques no pattern is seen in layer IVc in the cytochrome oxidase stain. In the Liesegang stain a pattern of alternating wide dark bands and thin pale bands is present normally. The dark bands are proposed to correspond to the 'core zones' of the ocular dominance columns; the pale bands consist of combined 'border strips' of adjacent ocular dominance columns. The square brackets marked 'r.e.' and 'l.e.' denote the boundaries of the ocular dominance columns occupied by geniculate terminals driven by the right eye and left eye respectively. If the right eye is deprived, Liesegang staining in core zones of the r.e. weakens, causing a pattern of alternating wide light bands and thin dark bands to emerge. Cytochrome oxidase staining also decreases in the r.e. core zones. However, it falls in l.e. and r.e. border strips too, causing a pattern to develop which appears similar to the pattern of Liesegang staining. The loss of cytochrome oxidase activity is slightly greater in the l.e. and r.e. border strips than the r.e. core zones, causing the r.e. core zones to appear faintly visible (diamond hatching) as indicated in figure 34*a* (long arrows).

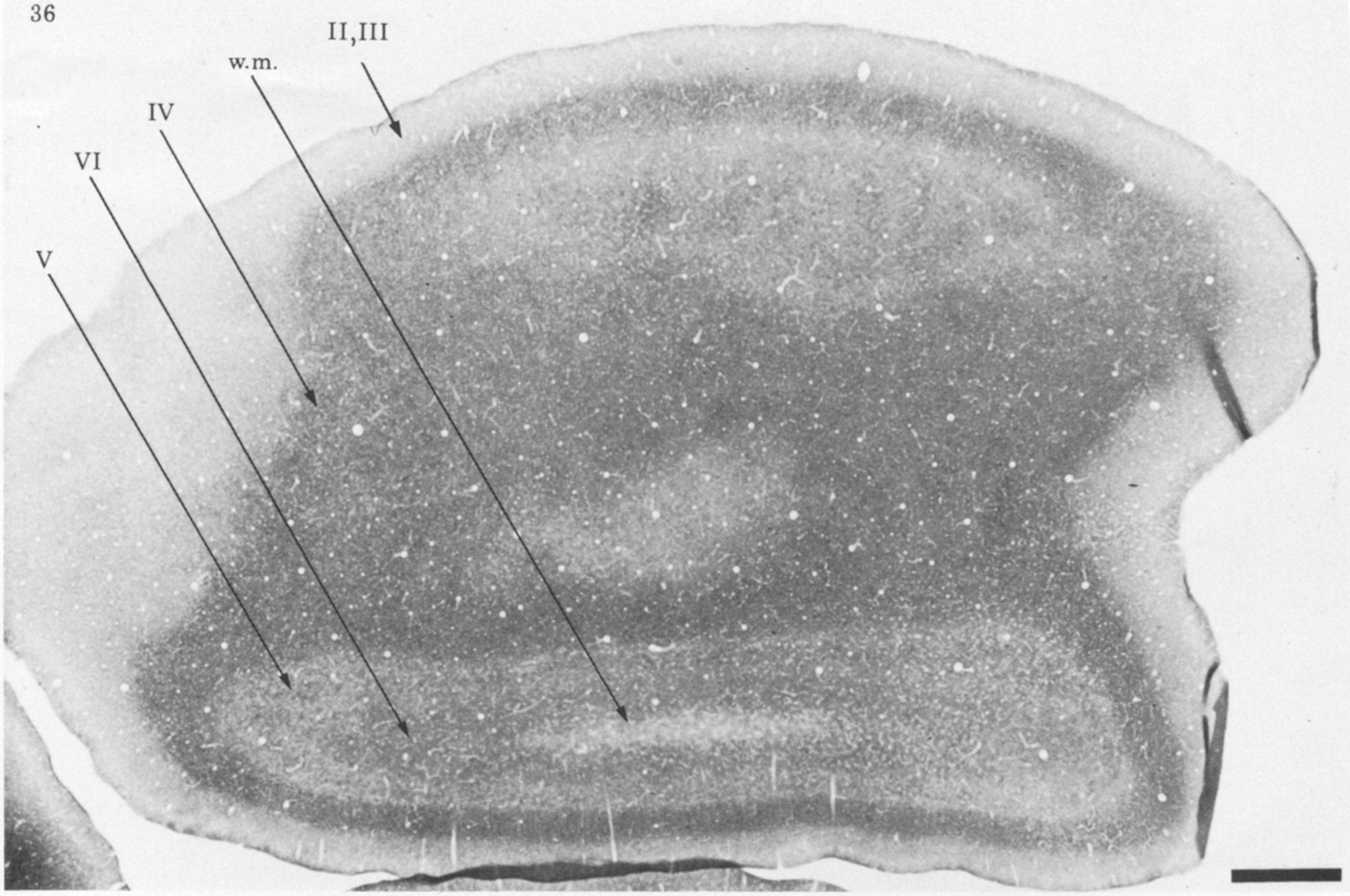





FIGURES 36 AND 38. For description see opposite.

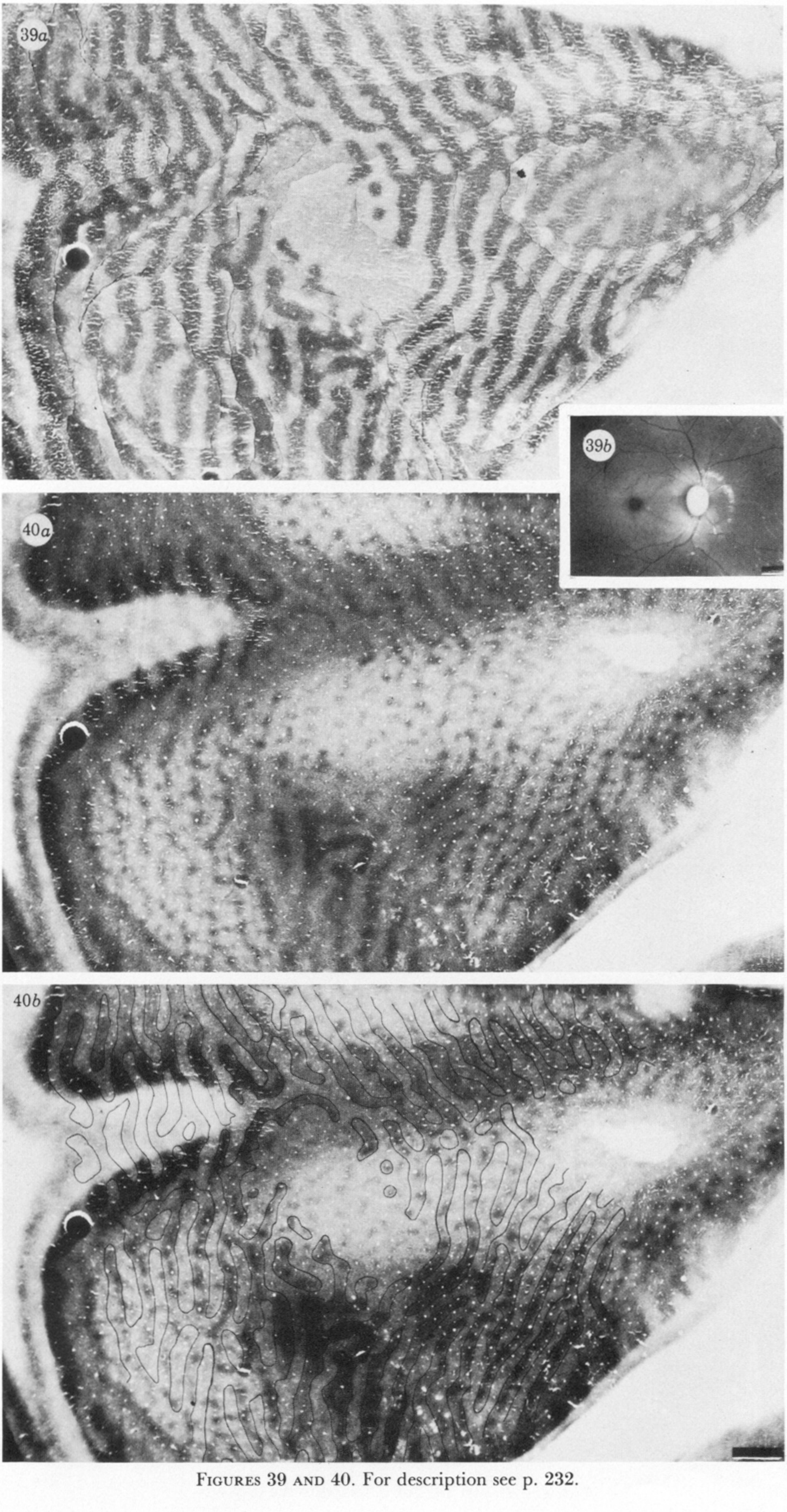


FIGURES 39 AND 40. For description see p. 232.

41*a*

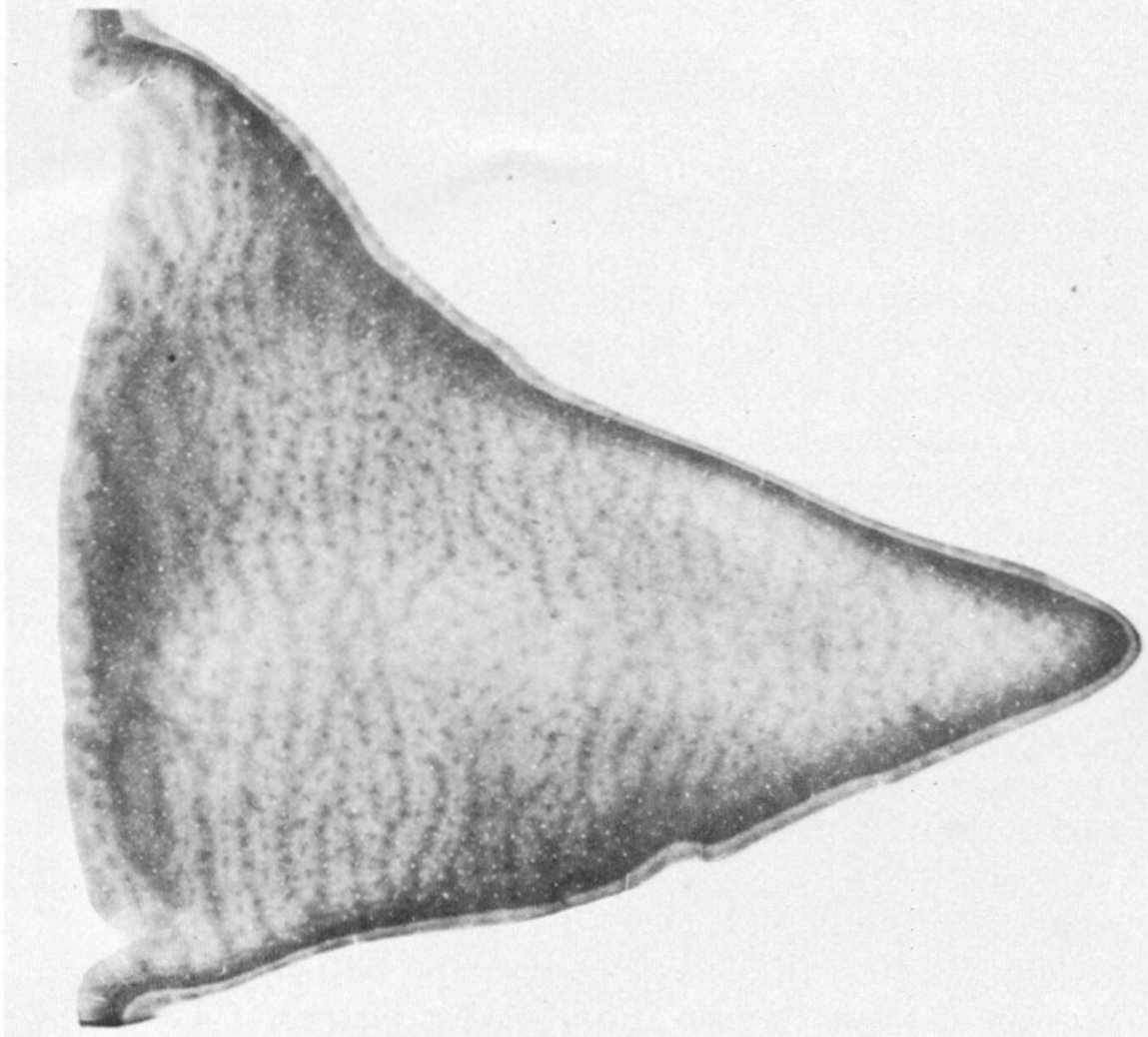

41*b*

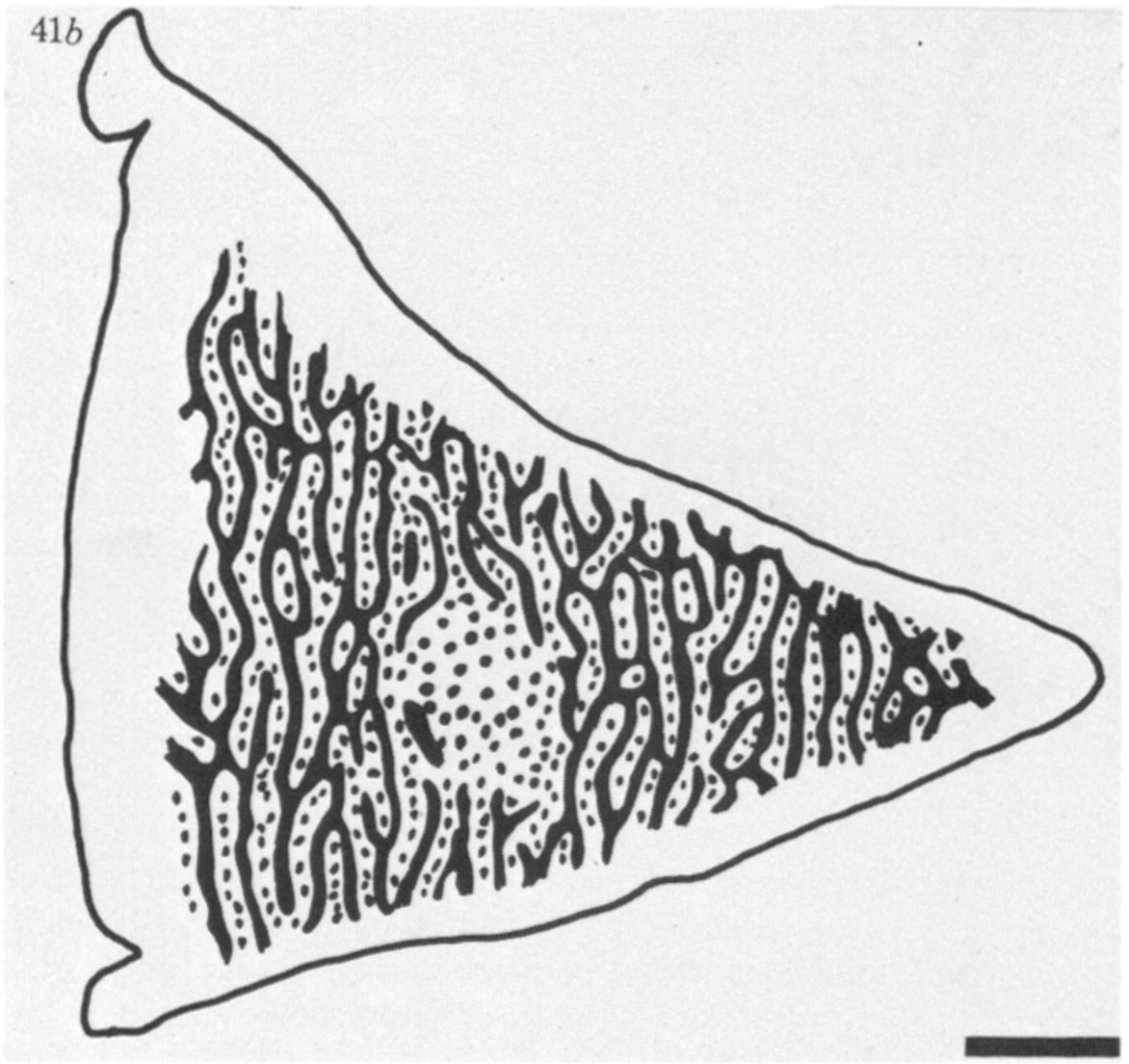

42*a*

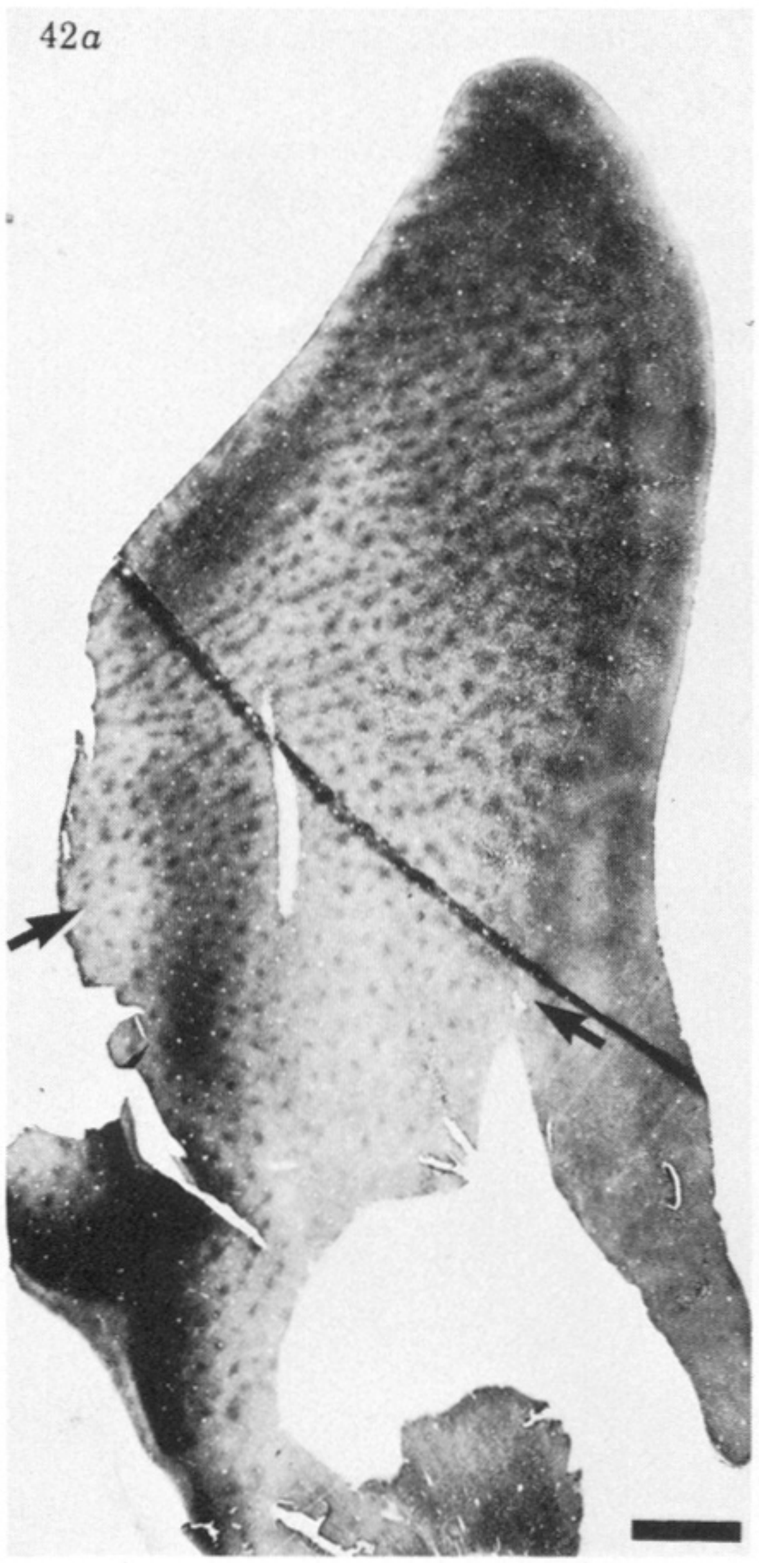

42*b*

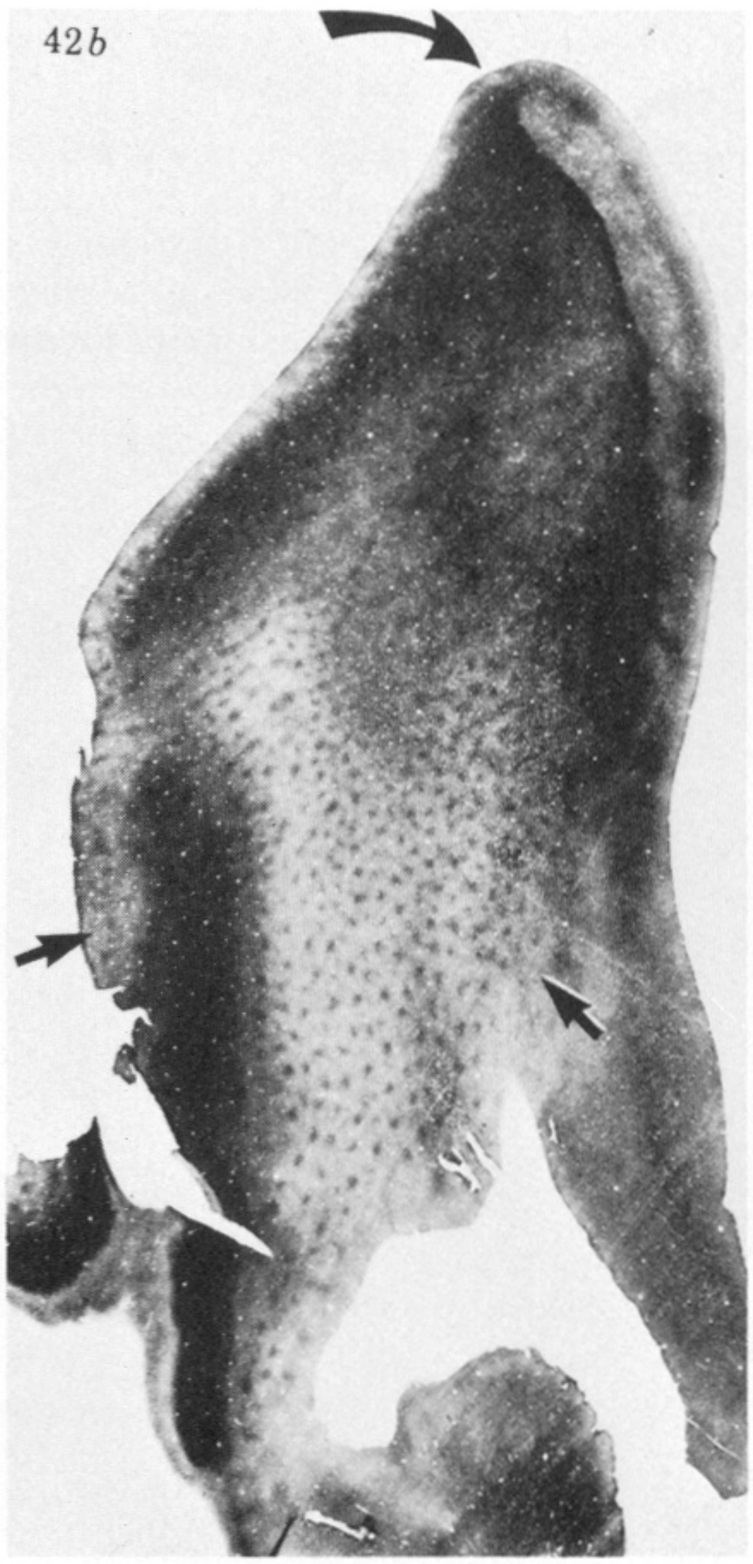

42*c*

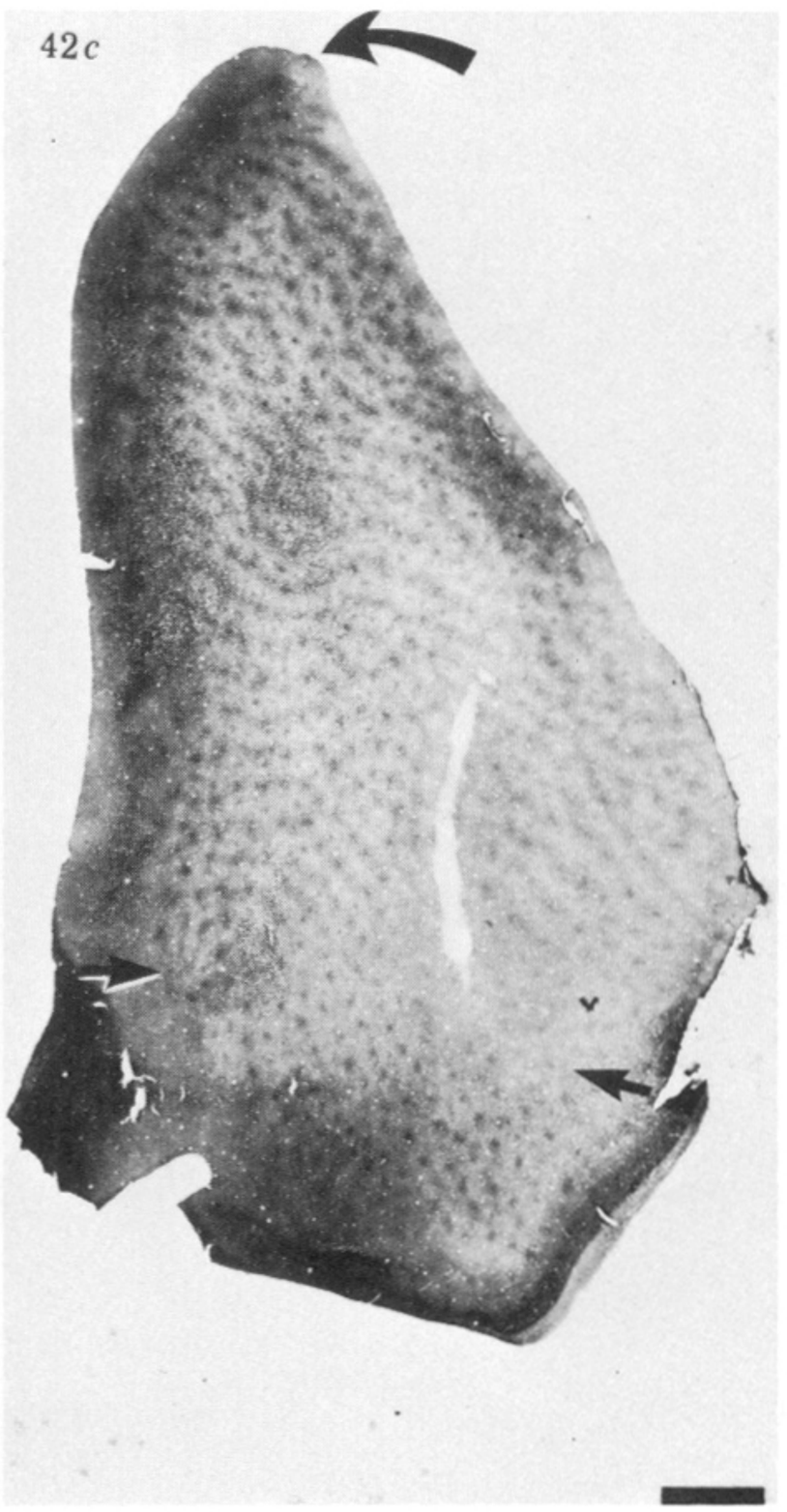

FIGURES 41 AND 42. For description see over.

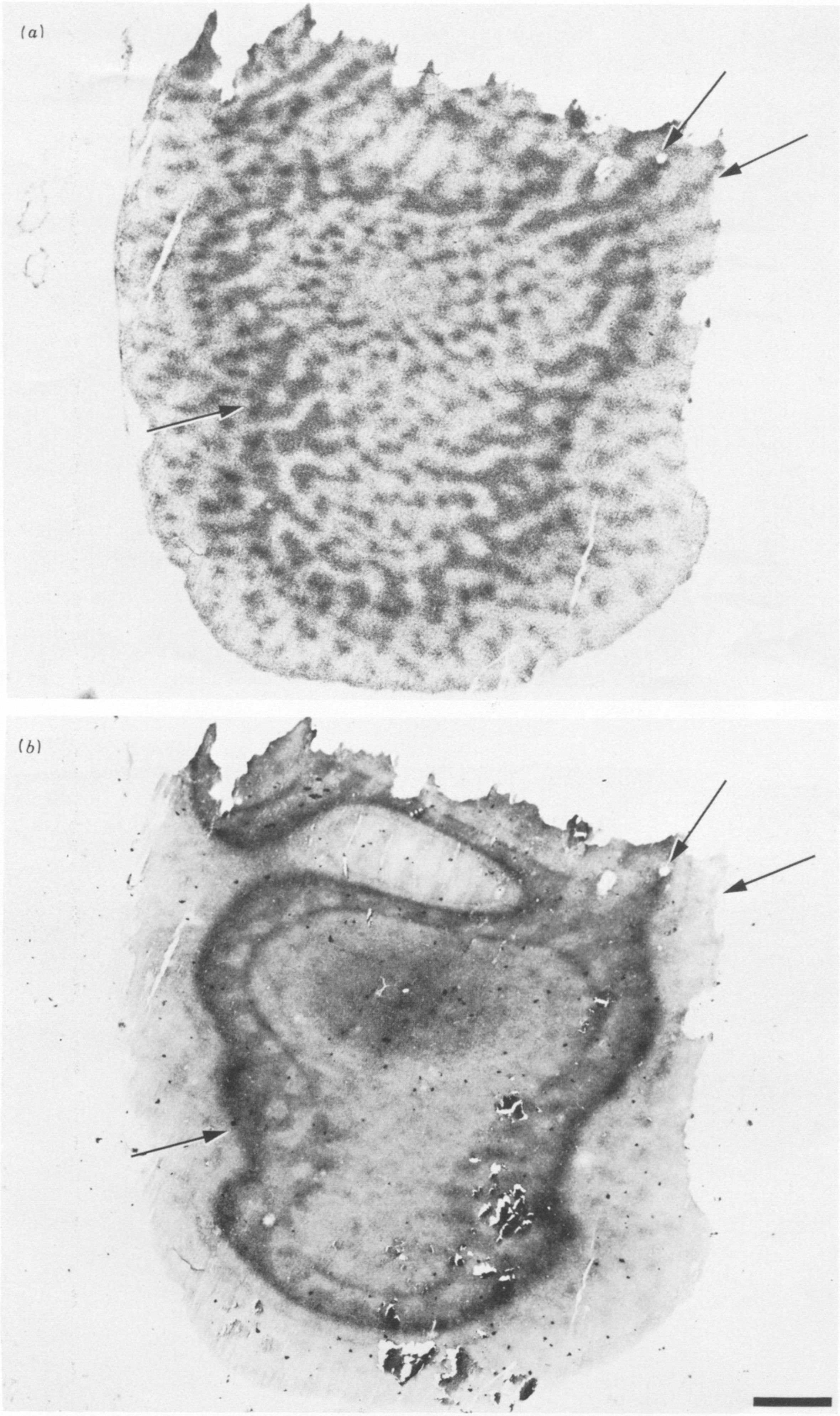


FIGURE 43. For description see opposite.

44*a*

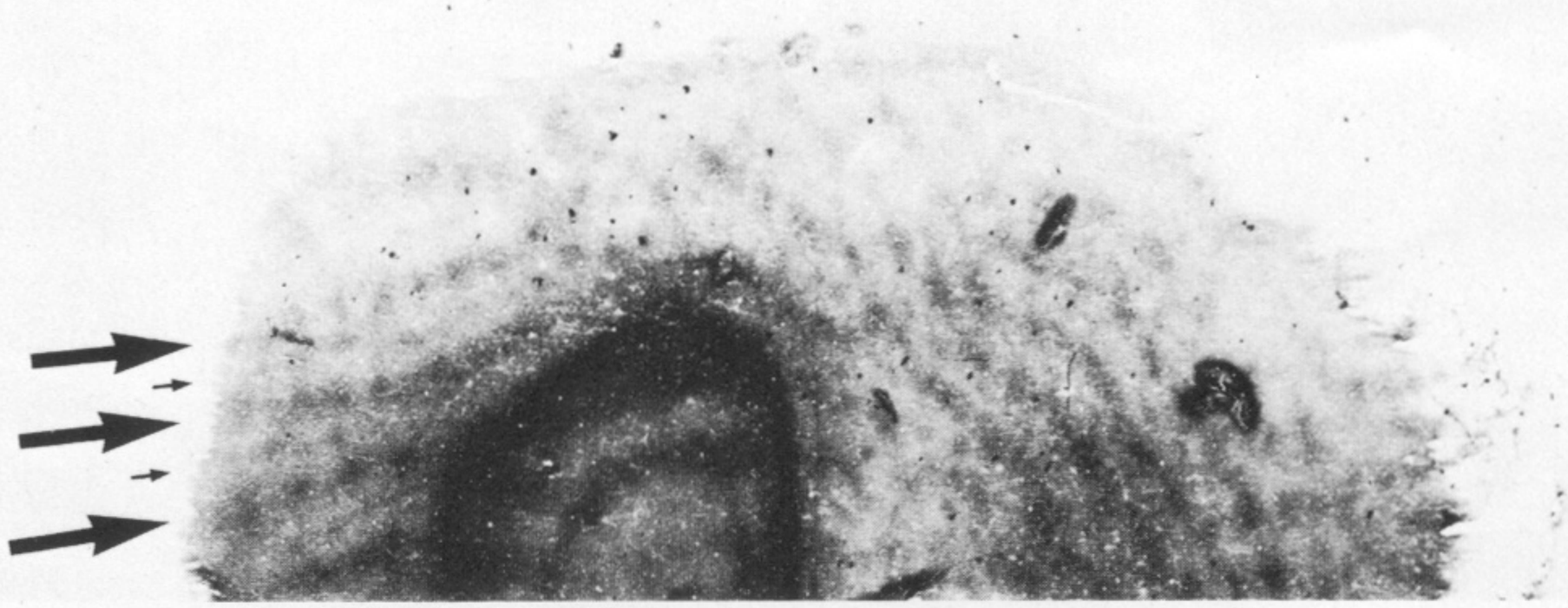

44*b*

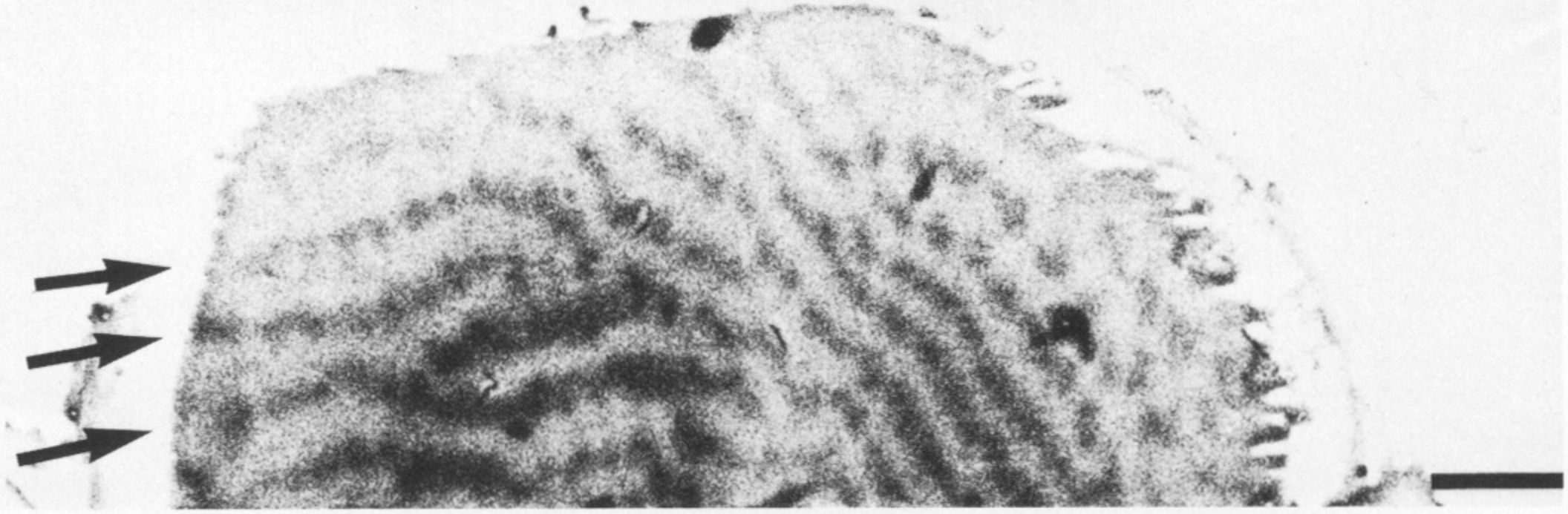

45

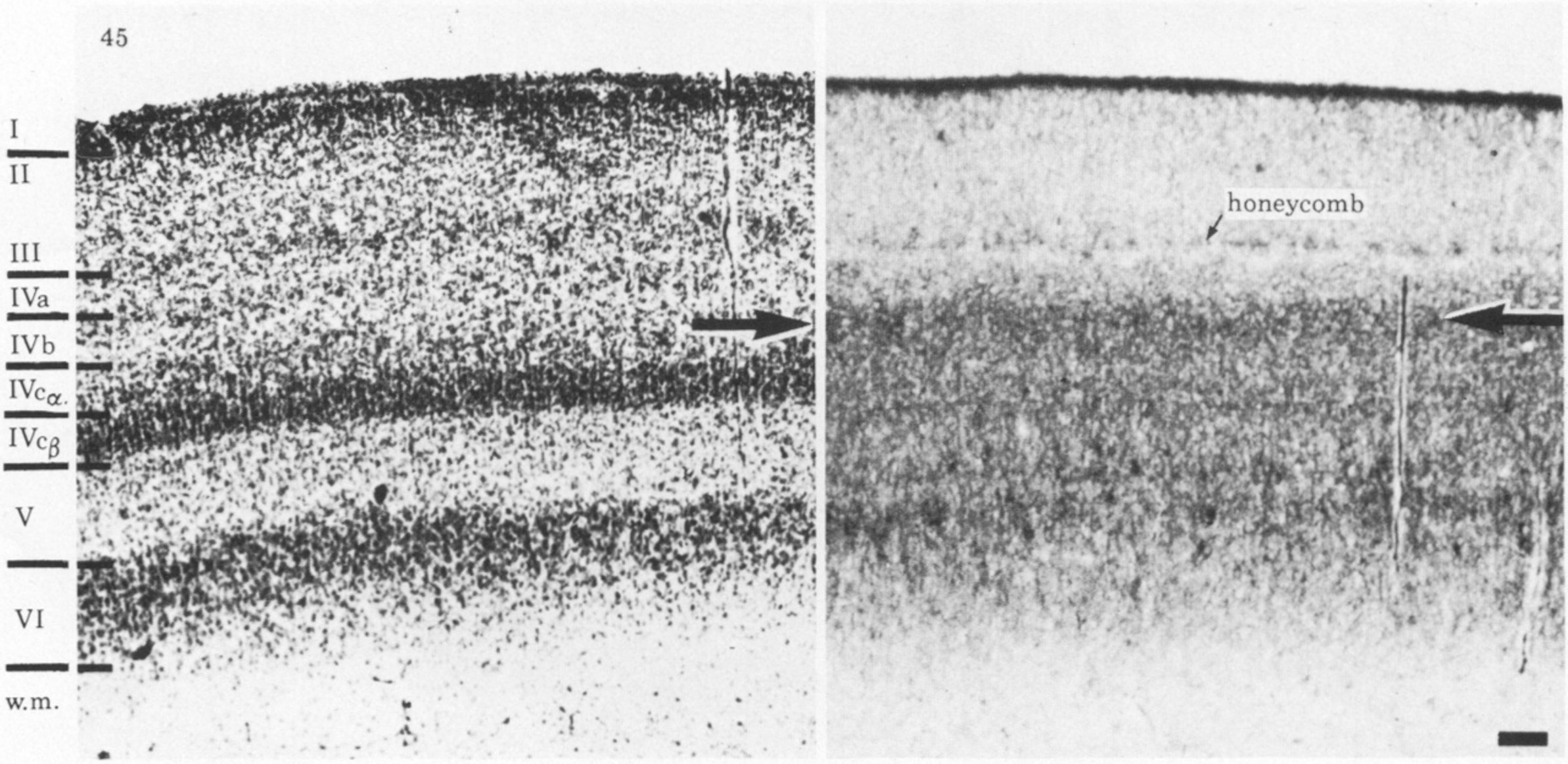


FIGURES 44 AND 45. For description see opposite.

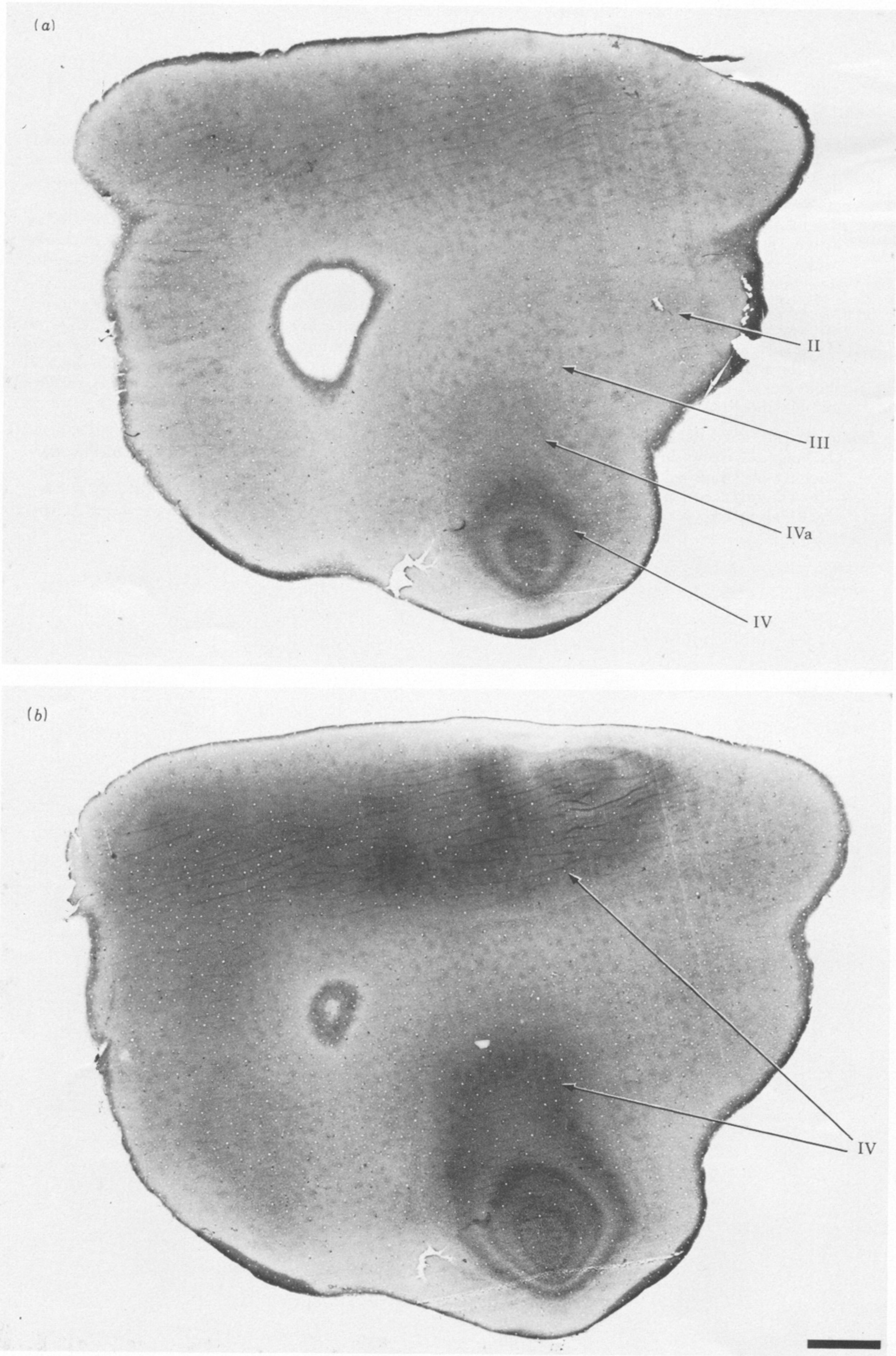


FIGURE 46. For description see previous page.

(a)

III

IV

(b)

IV

FIGURE 47. (*a*) Section from the roof of the left calcarine sulcus from the monkey illustrated in figure 46, showing patches in the upper layers.

(*b*) A deeper section from the same block grazing the dark band in layer IV, showing the patches more clearly. Scale = 2 mm. Inset: coarse pattern of cytochrome oxidase staining in layer IV a which closely resembles adult honeycomb pattern characteristic of layer IV a. Scale = 200 μm.